DEVELOPMENT OF FLUORINATED MONOMERS AND POLYMERS FOR ADVANCED PHOTOLITHOGRAPHIC APPLICATIONS

Thesis by

Daniel P. Sanders

In Partial Fulfillment of the Requirements for the Degree of

Doctor of Philosophy

CALIFORNIA INSTITUTE OF TECHNOLOGY

Pasadena, California

2005

(Defended December 8, 2004)

ACKNOWLEDGEMENTS

While I disagree that the acknowledgements section is the only portion of a Ph.D. thesis that is ever read, I do feel that it is by far and away the most important. I will take a few pages here to thank those whom have made this work possible. Here is my best effort to do justice to all of those to whom I owe so much. I would first and foremost like to thank my parents who did everything in their power to advance, encourage, and facilitate my education. At times, I am sure they thought I would never graduate, but would continually wander the earth collecting degrees in perpetuity. Now that the journey is complete, I hope they feel as much pride in this accomplishment as I do.

I would like to thank Prof. Jerome B. Lando (Case Western Reserve University), Dr. Ram S. Narang (Xerox), Prof. Hatsuo Ishida (Case Western Reserve University), and Dr. Joy P. Dunkers (NIST) for their assistance and guidance over the years.

The highlight of my initial visit to Caltech was visiting with the Grubbs group, sitting in the hallway on the second floor of Church drinking beer from a keg, talking sports with Arnab Chatterjee, and meeting Helen Blackwell (whose father I had taken classes from while I was at Case), Todd Younkin, Melanie Sanford, and many other members of the group. Although I was not sure what a Schlenk line really was for and I did not really understand why such a big deal was made out of a bunch of dirty bomb-like solvent purification cylinders, I *was* sure that Caltech was the place for me and that the Grubbs labs (specifically 214 Church) were by far the *worst* labs I had ever seen. Well, little did I know that the lab bay that I was so repulsed by would one day become my own and five years later I would be fretting about the remodeling of those same labs!

I would like to thank Bob Grubbs for affording me the opportunity to work in his group. Having seen the hard lessons learned by others during my Master's degree, I took awhile to choose a group at Caltech. I chose wisely. Joining the Grubbs group is not like joining a lab;

it is like joining a family. I would like to thank Bob, Helen, and their family for welcoming me into the fold. I have learned many things while in Bob's group, but two important lessons will stay with me. First, sometimes you just have to throw some stuff at some stuff and see what happens. That is how serendipity - the most useful tool in the arsenal of chemical discovery - works. It is the ideas that should not work that afford true insight when they miraculously do. Finally, if you find good people, treat them with respect, and give them the freedom to work on what they do best, good things happen.

Many other members of the Caltech community have assisted me throughout the years. First, I would like to thank the members of my committee: Professors Dave Tirrell, Brian Stoltz, Jack Beauchamp, and Pat Collier for their assistance and encouragement during my time at Caltech. Other members of the department staff were invaluable over the years, including Linda Clark, Dian Buchness, Scott Ross, Larry Henling, Mona Shahgholi, John Leite, Anne Penny, Steve Gould, Joe Drew, Chris Smith, and Cora from the VWR stockroom.

I have met some great people during my time in the Grubbs group who have helped me grow as a scientist and more importantly, as a person. I need to thank Eric Connor and Todd Younkin who helped teach me air sensitive chemistry as a first year graduate student. Their infectious good humor made the first year of graduate school at Caltech a great one. After Eric left, Christie Morrill became my new bay-mate for the next four years. I really could not have asked for someone better to work next to; Christie has always been willing to offer advice, encouragement, and commiseration during those (all too frequent) periods when seemingly every reaction ended in failure. In our bay, there are lies, damned lies, and then there are Tetrahedron Letters preps!!

I would like to thank Arnab Chatterjee for our productive collaboration on the trisubstituted olefin cross-metathesis work described in Chapter 7. Arnab's good humor and quality sports conversations made many hours in lab fly by. I need to thank Emmanuelle Despagnet-Ayoub who worked briefly with me on the ADMET chemistry described in Chapter 6.

I am grateful for Soon Hong's collaboration on our efforts to prevent/understand olefin isomerization. Finally, special thanks go out to Jolene Lau, a summer undergraduate student, who worked on the oxetane acetal structures presented in Chapter 4. I wish her all the best in her graduate career at Scripps.

Oren Scherman, Diego Benitez, and Tae-Lim Choi were my fellow classmates. Oren and his wife Cora have been good friends throughout graduate school. Oren was invaluable in offering advice on polymer chemistry, instigating never-ending political discussions, and bailing out our intramural basketball team with his patented drive/scoop shot. J.P. Morgan was a fellow member of the late night crew. Our many late nights working in lab while listening to Adam and Dr. Drew on Love Lines were "good times" as Adam would say. Fellow polymer chemists in the group with whom I have interacted include Chris Bielawski, Andreas Kilbinger, and Isaac Rutenberg. Melanie Sanford, Jen Love, Tina Trnka, and Bill Ward all helped me with catalyst-related issues throughout the years. Whenever my project seemed to be going nowhere, Andrew Waltman, one of the last remaining members of Team Nickel, could always be counted on to cheer things up with a spirited game of lab ball or a timely appearance of Surgical Elvis. Special thanks go to the class of Andy Hejl, Tim Funk, Jacob Berlin, and Jason Jordan for all the good times in lab the last three years.

A great number of post-docs have been helpful during my graduate career including (in chronological order): Adam Matzger, Mike Koscho, Janis Louie, John Seiders, Steve Goldberg, Justin Gallivan, Dean Toste, Jon Efskind, Eric Marinez, Brian Connell, Anatoly Chlenov, Paula Diaconescu, Anna Wenzel, Greg Beutner, and Al Nelson. A great benefit of working in the Grubbs lab is the opportunity to work with post-docs from all around the world. A few of them not mentioned previously include (in chronological order): Choon-Woo Lee, Hyun-Jin Kim, Jaesook Yun, James Tsai, Stu Cantrill, Sebastian Smidt, and Christiane Marti-Meyers. Thank you all for broadening my intellectual and cultural horizons. To the many post-docs and senior graduate students who have assisted me, I hope that I have repaid my debt in part by trying to

help the younger members of the lab as much as you helped me. I wish Donde Anderson, Erin Guidry, Irina Gorodetskaya, Ron Walker, Kevin Kuhn, and Michelle Robbins all the best.

Much of my work has been conducted in collaboration with a number other groups and industrial sponsors. The majority of this work has been done in collaboration with Professor C. Grant Willson's group at the University of Texas, Austin. The pervasive enthusiasm and energy of Prof. Willson is truly amazing. I consider myself truly blessed to have been able to work with not one, but two of the greatest professors and people in all of chemistry.

My primary collaborator in the Willson group was Brian Osborn. Brian is directly responsible for all the vacuum UV, VASE, and imaging measurements shown in this work. There is no way I can give him enough credit here. I also need to thank many of the other chemists in Dr. Willson's group for welcoming me into their group. I worked with Ray Hung and Shintaro Yamada on the norbornene addition polymers presented in Chapter 3. Matt Pinnow and I worked on mass-persistent resist platforms and I thank him for many excellent conversations. Other members of the group with whom I had great interaction include: Brian Trinque, Takashi Chiba, H. V. Tran, Charles Chambers, and Ryan Callahan.

My collaboration with UT-Austin was part of the Universities Resist Project (LITJ 102) funded by International SEMATECH and its member companies. I thank them for their generous funding of this work. I am grateful to Will "Hamburgers for Polymers" Conley and Paul Zimmerman, the SEMATECH academic liaisons for this project, and Gene Feit, the director of SEMATECH, for facilitating my involvement in this project. I also need to thank SEMATECH employees Danny Miller, Shashikant Patel, Vicky Graffenberg, and Georgia Rich, without whom all of the 157 nm imaging, vacuum UV, and VASE measurements would not have been possible. Finally, I would like to acknowledge the participating members of the Frechet group (UC-Berkeley), the DesMarteau group (Clemson), and the industrial members of SEMATECH for their helpful comments and advice, particularly Ralph Dammel of AZ-Clariant and Bob Allen of IBM. Special thanks go out to Dick Pederson, Yann Schrodi, Sharad Hajela, and Materia, Inc. for

their generous supply of various catalysts and assistance with patent-related issues. Paul Cahill, Exciton, Inc. and the U.S. Air Force are acknowledged for their generous supply of quadricyclane.

During my time at Caltech, a large number of people have helped me keep my sanity. Shawn Briglin (of the Lewis group) was my roommate for 3 years. Thanks to Shawn and his partner-in-arms, Dave Michalak, I made my first film appearance (providing a true LA experience!) when our living room was frequently turned into a production set and pre-production assembly area. After Shawn graduated, Andy Hejl became my roommate for the next 2+ years. Andy was responsible for introducing me to some of the finer things in life. Most notably, these include the George Foreman grill and TiVo - two truly life-changing technological developments without which I could not have made it through graduate school! Events like Andy and Tim Funk's Thanksgiving Extravaganza have made being so far away from home that much easier. Andy was also responsible for bringing Hodge the cat into our apartment. Hodge would always keep me company as I relaxed after late nights in the lab, although that usually resulted in me being covered with cat hair and cat drool. Thanks, Shawn, Andy, and Hodge for making the Catalinas a great home for the last five years.

Intramural sports have served as a greatly needed outlet for stress and aggression. Jacob Berlin deserves special recognition for tireless efforts to assemble various softball and basketball teams over the years. Thanks to all of those who competed alongside me through various seasons of softball, basketball, and soccer. A great part of intramurals was the chance to meet and befriend many members of other research groups over the years; a few of these include: Ryan Julian, Nick Graham, James Peterson, Jeremy Heidel, Steve Spronk, Rob Moncure, Ian Mangion, Jeremy May, Darren Beene, and the many members of the MacMillian group soccer team.

However, the longest running extracurricular activity in my graduate career has been flag football. Our feeble Eight Year Plan evolved into the Team Justice juggernaut and yearlong weekend football with a large number of friends/fanatics: Chad Schmutzer, Jake Wiener and his brother Dave, Brian Johnson, Brian McKay, Dave Anderson, Randy, Christine, Jim Falsey, Sean

Brown, Matt Pohlman, Ted Betley, Steve Brown, Brian Leigh, Mark Cappucci, Justin Romberg, Anand Vahedra, Andrew Mollner, Ron and Don Walker and many, many others. Thanks to all of you for helping me hold onto my youth just a little bit longer. It has been a great five years!

Well, I have probably forgotten many people in this acknowledgements section and for that, I apologize. To make up for it…and most importantly, I would like to thank (*insert name here*) for their (*insert contribution here*), without which none of this would have been possible.

Now if for some reason you still feel like you need to read this thesis, please either go lie down or have a few beers until that feeling goes away…..

ABSTRACT

The incorporation of fluorine into photoresist materials imparts a variety of highly desirable properties for deep ultraviolet lithography at 193 nm and 157 nm. Chief amongst these benefits are the high optical transparency of partially fluorinated materials and the high acidity of fluoroalcohols. While metal-catalyzed polymerizations historically have received less attention than radical polymerizations for photoresist synthesis due to concerns over residual metal contamination, the high deep UV transparency and etch-resistance of alicyclic norbornene monomers have revived interest in metal-catalyzed polymerizations for the development of advanced lithographic materials. Yet, significant challenges remain to incorporate sufficient fluorine for high transparency without adversely affecting the polymerization process or dissolution behavior.

Chapters 2 details the synthesis and characterization of a series of partially fluorinated tricyclo[4.2.1.$0^{2,5}$]non-7-ene (TCN) monomers. The fused cyclobutane ring serves as an additional scaffold onto which additional fluorinated groups can be substituted without adversely affecting the polymerization behavior of the monomer. Specifically, this allows the transparent α-trifluoromethyl carboxylic acid ester moiety to be incorporated into a polymerizable norbornene-like framework. The ability to incorporate additional fluorine allows for the synthesis of metal-catalyzed addition polymers with greatly enhanced transparency relative to their less-fluorinated norbornene analogues. The synthesis and imaging of TCN-based photoresist polymers are explored in Chapter 3.

Chapter 4 introduces a series of 3-oxa-tricyclonon-7-ene monomers synthesized from quadricyclane and fluorinated ketones. These oxetane-containing monomers undergo a facile Lewis acid-catalyzed isomerization to form the polycyclic 4-oxa-tricyclonon-8-enes. While the oxetane ring in oxatricyclononane structures was found to be largely unreactive, the similar high transparencies of addition and ring-opening metathesis polymers of fluorinated oxatricyclononenes detailed in chapter 5 reveal the effect of the alicyclic backbone structure on

transparency at 157 nm. 4-Oxatricyclononenes are valuable comonomers for the elevation of glass transition temperatures in ROMP polymers, while low molecular weight ROMP copolymers of 3-oxatricyclonene are being evaluated as crosslinking agents in negative tone resist formulations.

Chapter 6 details the use of cross-metathesis and ring-opening cross-metathesis in the synthesis of multifunctional monomers and oligomers for 193 nm immersion and 157 nm lithography. Cross-metathesis with unsaturated hexafluorocarbinols is a facile method to generate functionalized olefins without using toxic hexafluoroacetone gas. In certain instances, cross-metathesis reactions with these acidic alcohols were shown to proceed with unusual stereoselectivity. While investigating the nature of this stereoselectivity, simple carboxylic acids were found to eliminate problematic ruthenium-catalyzed olefin migration in specific substrates. These developments culminate in the synthesis of difunctional norbornenes containing both ester and hexafluorocarbinol functionalities. These ester-containing structures display dramatically increased transparency at 157 nm and will potentially afford unique dissolution behavior.

Finally, chapter 7 explores the synthesis of trisubstituted olefins via ruthenium-catalyzed cross-metathesis. Mechanistic investigations into the reaction pathways of isobutylene cross-metathesis revealed 2-methyl-2-butene to be a convenient isobutylene surrogate in the formation of prenyl groups via cross-metathesis. With less reactive olefins, a mechanistic reversal occurs which affords only 1,2-disubstituted products. Understanding of the reactivity of second-generation metathesis catalysts with 1,1-disubstituted and trisubstituted olefins has prompted the exploration of ring-opening cross-metathesis of low strain cyclic olefins and three component cross-metathesis reactions with high product selectivity.

TABLE OF CONTENTS

LIST OF FIGURES

Chapter 1

Chapter 3

Chapter 4

Chapter 5

Chapter 6

LIST OF TABLES

Chapter 6

Chapter 7

CHAPTER 1

Opportunities and Challenges for Transition Metal Catalysis in the Development of Materials for Deep Ultraviolet Lithography

Opportunities and Challenges for Transition Metal Catalysis in the Development of Materials for Deep Ultraviolet Lithography

Introduction and Historical Perspective

The last quarter of the 20th Century saw the rapid development and wide availability of powerful and reasonably priced microelectronics revolutionize nearly every aspect of our society from communications and science to shopping and entertainment. This rapid increase in affordable microprocessor power is directly attributable to the ability of the semiconductor industry to double the number of integrated circuit elements on the microprocessor roughly every 18 months, as described by Moore's Law.[1] This progress is driven by the associated cost advantages of producing more chips per wafer (2x more chips per wafer, 0.5x cost per chip). Advances in the science and engineering of lithography are critical to the continuation of this process.[2] At the forefront of these advances is the development of new imaging materials.

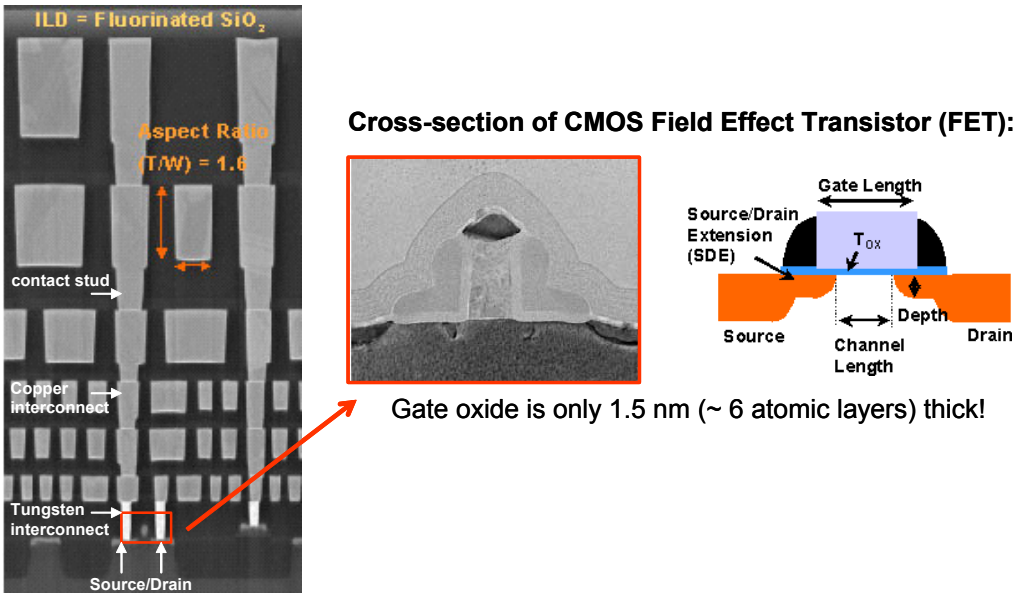

Figure 1.1. Cross-section of Intel Pentium® 4 (0.130 μm architecture)[3]

A cross-section of a commercially available computer chip (Intel Pentium® 4) based on 130 nm technology is shown in Figure 1.1.[3] The Pentium® 4 features 77 million transistors, 60 nm gate lengths, and 6 layers of copper interconnects. These complicated structures are built up layer-by-layer through a several hundred step production process that involves many iterations of lithography. While the pitch of the interconnects (1.2 mm at the top level, 350 nm at the first metal level) can be achieved using older generations of lithography, the wafer-level features require the highest level of resolution and the latest generation of lithography.

At the time the work presented in this thesis began (early 2000), 248 nm lithography was the current state of the art production lithographic technique, 193 nm lithography was moving into optimization and process evaluation, and early research into 157 nm lithography and related imaging materials had just begun. In 1999, the International Technology Roadmap for Semiconductors (ITRS)[4] put forth by the *International SEMATECH* detailed the timeline for possible lithographic solutions as shown in Table 1.1.

Table 1.1. 1999 ITRS Roadmap[4]

Year	1999	2002	2005	2008	20011
Feature Size	180 nm	130 nm	100 nm	70 nm	50 nm
Exposure Wavelength	248 nm	248 nm/193 nm	193 nm/**157 nm**	**157nm**/NGL	NGL
Radiation Source/Laser	KrF	KrF/ArF	ArF/**F_2**	**F_2**/EUV/EPL	EUV/EPL

While resist materials for 248 nm lithography had taken roughly 20 years to progress from initial discovery to final production quality performance and 193 nm resists had been under development for roughly 10 years, only five years remained for resist development before 157 nm lithography was expected to be introduced. The focus of this work as part of the *International SEMATECH* Universities Research Project (LITJ 102) was the development of advanced resist materials for 157 nm lithography. Although 157 nm lithography is no longer the lead candidate

to succeed 193 nm lithography as this is being written (late 2004) due to the rise to prominence of 193 nm immersion lithography,[5] the lessons learned in this pursuit have not been in vain. Many of the material advancements achieved in the quest for 157 nm resist materials are currently being applied to the development of advanced resist materials for 193 nm immersion and next generation lithographies (NGLs) and are being back-integrated into production 193 nm resists. If 157 nm lithography resurfaces as an immersion technique in the future, many of the developments described in this work will be directly applicable.[5a,e]

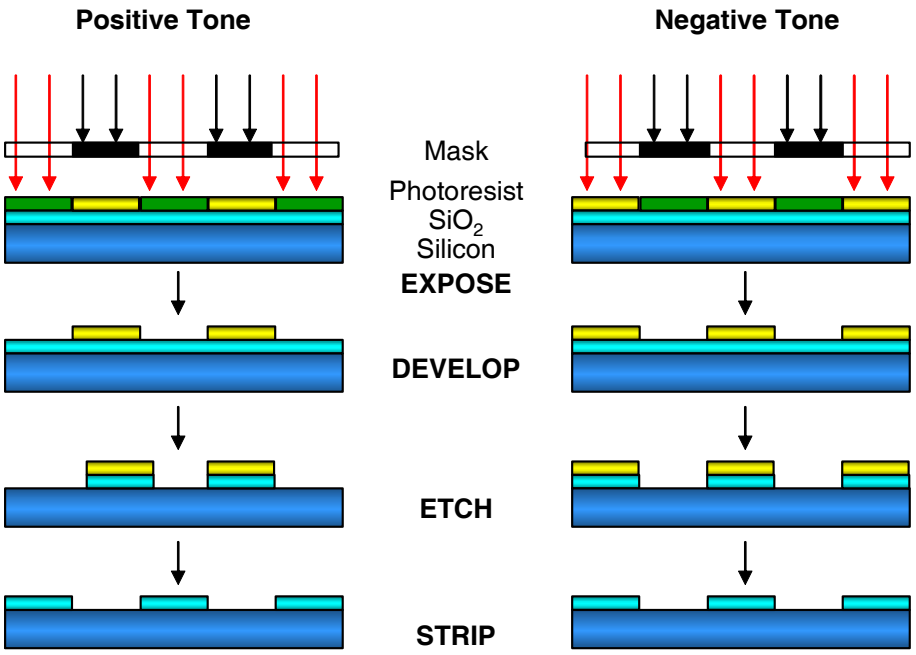

Figure 1.2. Photolithographic process

Introduction to Photoresists and Photolithography

Before the development of 157 nm resist material can be discussed, it is useful to review a brief description of photoresists and photolithography in order to understand the valuable resist design lessons learned during development of previous generations of lithographic materials. Optical lithography uses light to generate a pattern in a photosensitive polymer (photoresist) with subsequent transfer of that pattern onto the underlying substrate, as shown in Figure 1.2.[2] First, a

layer of photoresist is deposited onto a substrate via spin casting from a suitable solvent. Pattern formation is induced via illumination by a high-power laser light source through a complex series of optics involving a photomask. The interaction of the irradiating photons with the photosensitive elements in the photoresist leads to changes in the physical or chemical properties of the photoresist such as solubility, thermo-oxidative stability, molecular weight, etc. A dramatic change in solubility is the most commonly used approach, allowing the polymer in either the exposed (positive resist) or in the unexposed (negative resist) region to be washed away with an appropriate developing solvent. With the remaining photoresist acting as a protective layer, processes such as reactive ion etching (RIE) can be performed. Stripping of the remaining photoresist enables other post-lithography processes such as doping or dielectric deposition to be performed. In this fashion, IC devices are built layer-by-layer.

Ultimately, advances in lithography are governed by the physics of the optics. The resolution or feature size is governed by the "lens equation"

$$\text{Critical Dimension (resolution)} = k_1 \frac{\lambda}{\text{NA}},$$

k_1 is a process factor, λ is the wavelength of the light, and NA is the numerical aperture of the optics.[2] Unfortunately, the use of high power reduction optics (high numerical aperture) to minimize feature size results in a loss in depth of focus[2]

$$\text{Depth of Focus} \propto \frac{\lambda}{\text{NA}^2}.$$

Eventually, after optimization of exposure optics and process parameters, a shift to a shorter wavelength of light is required to achieve further reductions in feature sizes.

Photoresist Systems Photoresist systems are a complex mixture of matrix polymers, dissolution inhibitors, photoacid or photobase generators, buffers, and other additives.[2,6] Hereafter, the matrix polymers will be referred to as photoresists, although these polymers by themselves may not be photoactive. Positive tone photoresist polymers generally consist of units

selected to offer etch resistance, adhesion to the substrate of interest, and some form of solubility switch as shown in Figure 1.3.[7]

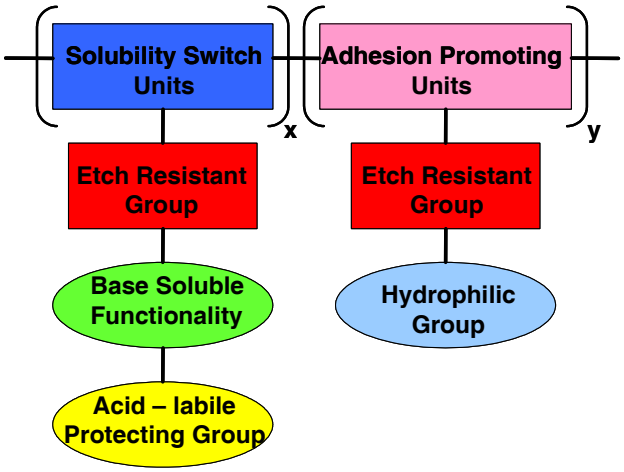

Figure 1.3. Design of a positive tone photoresist

Process	Required Photoresist Properties
Spin Casting	Solubility in suitable casting solvents Reasonable viscosity Good adhesion to wafer surface Phase compatibility with additives, photoacid generators...etc.
Post-application Bake	Thermal stability above T_g and b.p. of casting solvent
Exposure	Low absorbance at wavelength of irradiation ($\alpha_{10} < 0.7\ \mu m^{-1}$) High sensitivity of photoactive species Minimal outgassing of volatiles
Post -exposure Bake	Thermal stability above T_g to allow acid diffusion ($T_g > 120\ ^oC$) Rapid chemical reactions (low activation energies) (< 60 s, 120 - 140 ^oC) Minimal side reactions
Development	High contrast Good solubility in developer (0.262 N tetramethylammonium hydroxide) Rapid dissolution Low line edge roughness (M_n < 10,000 Da) Good mechanical properties to resist pattern collapse
Etching	Good etch resistance - Similar to APEX (High carbon/hydrogen ratio) - Ohnishi parater < 3 (Low structural oxygen content)
General Considerations	Synthesis via simple, rapid, inexpensive, tolerant polymerization Low residual metal contamination (< 20 ppb) Inexpensive, readily available, non-toxic materials

Figure 1.4. Material property requirements of a positive tone photoresist

The design of photoresist polymers is controlled by the large number of property requirements, some of which are outlined in Figure 1.4.[6] Selection of appropriate structures to fill the roles described in Figure 1.3 involves a complicated balance of trade-offs. For example, the etch rate of a polymer has been empirically modeled by Ohnishi *et al.* as

$$\text{Etch Rate} \propto \frac{N_{atoms}}{N_{carbons} - N_{oxygens}},$$

where N_{atoms}, $N_{carbons}$, and $N_{oxygens}$ are the numbers of atoms, carbons, and oxygens, respectively, in a repeat unit.[8] Etch resistance is enhanced by increasing the relative carbon content of the polymer; however, most hydrophilic and base-soluble groups contain large amounts of structural oxygen which decreases etch resistance.

Chemically Amplified Photoresists for 248 nm Lithography For years, above wavelength imaging had been accomplished using diazonaphthoquinone-based novolac resists.[2,6] Upon exposure to light, the diazonaphthoquinone is transformed via a Wolff rearrangement to an indene carboxylic acid. While the novolac matrix resin is insoluble in aqueous base in the presence of the diazonaphthoquinone, it becomes highly soluble in the presence of the carboxylic acid. Unfortunately, this dissolution inhibition approach does not possess high enough quantum efficiency for use with the less powerful laser light sources used in deep ultraviolet (≤ 248 nm) lithography.

In order to increase the quantum efficiency of the solubility switching reactions, a catalytic deprotection route was developed by Ito and Willson (Figure 1.5).[9] This "chemically amplified" technique relies on the ability of a single photogenerated acid to deprotect as many as 100-200 latent base-soluble groups in a few seconds during a post-exposure bake. The most successful 248 nm photoresists are based on protected polyhydroxystyrene (PHOST) or N-blocked maleimide/styrene copolymers and feature large amounts of aromatic structures for high etch resistance (Figure 1.6).[2,6,9] However, early chemically amplified resists showed extreme sensitivity to trace (< ppm) quantities of basic atmospheric compounds (primarily amine-based

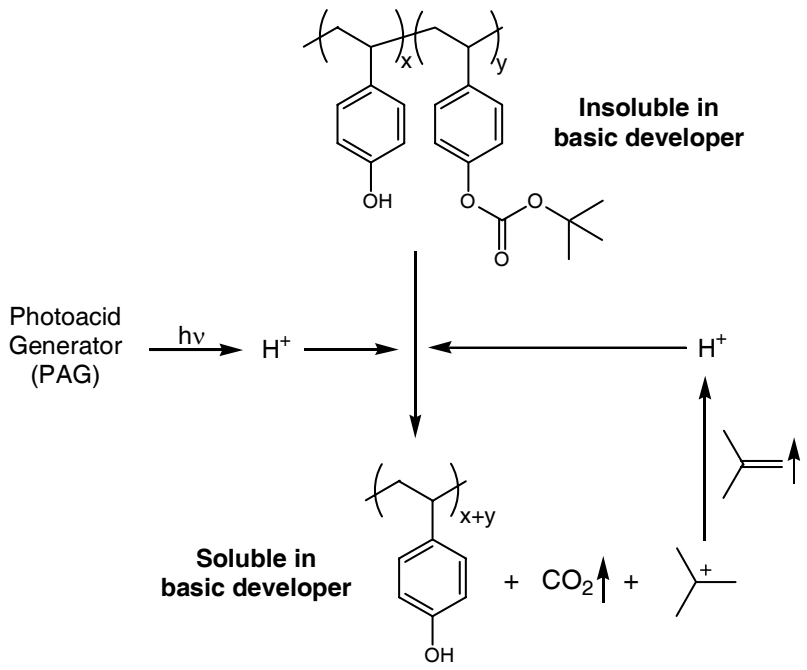

Figure 1.5. Chemical amplification

solvents used in paint and building materials). These airborne contaminants can penetrate the surface of the resist on the exposed wafer and quench the photogenerated acid, resulting in the production of an insoluble scum layer on the surface (T-topping). Environmentally stable, chemically amplified (ESCAP) resists were developed which incorporate a comonomer (such as *t*-butyl acrylate) which lowers the glass transition temperature (T_g) of the polymer below the

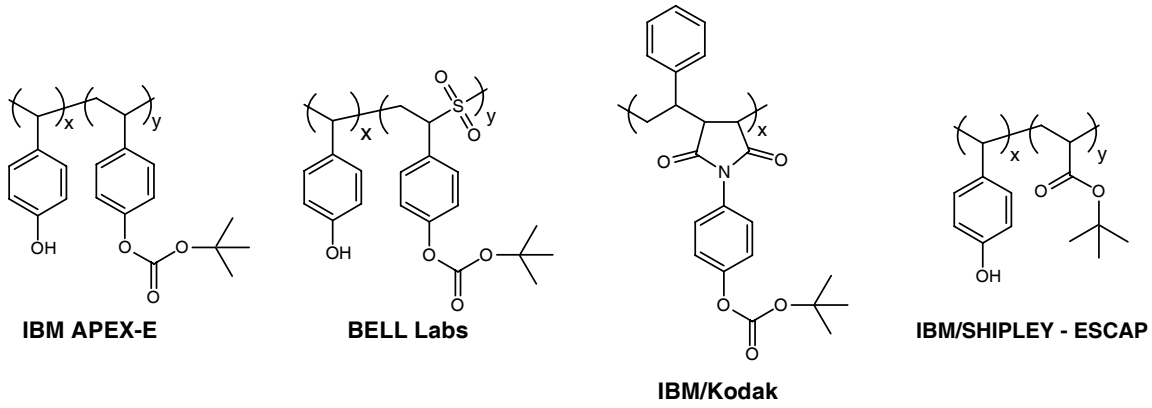

Figure 1.6. Commercially available 248 nm photoresists

thermal deprotection temperature.[9] Annealing the resists above their T_g results in reduction of free-volume which decreases the rate of sorption and diffusion of atmospheric contaminants.

Remarkably, these resist materials experience a very large solubility change over a relatively narrow range of deprotection (Figure 1.7). Consequently, the ability of a small number of deprotection reactions to induce a step-like large solubility change is responsible for the high sensitivity and high contrast of chemically amplified resists. Namely, it allows these materials to efficiently produce step-type profiles rather than simply mirror the sinusoidal optical intensity profiles experienced during exposure.

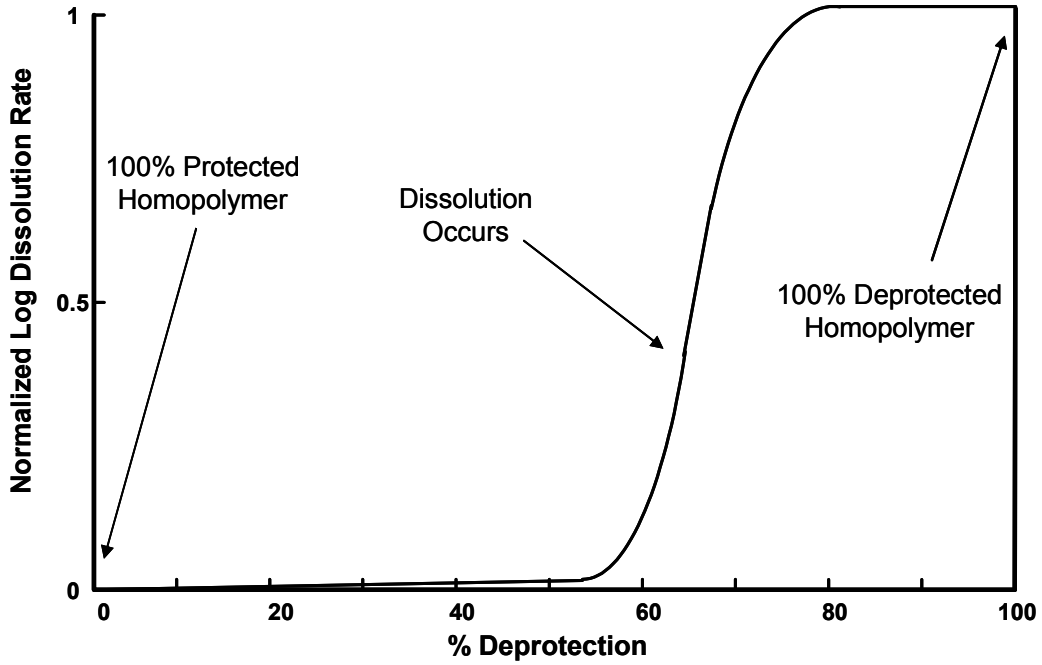

Figure 1.7. Dissolution rate as a function of deprotection for a model photoresist

193 nm Photoresists Unfortunately, the aromatic groups used to impart high etch resistance to 248 nm resists absorb too heavily for them to be useful at 193 nm.[10] With heavily absorbing materials, the light intensity falls quickly as a function of depth into the material, resulting in muted features rather than the sharp, step-type profiles required. Fortunately, carbon-rich alicyclic structures were found to serve as suitable etch-resistant replacements for the highly

absorbing aromatic structures used in previous generations of lithography.[10] A number of 193 nm resist platforms are under commercial development (Figure 1.8). Highly transparent acrylate and methacrylate polymers have been functionalized with alicyclic pendant groups (i.e., adamantyl and tricyclodecyl) to impart greater etch resistance to the oxygen-rich backbone.[11] Alternatively, functionalized norbornenes and tetracyclododecenes have been copolymerized with maleic anhydride via free radical techniques.[12] The anhydride group provides for excellent adhesion and serves as a latent water solubilizing group. Another leading class of commercial 193 nm photoresists in development is based on hybrid poly(methacrylate)-*co*-(norbornene-*alt*-maleic anhydride) copolymers.[10]

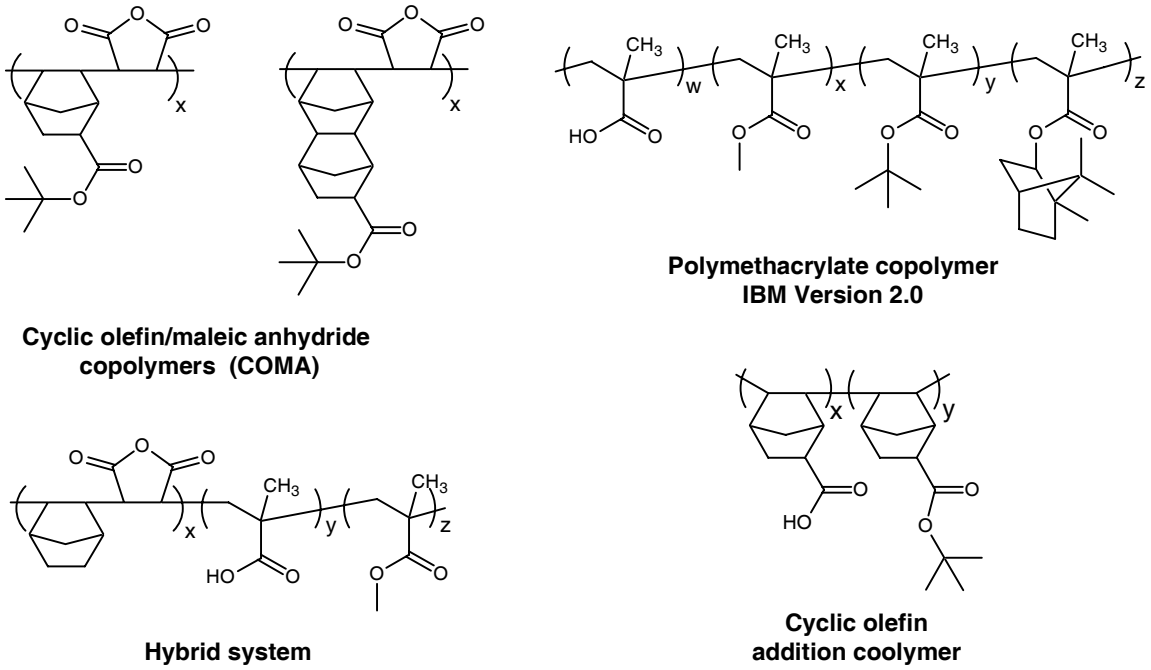

Figure 1.8. 193 nm photoresist polymers under development

Other groups have investigated metal-catalyzed polymerization of alicyclic monomers such as functionalized norbornenes and tetracyclododecenes.[13] Unable to radically homopolymerize efficiently,[14] norbornene-type monomers can be polymerized by transition metal catalysts to produce ring-opening metathesis (ROMP) or addition polymers. While a significant

amount of effort was expended exploring these polymers, the prospect of residual metal contamination has reduced the overall attractiveness of these materials.[10]

157 nm Materials Development

157 nm vacuum-ultraviolet (VUV) lithography initially appeared to be the most likely candidate for production of 100 nm structures around 2005.[4] The ability to continue to utilize the tremendous amount of physical and intellectual capital invested in optical lithography was a reassuring a prospect relative to the more risky option of adopting entirely new (and extremely expensive) next generation lithography (NGL) techniques such as extreme ultraviolet (13 nm, EUV), x-ray, and projection e-beam (SCALPEL, PREVAIL) lithography. While the development of a suitable illumination source (F_2 excimer laser, 157.6 nm) was achieved early on, it was the development and availability of the calcium fluoride optics which ultimately proved to be the stumbling block towards implementation.[15]

Early on, it appeared the chief optical problems were readily solvable; however, since O_2, water, and most polymers absorb heavily at 157 nm,[16,17] the development of high transparency photoresists was considered to be the primary challenge facing 157 nm photolithography. Since carbon 2p ground state electrons are primarily responsible for absorption at 157 nm, carbon-carbon double bonds (olefins, aromatics), carbon-oxygen double bonds (aldehydes, ketones, esters), and even to some extent, carbon-hydrogen single bonds (hydrocarbons) are all unsuitable for use in 157 nm photoresists.[16]

These results are reflected in the measured absorption coefficients of a variety of common polymers and photoresists shown in Table 1.2.[16] Due to their high absorbance at 157 nm, the use of the traditional photoresists used for 248 nm and 193 nm would require extremely thin films (30 - 50 nm) which would result in unacceptable levels of pinhole defects. In order for practical resist thicknesses (> 250 nm) to be employed, resist materials with an absorption coefficient less than 0.70 μm^{-1} is required. Silsesquioxanes and fluorocarbons are two classes of

Table 1.2. Necessary film thicknesses of common polymers and photoresists

Polymer	α_{10} [μm^{-1}]	Resist Thickness (optical density = 0.185) [nm]
Poly(hydrosilsesquioxane)	0.06[a]	3083
Perfluoropolymer	0.70[a]	264
Poly(norbornene-co-tetrafluoroethylene) (1:1)	1.10[b]	168
Poly(dimethylsiloxane)	1.61[a]	115
Poly(methyl trifluoromethacrylate)	2.68[c]	69
Poly(phenylsiloxane)	2.68[a]	69
Poly(vinyl alcohol))	4.16[a]	44
Poly(methyl methacrylate)	5.42[c]	34
Poly(norbornene) (addition)	6.10[a]	30
Polystyrene	6.20[a]	30
Poly(p-hydroxystyrene)	6.25[a]	30
Poly(norbornene) (ROMP)	6.80[a]	27
Sumitomo PAR-101	6.84[c]	27
Shipley UV6-2D	6.85[c]	27
IBM V1.0 acrylic terpolymer	8.20[a]	23
Poly(chlorostyrene)	10.15[a]	18
Poly(acrylic acid)	11.00[a]	16

[a] Data from ref. 16. [b] Data from ref. 29b. [c] Data from ref. 24a.

structures initially appearing to have sufficient transparency at 157 nm. However, while silicon-oxygen bonds are transparent at 157 nm, silicon-carbon bonds are only moderately transparent, complicating the development of resist materials. Additionally, the extremely large photon energy of 157 nm (~182 kcal/mol) results in significant amounts of homolytic bond cleavage of relatively weak chemical bonds such as carbon-chlorine and carbon-bromine bonds.[18]

The ability of moderate amounts of fluorine to greatly increase 157 nm transparency combined with the high stability of the carbon-fluorine bond led most research labs to initially explore hydrofluorocarbon materials for 157 nm resists. While synthesis of fluorinated polymers is not trivial in itself, synthesis of a heavily fluorinated photoresist capable of dissolving in an aqueous base developer is an even more daunting challenge. Since all common polar groups used for solubility switching (*t*-butyl esters, *t*-boc, etc.) and adhesion (carboxylic anhydrides, alcohols, carboxylic acids) in traditional photoresist are heavily absorbing at 157 nm, the development of a polar, base soluble functionality suitable for 157 nm was the most pressing priority. The

phenolics and carboxylic acids characteristic of 248 nm and 193 nm resists owe their acidity to the resonance stabilization of their conjugate bases; however, the π-bonds responsible for this stabilization are too absorbing for use at 157 nm. Alternatively, fluorinated alcohols exhibit enhanced acidities relative to non-fluorinated aliphatic alcohols due to the inductive stabilization of the conjugate base. As shown in Table 1.3, the presence of fluorine substituents is sufficient to afford a pKa comparable to the phenolic groups employed in 248 nm resists.[19] Fortunately, hexafluorocarbinols such as hexafluoroisopropanol are also highly transparent at 157 nm (Figure 1.9).[20] This discovery was particularly promising since the use of hexafluoroisopropyl alcohol groups had been investigated for use in 248 nm and 193 nm resists.[21]

Table 1.3. Acidity of fluorinated alcohols[19]

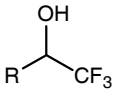

Acid	pKa
Water	18.3
R = H	14.5
Phenol	**11.8**
R = CF_3	**11.2**
Acetic acid	6.3
Pentafluorophenol	6.0

In 60/40 vol% DMSO/H_2O, 25 °C
Ionic strength 0.30 M (KCl)

In a search for chemical species that exhibit high transparency, several groups have used high level time-dependent density functional theory (TD-DFT) calculations to simulate the absorbance of simple chemical compounds at 157 nm.[22,23] However, an empirical correction of the calculated transition energies is required for good agreement with experimentally measured vacuum-UV (VUV) spectra.[22] Nevertheless, early computational results indicated that the absorption of esters could be dramatically decreased thru the addition of fluorinated substituents. The incorporation of fluorinated groups on the alkoxy portion of the ester results in a blue-shifting of the absorption band, while the addition of fluorinated substituents alpha to the ester

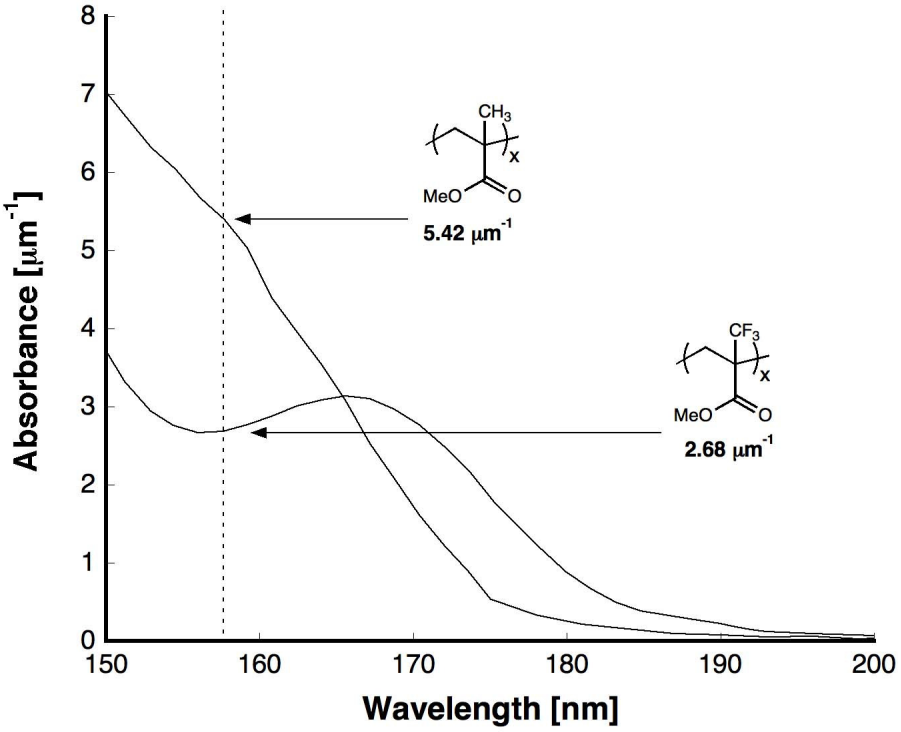

Figure 1.9. Effect of fluorination on transparency of polymethylmethacrylate[24]

opens a window of transparency at 157 nm by red-shifting the absorption band.[22] While a number of experimental VUV studies on model esters confirmed that ester transparency was increased with the incorporation of fluorinated substituents,[24] this is perhaps most dramatically illustrated by comparing the transparencies of poly(methyl methacrylate) and its fluorinated analogue[25] as measured by variable angle scanning ellipsometry (VASE)[26] (Figure 1.9).

With the discovery of a number of suitable polar groups, a number of photoresists based on fluorinated methacrylates,[27] fluorinated alcohols,[28] and hexafluorocarbinol-functionalized norbornene[29] were developed. However, the absorbance of these initial resist platforms, while being considerably more transparent than commercialized 248 nm and 193 nm resists, was still unacceptably high (~ 2-3.5 μm^{-1})[24a] (Figure 1.10). The transparency of these 157 nm resists was a far cry from the transparency of successful 248 nm and 193 nm resists at their respective wavelengths as shown in Table 1.4.

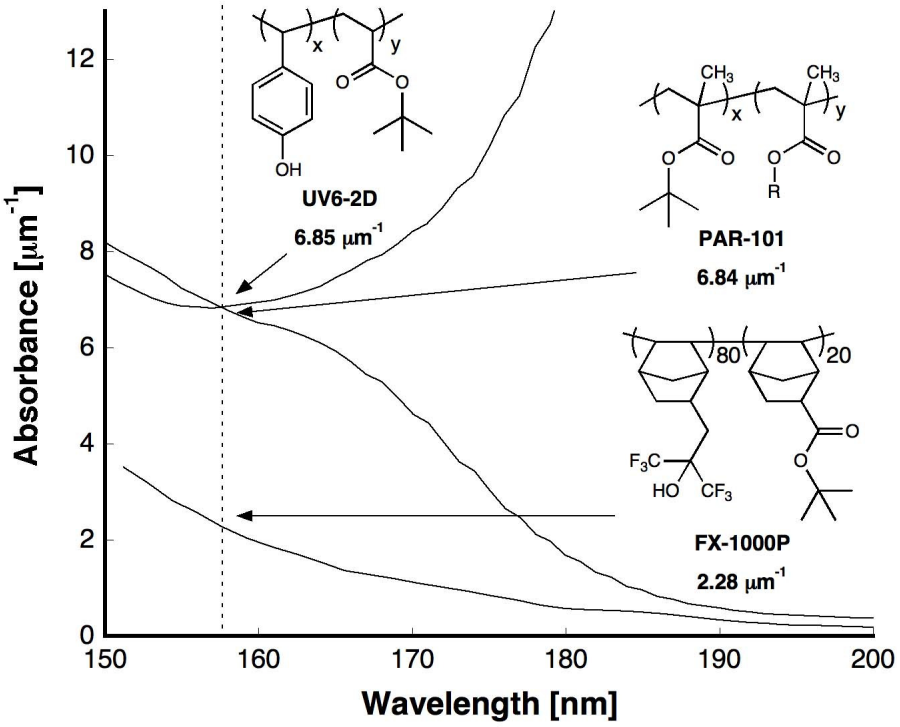

Figure 1.10. Comparison of initial 157 nm resist with previous generations (Structures shown for UV6-2D and PAR-101 only denote general class of resist)[24a]

Table 1.4. Performance comparison of three generations of photoresists[24a]

Resist	157 nm	193 nm	248 nm
UV6-2D (Shipley)	6.85	24.94	***0.37***
PAR-101 (Sumitomo)	6.84	***0.47***	0.06
FX-1000P (AZ-Clariant)	***2.28***	0.26	0.04

In order to increase the transparency of resist materials for 157 nm lithography, the incorporation of additional fluorine into the polymer backbone was required. Three distinct approaches emerged from the research community as shown in Figure 1.11. The metal-catalyzed norbornene addition polymer platform[29] was the first to be commercialized and offers high etch resistance (due to its purely alicyclic backbone), but suffers from relatively poor transparency. A series of radically polymerized aliphatic cyclopolymers[30] emerged which exhibit outstanding

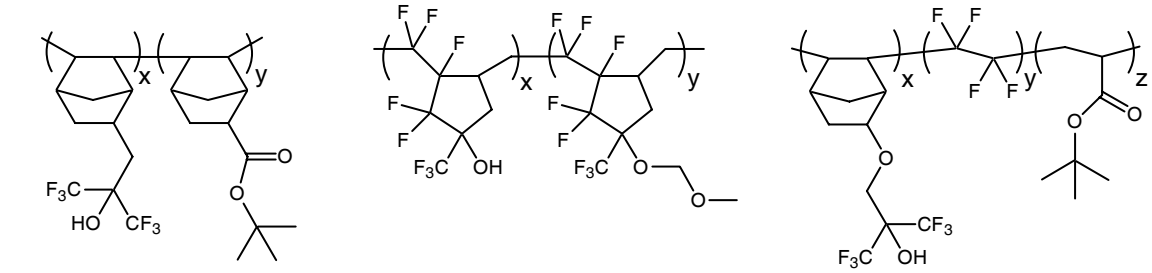

Figure 1.11. Three 157 nm photoresist platforms under development

transparency at 157nm (~0.5 – 0.7 μm^{-1}); however, they offer lower resistance to etch processes. Free-radical copolymers of functionalized norbornenes with tetrafluoroethylene[31] offer a good balance of transparency and etch resistance, while avoiding the issue of residual metal contamination.

Challenges and Opportunities for Metal Catalysis in Resist Development

While norbornene-type monomers do not undergo efficient radical homopolymerization, they can be copolymerized with electron deficient olefins such as maleic anhydride or tetrafluoroethylene to produce alternating copolymers described previously. Cationic polymerization of norbornenes is also inefficient and similarly results in polymers with 2,7-linkages rather than 2,3-linkages.[14] Transition metal catalysis offers two routes to the efficient homopolymerization of norbornenes and functionalized norbornenes.[13] Addition polymerization affords polynorbornenes with high glass transition temperatures (> 300 °C) due to the rigid backbone formed by 2,3-enchainment. Alternatively, ring-opening metathesis polymerization (ROMP) affords polymers with an unsaturated backbone and reduced glass transition temperatures. After hydrogenation, the ROMP polymers resemble the aliphatic cyclopolymer shown in Figure 1.11, but with 1,3-disubstitution of the cyclopentane structures rather than 1,2-disubstitution.

The focus of the work described in this dissertation is the improvement of the performance of metal-catalyzed addition and ring-opening metathesis polymers of norbornene via

the incorporation of additional fluorinated substituents and the resolution of the metal-catalyzed polymerization issues associated with these modifications.

Metal-catalyzed Addition Polymerization

The presence of much polar functionality in resist materials requires a great deal of functional group tolerance by the metal catalyst. A large number of neutral nickel[32] and cationic palladium[33,34,35] catalysts have been developed for the addition polymerization of functionalized norbornenes, a few of which are shown in Figure 1.12. Cationic palladium catalysts such as the (π-allyl) palladium catalysts developed by Risse *et al.* have been heavily studied in the literature.[34] The mechanism of norbornene polymerization for this catalyst is shown in Figure 1.13.[36] The active catalyst is formed via anion exchange of the chloride for a less coordinating anionic ligand. Norbornene displaces solvent and binds to the catalyst from its exo-face prior to insertion into the allyl palladium bond. The resulting allyl group forms a chelated intermediate which is a stable resting state for the catalyst. The dissociation/displacement of this chelated group by another norbornene monomer and subsequent norbornene insertion appears to be the rate limiting initiation step.[36] Subsequent polymerization is extremely rapid, with complete

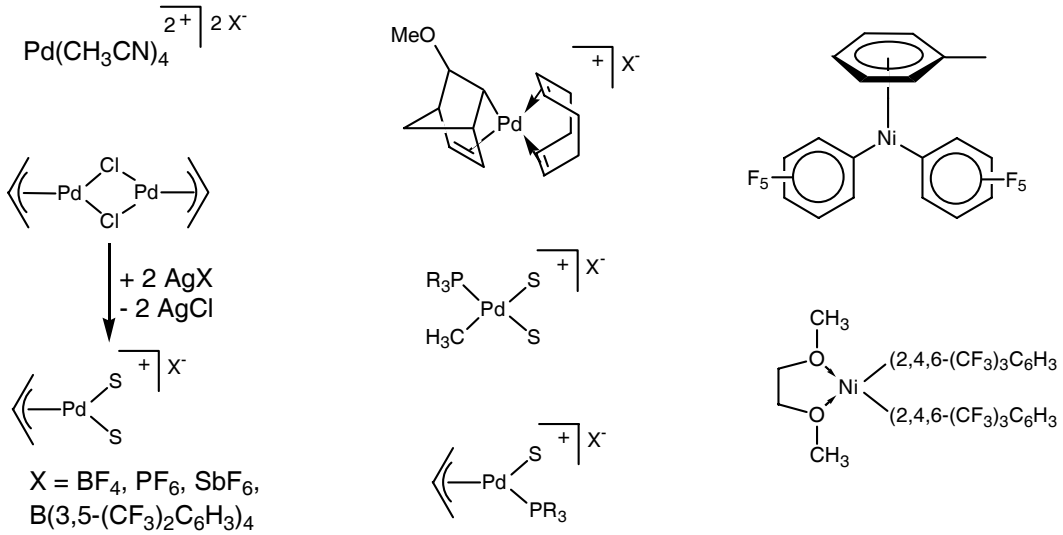

Figure 1.12. Common nickel and palladium addition catalysts

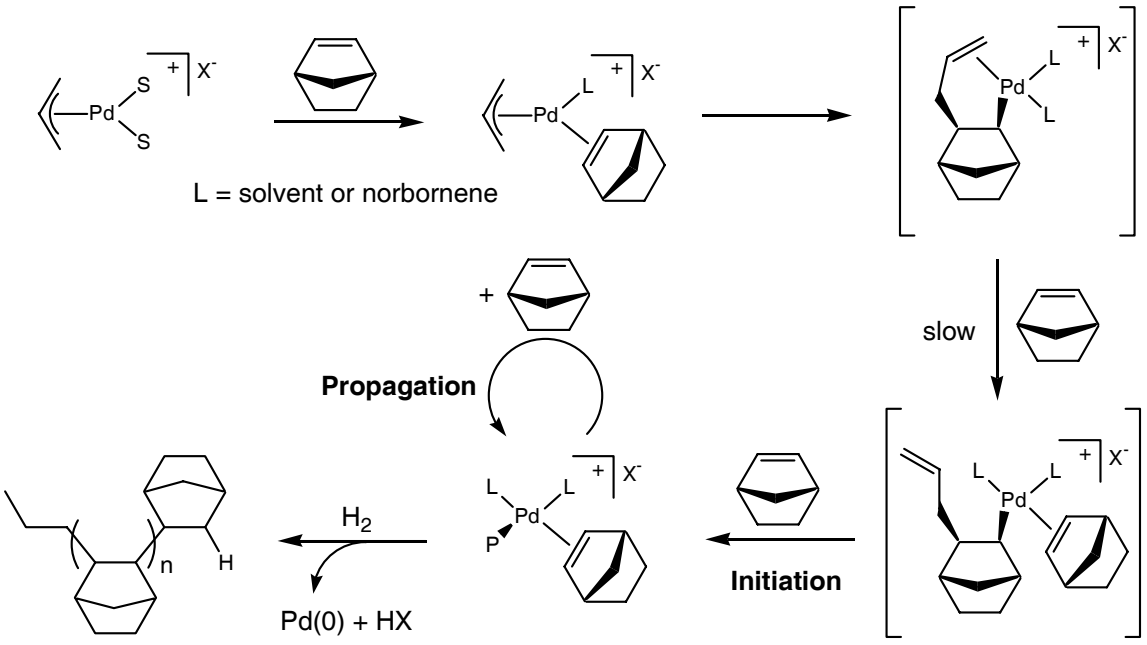

Figure 1.13. Mechanism of metal-catalyzed addition polymerization of norbornene

consumption of monomer within seconds. Polymerization of norbornene to high molecular weights is enabled by the absence of accessible β-hydrogens on the rigid alicyclic structure. The addition of small amounts of α-olefins provides for the β-hydrogens necessary for β-hydride elimination.[32-33] This approach has been used to control the molecular weight of addition polymers; however, the resultant unstable palladium hydride often decomposes to palladium(0) rather than reinitiate another chain. Alternatively, dihydrogen can be used to remove the catalyst from the end of the polymer chain.

The presence of polar substituents on the norbornene typically results in a dramatic reduction in the rate of polymerization.[34] In addition, the rate of polymerization is highly dependent upon the exo/endo configuration of the substituent group on the norbornene, with endo isomers polymerizing significantly more slowly.[37] Unfortunately, the endo isomer is commonly the major product of the Diels-Alder synthesis of functionalized norbornenes.[38] The large difference in the rates of polymerization between *exo*- and *endo*-*n*-butyl-2-norbornene has been attributed to the steric compression of the vinyl hydrogen with the endo-functionality as it is

rehybridized from sp^2 to sp^3 during insertion.[37] For functionalized norbornenes, the chelation of the catalyst by the polar functional group to the endo-face of the norbornene was speculated to be also responsible for the reduction in polymerization rate. Geminally disubstituted norbornenes like the one shown in Figure 1.14 polymerize ~10 times slower despite the predominant exo-configuration of the ester group.[39] Subsequent work by Sen *et al.* has shown that the predominant rate decelerating interaction is the simple binding of the polar functional group to the cationic metal center.[37b] As a result of their theoretical calculations, Ziegler *et al.* proposed that neutral catalysts offer potentially superior performance due to their reduced preference for polar functional groups while retaining similar ability as cationic metal centers to bind olefins.[40] Recently, Sen *et al.* confirmed this by demonstrating the ability of a neutral palladium catalyst to polymerize exo and endo isomers of functionalized norbornenes at more similar rates; however, these catalysts currently have insufficient activity to be useful.[37a]

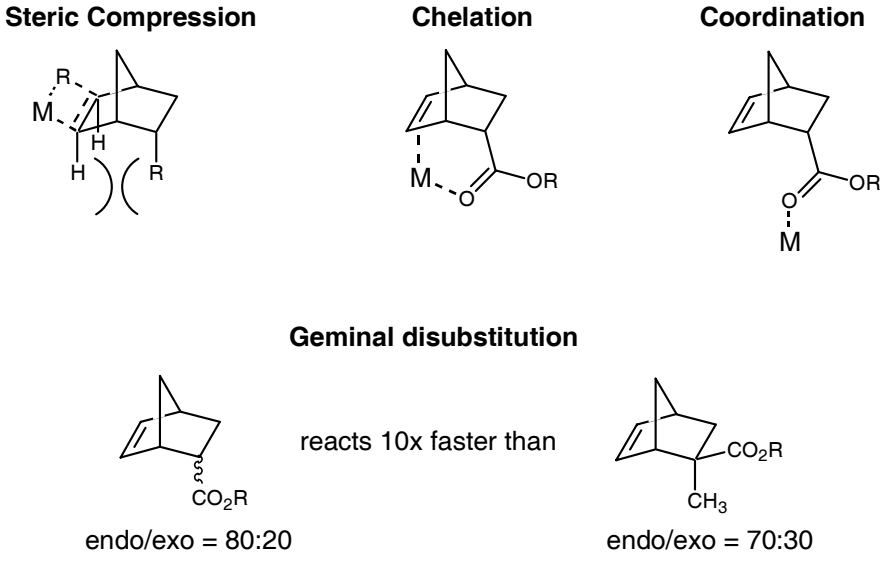

Figure 1.14. Issues in the polymerization of functionalized norbornenes

Design of Transparent Addition Polymers for 157 nm Photoresists In order to design fluorinated norbornenes with higher transparencies, careful attention must be paid to the effects of fluorine on the polymerization activities of the resulting monomers. For example,

fluorinated olefins have insufficient electron density to bind to metal centers and undergo polymerization. A number of partially fluorinated norbornanes have been synthesized and examined by vacuum ultraviolet spectroscopy by Willson *et al.* (Figure 1.15).[41] It can be seen that di-substitution is more effective at increasing transparency than mono-substitution, and substitution at the 2-position is more effective than substitution at the 7-position.

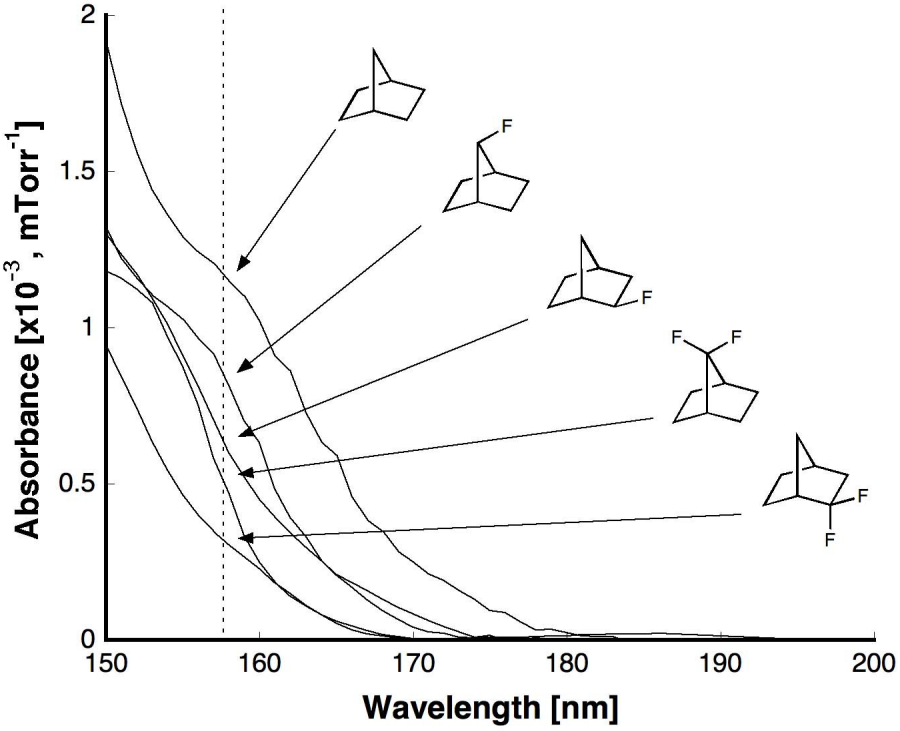

Figure 1.15. Effects of fluorination on norbornane transparency[41]

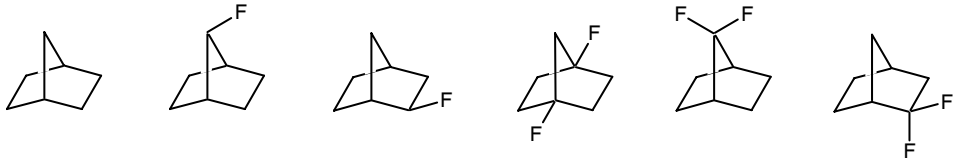

Itani *et al.*[42c]	100	-	-	30	14	12
Dixon *et al.*[42a/b]	100	61	52	52	29	25
Experimental[41]	100	76	58	-	48	29

Figure 1.16. Relative calculated absorbances of fluorinated norbornanes

While theoretical calculations of the vacuum ultraviolet spectra of a number of fluorinated norbornanes qualitatively agree with the experimental observations,[42] the calculated values tend to overestimate the relative transparency when compared to experimentally determined values, even with empirical corrections (Figure 1.16).

Alternatively, several other bicyclic olefin systems exist which have additional carbons where fluorinated substituents could be placed. Chief among these are bicyclo[2.2.2]oct-2-enes formed via the Diels-Alder reaction of 1,4-cyclohexadiene with electron deficient olefins. Unfortunately, bicyclo[2.2.2]oct-2-ene is unreactive towards metal-catalyzed addition polymerization.[43] This lack of reactivity is illustrated by the relative rates of dipolar cycloaddition shown in Table 1.5.[44,45] The low ring-strain of the [2.2.2] system (similar to that of cyclohexene) results in poor reactivity.[44] However, norbornene exhibits reactivities even greater

Table 1.5. Reactivities of cyclic and bicyclic olefins[44,45]

	Strain Energy (kcal/mol)	Relative Strain Energy (to saturated compound) (kcal/mol)	Relative rate of Dipolar Cycloaddition*
	15.8	**6.0**	**3000**
	25.2	9.0	
	10.3-11.7	**0.8-2.2**	**5**
	1.4	1.5	1
	5.9	-0.3	
		10.0*	2300
		8.9*	2300

* 2,4,6-trimethyl benzonitrile oxide, CCl_4, 25 °C[44]

than its ring strain would predict. The asymmetric distribution of the π-bond electron density from exo face of the olefin coupled with the low steric shielding of the exo face results in particularly high reactivity. Unlike norbornene, the methylene protons in bicyclo[2.2.2]oct-2-ene may also sterically hinder approach of a metal catalyst to the olefin. A few other highly strained bicyclic systems exist, but their synthesis is not trivial and unlikely to be successful on the scales required for application as photoresist materials. As a result, norbornene-type monomers are the only practical bicyclic olefins for use in resist material development.

Having determined the effect of fluorination on transparency, a second-generation addition polymer featuring was designed as shown in Figure 1.17. Since the absorbance of the ester-functionalized norbornane in the first-generation addition polymer is far greater than the more transparent hexafluorocarbinol-functionalized monomer, the effect of an additional trifluoromethyl group on the overall absorbance of the copolymer was expected to be dramatic.

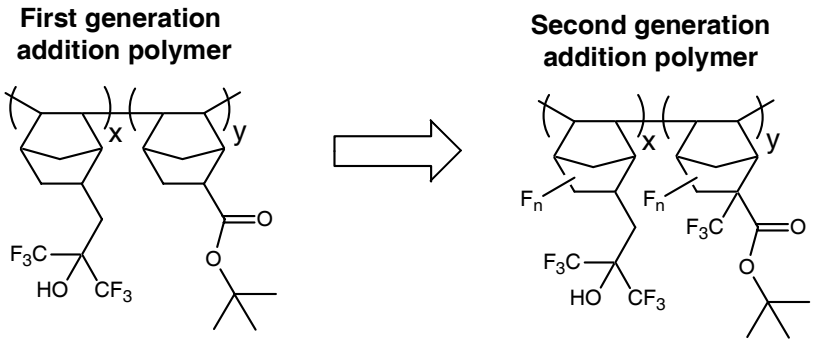

Figure 1.17. Design of transparent addition polymers for 157 nm lithography

The synthesis of an ester-functionalized norbornene from the 2-trifluoromethyl-acrylate proceeded smoothly and the saturated analogue exhibited improved transparency at 157 nm as expected (Figure 1.18).[24] Unfortunately, this monomer was found to be unreactive towards metal-catalyzed addition polymerization with both nickel and palladium catalysts.[29] Only trace amounts were incorporated with copolymerizations with the hexafluorocarbinol-functionalized

norbornene. The two heavily electron-withdrawing substituent groups reduce the polymerization activity by reducing the electron density of the norbornene via induction. When this inductive deactivation is coupled with the additional order of magnitude lower reactivity of norbornenes with geminal substituents, the result is a monomer with virtually no polymerization activity.

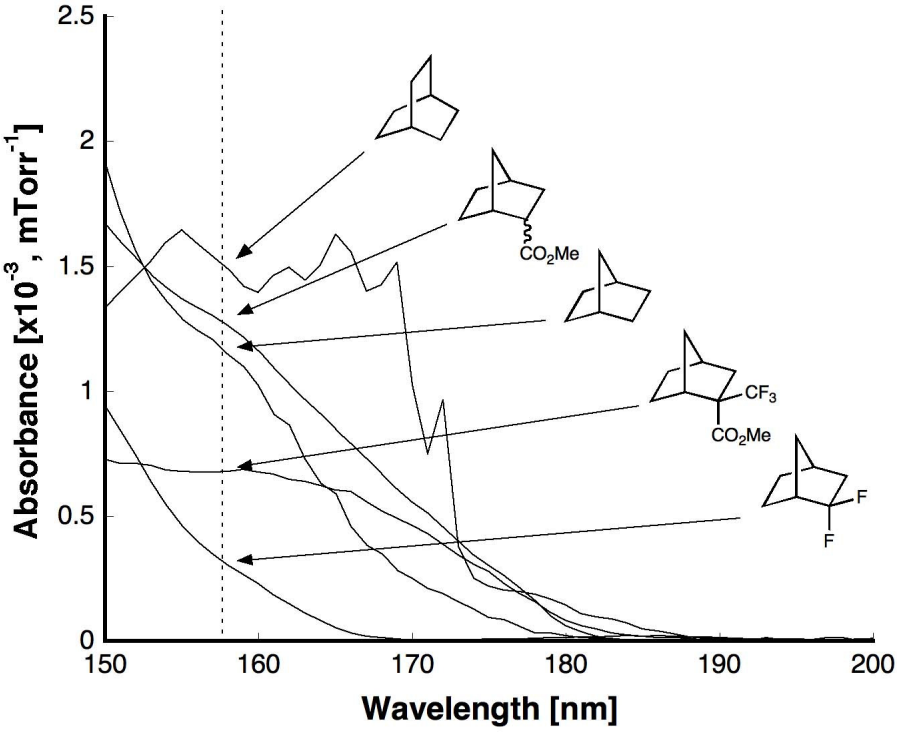

Figure 1.18. Transparency of fluorinated norbornanes for 157 nm photoresists[24]
(Poor spectrum of bicyclo[2.2.2]octane due to low volatility)

Synthesis of difluorinated versions of the hexafluorocarbinol-functionalized norbornane resulted in similarly discouraging results (Figure 1.19).[46] First, the structures exhibited *increased* absorbance relative to the base monomer. Secondly, the more fluorinated monomers were found to unreactive towards metal-catalyzed addition polymerization. The larger fluorine substitutent in the 7-syn position may sterically block or interact with the approaching catalyst and thereby prevent polymerization. However, the detrimental impact of additional fluorine incorporation at the 2-position was surprising. These efforts to produce norbornene addition polymers with

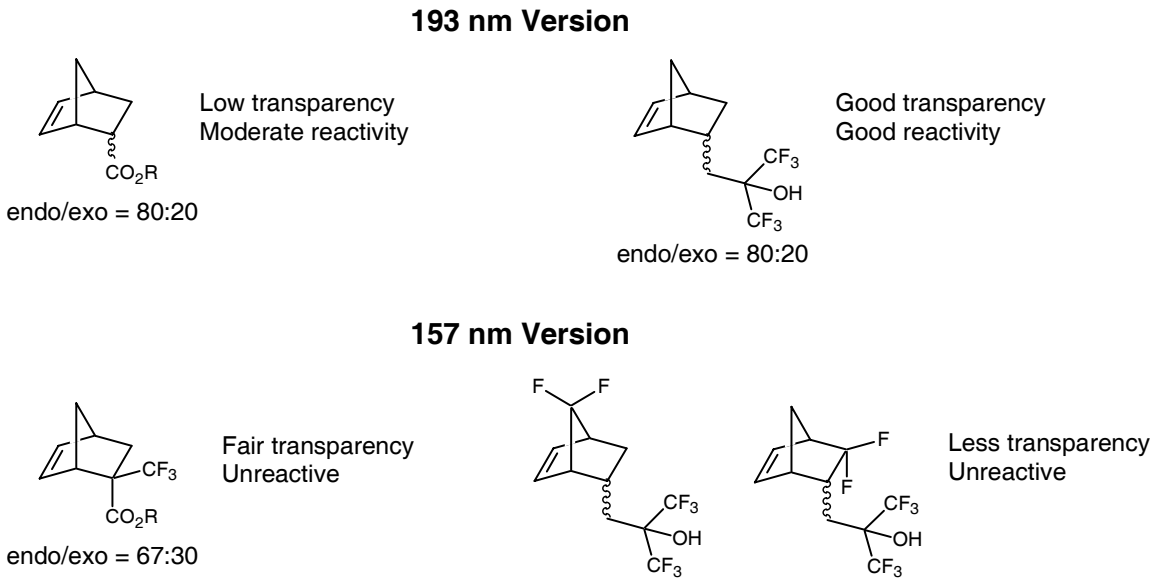

Figure 1.19. Detrimental effects of increased fluorination

enhanced transparency at 157 nm through the selective incorporation of additional fluorine are summarized in Figure 1.19. Two key lessons have been learned through these failures; geminal disubstitution must be avoided and the additional fluorine must be placed as far away from the reactive olefin as possible.

We hypothesized that the incorporation of additional cyclic units on the norbornene could provide a scaffold for additional fluorinated substituents while reducing the steric and electron interference with the subsequent polymerization. Chapters 2 and 3 of this thesis detail the synthesis and polymerization of new fluorinated tricyclo[4.2.1.$0^{2,5}$]non-7-enes, respectively. Similarly, chapters 4 and 5 describe the synthesis and polymerization of two new classes of alicyclic olefins, 3-oxa-tricyclo[4.2.1.$0^{2,5}$]non-7-enes and 4-oxa-tricyclo[4.3.$0^{1,6}$.$0^{3,7}$]non-8-enes. Finally, the synthesis of new, transparent difunctional monomers containing both hexafluorocarbinol and ester functionalities are described in Chapter 6. These new classes of monomers and materials illustrate potential highly transparent resist materials for 157 nm lithography.

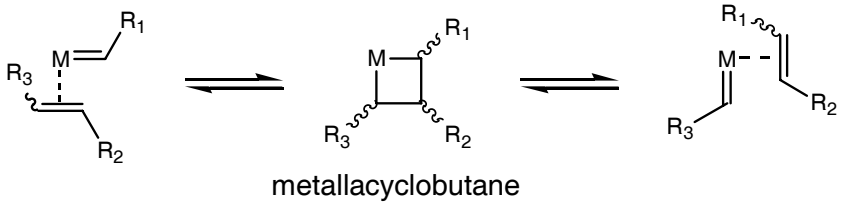

Figure 1.20. Olefin metathesis

Ruthenium-catalyzed Olefin Metathesis

Olefin metathesis involves the metal-carbene mediated cleavage and recombination of carbon-carbon double bonds as shown in Figure 1.20.[47] The process proceeds through the formation of a metallacyclobutane intermediate. When the reaction is used to α,ω-diene can undergo ring-closing metathesis (RCM)[49] to form a cyclic olefin if the resultant ring has low ring-strain (usually 5, 6, and 7-membered rings), as shown in Figure 1.21. Otherwise, the α,ω-diene may undergo acyclic diene metathesis (ADMET)[50] polymerization to form oligomeric and eventually polymeric materials in a step-growth process. However, the most facile route to polymeric material is the polymerization of strained cyclic olefins such as norbornene via chain-

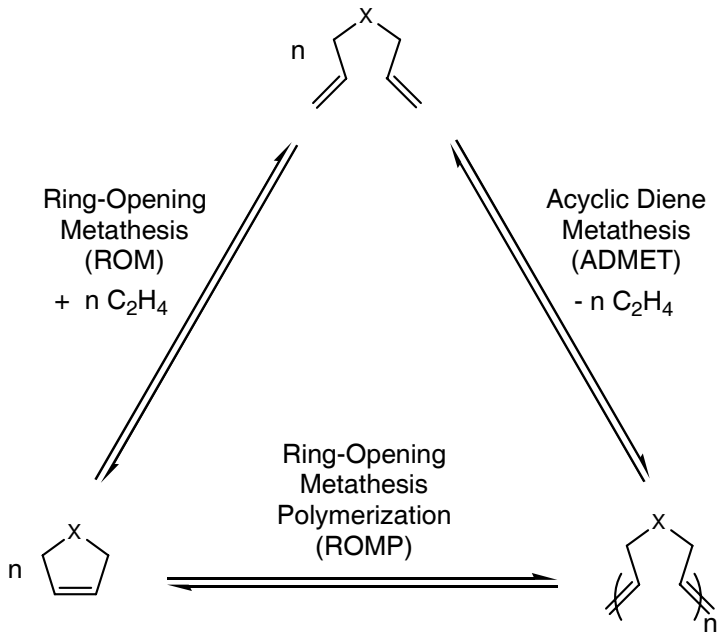

Figure 1.21. Olefin metathesis processes

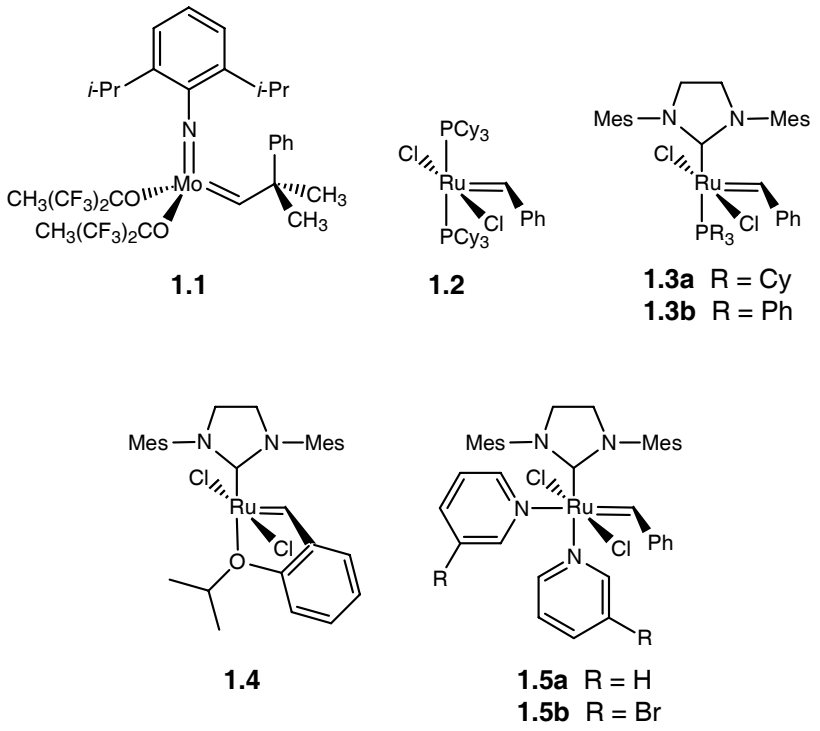

Figure 1.22. Olefin metathesis catalysts

growth ring-opening metathesis polymerization (ROMP).[51,52]

The use of olefin metathesis has mirrored the development of well-defined metal carbene olefin metathesis catalysts such as catalyst **1.1** (Figure 1.22).[53] However, early transition metal molybdenum and tungsten catalysts have limited abilities to tolerate polar functional groups (such as alcohols, ketones, and esters) and require rigorous purification and drying of reagents and reaction solvents.[54] Fortunately, a renaissance in olefin metathesis has occurred over the last 8 years with the development of highly active, functional group tolerant olefin metathesis catalysts based on ruthenium such as **1.2**.[55] More recently, the use of strongly donating N-heterocyclic carbene ligands has resulted in the recovery of the activity loss once associated with the move to a late transition metal and afforded catalysts such as **1.3** with higher activities, stabilities, and functional group tolerances.[53,56] In further optimization of the ligand set, phosphine-free systems with enhanced stability or initiation rates have been developed (catalysts **1.4** and **1.5**, respectively).[57,58] While **1.2** has been used to catalyze the controlled living polymerization of

functionalized norbornenes, the greater reactivity and much higher initiation rates of catalyst **1.5** allows the living polymerization of less reactive endo-substituted norbornenes and results in polymers with narrower polydispersities.[59]

These recent developments in metathesis catalysts are particularly beneficial to the potential synthesis of highly functionalized photoresist polymers via ROMP. A particular benefit of ROMP is the facile control of molecular weight via chain transfer, a process that is not trivial in metal-catalyzed addition polymerizations. The ability to control molecular weight by chain transfer offers the ability to employ very low catalyst loadings. Polymer molecular weights may be controlled either kinetically or thermodynamically through the use of terminal or internal olefinic chain transfer agents (CTAs) (Figure 1.23).[60] The first generation, bisphosphine-based catalyst **1.2** cannot perform secondary metathesis reactions on the olefins in the polymeric backbone and is significantly more reactive towards terminal rather than 1,2-disubstituted olefins.

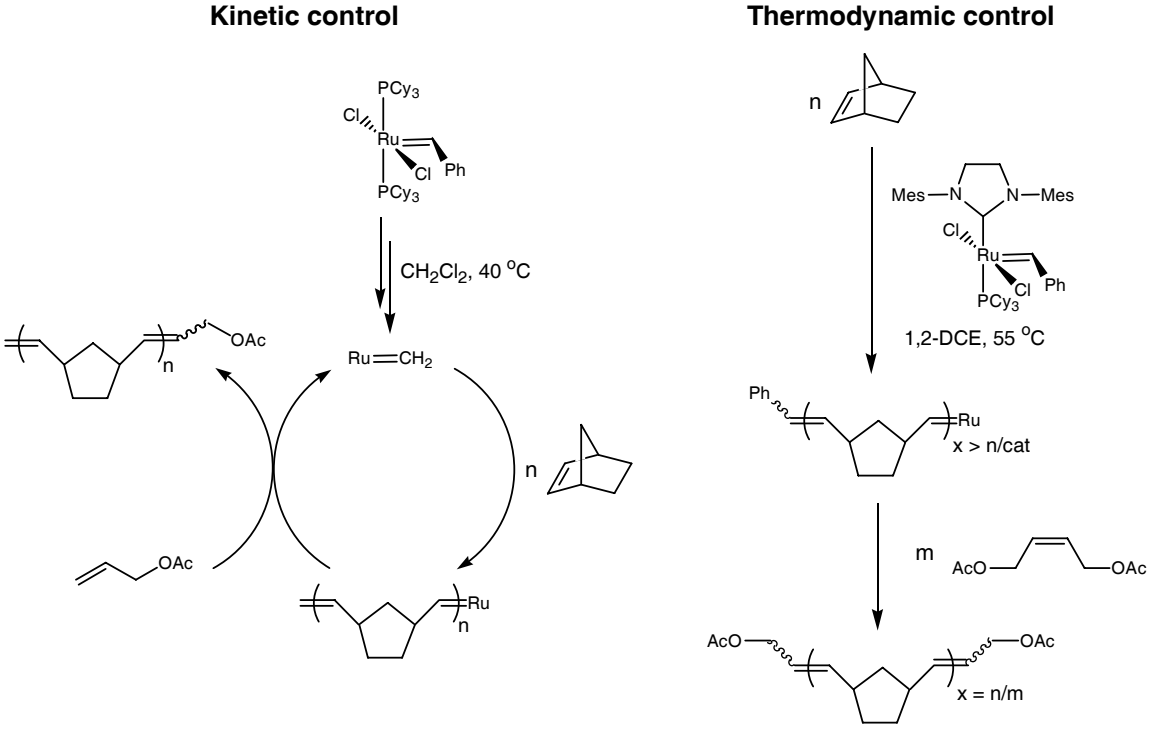

Figure 1.23. Control of molecular weight via chain transfer in ROMP

Therefore, the use of terminal olefin CTAs affords a kinetic control of the molecular weight that is dependent upon the monomer to chain transfer agent ratio [M]/[CTA]. The use of a functionalized CTA results in the formation of end-functionalized poly(norbornene)s.[60]

Alternatively, the second generation catalyst **1.3** can perform secondary metathesis on the backbone olefins of poly(norbornene) at slightly higher temperatures. The slow initiation rate and fast propagation typically results in the formation of very high molecular weight material. Secondary metathesis reactions subsequently redistribute the end-groups introduced by the presence of a chain transfer agent to afford a molecular weight distribution that is determined by the monomer to chain transfer agent ratio [M]/[CTA]. The use of a symmetric chain transfer agent has been used to produce telechelic poly(norbornene)s.[60]

Design of a ROMP-based 157nm Photoresist The major disadvantages of norbornene ROMP polymers are the residual double bonds which must be hydrogenated to afford the polymer with acceptable oxidative stability and the resulting low glass transition (T_g) temperatures. The glass transition temperature of norbornene ROMP polymers typically fall by around 30 °C after hydrogenation.[61] A series of norbornene ROMP polymers and their glass transition temperatures are shown in Figure 1.24. It should be noted that the glass transition temperature of ROMP polymers is heavily influenced by the cis/trans ratios of the backbone olefins and the polymer tacticity, both of which are highly catalyst dependent. The examples shown in this chapter are taken from the literature and are not polymerized under identical conditions; therefore, the glass

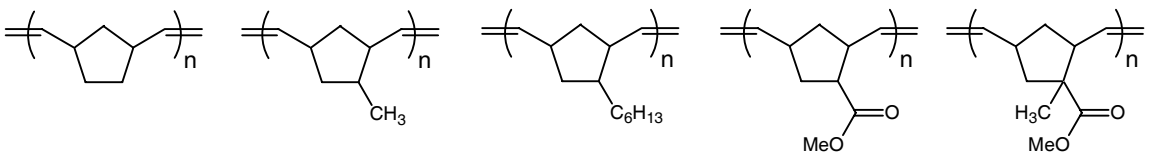

Figure 1.24. Glass transition temperatures of norbornene ROMP polymers[61-63]
Values in parentheses are for the hydrogenated analogues

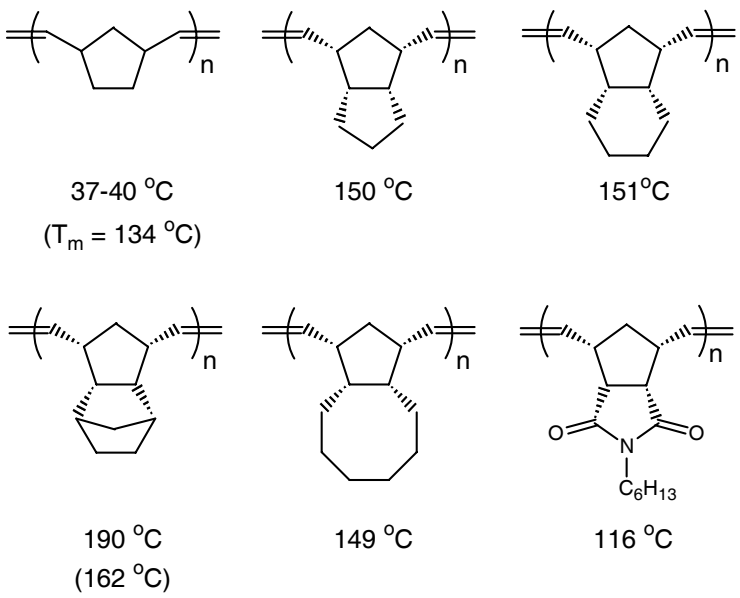

Figure 1.25. Effect of additional cyclic units on glass transition temperature[61,63,64] Values in parentheses are for the hydrogenated analogues.

transition temperatures cited here are only useful for a general comparison. The difference in T_g between the ROMP polymers shown here and norbornene addition polymers (> 300 °C) is dramatic.

In order to increase the glass transition temperature of ROMP polymers, additional cyclic structures are often incorporated; however, Stelzer *et al.* have shown that the T_g is relatively unaffected by the size of the additional cyclic structure (Figure 1.25).[64] Tetracyclo[4.4.0.$1^{2,5}$.$1^{7,10}$]dodec-3-enes (TCDs) are synthesized during the Diels-Alder synthesis of norbornenes via the addition of an extra cyclopentadiene unit. ROMP polymers of several TCDs have acceptable glass transition temperatures for use as photoresists. Incorporation of polar ester substituents can raise the glass transition temperature. However, additional steric bulk has a decreased effect on the T_g the further it is away from the backbone. For example, while the addition of a methyl group alpha to the ester raises the T_g of a polynorbornene by ~ 20 °C (Figure 1.24), it has virtually no effect on a TCD ROMP polymer (Figure 1.26). Extremely large groups such as the adamantyl group in the maleimide-functionalized poly(norbornene) are required to

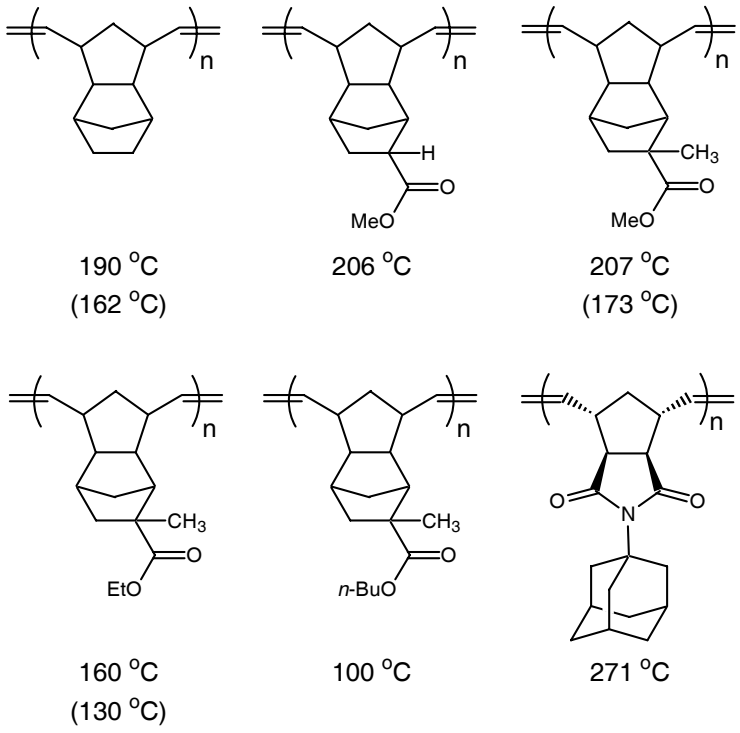

Figure 1.26. Effect of substituents on glass transition temperature[61,63,65]
Values in parentheses are for the hydrogenated analogues.

boost the T_g above 250 °C.[65] In addition, the presence of long, flexible substituents counteracts the benefits of the extra cyclic structure and significantly reduces the polymer's T_g.

While the tricyclodecane backbone structure of a TCD ROMP polymer should have similar etch resistance to adamantane given its similar Ohnishi parameter,[12e] theoretical calculations suggest that the tricyclodecane structure should have higher absorption at 157 nm than many other alicyclic structures (cyclopentane < norbornane < cyclohexanone = adamantane < tricyclodecane).[42] In fact, tricyclodecane appeared to be about 3 times more absorbing than cyclopentane and around 0.33 times more absorbing than norbornane. These calculations suggest that an absorption penalty will be incurred by using additional cyclic units to boost T_g. The use of additional fluorine substituents will be necessary to offset this inherent disadvantage.

ROMP of fluorinated norbornenes and norbornene-type monomers has been explored with a wide variety of ill-defined and early transition metal catalysts.[66] A few examples of

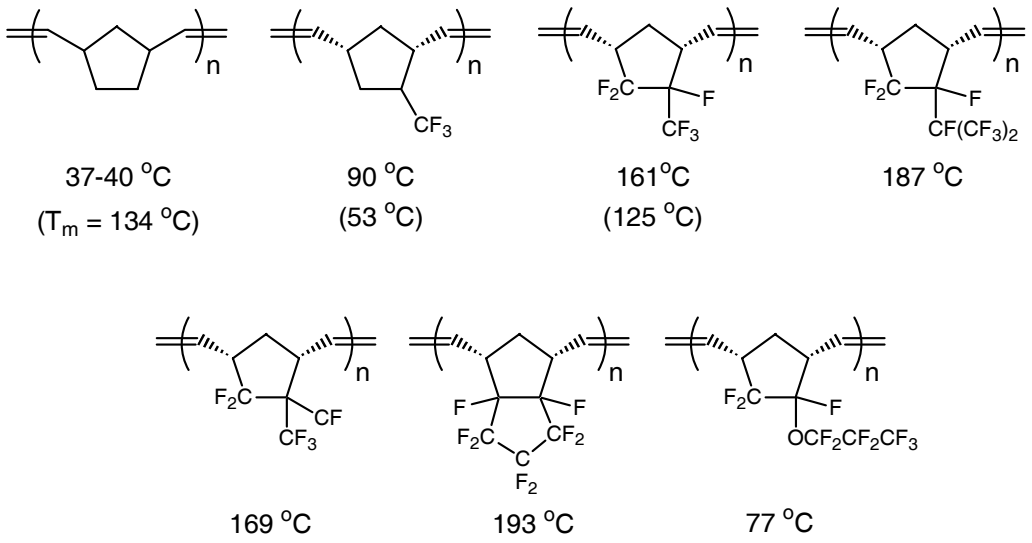

Figure 1.27. ROMP polymers of fluorinated norbornenes[65]

ROMP polymers of fluorinated norbornenes that have been studied are shown in Figure 1.27. The activity of the newer second-generation ruthenium metathesis catalysts is likely high enough to polymerize these fluorinated norbornenes. While the glass transition temperatures of several of these monomers appear to be promising for use as 157 nm resist materials, the location of the fluorinated groups so close to the olefin raises the distinct possibility of reactivity ratio concerns when copolymerized with more electron-rich monomers. Unfortunately, these fluorinated ROMP polymers are reportedly difficult to hydrogenate fully (perhaps due to their unique solubilities).

Ring-opening metathesis polymers were briefly examined for use as 193 nm resists.[13] A number of copolymers of functionalized norbornene and TCD monomers were synthesized using an ill-defined iridium catalyst. In order to achieve acceptable glass transition temperatures, the incorporation of a significant quantity of free carboxylic acid was required (Figure 28).[67] These polymers exhibited swelling problems, poor adhesion, slow dissolution, and phase incompatibility with several photoacid generators. In order to overcome this past poor performance, the use of more active, second generation ruthenium catalysts is expected to provide substantially better molecular weight control and lower residual metal content. The good

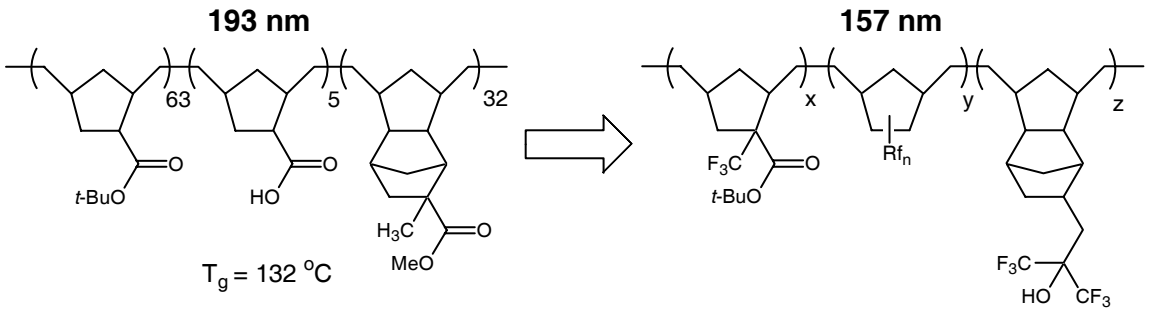

Figure 1.28. Design of ROMP-based resists for 157 nm lithography

dissolution behavior and adhesion properties of hexafluorocarbinols are expected to overcome related problems with the 193 nm ROMP materials. An additional fluorinated norbornene-type monomer (possibly of the type shown in Figure 1.28) will be necessary in order to afford acceptable glass transition temperatures and to offset the potentially higher absorbance of the tricyclodecane structure. Chapter 5 of this thesis details the synthesis of a new class of transparent, fluorinated 4-oxa-tricyclo[4.3.$0^{1,6}$.$0^{3,7}$]non-8-ene monomers suitable for increasing the glass transition temperature of ROMP polymers. Finally, chapter 6 describes a few aspects of ROMP polymerization of the hexafluorocarbinol-functionalized TCD monomer related to polymer transparency at 157 nm and the exploration of several other alicyclic structures for high T_g, metathesis-based materials.

References and Notes

(1) (a). Moore, G. E. *Electronics* **1965**, *38*, 114. (b). Moore, G. E. *Proc. SPIE* **1995**, *2439*, 2.

(2) (a). Walraff, G. M.; Hinsberg, W. D. *Chem. Rev.* **1999**, *99*, 1801-1821. (b). Brunner, T. A. *J. Vac. Sci. Technol. B* **2003**, *21*, 2632-2637.

(3) Thompson, S.; Alavi, M.; Hussein, M.; Jacob, P.; Kenyon, C.; Moon, P.; Prince, M.; Sivakumar, S.; Tyagi, S., Jr.; Bohr, M. *Intel Technol. J.* **2002**, *6*, 5-13. Graphs used by permission from Intel Corporation as published in Thompson, S.; Alavi, M.; Hussein, M.; Jacob, P.; Kenyon, C.; Moon, P.; Prince, M.; Sivakumar, S.; Tyagi, S., Jr.; Bohr, M. “

130nm Logic Technology Featuring 60nm Transisitors, Low-K Dielectrics, and Cu Interconnects." *Intel Technol. J.* **2002**, *6*, 5-13. http://developer.intel.com/technology/itj/2002/volume06issue02/.

(4) (a). *International Technology Roadmap for Semiconductors*. International SEMATECH: Austin, Tx. **1999**. ITRS documents can be accessed free of charge at http://public.itrs.net/. (b). Burggraaf, P. *Solid State Technol.* **2000**, *43*, pp. 31, 36.

(5) (a). Lin, B. J. *J. Microlitho. Microfab. Microsys.* **2004**, *3*, 377-395. (b). Owa, S.; Nagasaka, H. *J. Microlith. Microfabr. Microsys.* **2004**, *3*, 97-103. (c). Smith, B. W.; Bourov, A.; Kang, H.; Cropanese, F.; Fan, Y.; Lafferty, N.; Zavyalova, L. *J. Microlith. Microfabr. Microsys.* **2004**, *3*, 44-51. (d). Dammel, R. R.; Houlihan, F. M.; Sakamuri, R.; Rentkiewicz, D.; Romano, A. *J. Photopolym. Sci. Technol.* **2004**, *17*, 587-602. (e). Switkes, M.; Rothschild, M. *J. Vac. Sci. Technol. B* **2001**, *19*, 2353-2356.

(6) For reviews of the role of photoresists in lithography, see: (a) Steppan, H.; Buhr, G.; Vollman, H. *Angew. Chem. Int. Ed. Engl.* **1982**, *21*, 455-554. (b). Reichmanis, E.; Thompson, L. F. *Chem. Rev.* **1989**, *89*, 1273-1289. (c). Hinsberg, W. D.; Wallraff, G. M.; Allen, R. D. "Lithographic Resists" In *Kirk-Othmer Encyclopedia of Chemical Technology*, John Wiley & Sons. **1998**. (d). Roy, D.; Basu, P. K.; Eswaran, S. V. *Resonance* **2002**, 44-53.

(7) Patterson, K.; Somervell, M.; Willson, C. G. *Solid State Technol.* **2000**, *43*, 41-48.

(8) Gokan, H.; Esho, S.; Ohnishi, Y. *J. Electrochem. Soc.* **1983**, *130*, 143-146.

(9) For reviews of the development of chemically amplified resists, see: (a). Willson, C. G.; Ito, H.; Frechet, J. M. J.; Tessier, T. G.; Houlihian, F. M. *J. Electrochem. Soc.* **1986**, *133*, 181-187. (b). Reichmanis, E.; Houlihan, F. M.; Nalamasu, O.; Neenan, T. X. *Chem. Mater.* **1991**, *3*, 394-407. (c). MacDonald, S. A.; Willson, C. G.; Frechet, J. M. *Acc. Chem. Res.* **1994**, *27*, 151-158. (d). Ito, J. *IBM J. Res. Dev.* **1997**, *41*, 69-80. (e). Stewart, M. D.;

Patterson, K.; Somervell, M. H.; Willson, C. G. *J. Phys. Org. Chem.* **2000**, *13*, 767-774. (f). Ito, H. *J. Polym. Sci. A: Polym. Chem.* **2003**, *41*, 3863-3870.

(10) (a). Reichmanis, E.; Nalamasu, O.; Houlihan, F. M. *Acc. Chem. Res.* **1999**, *32*, 659-667. (b). Allen, R. D.; Opitz, J.; Ito, H.; Wallow, T. I.; Casmier, D. V.; DiPietro, R. A.; Brock, P.; Breyta, G.; Sooriyakumaran, R.; Larson, C. E.; Hofer, D. C.; Varanasi, P. R.; Mewherter, A. M.; Jayaraman, S.; Vicari, R.; Rhodes, L. F.; S. Sun. *Proc. SPIE* **1999**, *3678*, 66-77.

(11) (a). Allen, R. D.; Wallraff, G. M.; Hofer, D. C.; Kunz, R. R. *IBM J. Res. Dev.* **1997**, *41*, 95-104. (b). Allen, R. D.; Wallraff, G. M.; DiPietro, R. A.; Hofer, D. C.; Kunz, R. R. *J. Photopolym. Sci. Technol.* **1995**, *8*, 623-636. (c). Kunz, R .R.; Allen, R. D.; Hinsberg, W. D.; Walraff, G. M. *Proc. SPIE* **1993**, *1925,* 167-175.

(12) (a). Houlihan, F. M.; Wallow, T. I.; Nalamasu, O.; Reichmanis, E. *Macromolecules* **1997**, *30*, 6517-6524. (b). Reichmanis, E.; Nalamasu, O.; Houlihan, F. M.; Wallow, T. I.; Timko, A. G.; Cirelli, R. A.; Dabbagh, G.; Hutton, R. S.; Novembre, A. E.; Smith, B. W. *J. Vac. Sci, Technol. B* **1997**, *5,* 2528-2533. (c). Nalamasu, O.; Houlihan, F. M.; Cirelli, R. A.; Timko, A. G.; Watson, G. P.; Hutton, R. S.; Gabor, A.; Medina, A.; Slater, S. *J. Vac. Sci, Technol. B* **1998**, *16*, 3716-3721. (d). Byers, J.; Patterson, K.; Cho, S.; McCallum, M.; Willson, C. G. *J. Photopolym. Sci. Technol.* **1998**, *11*, 465-474. (e). Douki, K.; Kajita, T.; Shimokawa, T. *Proc. SPIE* **2000**, *3999*, 1128-1135. (f). Park, J.-H.; Kim, J.-Y.; Seo, D.-C.; Park, S.-Y.; Lee, H.; Kim, S.-J.; Jung, J.-C.; Baik, K.-H. *Proc. SPIE* **2000**, *3999*, 1163-1170.

(13) (a). Okoroanyanwu, U.; Shimokawa, T.; Byers, J.; Willson, C. G. *Chem. Mater.* **1998**, *10*, 3319-3327. (b). Okoroanyanwu, U.; Byers, J.; Shimokawa, T.; Willson, C. G. *Chem. Mater.* **1998**, *10*, 3328-3333. (c). Okoroanyanwu, U.; Shimokawa, T.; Byers, J.; Willson, C. G. *J. Molec. Catal. A* **1998**, *133*, 93-114. (d). Varanasi, P. R.; Jordhamo, G.; Lawson, M. C.; Chen, R.; Brunsvold, W. R.; Hughes, T.; Keller, R.; Khojasteh, M.; Li, W.; Allen, R.

D.; Ito, H.; Opitz, J.; Truong, H.; Wallow, T. *Proc. SPIE* **2000**, *3999*, 1157-1162. (e). Allen, R. D.; Opitz, J.; Wallow, T.; DiPietro, R. A.; Hofer, D. C.; Jayaraman, S.; Hullihan, K. A.; Rhodes, B. L.; Shick, R. A. *Proc. SPIE* **1998**, *3333*, 463-471.

(14) (a). Gaylord, N .G.; Mandal, B. M. *J. Polym. Sci. Polym. Lett. Ed.* **1976**, *14*, 555-559. (b). Gaylord, N. G.; Desphande, A. B.; Mandal, B. M.; Marton, M.; *J. Macromol. Sci. Chem. A* **1977**, *11*, 1053-1070. (c). Crivello, J. V.; Shim, S.-Y. *Chem. Mater.* **1996**, *8*, 376-381.

(15) (a). Rothschild, M.; Bloomstein, T. M.; Curtin, J. E.; Downs, D. K.; Fedynyshyn, T. H.; Hardy, D. E.; Kunz, R. R.; Liberman, V.; Sedlacek, J. H. C.; Uttaro, R. S.; Bates, A. K.; Van Peski, C. *J. Vac. Sci, Technol. B* **1999**, *17*, 3262-3266. (b). Bloomstein, T. M.; Rothschild, M.; Kunz. R. R.; Hardy, D. E., Goodman, R. B.; Palmacci, S. T. *J. Vac. Sci, Technol. B* **1998**, *16*, 3154-3157. (c). Rothschild, M.; Bloomstein, T. M.; Fedynyshyn, T. H.; Liberman, V.; Mowers, W.; Sinta, R.; Switkes, M.; Grenvile, A.; Orvek, K. *J. Fluor. Chem.* **2003**, *122*, 3-10. (d). Wagner, C.; Kaiser, W.; Mulkens, J.; Flagello, D. G. *Solid State Technol.* **2000**, *43*(9), 97-108.

(16) (a). Kunz, R. R.; Bloomstein, T. M.; Hardy, D. E.; Goodman, R. B.; Downs, D. K., Curtin, J. E. *J. Vac. Sci. Technol. B* **1999**, *17*, 3267-3272. (b). Kunz, R. R.; Bloomstein, T. M.; Hardy, D. E.; Goodman, R. B.; Downs, D. K.; Curtin, J. E. *J. Photopolym. Sci. Technol.* **1999**, *12*, 561-570.

(17) (a). Fedynyshyn, T. H.; Kunz, R. R.; Doran, S. P.; Goodman, R. B.; Lind, M. L.; Curtin, J. E. *Proc. SPIE* **2000**, *3999*, 335-346. (b). Cefalas, A. C.; Sarantopoulou, E.; Gogolides, E.; Argitis, P. *Microelectron. Eng.* **2000**, *53*, 123-126.

(18) Fedynyshyn, T. H.; Kunz, R. R.; Sinta, R. F.; Goodman, R. B.; Dorna, S. P. *J. Vac. Sci. Technol. B* **2000**, *18*, 3332-3339.

(19) Grandler, J. R.; Jencks, W. P. *J. Am. Chem. Soc.* **1982**, *104*, 1937-1951.

(20) Patterson, K.; Yamachika, M.; Hung, R.; Brodsky, C.; Yamada, S.; Somervell, M.; Osborn, B.; Hall, B.; Dukovic, G.; Byers, J.; Conley, W.; Willson, C. G. *Proc. SPIE*, **2000**, *3999*, 365-374.

(21) (a). Przybilla, K. J.; Roschert, H.; Pawlowski, G. *Proc. SPIE*, **1992**, *1672*, 500-512. (b). Ito, H.; Seehof, N.; Sato, R. *Polym. Mater. Sci. Eng.* **1997**, *77*, 449-450. (c). Ito, H.; Seehof, N.; Sato, R.; Nakayama, T.; Ueda, M. *ACS Symp. Ser.* **1998**, *706*, 208-223. (d). Ito, H. *IBM. J. Res. Dev.* **2001**, *45*, 683-695.

(22) For calculations of the VUV spectra of polar, fluorinated compounds, see: (a). Matsuzawa, N. N.; Mori, S.; Yano, E.; Okazaki, S.; Ishitani, A.; Dixon, D.A. *Proc. SPIE* **2000**, *3999*, 375-383. (b). Ando, S.; Fujigaya, T.; Ueda, M. *Jpn. J. Appl. Phys.* **2002**, *41*, L105-L108. (c). Toriumi, M.; Satou, I.; Itani, T. *J. Vac. Sci. Technol. B* **2000**, *18*, 3328-3331.

(23) For calculations of the VUV spectra of fluorinated alkanes, see: (a). Waterland, R. L.; Dobbs, K. D.; Rinehart, A. M.; Feiring, A. E.; Wheland, R. C.; Smart, B. E. *J. Fluor. Chem.* **2003**, *122*, 37-46. (b). Zhan, C. G.; Dixon, D. A.; Matsuzawa, N. N.; Ishitani, A.; Uda, T. *J. Fluor. Chem.* **2003**, *122*, 27-35.

(24) (a). Brodsky, C.; Byers, J.; Conley, W.; Hung, R.; Yamada, S.; Patterson, K.; Somervell, M.; Trinque, B.; Tran, H. V.; Cho, S.; Chiba, T.; Lin, S. H.; Jamieson, A.; Johnson, H.; Vander Heyden, T.; Willson, C. G. *J. Vac. Sci. Technol. B* **2000**, *18*, 3396-3401. (b). Chiba, T.; Hung, R. J.; Yamada, S.; Trinque, B.; Yamachika, M. Brodsky, C.; Patterson, K.; Vander Heyden, A.; Jamison, A.; Lin, S. H.; Somervell, M.; Byers, J.; Conley, W.; Willson, C.G. *J. Photopolymer Sci. Technol*. **2000**, *13*, 657-664.

(25) (a). Ito, H.; Miller, D. C.; Willson, C. G. *Macromolecules* **1982**, *15*, 915-920. (b). Wilson, C. G.; Ito, H.; Miller, D. C.; Tessier, T. G. *Polym. Eng. Sci.* **1983**, *23*, 1000-1003.

(26) (a). French, R. H.; Wheland, R. C.; Jones, D. J.; Hilfiker, J. N.; Synowicki, R. A.; Zumsteg, F. C.; Fledman, J.; Feiring, A. E. *Proc. SPIE* **2000**, *4000*, 1491-1502. (b). Johs, B.; French, R. C.; Kalk, F. D.; McGahan, W. A.; Woollam, J. A. *Proc. SPIE* **1994**, *2253*, 1098-1106.

(27) (a). Ito, H.; Wallraff, G. M.; Brock, P.; Fender, N.; Truong, H.; Breyta, G.; Miller, D. C.; Sherwood, M. H.; Allen, R. D. *Proc. SPIE* **2001**, *4345*, 273-284. (b). Trinque, B. C.; Chiba, T.; Hung, R. J.; Chambers, C. R.; Pinnow, M. J.; Osborn, B. P.; Tran, H. V.; Wunderlich, J.; Hsieh, Y.-T.; Thomas, B. H.; Shafer, G.; DesMarteau, D. D.; Conley, W.; Willson, C. G. *J. Vac. Sci. Technol. B* **2002**, *20*, 531-536. (c). Ito, H.; Okazaki, M.; Miller, D. C. *J. Polym. Sci. A: Polym. Chem.* **2004**, *42*, 1468-1477.

(28) Schmaljohann, D.; Bae, Y. C.; Weibel, G. L.; Hamad, A. H.; Ober, C. K. *Proc. SPIE* **2000**, *3999*, 330-334. (b). Schmaljohann, D.; Bae, Y. C.; Dai, J.; Weibel, G. L.; Hamad, A.; Ober, C. K. *J. Photopolym. Sci. Technol.* **2000**, *13*, 451-458.

(29) (a). Tran, H. V.; Hung, R. J.; Chiba, T.; Yamada, S.; Mrozek, T.; Hsieh, Y.-T.; Chambers, C. R.; Osborn, B. P.; Trinque, B. C.; Pinnow, M. J.; Sanders, D. P.; Connor, E. F.; Grubbs, R. H.; Conley, W.; MacDonald, S. A.; Willson, C. G. *J. Photopolym. Sci. Technol.* **2001**, *14*, 669-674. (b). Hung, R.; Tran, H. V.; Trinque, B. Chiba, T.; Yamada, S.; Osborn, B.; Brodsky, C.; Vander Heyden, A.; Sanders, D.; Grubbs, R.; Klopp, J.; Frechet, J.; Thomas, B.; Shafer, G.; , D.; Conley, W.; Willson, C. G. *Proc. SPIE.* **2001**, *4345*, 385-395. (c). Willson, C. G.; Trinque, B. C.; Osborn, B. P.; Chambers, C. R.; Hsieh, Y.-T.; Chiba, T.; Zimmerman, P.; Miller, D.; Conley, W. *J. Photopolym. Sci. Technol.* **2002**, *15*, 583-590. (d). Hoskins, T.; Chung, W. J.; Agrawal, A.; Ludovice, P. J.; Henderson, C. L.; Seger, L. D.; Rhodes, L. F.; Shick, R. A. *Macromolecules* **2004**, *37*, 4512-4518.

(30) (a). Kodama, S.; Kaneko, I.; Takebe, Y.; Okada, S.; Kawaguchi, Y.; Shida, N.; Ishikawa, S.; Toriumi, M.; Itani, T. *Proc. SPIE* **2002**, *4690*, 76-83. (b). Toriumi, M.; Shida, N.; Watanabe, H.; Yamazaki, T.; Ishikawa, S.; Itani, T. *Proc. SPIE* **2002**, *4690,* 191-199. (c). Shida, N.; Watanabe, H.; Yamazaki, T.; Ishikawa, S.; Toriumi, M.; Itani, T. *Proc. SPIE* **2002**, *4690*, 497-503.

(31) (a). Crawford, M. K.; Feiring, A. E.; Fledman, J.; French, R. H.; Periyasamy, M.; Schadt, F. L., III.; Smalley, R. J.; Zumsteg, F. C.; Kunz, R. R.; Rao, V.; Liao, L.; Holl, S. M. *Proc.*

SPIE **2000**, *3999*, 357-364. (b). French, R. C.; Feldman, J.; Zumsteg, F. C.; Crawford, M. K.; Feiring, A. E.; Petrov, V. A.; Schadt, F. L., III.; Wheland, R. C.; Gordon, J.; Zhang, E. *Semicond. FABTECH* **2001**, *14*, 167-175. (c). Feiring, A. E.; Crawford, M. K.; Farnham, W. B.; Feldman, J.; French, R. H.; Leffew, K. W.; Petrov, V. A.; Schadt, F. L., III.; Wheland, R. C.; Zumsteg, F. C. *J. Fluor. Chem.* **2003**, *122*, 11-16. (d). Toriumi, M.; Ishikawa, T.; Kodani, T.; Koh, M.; Moriya, T.; Araki, T.; Aoyama, H.; Yamashita, T.; Yamazaki, T.; Furukawa, T.; Itani, T. *J. Photopolym. Sci. Technol.* **2003**, *16*, 607-614. (e). Toriumi, M.; Ishikawa, T.; Kodani, T.; Koh, M.; Moriya, T.; Yamashita, T.; Araki, T.; Aoyama, H.; Yamazaki, T.; Furukawa, T.; Itani, T. *J. Vac. Sci. Technol. B* **2004**, *22*, 27-30.

(32) (a). Barnes, D. A.; Benedikt, G. M.; Goodall, B. L.; Huang, S. S.; Kalamarides, H. A.; Lenhard, S.; McIntosh, L. H., III.; Selvy, K. T.; Shick, R. A.; Rhodes, L. F. *Macromolecules* **2003**, *36*, 2623-2632. (b). Park, K. H.; Twieg, R. J.; Ravikiran, R.; Rhodes, L. F.; Shick, R. A.; Yankelevich, D.; Knoesen, A. *Macromolecules* **2004**, *37*, 5163-5178. (c). Lin, S. T; Narske, R. N.; Klabunde, K. J. *Organometallics* **1985**, *4*, 571-574.

(33) (a). Sen, A.; Lai, T.-L. *Organometallics* **1982**, *1*, 415-417. (b) Sen, A.; Lai, T-W; Thomas, R. R. *J. Organomet. Chem.* **1988**, *358*, 567-588. (c) Mehler, C.; Risse, W. *Makromol. Chem. Rapid. Commun.* **1991**, *12*, 255-259. (d). Mehler, C.; Risse, W. *Macromolecules* **1992**, *12*, 4226-4228. (e). Seehof, N.; Mehler, C.; Breunig, S.; Risse, W. *J. Molec. Catal.* **1992**, *76*, 219-228. (f). Lipian, J.; Mimna, R. A.; Fondran, J. C.; Yandulov, D.; Shick, R. A.; Goodall, B. L.; Rhodes, L. F.; Huffman, J. C. *Macromolecules* **2002**, *35*, 8969-8977.

(34) (a). Breunig, S.; Risse, W. *Makromol. Chem.* **1992**, *193*, 2915-2927. (b). Mehler, C.; Risse, W. *Makromol. Chem., Rapid Commun*. **1992**, *13*, 455-459. (c). Reinmuth, A.; Mathew, J. P.; Melia, J.; Risse, W. *Macromol. Rapid Commun*. **1996**, *17*, 173-180. (d). Mathew, J. P.; Reinmuth, A.; Melia, J.; Swords, N.; Risse, W. *Macromolecules* **1996**, *39*, 2755-2763.

(35) (a). Hennis, A. D.; Polley, J. D.; Long, G. S.; Sen, A.; Yandulov, D.; Lipian, J.; Benedikt, G. M.; Rhodes, L. F.; Huffman, J. *Organometallics* **2001**, *20*, 2802-2812. (b). Goodall, B. L.; Barnes, D. A.; Benedikt, G. M.; McIntosh, L. H.; Rhodes, L. F. *Polym. Mat. Sci. Eng.* **1997**, *76*, 56-57.

(36) Peruch, F.; Risse, W. *Polym. Prepr.* **2000**, *41*, 1916-1917.

(37) (a). Kang, M.; Sen, A. *Organometallics* **2004**, 23, 5396-5398. (b). Funk, J. K.; Andes, C. E.; Sen, A. *Organometallics* **2004**, *23*, 1680-1683. (c). Funk, J. K.; Andes, C.; Sen, A. *Polym. Prepr.* **2003**, *44*, 681-682. (d). Hennis, A. D.; Sen, A. *Polym. Prepr.* **2000**, *41*, 1933-1934.

(38) (a). Martin, J. G.; Hill, R. K. *Chem. Rev.* **1961**, *16*, 537-562. (b). Madan, R.; Srivastava, A.; Anand, R. C.; Varma, I. K. *Prog. Polym. Sci.* **1998**, *23*, 621-663.

(39) Heinz, B. S.; Alt, F. P.; Heitz, W. *Macromol. Rapid. Commun.* **1998**, *19*, 251-256.

(40) (a). Michalak, A.; Ziegler, T. *Organometallics* **2004**, *23*, 5565-5572. (b). Michalak, A.; Ziegler, T. *Organometallics* **2001**, *20*, 1521-1532.

(41) (a). Trinque, B. C.; Chambers, C. R.; Osborn, B. P.; Callahan, R. P.; Lee, G. S. Kusumoto, S.; Sanders, D. P.; Grubbs, R. H.; Conley, W. E.; Willson, C. G. *J. Fluor. Chem.* **2003**, *122*, 17-26. (b). Trinque, B. C.; Osborn, B. P.; Chambers, C. R.; Hsieh, Y.-T.; Corry, S.; Chiba, T.; Hung, R. J.; Tran, H. V.; Zimmerman, P.; Miller, D.; Conley, W.; Wilson, C. G. *Proc. SPIE* **2002**, *4690*, 58-68.

(42) Osborn, B. P.; Chiba, T.; Trinque, B. C.; Brodsky, C. J.; Hung, R. J.; Tran, H. V.; Chambers, C. R.; Callahan, R. P.; Carpenter, II., L. E.; Pinnow, M. J.; Lee, G. S.; Yamachika, M.; Willson, C. G.; Sanders, D. P.; Grubbs, R. H.; Dixon, D. A.; Miller, D. A.; Conley, W. E. Manuscript in preparation. For more calculations of the VUV spectra of fluorinated norbornenes, see: (a). Dixon, D. A.; Matsuzawa, N. N.; Ishitani, A.; Uda, T. *Phys. Stat. Sol B* **2001**, *226*, 69-77. (b). Matsuzawa, N. N.; Ishitani, A.; Dixon, D. A.; Uda,

T. *Proc. SPIE* **2001**, *4345*, 396-405. (c). Yamazaki, T.; Itani, T. *Jpn. J. Appl. Phys.* **2003**, *42*, 3881-3884.

(43) Exposure of bicyclo[2.2.2]oct-2-ene to a (π-allyl) palladium hexafluoroantimonate catalyst results in no polymer formation.

(44) Huisgen, R. Ooms, P. H. J.; Mingin, M.; Allinger, N. A. *J. Am. Chem. Soc.* **1980**, *102*, 3951-3953.

(45) Atkinson, R.; Aschmann, S. M.; Carter, W. P. L.; Pitts, J. N., Jr. *Int. J. Chem. Kinetics* **1983**, *15*, 721-731.

(46) Osborn, B. P. *Ph.D. Dissertation* University of Texas-Austin, **2004**.

(47) (a). Grubbs, R. H.; Trnka, T. M.; Sanford, M. S. *Curr. Meth. Inorg. Chem.* **2003**, 187- 231. (b). Grubbs, R. H. *Tetrahedron* **2004**, *60*, 7117-7140.

(48) For recent reviews on olefin cross-metathesis, see: (a). Chatterjee, A. K. In *Handbook of Olefin Metathesis*, vol. 2., Grubbs, R. H., Ed. Wiley-VCH: Weinheim, Ge., **2004**, pp. 246-295. (b). Connon, S. J.; Blechert, S. *Angew. Chem. Int. Ed.* **2003**, *42*, 1900-1923.

(49) For reviews on ring-closing metathesis, see: (a). Maier, M. E. *Angew. Chem. Int. Ed.* **2000**, *39*, 2073-2077. (b). Grubbs, R. H.; Miller, S. J.; Fu, G. C. *Acc. Chem. Rec.* **1995**, *28*, 446-452.

(50) For a recent review on ADMET, see: Schwendeman, J. E.; Church, A. C.; Wagener, K. B. *Adv. Synth. Catal.* **2002**, *344*, 597-613.

(51) For recent reviews on development of olefin metathesis catalysts and their application to ring-opening metathesis polymerization, see: (a). Buchmeiser, M. R. *Chem. Rev.* **2000**, *100*, 1565-1604. (b) Frenzel, U.; Nuyken, O. *J. Polym. Sci. A Polym. Chem.* **2002**, *40*, 2895-2916. (c). Slugovc, C. *Macromol. Rapid Commun.* **2004**, *25*, 1283-1297. (d). Trnka, T. M.; Grubbs, R. H. *Acc. Chem. Res.* **2001**, *34*, 18-29.

(52) Ivin, K. J. *Makromol. Chem. Macromo., Symp.* **1991**, *42/43*, 1-14.

(53) For recent reviews on development of olefin metathesis catalysts, see: (a) Schrock, R. R. In *Handbook of Olefin Metathesis*, vol. 1., Grubbs, R. H., Ed. Wiley-VCH: Weinheim, Ge., **2004**, pp. 8-32. (b). Nguyen, S. T..; Trnka, T. M. In *Handbook of Olefin Metathesis*, vol. 1., Grubbs, R. H., Ed. Wiley-VCH: Weinheim, Ge., **2004**, pp. 61-85. (c) Trnka, T. M.; Grubbs, R. H. *Acc. Chem. Res.* **2001**, *34*, 18-29.

(54) (a) Schrock, R. R.; Murdzek, J. S.; Bazan, G. C.; Robbins, J.; Dimare, M.; O'Regan, M. *J. Am. Chem. Soc.* **1990**, *112*, 3875-3886. (b) Bazan, G. C.; Khosravi, E.; Schrock, R. R.; Feast, W. J.; Gibson, V. C.; O'Regan, M. B.; Thomas, J. K.; Davis, W. M. *J. Am. Chem. Soc.* **1990**, *112*, 8378-8387. (c) Bazan, G. C.; Oskam, J. H.; Cho, H. N.; Park, L. Y.; Schrock, R. R. *J. Am. Chem. Soc.* **1991**, *113*, 6899-6907.

(55) (a) Schwab, P.; France, M. B.; Ziller, J. W.; Grubbs, R. H. *Angew. Chem. Int. Ed. Eng.* **1995**, *34*, 2039-2041. (b) Schwab, P.; Grubbs, R. H.; Ziller, J. W. *J. Am. Chem. Soc.* **1996**, *118*, 100-110. (c) Belderrain, T. R.; Grubbs, R. H. *Organometallics* **1997**, *16*, 4001-4003.

(56) (a) Scholl, M.; Ding, S.; Lee, C. W.; Grubbs, R. H. *Org. Lett.* **1999**, *1*, 953-956. (b) Sanford, M. S.; Love, J. A.; Grubbs, R. H. *J. Am. Chem. Soc.* **2001**, *123*, 6543-6554.

(57) For a recent review, see: (a). Hoveyda, A. H.; Gillingham, D. G.; Van, Velhuizen, J. J.; Kataoka, O.; Garber, S. B.; Kingsbury, J. S.; Harrity, J. P. A. *Org. Biomol. Chem.* **2004**, *2*, 8-23. Also: (b). Kingsbury, J. S.; Harrity, J. P. A.; Bonitatebus, P. J.; Hoveyda, A. H. *J. Am. Chem. Soc.* **1999**, *121*, 791-799. (c). Garber, S. B.; Kingsbury, J. S.; Gray, B. L.; Hoveyda, A. *J. Am. Chem. Soc.* **2000**, *122*, 8168-8179.

(58) (a). Sanford, M. S.; Love, J. A.; Grubbs, R. H. *Organometallics* **2001**, *20*, 5314-5318. (b). Love, J. A.; Morgan, J. P.; Trnka, T. M.; Grubbs, R. H. *Angew. Chem. Int. Ed.* **2002**, *41*, 4035-4037.

(59) (a). Slugovc, C.; Demel, S.; Stelzer, F. *Chem. Commun.* **2002**, 2572-3. (b) Choi, T.-L.; Grubbs, R. H. *Angew. Chem. Int. Ed.* **2003**, *42*, 1743-1746. (c). Slogovc, C.; Riegler, S.; Hayn, G.; Saf, R.; Stelzer, F. *Macromol. Rapid. Commun.* **2003**, *24*, 435-439.

(60) Bielawski, C. W.; Benitez, D.; Morita, T.; Grubbs, R. H. *Macromolecules* **2001**, *34*, 8610-8618.

(61) (a). Yoshida, Y.; Goto, K.; Komiya, Z. *J. Appl. Polym. Sci.* **1997**, *66*, 367-375. (b). Otsuki, T.; Goto, K.; Komiya, Z. *J. Polym. Sci. A: Polym. Chem.* **2000**, *66*, 367-375.

(62) Hatjopoulos, J. D.; Register, R. A. *Polym. Mat. Sci. Eng.* **2004**, *91*, 971-972.

(63) (a). Mol, J. C. *J. Molec. Catal. A: Chem.* **2004**, *213*, 39-45. (b). Yamazaki, M. *J. Molec. Catal. A: Chem.* **2004**, *213*, 81-87. (c). Six, C.; Beck, K.; Wegner, A.; Leitner, W. *Organometallics* **2000**, *19*, 4639-4642.

(64) Preishuber-Pfugl, P.; Eder, E.; Stelzer, F.; Reisinger, H.; Mulaupt, R.; Forsyth, J.; Perena, J. M. *Macromol. Chem. Phys.* **2001**, *202*, 1130-1137.

(65) Contrearas, A. P.; Cerda, A. M.; Tlenkopatchev, M. A. *Macromol. Chem. Phys.* **2002**, *203*, 1811-1818.

(66) (a). Feast, W. J.; Gimeno, M.; Khosravi, E. *Polymer* **2003**, *44*, 6111-6121. (b). Feast, W. J.; Gimeno, M.; Khosravi, E. *J. Molec. Catal. A: Chem.* **2004**, *44*, 9-14. (c). Feast, W. J.; Gimeno, M.; Khosravi, E. *J. Fluor. Chem.* **1999**, *100*, 117-125. (d). Yampol'skii, Y. P.; Bespalova, N. B.; Finkelshtein, E. S.; Bondar, V. I.; Popov, A. V. *Macromolecules* **1994**, *27*, 2872-2878. (e). Seehof, N.; Grutke, S.; Risse, W. *Macromolecules* **1993**, *26*, 695-700.

(67) Patterson, K. W. *Ph.D. Dissertation* University of Texas, Austin, **2000**.

CHAPTER 2

Development of Fluorinated Tricyclononenes: Transparent, Ester-Functionalized Monomers for 157 nm Lithography

Development of Fluorinated Tricyclononenes: Transparent, Ester-Functionalized Monomers for 157 nm Lithography

Abstract While metal-catalyzed addition polymers of ester-functionalized norbornenes have the high etch-resistance and glass transition temperatures required for photoresist polymers, they absorb too heavily to be useful for 157 nm lithography. The incorporation of a geminal trifluoromethyl group, while dramatically increasing transparency, renders the monomer unreactive towards metal-catalyzed addition polymerization. The exo-configuration of the additional cyclobutane ring in tricyclo[4.2.1.$0^{2,5}$]non-7-enes serves as a scaffold suitable for the incorporation of additional fluorinated substituents while reducing the steric and electronic effects of these groups on the subsequent polymerization. Novel fluorinated tricyclononene-3-carboxylic acid esters are synthesized via the cycloaddition of quadricyclane with a number of fluorinated acrylic acid esters. Fluorinated tricyclononane esters possess enhanced transparencies at 157 nm relative to non-fluorinated norbornane analogues as determined by gas phase vacuum-ultraviolet (V-UV) spectroscopy. Further extension of this approach to the synthesis of hexafluorocarbinol-functionalized tricyclononenes is limited by the isomerization of quadricyclane to norbornadiene at higher temperatures. As a result, cycloaddition with less reactive dienophiles such as 1-acetoxy-1-trifluoromethyl-ethene is unsuccessful. Additionally, reaction with unsaturated hexafluorocarbinols results in the exclusive formation of norbornenyl ethers.

Introduction

Specialized, alicyclic fluoropolymers are the focus of intense research as the semiconductor industry attempts to develop the functional photoresists required to enable the timely introduction of 157 nm optical lithography, as outlined in the International Technical Roadmap for Semiconductors (ITRS) timeline.[1,2] A prominent concern for 157 nm lithography is the feasibility of employing a practical resist thickness (> 200 nm), which requires a photoresist

with a low absorption coefficient.[3] In order to fulfill this requirement while retaining optimal imaging properties, a critical balance of several, often competing, material properties, such as transparency, etch resistance, glass transition temperature, thermal stability, and dissolution behavior must be achieved. Carbon-rich and heteroatom-deficient norbornene structures such as the norbornene *t*-butyl ester (NTBE, **2.1**, Figure 2.1) were developed for use at 193 nm, proving to be suitable replacements for the heavily absorbing, etch-resistant aromatics used in previous generations of photoresists. Unfortunately, while the majority of the polar functionalities (esters, carbonates, alcohols, and anhydrides) used in resist chemistry are transparent at 193 nm, the absorption coefficients of carbon-carbon double bonds, carbon-oxygen single bonds, carbon-oxygen double bonds, and even some carbon-hydrogen bonds are all too high at 157 nm for these functionalities to be useful.[4]

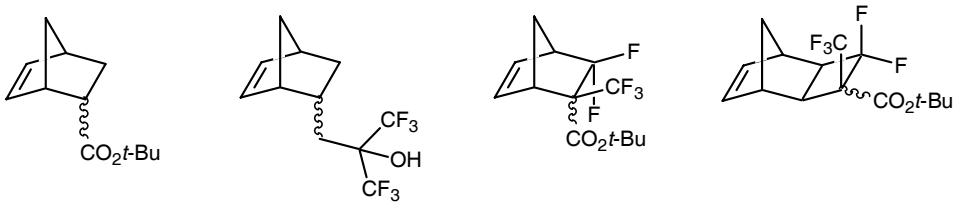

Figure 2.1. Norbornene-type monomers for lithographic applications

Fortunately, through computational[5] and experimental[6] efforts, it was discovered that the incorporation of fluorinated substituents dramatically reduces the absorption of various structures at 157 nm. For example, the hexafluoroisopropyl alcohol functionalized norbornene (NBHFA, **2.2**) was found to be highly transparent.[6] In addition, due to the inductive effects of the two trifluoromethyl groups, the acidity of the this type of fluorinated alcohol is similar to phenol,[7] allowing this polar monomer to replace the highly absorbing phenolic structures used in previous generations of resists. This discovery has renewed interest in resists based on metal-catalyzed addition polymers of functionalized norbornenes, originally developed for 193 nm,[8] as promising

candidates for 157 nm photoresists. Protection of the hexafluoroisopropyl alcohol functionality of **2** with *t*-BOC groups has produced monomers suitable for resist development.[6] Efforts to expand the scope of 157 nm resists to include those based on the more thermally stable *t*-butyl and tetrahydropyranyl esters have achieved only partial success due to the high absorbance of ester-functionalized monomers such as **2.1** at 157 nm. Fortunately, the incorporation of an α-trifluoromethyl group was found to significantly reduce the absorption of these esters.[6] Similarly, the absorbance of norbornane structures could be reduced by the incorporation of judiciously positioned fluorine substituents.[6] The fluorinated monomer **2.3** was subsequently designed as an ideal replacement for the highly absorbing norbornene **2.1**. Unfortunately, norbornene monomers of this type with geminal electron-withdrawing ester and trifluoromethyl substituents were found to be unsuitable for polymerization with common nickel and palladium catalysts.[9] The addition of an α-trifluoromethyl group in **2.3**, while addressing the transparency problem, hinders the polymerization. Thus, alternative approaches towards a polymerizeable monomer incorporating these transparent esters were investigated.

Recently, Grubbs *et al.* reported that, in the copolymerization of ethylene and functionalized norbornene-type monomers to produce functionalized polyethylene, high incorporation (up to 31 mol %) of polar functionalities could be achieved through the use of functionalized tricyclo[4.2.1.$0^{2,5}$]non-7-ene (TCN) monomers.[10] The combination of reduced steric interference due to the 100% exo configuration of the cyclobutane ring (moving the geminal electron-withdrawing functionalities an additional carbon away from the double bond) and increased ring strain improved the reactivity of the tricyclononene monomers towards metal-catalyzed addition polymerization. The use of TCN chemistry in photoresists is a potential solution to the polymerization difficulties of the partially fluorinated norbornenes mentioned previously.

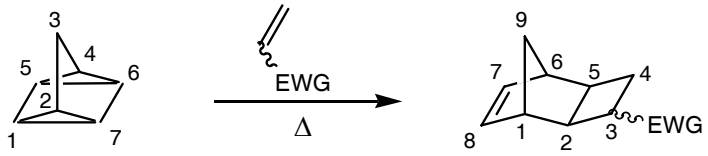

Tetracyclo[3.2.0.0^{2,7}.0^{4,6}]heptane (Quadricyclane)

3-EWG-tricyclo[4.2.1.0^{2,5}]non-7-ene

Figure 2.2. Cyclizations of quadricyclane with electron deficient olefins (EWG = electron withdrawing group)

Tricyclo[4.2.1.0^{2,5}]non-7-enes (TCNs) are formed from the [2σ + 2 σ + 2π] cycloaddition of quadricyclane (tetracyclo[3.2.0.0^{2,7}.0^{4,6}]heptane) with electron deficient dienophiles such as alkenes, alkynes, and azo compounds (Figure 2.2).[11,12] The cycloadditions proceed readily at moderate temperature with electron-deficient olefins to produce norbornene-like structures with a fused cyclobutane ring in the exo configuration. While the allowed thermal homo-Diels-Alder [2π + 2π + 2π] reaction between norbornadiene and electron deficient olefins[13] can be catalyzed by nickel and cobalt species[14] to produce deltacyclanes, in certain cases, metal-catalyzed [2π + 2π] cycloadditions can also occur to produce a mixture of tricyclononenes in which the cyclobutane ring appears be in either the exo or the endo configuration.[14b,15] Unfortunately, the tri- and tetra-substituted double bonds of the resulting tricyclononenes,[16] coupled with the complex mixture of exo and endo isomers, renders this route unattractive for the production of valuable monomers. At present, the quadricyclane pathway is the only viable synthetic route towards TCN monomers suitable for metal-catalyzed addition polymerization.

The wide variety of electron-withdrawing groups (nitriles, anhydrides, esters, etc.) able to undergo cyclizations with quadricyclane allows TCNs to retain the versatility of established norbornene chemistry. While most reports of TCN chemistry to date have investigated the regio- and stereospecificity[11] and concertedness of the cyclization reaction,[17] the value of photoresist materials prompted us to consider these compounds for materials development. In this chapter, we report the development of partially fluorinated tricyclo[4.2.1.0^{2,5}]non-7-ene-3-carboxylic acid

esters, such as monomer **2.4**, as transparent, ester-functionalized norbornene-like monomers useful for incorporation into addition-type photoresist polymers.

Results and Discussion

Synthesis of TCN Monomers A series of tricyclononene compounds (**2.5-2.9**, Table 2.1) were synthesized from quadricyclane and the appropriate olefin as shown in Figure 2.3. The numbering system and nomenclature used is shown in Figure 2.2 and Table 2.1, respectively. The methylene bridge (C9) hydrogens will be referred to as either syn or anti to the C(7)-C(8) olefin. The most important substituent (nitrile or ester) at C(3) on the cyclobutane ring will be referred to as being syn or anti to the C(1)-C(2) bond, to avoid confusion with the exo notation used to describe the cyclobutane ring fusion. Since the majority of TCN compounds reported in the literature[11] were made from symmetrical 1,1- or 1,2-disubstituted olefins, less is known about the resultant TCN isomer distribution produced using non-symmetrical 1,1-disubstituted olefins. Particular attention will be paid to the syn/anti isomer distribution as it may significantly affect the rate of polymerization and/or incorporation ratio in copolymerizations. The syn/anti isomer distributions produced by the quadricyclane cyclizations will be compared with the more familiar exo/endo isomer distributions achieved by Diels-Alder reactions with cyclopentadiene. Finally, while esters with readily removable *t*-butyl or cyclic acetal protecting groups are required for use as imageable photoresists, the more synthetically and commercially accessible methyl esters of

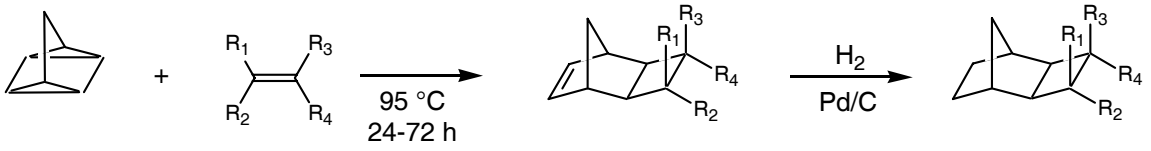

R_1,R_2 = H R_3 = H	R_4 = CO_2H	**2.5**	35 % (2 steps from nitrile)
R_1,R_2 = H R_3 = H	R_4 = $CO_2{}^tBu$	**2.6**	80 %
R_1,R_2 = H R_3 = CH_3	R_4 = CO_2Me	**2.7**	8 %
R_1,R_2 = F R_3 = CF_3	R_4 = CO_2Me	**2.8**	94 %
R_1,R_2 = F R_3 = CF_3	R_4 = CO_2Me	**2.9**	73 %

Figure 2.3. Synthesis of tricyclononene monomers and model compounds

Table 2.1. Selectivity in TCN monomer synthesis

Olefin	TCN Products		
	syn		anti
			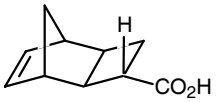
	2 %	**2.5***	98 %
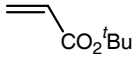	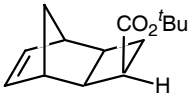		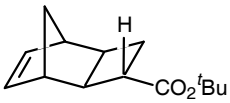
	57 %	**2.6**	43 %
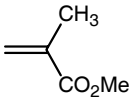	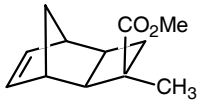		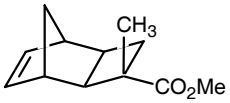
	55 %	**2.7**	45 %
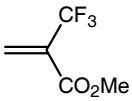	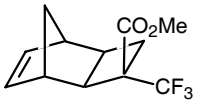		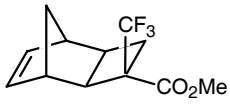
	32 %	**2.8**	68 %
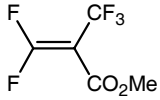	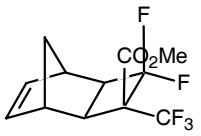		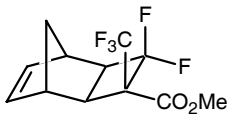
	49 %	**2.9**	51 %

* After hydrolysis of nitrile

the fluorinated acrylates were employed in this initial study.

The nitrile-functionalized TCN monomer was synthesized by the cycloaddition of quadricyclane and acrylonitrile using the procedure of Noyori[18] to produce 3-cyano-tricyclo[4.2.1.$0^{2,5}$]non-7-ene with a 2:1 syn:anti ratio and 100% exo cyclobutane ring fusion. Subsequent base catalyzed hydrolysis of the nitrile afforded the carboxylic acid (**2.5**) with a syn:anti ratio of approximately 2:98. During the hydrolysis, epimerization around the C(3)

position converts the syn isomer into the more stable anti isomer, consistent with the results of Tabushi *et al*.[11e] regarding the base-catalyzed isomerization of cis and trans di-ester and di-nitrile-substituted tricyclononenes.

Cycloaddition of quadricyclane with acrylonitrile or *t*-butyl acrylate produced high yields (80%+ with respect to quadricyclane) of TCN products with a preference for the syn product. While this syn structure is formed via a transition state with the maximal orbital overlap on C(2) and C(4) of quadricyclane as is the case in Diels-Alder reactions, the role of electrostatic effects or intermolecular attractive forces remains unknown. The predominant by-products of the reaction are norbornadiene formed by slow isomerization of quadricyclane under the reaction conditions and acrylate or acrylonitrile homopolymer.[19]

t-Butyl methacrylate and methacrylonitrile also undergo cyclizations with quadricyclane, albeit in dramatically reduced yields (~8 % for *t*-butyl methacrylate).[20] Interestingly, no appreciable difference in the syn/anti ratio is observed despite the introduction of the α-methyl group. This is in direct contrast to the cycloaddition behavior of cyclopentadiene, as shown in Table 2.2. In cycloadditions with cyclopentadiene, the presence of an α-methyl group on an acrylate induces a preference for the exo isomer (~70% exo v. ~30% exo for acrylate), while a trans β-methyl group has only a small effect.[21] This deviation from endo selectivity has been attributed either to steric interference between the α-methyl group and the methylene hydrogens of cyclopentadiene or secondary attractive forces between the methyl and the unsaturated carbons.[21] Since the transition state in the quadricyclane cycloaddition is centered on C(6) and C(7) (Figure 2.2), steric interference by the C-3 methylene hydrogens appears to be minimal as exhibited in the small effect on the syn/anti ratio upon incorporation of the α-methyl group (**2.6** and **2.7,** Table 2.1).

Table 2.2. Comparison of cyclopentadiene and quadricyclane cycloadditions

Olefin	Cyclopentadiene (% endo, 25 °C)	Cyclopentadiene (% endo, 100 °C)	Quadricyclane (% syn, 97 °C)
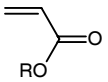	74.3 (R = Me)[21c]	70.5 (R = Me)[21c]	57 (R = ^{t}Bu)
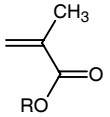	30.1 (R = Me)[21c]	31.8 (R = Me)[21c]	55 (R = ^{t}Bu)
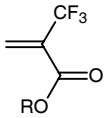	67 (R = Me)[25]		32 (R = Me)
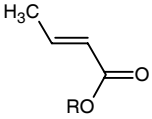	50.9 (R = Me)[21c]	50.8 (R = Me)[21c]	
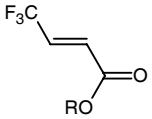	26.3 (R = Me)[24d]		

Cyclization of quadricyclane with methyl 2-(trifluoromethyl)acrylate proceeded nearly quantitatively by ^{1}H NMR to produce **2.8** in 94% isolated yield after 72 hours. The inability of the fluorinated methacrylate to undergo radical homopolymerization prevents it from being consumed in the production of polymeric by-products, leading to a high yield. The facile cycloaddition is consistent with the observed behavior of olefins with trifluoromethyl substituents in 1,3-dipolar[22] and Diels-Alder cycloaddition reactions.[23] Unlike the previous acrylate and methacrylate cyclizations, this reaction produced predominantly the anti product (syn/anti = 32:68), similar to the cycloaddition of cyclopentadiene and either *trans*-crotonic acid or *trans*-4,4,4-trifluorocrotonic acid (Table 2.2).[24] In contrast, the cycloaddition of 2-(trifluoromethyl)acrylic acid with cyclopentadiene exhibits little change in exo/endo preference relative to acrylic acid.[25] Since the trifluoromethyl group is more sterically bulky than a methyl

group (being more similar to an isopropyl group),[26] the high yield in the cyclization with the methyl 2-(trifluoromethyl)acrylate (unlike the cyclizations with *t*-butyl methacrylate or methacrylonitrile) demonstrates the importance of the electronics of the dienophile in cyclizations with quadricyclane.

Unfortunately, the cyclization with the methyl 3,3-difluoro-2-(trifluoromethyl)acrylate produced only a moderate yield (~25%) of TCN **2.9** after 72 hours. This was in distinct contrast to the excellent yields obtained in the Diels-Alder reaction of this perfluorinated olefin with cyclopentadiene. The yield was increased to 73% upon allowing the reaction mixture to continue at room temperature for several days. This is similar to some cycloadditions with furan in which high yields are observed after long reaction times at room temperature.[27] Further work is required to explain the reluctance of this fluorinated methacrylate to undergo cyclization with quadricyclane.

Assignment of TCN Isomers As previously mentioned, little has been published on TCN compounds obtained from non-symmetric 1,1-disubstituted olefins. Therefore, we endeavored to find a simple diagnostic to determine the isomeric product distribution in these compounds. Fortunately, due to epimerization during the hydrolysis reaction, the TCN carboxylic acid (**2.5**) is almost exclusively the anti isomer. ^{1}H, ^{13}C, ^{13}C DEPT, ^{1}H-^{1}H COSY, and ^{1}H-^{13}C HMQC and HETCOR NMR experiments were used to assign the carbon and proton resonances in this compound. The spectra were compared with the available published spectral data[10e,16,27] for other tricyclo[4.2.1.0^{2,5}]non-7-ene compounds. The exo configuration of the cyclobutane ring fusion was established by the W-coupling between H(9$_{syn}$) and H(2) and H(5) (^{4}J = 1.7 Hz), that is similar to the reported values for *exo*-3-thiatricyclo[4.2.1.0^{2,5}]non-7-ene-3,3-dioxide.[28]

The bridgehead protons H(1) and H(6) each appear as distinct unresolved multiplets with the H(1) proton appearing about 0.08 ppm downfield from H(6). The $\Delta\delta$ for H(1)-H(6) is diagnostic of syn and anti due to deshielding by the nearby substituents on C(3). For example, in the t-butyl ester TCN compound (**2.6**), H(6) of both the syn and anti isomer are identical;

however, while H(1) of the anti isomer appears 0.07 ppm downfield of H(6), H(1) of the syn isomer is shifted 0.27 ppm downfield due to closer proximity of the ester group, in agreement with the reported NMR assignments for the isolated anti isomer of **2.6**.[10] Since the bridgehead hydrogens in TCNs **2.5-2.9** appear between 2.5 and 3.6 ppm (well resolved from each other and the other protons in these compounds) and agree with the integration of the protons belonging to any ester substituents for the corresponding isomer, the isomer ratio for each compound was determined by integration of the H(1) and H(6) bridgehead protons.

The hydrolysis of the fluorinated TCN methyl ester (**2.9**) produced a mixture of carboxylic acid isomers, one of which was isolated by crystallization. X-ray crystallographic analysis revealed that this isomer is the *syn* compound (**2.10**, Figure 2.4). The crystal structure of **2.10** is similar to that of an imide-functionalized TCN structure reported in the literature.[29] From the crystal structure, the proximity of the carboxylic acid in the syn position to the bridgehead H(1) proton (responsible for significant deshielding of the proton) is apparent. The crystal structure and NMR data from the *syn* isomer of the fluorinated TCN carboxylic acid (**2.10**) complement the NMR data from the anti isomer of the non-fluorinated TCN carboxylic acid

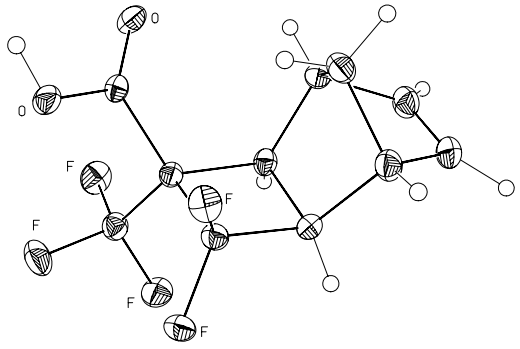

Figure 2.4. X-ray crystal structure of the carboxylic acid **2.10**
Displacement ellipsoids are scaled to the 30% probability level.
Hydrogen atoms are drawn to an arbitrary size.

(**2.5**), confirming the assignments of the isomers and the validity of using the Δδ for H(1)-H(6) as a diagnostic.

Synthesis of Saturated TCN Compounds The first concern with these TCN monomers was preservation of the transparency demonstrated in the analogous norbornane structures. It was unknown whether the addition of the fused cyclobutane ring would pose any absorbance problems at 157 nm, similar to those of cyclopropane rings in nortricyclane-based polymers at 193 nm.[30] To investigate this, several tricyclononane compounds were produced by hydrogenating the double bonds of various TCN monomers. Gas-phase vacuum ultraviolet (VUV) spectra of the fluorinated tricyclononane compounds shown in Figure 2.5 reveal promising transparency. In fact, the saturated version of **2.9** exhibits even higher transparency than norbornane. While still more heavily absorbing than 2,2-difluoronorbornane (one of the most transparent norbornanes at 157 nm discovered to date), these results are encouraging enough

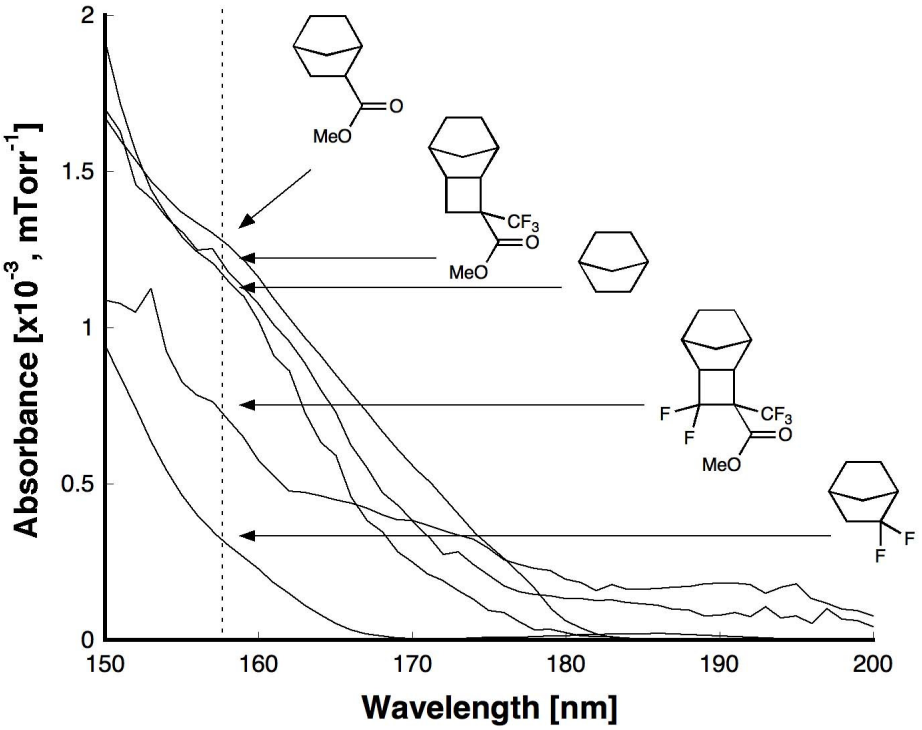

Figure 2.5. Vacuum UV spectra of model tricyclononane structures

to warrant additional experimental verification of transparency through the synthesis of TCN addition polymers for analysis by variable angle spectroscopic ellipsometry (VASE)[31]. The additional cyclobutane ring of the TCN monomer produces only a small increase in absorbance at 157 nm which can be more than compensated for by the incorporation of additional fluorinated groups as shown in Figure 2.6. It should be noted that the lower volatilities of some of the TCN compounds results in the lower signal to noise ratios of the spectra shown in Figures 2.5 and 2.6. Therefore, VASE analysis of TCN homopolymers may be a more accurate determination of the effect of fluorination and the additional cyclobutane ring on the transparency at 157 nm.

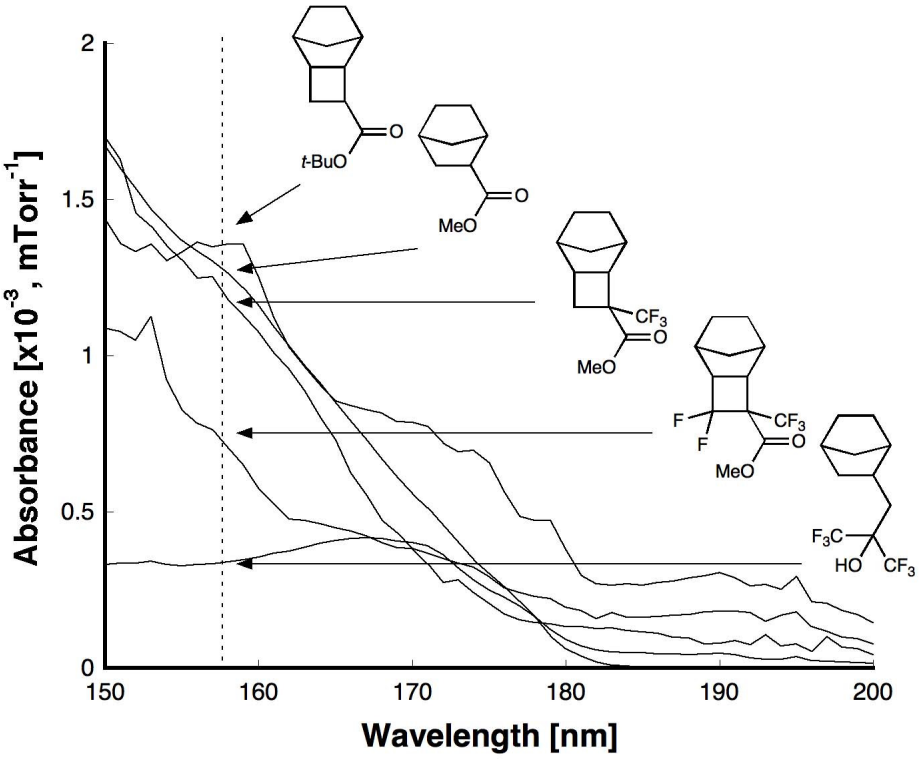

Figure 2.6. Vacuum UV spectra of model tricyclononane structures

Attempted Synthesis of Hexafluorocarbinol-functionalized Tricyclononenes

Given the high transparency of **2.1**, the incorporation of additional fluorine was expected to offer additional transparency enhancements;[6b] however, the more fluorinated analogues **2.11**

and **2.12** were shown to be more absorbing and unreactive towards metal-catalyzed addition polymerization.[32] Similarly, the trifluorocarbinol **2.13** and pentafluorocarbinol **2.14** are easily synthesized via the Diels-Alder reaction with the corresponding vinyl acetate followed by hydrolysis.[6a,33] While alcohol **2.13** does not have sufficient acidity or transparency to be useful, **2.14** offers sufficient acidity and high transparency. Since the additional cyclobutane ring of the TCN framework has little effect on the absorbance at 157 nm and results in superior activity towards metal-catalyzed addition, we sought to synthesize hexafluorocarbinol-functionalized TCN analogues of **2.12 – 2.14**, such as **2.15** and **2.16**.

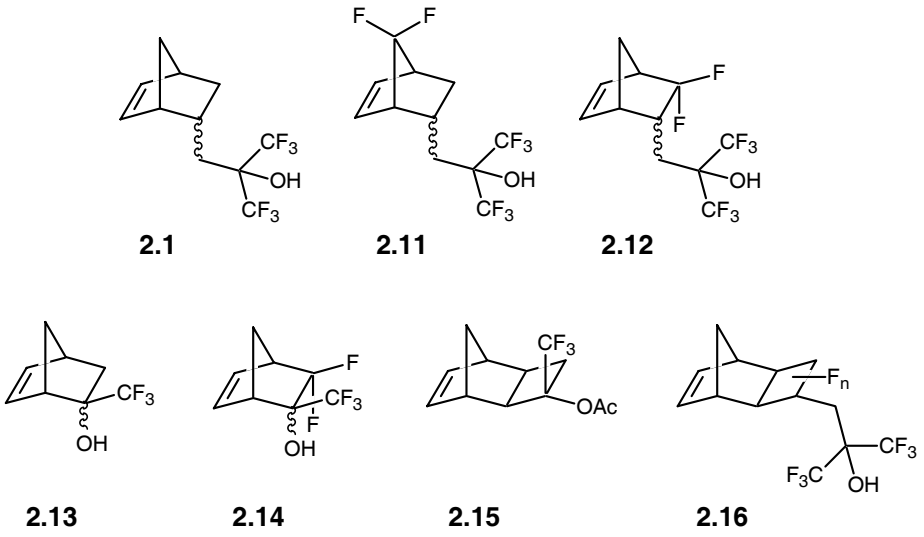

Figure 2.7. Hexafluorocarbinol-functionalized monomers

Unfortunately, reaction of 1-acetoxy-1-trifluoromethyl-ethene with quadricyclane was unsuccessful (Figure 2.8). Extended heating of the reaction mixture at higher temperatures resulted only in the isomerization of quadricyclane back to norbornadiene. Unlike Diels-Alder reactions with cyclopentadiene which can be performed at elevated temperatures for prolonged periods of time in order to achieve acceptable yields of cycloaddition products with moderate dienophiles, reactions with quadricyclane must be performed below 140 °C to prevent isomerization to the unreactive norbornadiene. The lower reactivity of quadricyclane requires

extremely reactive dienophiles for acceptable cycloaddition yields. Consistent with these results, reaction of quadricyclane with the homoallylic hexafluorocarbinol **2.17** did not afford any tricyclononene product; instead however, a 1.4:1 mixture of the norbornenyl and nortricyclyl ethers **2.18a** and **2.18b**, respectively, was isolated. Several iterations of silica gel column chromatography were sufficient to separate the isomers to afford a clean sample of the norbornenyl ether **2.18a** for analysis. These results are similar to those of Dauben *et al.*, who reported the reaction of acetic acid with quadricyclane to afford a mixture of norbornene and nortricyclane esters.[34] When the alcohol is protected (as with the *t*-butyldimethylsilyl-protected hexafluorocarbinol **2.19**), no reaction with quadricyclane is observed. While these failures persuaded us to focus on alternative monomers, the reaction of quadricyclane with fluorinated alcohols was pursued independently with some success by another laboratory.[35]

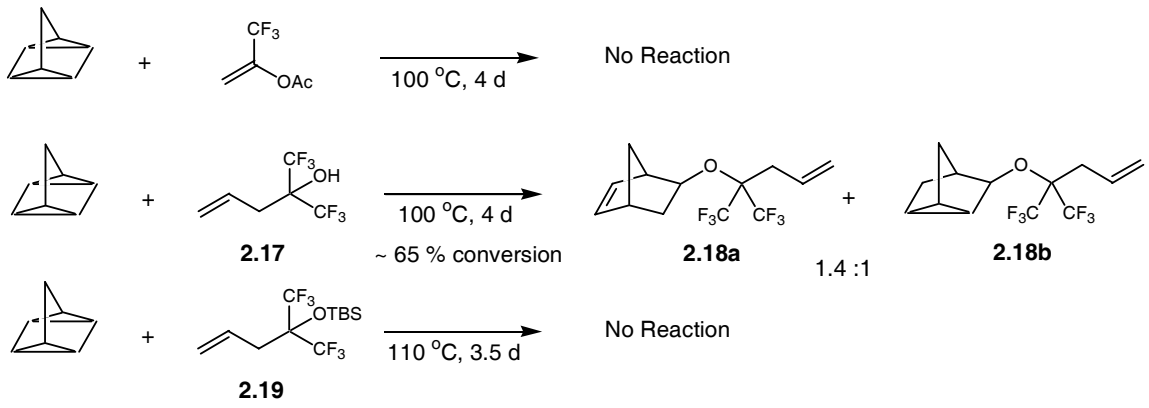

Figure 2.8. Attempted syntheses of hexafluorocarbinol-functionalized tricyclononenes

Conclusions

A number of non- and partially-fluorinated acrylic and methacrylic acid esters undergo cyclizations with quadricyclane to produce tricyclononene structures in moderate to high yield. The *exo*-configuration of the cyclobutane ring relieves steric crowding of the olefin and reduces inductive effects by locating the highly electron-withdrawing fluorine, trifluoromethyl, and carboxylic acid ester functionalities further from the double bond. In this way, the electronic and

steric issues which affect polymerization activity can be balanced with the degree of fluorination required for acceptable transparency. Vacuum-UV measurements on saturated model TCN systems demonstrate the increased transparency imparted by the selective incorporation of trifluoromethyl and fluorine substituents. Further extension of this approach to the synthesis of hexafluorocarbinol-functionalized tricyclononenes is limited by the isomerization of quadricyclane to norbornadiene at higher temperatures. As a result, cycloaddition with less reactive dienophiles such as 1-acetoxy-1-trifluoromethyl-ethene was unsuccessful. Additionally, reaction with unsaturated hexafluorocarbinols resulted in the exclusive formation of norbornenyl and nortricylanyl ethers. Nevertheless, fluorinated tricyclononenes constitute a new viable route towards photoresist materials for 157 nm lithography with enhanced transparencies.

Experimental

Materials: All manipulations and polymerizations were carried out in an N_2-filled drybox or using standard Schlenk techniques. Argon was purified by passage through columns of BASF RS-11 (Chemalog) and Linde 4-Å[36] molecular sieves. Dichloromethane was rigorously degassed in 18 L reservoirs and passed through two sequential purification columns consisting of activated alumina. All starting materials were procured from Aldrich except methyl 2-(trifluoromethyl)-3,3,3-trifluoropropenoate (Synquest), (2-trifluoromethyl)acrylic acid (Honeywell), and 1,1,1-trifluoro-2-trifluoromethyl-pent-4-ene-2-ol (**2.17**) (Oakwood) and were used as received unless noted otherwise. Compounds **2.10**, methyl bicyclo[2.2.1]heptane-2-carboxylate, 2,2-difluoronorbornane[6a], and 3-(bicyclo[2.2.1]heptan-2-yl)-1,1,1-trifluoro-2-(trifluoromethyl)propan-2-ol were synthesized by colleagues at the University of Texas, Austin. All liquid reagents used for vacuum UV measurements were distilled from appropriate drying agents, thoroughly degassed by freeze, pump, thaw cycles and sealed in glass ampoules under vacuum.

Methods: Nuclear magnetic resonance (NMR) spectra were obtained using either a Bruker AMX300, Varian *Unity Plus 300*, Varian *Gemini 300*, or Varian *Mercury 300* spectrometer (^{1}H:

300 MHz, ^{13}C: 75 MHz, ^{19}F: 282 MHz). Select NMR spectra for compound 2.10 were obtained using a Varian 500 MHz spectrometer (^{13}C: 125 MHz, ^{19}F: 470 MHz). Shifts for NMR spectra are reported in ppm relative to TMS (for ^{19}F, $CFCl_3$ unless otherwise noted) or to the chemical shift of the residual proteo solvent. Infrared spectra were recorded on either a Nicolet Avatar 360 or a Perkin-Elmer Paragon 1000 IR spectrometer. Mass spectra were measured on a Finnigan *MAT TSQ-700* spectrometer. Gas chromatographs were recorded on a Hewlett Packard *5890 Series II* with an *HP-5* (crosslinked 5% PH ME siloxane) capillary column and flame ionization detector (FID).

X-ray Crystallography: X-ray crystallographic analysis of **2.10** was performed by the X-ray crystallography facility at the University of Texas, Austin. Crystallographic data (experimental procedure, labeled drawings, table of atomic coordinates, complete bond distances and angles, and anisotropic displacement parameters) for compound **2.10** can be found in Appendix A.

Vacuum UV Spectroscopy: Gas phase VUV measurements were made on an Acton *CAMS-507* spectrophotometer fitted with a custom-made gas cell attachment. The details of the cell design and implementation have been described previously.[37] VUV spectra of polymer films were calculated from measurements made with a J. A. Woollam *VU301* variable angle spectroscopic ellipsometer (VASE) and/or measured with the Acton *CAMS-507* spectrophotometer. The films were cast on either silicon wafers (VASE) or calcium fluoride disks (Acton) from solutions in propylene glycol methyl ether acetate (PGMEA) or cyclohexanone and baked at 100-130°C for at least 5 minutes prior to analysis. All absorbance data reported are in base 10.

General Synthesis Procedure for Tricyclononene Compounds: One equivalent of tetracyclo[3.2.0.$0^{2,7}$.$0^{4,6}$]heptane (quadricyclane) and 1-3 equivalents of acrylate were placed in a thick-walled Schlenk tube. The components were degassed and the flask sealed under an atmosphere of argon. For reactions in which radical polymerization of the olefin occurs readily, small amounts (0.001 equiv.) of suitable radical inhibitor such as hydroquinone was added. The reaction mixture was heated to 96 °C for 24-72 hours. The tricyclononene product was separated

from the residual quadricyclane starting material and norbornadiene and polymeric by-products by Kugelrohr vacuum distillation to yield colorless liquids (or solids).

Tricyclo[4.2.1.0^{2,5}]non-7-ene-3-carboxylic acid (2.5). 3-Cyano-tricyclo[4.2.1.0^{2,5}]non-7-ene (prepared by the cycloaddition of quadricyclane with acrylonitrile[18]) (23.6 g, 0.162 mol) was dissolved into 40 mL of ethylene glycol and added to a 250 mL round-bottom flask charged with 1.5 equivalents of potassium hydroxide (13.7 g, 0.244 mol) in 25 mL H_2O. The resulting biphasic system was stirred vigorously while refluxing at 140 °C for 24 hours. The resulting mixture was acidified with 20 mL of HCl (37% solution in H_2O). The product was extracted into ethyl ether and dried over $MgSO_4$. Removal of the solvent *in vacuo* produced a viscous, colorless oil, which crystallized overnight into a white crystalline material. Removal of residual ethylene glycol was achieved via Kugelrohr distillation (80 °C, 60 mTorr) to produce 16.4 g (0.098 mol) of a viscous, colorless oil, which crystallized overnight into a white crystalline material. Yield: 60% (35% over 2 steps from acrylonitrile). Isomer composition: > 98 % anti. Anti isomer: ^{1}H NMR ($CDCl_3$, 300 MHz, ppm): δ 11.27 (br s, COOH), 6.01 (dd, *J* = 2.7, 6.0 Hz, 1H, H-7), 5.96 (dd, *J* = 2.7, 6.0 Hz, 1H, H-8), 2.78 (s, 1H, H-1), 2.70 (s, 1H, H-6), 2.50 (m, 1H, H-3), 2.40 (m, 1H, H-4), 2.23 (m, 1H, H-2), 2.05 (m, 1H, H-5), 1.67 (d, *J* = 8.7 Hz, 1H, H-9 anti), 1.62 (m, 1H, H-4), 1.37 (dt, *J* = 1.7, 9.6 Hz, 1H, H-9 syn). ^{13}C NMR ($CDCl_3$, 75 MHz, ppm): δ 182.91 (COOH), 136.07 (CH, C-7), 134.68 (CH, C-8), 44.31 (CH, C-6), 44.13 (CH, C-1), 40.72 (CH, C-2), 40.48 (CH_2, C-9), 37.55 (CH, C-3), 34.47 (CH, C-5), 24.02 (CH_2, C-4). IR (KBr, Nujol, cm^{-1}): 3050, 1700, 1464, 1417, 1267, 1240, 1211, 927, 692. HRMS-EI (*m/z*): $[M + H]^+$ calcd for $C_{10}H_{13}O_2$, 165.0916; found, 165.0903

***t*-Butyl tricyclo[4.2.1.0^{2,5}]non-7-ene-3-carboxylate (2.6).** Quadricyclane (15 mL, 14.7 g, 0.16 mol) and 4 equiv. *t*-butyl acrylate (92 mL, 80.7 g, 0.63 mol) were reacted according to the general procedure mentioned above to produce, after Kugelrohr vacuum distillation, 28.0 g (0.13 mol) of colorless liquid. Yield: 80%. Isomer composition: 57 % syn, 43 % anti. ^{1}H NMR ($CDCl_3$, 300 MHz, ppm): δ 5.94 (m, 4H, H-7+H-8, syn+anti), 3.12 (ddd, *J* = 7.8, 9.6, 11.1 Hz, 1H, H-3, syn),

2.90 (s, 1H, H-1, syn), 2.70 (s, 1H, H-1, anti), 2.63 (s, 2H, H-6, syn+anti), 2.34-2.05 (5H, syn+anti), 2.02-1.87 (2H, H-5 syn+anti), 1.68 (dd, J = 4.8, 7.8 Hz, 1H, H-4, syn), 1.65-1.58 (2H, H-9 anti, syn+anti), 1.57-1.48 (1H, H-4, anti), 1.44 (s, 9H, C(CH_3)$_3$, syn), 1.43 (s, 9H, C(CH_3)$_3$, anti), δ 1.29 (dt, J = 1.5, 8.1 Hz, 1H, H-9 syn, anti), 1.17 (dt, J = 1.5, 9.6 Hz, 1H, H-9 syn, syn). ^{13}C NMR ($CDCl_3$, 75 MHz, ppm): δ 175.22 (*C*OOtBu, anti), δ 173.40 (*C*OOtBu, syn), 136.07 (olefin C, syn), 135.81 (olefin C, anti), 135.13 (olefin C, syn), 134.61 (olefin C, anti), 80.03 (*C*(CH$_3$)$_3$, syn), 79.77 (*C*(CH$_3$)$_3$, anti), 44.92 (CH, C-6, syn), 44.17 (CH, C-6, anti), 43.96 (CH, C-1, anti), 42.46 (CH, C-1, syn), 40.57 (CH, C-2, anti), 40.41 (CH_2, C-9, anti), 40.36 (CH_2, C-9, syn), 40.14 (CH, C-2, syn), 38.48 (CH, C-3, anti), 35.56 (CH, C-3, syn), 34.26 (CH, C-5, anti), 33.50 (CH, C-5, syn), 28.30 (COOC(*C*H$_3$)$_3$, syn), 28.18 (COOC(*C*H$_3$)$_3$, anti), 23.79 (CH_2, C-4, anti), 23.07 (CH_2, C-4, syn). IR (KBr, cm^{-1}): 3057 (alkene), 2972, 1723 (C=O), 1456, 1391, 1367, 1349, 1322, 1256, 1228, 1215, 1154, 848, 754, 698. HRMS-EI (*m/z*): [M + H]$^+$ calcd for $C_{14}H_{21}O_2$, 221.1542; found, 221.1546.

***t*-Butyl 3-(methyl)tricyclo[4.2.1.0^{2,5}]non-7-ene-3-carboxylate (2.7).** Quadricyclane (15 mL, 14.7 g, 0.16 mol) and 3 equiv. *t*-butyl methacrylate (78 mL, 68.2 g, 0.48 mol) were reacted according to the general procedure mentioned above to produce, after Kugelrohr vacuum distillation, 3.0 g (0.013 mol) of colorless liquid. Yield: 8%. Isomer composition: 55 % syn, 45 % anti. ^{1}H NMR ($CDCl_3$, 300 MHz, ppm): δ 5.98 (m, 4H, H-7+8, syn+anti), 2.95 (s, 1H, H-1, syn), 2.74 (s, 1H, H-1, anti), 2.65 (s, 2H, H-6, syn+anti), 2.44 (m, 1H), 2.1-1.6 (6H, syn+anti), 1.56-1.48 (m, 1H), 1.46 (s, 9H, C(CH_3)$_3$, syn), 1.45 (s, 9H, C(CH_3)$_3$, anti), 1.40 (d, 3H, -CH_3, syn), 1.36-1.18 (4H, syn+anti), 1.16 (d, 3H, -CH_3, anti). ^{13}C NMR ($CDCl_3$, 75 MHz, ppm): δ 178.25 (*C*OOtBu, anti), 176.43 (*C*OOtBu, syn), 136.37 (olefin C, anti), 136.23 (olefin C, syn), 135.71 (olefin C, anti), 135.48 (olefin C, syn), 79.94 (C(CH$_3$)$_3$, syn), 79.79 (C(CH$_3$)$_3$, anti), 48.91 (CH, C-2, syn), 44.63 (CH, C-6, syn), 44.30 (CH, C-2, anti), 43.53 (CH, C-6, anti), 42.99 (CH, C-1, syn), 41.88 (CH_2, C-9, anti), 41.52 (CH, C-1, anti), 41.35 (quat. C, C-3, syn), 41.07 (quat. C, C-3, anti), 40.65 (CH_2, C-9, syn), 33.09 (CH, C-5, anti), 31.36 (CH_2, C-4, anti), 31.08 (CH_2, C-4,

syn), 30.48 (CH, C-5, syn), 28.37 (CH_3, syn), 28.32 ($C(CH_3)_3$, syn), 28.17 ($C(CH_3)_3$, anti), 16.91 (CH_3, anti). IR (KBr, cm^{-1}): 3057 (alkene), 2972, 1720 (C=O), 1470, 1456, 1391, 1367, 1313, 1281, 1256, 1227, 1131, 849, 757, 703. HRMS-EI (*m/z*): $[M + H]^+$ calcd for $C_{15}H_{23}O_2$, 235.1698; found, 235.1698.

Methyl 3-(trifluoromethyl)tricyclo[4.2.1.0^{2,5}]non-7-ene-3-carboxylate (2.8). Quadricyclane (1.5 equiv., 4.25 g, 0.046 mol) and methyl (2-trifluoromethyl)acrylate[6a] (1 equiv., 4.55 g, 0.30 mol) were reacted according to the general procedure mentioned above to produce, after Kugelrohr vacuum distillation, 6.78 g (0.028 mol) of colorless liquid. Yield: 94%. Isomer composition: 32 % syn, 68 % anti. ^{1}H NMR ($CDCl_3$, 300 MHz, ppm): 6.1-5.9 (m, 4H, H-7+H-8, syn+anti), 3.80 (s, 3H, COOC*H*$_3$, syn), 3.78 (s, 3H, COOC*H*$_3$, anti), 3.06 (s, 1H, H-1, syn), 2.99 (s, 1H, H-1, anti), 2.82 (s, 1H, H-6, syn), 2.74 (s, 1H, H-6, anti), 2.68 (ddd, *J* = 3.0, 7.5, 13.2 Hz, 1H, anti), 2.5-1.9 (7 H), 1.48-1.24 (4 H). ^{13}C NMR ($CDCl_3$, 75 MHz, ppm): δ 171.16 (d, *J* = 2.9 Hz, *C*OOMe, syn), 168.85 (d, *J* = 2.4 Hz, *C*OOMe, anti), 136.74 (olefin C, anti), 136.62 (olefin C, syn), 135.24 (olefin C, syn), 135.06 (olefin C, anti), 126.32 (q, *J* = 280 Hz, CF_3, anti), 125.16 (q, *J* = 281 Hz, CF_3, syn), 53.30 (COO*C*H3, syn), 52.81 (COO*C*H$_3$, anti), 49.56 (q, *J* = 28.6 Hz, quat. C, C-3, syn), 49.40 (q, *J* = 26.5 Hz, quat. C, C-3, anti), 44.50 (CH, C-6, anti) 44.18 (CH, C-6, syn), 44.15(CH, C-2, syn), 42.86 (CH, C-1, syn), 42.50 (CH, C-1, anti), 41.95 (m, *J* = 2.0 Hz, CH, C-2 anti), 41.14 (m, CH_2, C-9, anti), 40.71 (CH_2, C-9, syn), 32.98 (CH, C-5, syn), 32.83 (CH, C-5, anti), 26.07 (d, *J* = 2.4 Hz, CH_2, C-4, anti), 25.93 (d, *J* = 1.9 Hz, CH_2, C-4, syn). ^{19}F NMR ($CDCl_3$, 282 MHz, ppm) (referenced to external C_6F_6 standard at -166.717 ppm): δ -66.25 (s, 3F, -CF_3, syn), -75.13 (s, 3F, -CF_3,, anti). IR (KBr, cm^{-1}): 3060 (alkene), 2970, 2892, 1742 (C=O), 1473, 1436, 1333, 1322, 1275, 1225, 1163, 1132, 1087, 712, 671. HRMS-EI (*m/z*): $[M]^+$ calcd for $C_{12}H_{14}F_3O_2$, 246.0868; found, 246.0868 .

Triethylaminoboron trifluoride.[38] To a cooled (dry ice/acetone) 250 mL round-bottom flask equipped with a stir bar and addition funnel was added boron trifluoride diethyl etherate (30 g, 211 mmol). Triethylamine (60 mL) was added dropwise to the flask via an addition funnel. The

formation of white precipitate was immediately observed. After the addition of triethylamine, the reaction was allowed to warm to room temperature, and excess triethylamine was removed *in vacuo*. The white residue was purified by vacuum fractional distillation (85°C / 3 mm Hg) to give a white solid (32.0 g, 91%), which melted at approximately 25°C. The compound was kept in the refrigerator and used in the next step without further purification.

Methyl 3,3-difluoro-2-(trifluoromethyl)acrylate. A slight modification of the literature procedure was used.[39] To a 100 mL round-bottom flask equipped with a magnetic stir bar and reflux condenser were added triethylaminoboron trifluoride (32.0 g, 189 mmol) and methyl 2-(trifluoromethyl)-3,3,3-trifluoropropionate (30.5 g, 145 mmol). The reaction mixture was refluxed for 3 h and then cooled to room temperature. The residue was purified by vacuum transfer (bulb to bulb distillation) to give a clear oil (19.8 g, 71%). ^{1}H NMR ($CDCl_3$, 300 MHz, ppm): δ 3.84 (s, 3H, methyl). ^{19}F NMR (CD_3OD, 282 MHz, ppm): δ -58.5 (m, 1F, RC=CF_2), -59.1 (m, 3F, CF_3), -59.5 (m, 1F, RC=CF_2). IR (NaCl, cm^{-1}): 2960, 1767 (C=O), 1710, 1439, 1372, 1152, 1081, 1040, 1024. HRMS-CI (*m/z*): $[M + H]^+$ calcd for $C_5H_3F_5O_2$, 191.0131; found, 191.014.

Methyl 4,4-difluoro-3-(trifluoromethyl)tricyclo-[4.2.1.0^{2,5}]non-7-ene-3-carboxylate (2.9). To a 300 mL Parr pressure reactor equipped with a magnetic stir bar were added quadricyclane (1.5 g, 16.3 mmol) and methyl 3,3-difluoro-2-(trifluoromethyl)acrylate (3.9 g, 20.4 mmol). The pressure vessel was sealed, and the reaction mixture was stirred at 100°C for 72 hours. After cooling to room temperature, the residue was purified by fractional vacuum distillation (39-40°C / 0.30 mm Hg) to yield a clear oil (1.0 g, 22%). In a subsequent synthesis, it was found that if the reaction was allowed to sit at room temperature for 14 days after the initial heating, the isolated yield increased to 73%. Isomer composition: 49% syn, 51% anti. ^{1}H NMR ($CDCl_3$, 300 MHz, ppm): δ 6.27 (dd, *J* = 2.7, 5.7 Hz, olefin H, 1H, anti), 6.05-6.15 (m, olefin H, 3H, 2 syn+1 anti), 3.87 (s, COOCH_3, 3H, anti), 3.86 (s, COOCH_3, 3H, syn), 3.53 (s, 1H, H-1, syn), 3.22 (2H, H-1,

H-6, anti), 3.13 (s, 1H, H-6, syn), 2.84-2.75 (m, 1H, H-5, anti), 2.75-2.6 (m, 1H, H-5, syn), 2.39-2.31 (m, 1H, H-2, syn), 2.10 (d, *J* = 10.2 Hz, 1H, H-2, anti), 1.50-1.30 (m, 4H, H-9 syn, H-9 anti, syn+anti). ^{13}C NMR (C_6D_6, 75 MHz, ppm): 165.11 (COOMe, syn), 162.91 (COOMe, anti), 139.62 (olefin C, anti), 137.82 (olefin C, syn), 136.93 (olefin C, syn), 136.77 (olefin C, anti), 123.97, (q, J = 283 Hz, CF_3, syn), 123.68 (q, J = 280 Hz, CF_3, anti), 116.72 (t, *J* = 292 Hz, C-5), 114.09, (t, *J* = 296 Hz, C-5), 53.32 (COO*C*H$_3$, anti), 52.64 (COO*C*H$_3$, syn), 50.70 (dd, *J* = 19.2, 26 Hz, CH, C-5, anti), 50.36 (t, *J* =23 Hz, CH, C-5, syn), 43.71 (CH, C-1, anti), 43.26 (CH, C-1, syn), 43.11 (dd, *J* = 4.4, 8.2 Hz, CH_2, C-9, anti), 42.82 (d, *J* = 6.6 Hz, CH_2, C-9, syn), 42.08 (CH, C-6, anti), 41.29 (t, *J* = 2.3 Hz, CH, C-6, syn), 37.21(dd, J = 4.9, 12 Hz, CH, C-2, anti), 36.90 (m, CH, C-2, syn). ^{19}F NMR (Acetone, 282 MHz, ppm): δ –61.67 (d, *J* = 6.7 Hz, 3F, CF_3, anti), -68.36 (d, *J* = 2.0 Hz, 3F, CF_3, syn), -85.70 (dm, *J* = 211 Hz, 1F, F-4 syn, anti), -97.15 (dm, *J* = 217 Hz, 1F, F-4 anti, syn), -106.87 (d, *J* = 217 Hz, 1F, F-4 syn, syn), -113.94 (d, *J* = 211 Hz, 1F, F-4 anti, anti). IR (NaCl, cm^{-1}): 3058 (alkene), 2991, 2909, 1752 (C=O), 1429, 1317, 1219, 1045, 897, 794, 697. HRMS-CI (*m/z*): $[M + H]^+$ calcd for $C_{12}H_{12}F_5O_2$, 283.0757; found, 283.0755.

4,4-Difluoro-3-(trifluoromethyl)tricyclo-[4.2.1.0^{2,5}]non-7-ene-3-carboxylic acid (2.10). Hydrolysis of **2.9** with KOH and water under standard conditions produced the carboxylic acid. One of the isomers selectively crystallized from solution and was determined to be the syn isomer by x-ray crystallography. Syn isomer: ^{1}H NMR ($CDCl_3$, 300 MHz, ppm): δ 9.6-8.4 (br s, 1H, COOH), 6.16 (m, 2H, H-7+H-8), 3.50 (s, 1H, H-1), 3.16 (s, 1H, H-6), 2.69 (m, *J* = 4.2 Hz, 1H, H-5), 2.35 (m, 1H, H-2), 1.45 (s, 2H, H-9 syn, H-9 anti). ^{13}C NMR ($CDCl_3$, 125 MHz, ppm): δ 167.63 (COOH), 137.94 (C-8), 137.082 (C-7), 122.93 (q, *J* = 282 Hz, CF_3), 116.08 (t, *J* =290 Hz, C-4), 59.5 (quat. C, C-3), 50.25 (t, *J* =23 Hz, CH, C-5), 43.04 (CH, C-1), 42.80 (d, *J* = 6.4 Hz, CH_2, C-9), 41.25 (t, *J* = 1.8 Hz, CH, C-6), 36.77 (m, CH, C-2). ^{19}F NMR ($CDCl_3$, 470 MHz, ppm): δ -68.94 (dd, *J* = 2.4, 17.0 Hz, 3F, CF_3), -97.81 (dm, *J* = 217 Hz, 1F, F-4 anti), -107.95 (d, *J* = 217 Hz, 1F, F-4 syn). HRMS-CI (*m/z*): $[M + H]^+$ calcd for $C_{11}H_{10}F_5O_2$, 269.0601; found, 269.0589.

General Hydrogenation Procedure: Norbornene or tricyclononene monomer (5.86 mmol) was dissolved in 16 mL ethyl acetate in a 250 mL Parr bomb (Parr Instrument Company, MAWP 3000psi at 350 °C). Palladium (10 % on carbon, 0.015g) was added to the bomb, which was pressurized to 50 psi with H_2. The reaction mixture was stirred overnight at room temperature, the catalyst was removed with a 0.45 μm PTFE syringe filter, and the solvent was removed by rotary evaporation to yield a clear oil.

1,1,1-Trifluoro-2-trifluoromethyl-pent-4-ene-2-ol (2.17). ^{1}H NMR ($CDCl_3$, 300 MHz, ppm): δ 6.22 (m, 1H), 5.93 (m, 1H), 5.85 (m, 1 H), 5.24 (dm, 1H), 5.19 (m, 1H), 4.10 (d, 1H, *J* = 6.6 Hz), 2.83 (br s, 2H), 2.76 (d, 2H, *J* = 7.2 Hz), 1.8-1.4 (4H). ^{13}C NMR ($CDCl_3$, 75.46 MHz, ppm): δ 141.78, 132.93, 129.38, 120.23, 48.97, 46.24, 40.58, 36.41, 34.10. ^{19}F NMR ($CDCl_3$, 282 MHz, ppm) (referenced to internal C_6F_6 at -162.2 ppm): δ -77.03 (s).

5-(1,1-Bis-trifluoromethyl-but-3-enyloxy)-bicyclo[2.2.1]hept-2-ene (2.18a). Quadricyclane (0.50g, 5.43 mmol) and 1,1,1-trifluoro-2-trifluoromethyl-pent-4-ene-2-ol (**2.17**) (1.13 g, .43 mmol) were added to a Schlenk tube and degassed via 3 free-pump-thaw cycles. The tube was sealed and heated at 95 °C for3 days. Silica gel column chromatography (20:1 pentane: ether) afforded a 1.4:1 mixture of **2.18a** and 3-(1,1-bis-trifluoromethyl-but-3-enyloxy)-tricyclo[2.2.1.0^{2,6}]heptane (**2.18b**). The norbornenyl ether **2.18a** was separated from **2.18b** via 3 successive silica gel columns (100% pentane) to afford **2.18a** as a colorless liquid. **2.18a** R_f = 0.61 (100% hexane), **2.18b** R_f = 0.56 (100% hexane). Characterization for **2.18a**: ^{1}H NMR ($CDCl_3$, 300 MHz, ppm): δ 6.22 (m, 1H), 5.93 (m, 1H), 5.85 (m, 1 H), 5.24 (dm, 1H), 5.19 (m, 1H), 4.10 (d, 1H, *J* = 6.6 Hz), 2.83 (br s, 2H), 2.76 (d, 2H, *J* = 7.2 Hz), 1.8-1.4 (4H). ^{13}C NMR ($CDCl_3$, 75.46 MHz, ppm): δ 141.78, 132.93, 129.38, 120.23, 48.97, 46.24, 40.58, 36.41, 34.10. ^{19}F NMR ($CDCl_3$, 282 MHz, ppm): δ -72.28 (s). *g*HSQC and *g*COSY experiments confirmed the assigned structure. HRMS-EI/GC (*m/z*): $[M\bullet]^+$ calc'd for $C_{13}H_{14}F_6O$, 300.0949; found, 300.0958. Characterization for **2.18b**: ^{1}H NMR ($CDCl_3$, 300 MHz, ppm): δ 5.86 (m, 1H), 5.25 (dm, 1H),

5.19 (m, 1H), 4.13 (s, 1H, J = 6.6 Hz), 2.76 (d, 2H, J = 6.9 Hz), 2.0-1.9 (m, 2H), 1.4-1.2 (6H). ^{19}F NMR ($CDCl_3$, 282 MHz, ppm): δ -76.75 (m, 3F), -77.19 (m. 3F).

1,1,1-Trifluoro-2-(*t*-butyldimethylsilyloxy)-2-trifluoromethyl-pent-4-ene (2.19). 1,1,1-trifluoro-2-trifluoromethyl-pent-4-ene-2-ol (**2.17**)[6a] (3.0 g, 14.4 mmol) was added slowly to a 30 mL suspension of sodium hydride (0.38 g, 15.8 mmol, 1.1 eq.) in dry tetrahydrofuran. The reaction was stirred at 40 °C for 1 hour to ensure complete reaction. Subsequently, the reaction was cooled to 0 °C and a solution of t-butyldimethylsilyl chloride (2.39g, 15.8 mmol, 1.1 equiv) in 5 mL of tetrahydrofuran was added. The reaction was heated at 40 °C overnight. The reaction mixture was concentrated and the reaction product purified via silica gel chromatography (50:1 pentane:ether) to afford 4.16 g (90 %) of **2.19** as a colorless liquid. R_f = 0.91 (20:1 hexane/ethyl acetate). ^{1}H NMR ($CDCl_3$, 300 MHz, ppm): δ 5.82 (m, 1 H), 5.23 (dm, 1H), 5.18 (m, 1H), 2.70 (d, 2H, J = 7.2 Hz), 0.91, (s, 9H), 0.19 (s, 6H).). ^{13}C NMR ($CDCl_3$, 75.46 MHz, ppm): δ 129.32, 123.18 (q, J = 289 Hz, CF_3), 120.36, 37.23, 25.62, -3.33. ^{19}F NMR ($CDCl_3$, 282 MHz, ppm) (Referenced to internal C_6F_6 at -162.2 ppm): δ -75.37 (s).

References and Notes

(1) *International Technology Roadmap for Semiconductors, 2000 Update*, SRC, http://public.itrs.net/Files/2000UpdateFinal/ORTC2000final.pdf.

(2) Patterson, K.; Somervell, M.; Willson, C. G. *Solid State Technol.* **2000**, *43(3)*, 41-48.

(3) (a). Bloomstein, T. M.; Rothschild, M.; Kunz, R. R.; Hardy, D. E.; Goodman, R. B.; Palmacci, S. T. *J. Vac. Sci. Technol. B* **1998**, *16*, 3154-3157. (b). Rothschild, M.; Bloomstein, T. M.; Curtin, J. E.; Downs, D. K.; Fedynyshyn, T. H.; Hardy, D. E.; Kunz, R. R.; Liberman, V.; Sedlacek, J. H. C.; Uttaro, R. S.; Bates, A. K.; Van Peski, C. *J. Vac. Sci. Technol. B* **1999**, *17*, 3262-3266.

(4) (a). Kunz, R. R.; Bloomstein, T. M.; Hardy, D. E.; Goodman, R. B.; Downs, D. K.; Curtin, J. E. *J. Vac. Sci. Technol. B* **1999**, *17*, 3267-3272. (b). Kunz, R. R.; Bloomstein, T. M.;

Hardy, D. E.; Goodman, R. B.; Downs, D. K.; Curtin, J. E. *J. Photopolym. Sci. Technol.* **1999**, *12*, 561-570.

(5) (a). Matsuzawa, N. N.; Mori, S.; Yano, E.; Okasaki, S.; Ishitani, A.; Dixon, D. A. *Proc. SPIE*, **2000**, *3999*, 375-384. (b). Toriumi, M.; Satou, I.; Itani, T. *J. Vac. Sci. Technol. B* **2000**, *18*, 3328-3331.

(6) (a). Chiba, T.; Hung, R. J.; Yamada, S.; Trinque, B.; Yamachika, M.; Brodsky, C.; Patterson, K.; Vander Heyden, A.; Jamison, A.; Lin, S. H.; Somervell, M.; Byers, J.; Conley, W.; Willson, C. G. *J. Photopolymer Sci. Technol.* **2000**, *13*, 657-664. (b). Brodsky, C.; Byers, J.; Conley, W.; Hung, R.; Yamada, S.; Patterson, K.; Somervell, M.; Trinque, B.; Tran, H. V.; Cho, S.; Chiba, T.; Lin, S-H.; Jamieson, A.; Johnson, H.; Vander Heyden, T.; Willson, C. G. *J. Vac. Sci. Technol. B.* **2000**, *18*, 3396-3401.

(7) Grandler, J. R.; Jencks, W. P. *J. Am. Chem. Soc.* **1982**, *104*, 1937-1951.

(8) (a). Okoranynawu, U.; Shimokawa, T.; Byers, J.; Willson, C. G. *Chem. Mater.* **1998**, *10*, 3319-3327. (b). Okoranynawu, U.; Byers, J.; Shimokawa, T.; Willson, C. G. *Chem. Mater.* **1998**, *10*, 3328-3333. (c). Allen, R. D.; Opitz, J.; Wallow, T. I.; DiPietro, R. A.; Hofer, D. C.; Jayaraman, S.; Hullihan, K. A.; Rhodes, L. F.; Goodall, B. L.; Shick, R. A. *Proc. SPIE* **1998**, *3333*, 463-471. (d). Goodall, B. L., Jayaraman, S.; Shick, R. A.; Rhodes, L. F. *PCT Int. Appl. WO 9733198*, **1997**.

(9) No homopolymer of methyl 2-(trifluoromethyl)-norborn-5-ene-2 carboxylate was isolated after attempted polymerization with palladium or nickel catalysts. In copolymerizations with the hexafluoroisopropyl alcohol norbornene **2.2**, the geminally di-substituted norbornene was incorporated in significantly lower than stoichiometric amounts and low (< 10%) overall yields were observed. (a). Hung, R. J.; Tran, H. V.; Trinque, B. C.; Chiba, T.; Yamada, S.; Sanders, D.; Connor, E. F.; Grubbs, R. H.; Klopp, J. M.; Frechet, J. M. J.; Thomas, B. H.; Shafer, G. J.; DesMarteau, D. D.; Conley, W.; Willson, C. G. *Proc. SPIE* **2001**, *4345*, 385-395. (b). Tran, H. V.; Hung, R. J.; Chiba, T.; Yamada, S.; Mrozek, T.;

Hsieh, Y-T.; Chambers, C. R.; Osborn, B. P.; Trinque, B. C.; Pinnow, M. J.; Sanders, D. P.; Connor, E. F.; Grubbs, R. H.; Conley, W.; MacDonald, S. A.; Willson, C. G. *J. Photopolym. Sci. Technol.* **2001**, *14*, 669-674.

(10) Connor, E. F.; Younkin, T. R.; Henderson, J. I.; Grubbs, R. H.; Roberts, W. P.; Litzau, J. J. *J. Polym. Sci. A: Polym. Chem.* **2002**, *40*, 2842-2854.

(11) (a). Smith, C. D. *J. Am. Chem. Soc.* **1966**, *88*, 4273-4274. (b). Prinzbach, H; Rivier, J. *Angew. Chem., Int. Ed. Engl.* **1967**, *6*, 1069-1070. (c). Prinzbach, H. *Pure Appl. Chem.* **1968**, *16*, 17-46. (d). Rieber, N.; Alberts, J.; Lipsky, J. A.; Lemal, D. M. *J. Am. Chem. Soc.* **1969**, *91*, 5668-5669. (e). Tabushi, I.; Yamamura, K.; Yoshida, Z. *J. Am. Chem. Soc.* **1972**, *94*, 787-792.

(12) The addition of the olefin to quadricyclane by a thermal homo-*endo*-type cyclization to produce a tetracyclo[4.3.0.$0^{2,4}$.$0^{3,7}$]nonane (deltacyclane) is a forbiddden process,[11d] although this cycloaddition proceeds in the presence of nickel(0) complexes. Noyori, R.; Umeda, I.; Kawauchi, H.; Takaya, H. *J. Am. Chem. Soc.* **1975**, *97*, 812-820.

(13) The allowed thermal homo-Diels-Alder cycloaddition of norbornadiene with electron deficient olefins produces tetracyclononane (deltacyclane) compounds. (a). Ullman, E. F. *Chem. Ind. (London)* **1958**, 1171-1174. (b). Blomquist, A. T.; Meinwald, Y. C. *J. Am. Chem. Soc.* **1959**, *81*, 667-672. (c). Hall, H. K., Jr. *J. Org. Chem.* **1960**, *25*, 42-44. (d). Cookson, R. C.; Dance, J.; Hudec, J. *J. Chem. Soc.* **1964**, 5416-5422. (e). For additional references see reference 11 within reference 14b.

(14) (a). Lautens, M.; Tam, W.; Lautens, J. C.; Edwards, L. G.; Crudden, C. M.; Smith, A. C. *J. Am. Chem. Soc.* **1995**, *117*, 6863-6879. (b). Lautens, M.; Edwards, L. G.; Tam, W.; Lough, A. J. *J. Am. Chem. Soc.* **1995**, *117*, 10276-10291 and references therein.

(15) Schrauzer, G. N.; Glockner, P. *Chem. Ber.* **1964**, *97*, 2451-2462.

(16) The norbornadienes found to undergo such reactions were substituted at one double bond with either electron-donating methoxy or electron-withdrawing ester functionalities. See reference 14b.

(17) (a). Haselbach, E.; Martin, H-D. *Helv. Chim. Acta* **1974**, *57*, 472-480. (b). Papadopoulos, M.; Jenner, G. *Nouv. J. Chim.* **1983**, *7*, 463-464. (c). Papadopoulos, M.; Jenner, G. *Nouv. J. Chim.* **1984**, *8*, 729-732. (d). Paquette, L. A.; Kesselmayer, M. A.; Kunzer, H. *J. Org. Chem.* **1988**, *53*, 5183-5185. (e). Jones, G. A.; Shepard, M. J.; Paddon-Row, M. N.; Beno, B. R.; Houk, K. N.; Redmond, K.; Carpenter, B. K. *J. Am. Chem. Soc.* **1999**, *121*, 4334-4339.

(18) Takaya, H.; Yamakawa, M.; Noyori, R. *Bull. Chem. Soc. Jpn.* **1982**, *55*, 852-858.

(19) Since the reactivity of norbornadiene (formed during the reaction) towards the electron-deficient olefins is considerably less than that of quadricyclane,[10e] no tetracyclononane products were observed to form by ^{1}H NMR under the reaction conditions used in this study.

(20) Previously, these compounds have been synthesized as components of complex product mixtures formed by heating methyl methacrylate or methacrylonitrile with norbornadiene at 200 °C for 12 hours. Applequist, D. E.; England, D. C. *US Pat. 2940984*, **1960**.

(21) (a). Meek, J. S.; Trapp, W. B. *J. Am. Chem. Soc.* **1957**, *79*, 3909-3912. (b). Martin, J. G.; Hill, R. K. *Chem. Rev.* **1961**, *61*, 537-562. (c). Kobuke, Y.; Fueno, T.; Furukawa, J. *J. Am. Chem. Soc.* **1970**, *92*, 6548-6553. (d). Kobuke, Y.; Sugimoto, T.; Furukawa, J.; Fueno, T. *J. Am. Chem. Soc.* **1972**, *94*, 3363-3365.

(22) (a). Begue, J. P.; Bonnet-Delphon, D.; Lequeux, T.; d'Angelo, J.; Guingant, A. *Synlett* **1992**, 146-148. (b). Bruckner, R.; Huisgen, R.; *Tetrahedron Lett.* **1994**, *35*, 3285-3288.

(23) Rate acceleration in Diels-Alder type reactions by trifluoromethyl groups has been attributed to the enhanced lowering of the LUMO of the dienophile over that achieved by a

methyl group. Pascal, Y. L.; Chanet-Ray, J.; Vessiere, R.; Zeroual, A. *Tetrahedron*, **1992**, *48*, 7197-7208.

(24) (a). McBee, E. T.; Hsu, C. G.; Roberts, C. W. *J. Am. Chem. Soc.* **1956**, *78*, 3389-3392. (b). McBee, E. T.; Hsu, C. G.; Roberts, C. W. *J. Am. Chem. Soc.* **1956**, *78*, 3393-3394. (c). Braedlin, H. P.; Zielinski, A. Z.; McBee, E. T. *J. Am. Chem. Soc.* **1962**, *84*, 2109-2112. (d). McBee, E. T.; Keogh, M. J.; Levek, R. P.; Wesseler, E. P. *J. Org. Chem.* **1973**, *38*, 632-636.

(25) (a). Hanzawa, Y.; Suzuki, M.; Kobayashi, Y. *Tetrahedron Lett.* **1989**, *30*, 571-574. (b). Hanzawa, Y.; Suzuki, M.; Kobayashi, Y.; Taguchi, T.; Itaka, Y. *J. Org. Chem.* **1991**, *56*, 1718-1725.

(26) Bott, G.; Field, L. D.; Sternhell, S. *J. Am. Chem. Soc.* **1980**, *102*, 5618-5626.

(27) Leroy, J.; Fischer, N.; Wakselman, C. *J. Chem. Soc. Perkin Trans. I* **1990**, 1281-1287.

(28) Martin, H. D.; Iden, R.; Scheutzow, D.; Jackman, L. M. *Org. Magn. Res.* **1980**, *14*, 192-197.

(29) Edwards, L. G.; Lautens, M.; Lough, A. J. *Z. Kristall.* **1996**, *211*, 919-923.

(30) Niu, Q. J.; Frechet, J. M. J. *Angew. Chem. Int. Ed.* **1998**, *37*, 667-670.

(31) (a). Johs, B.; French, R. H.; Kalk, F. D.; McGahan, W. A.; Woollam, J. A. *Proc. SPIE*, **1994**, *2253*, 1098-1106. (b). French, R. H.; Whelan, R. C.; Jones, D. J.; Hilfiker, J. N.; Synowicki, R. A.; Zumsteg, F. C.; Feldman, J.; Feiring, A. E. *Proc. SPIE* **2000**, *4000*, 1491-1502.

(32) Osborn, B. P. *Ph.D. Dissertation* University of Texas, Austin, **2004**.

(33) Trinque, B. C.; Chambers, C. R.; Osborn, B. P.; Callahan, R. P.; Lee, G. S.; Kusomoto, S.; Sandes, D. P.; Grubbs, R. H.; Conley, W. E.; Willson, C. G. *J. Fluor. Chem.* **2003**, *122*, 17-26.

(34) Dauben, W. G.; Cargill, R. L. *Tetrahedron* **1961**, *15*, 197-201.

(35) Following our publication of the advantages of the tricyclononene framework, researchers at Air Products, Inc. attempted a similar cycloaddition between quadricyclane and bis(hexafluorocarbinol)-functionalized alkenes. They also observed the exclusive formation of norbornenyl ethers. Metal-catalyzed addition polymers of these hexafluorocarbinol-functionalized norbornenyl ethers afforded the some of the most transparent addition polymers to date. (A_{10}^{157nm} = 0.8 μm^{-1}). Marsela, J. A.; Abdourazak, A. H.; Carr, R. V. C.; Markley, T. J.; Robertson, E. A., III. *Proc. SPIE* **2004**, *5376*, 266-275.

(36) Pangborn, A. B.; Giardello, M. A.; Grubbs, R. H.; Rosen, R. K.; Timmers, F. J. *Organometallics* **1996**, *15*, 1518-1520.

(37) Brodsky, C.; Byers, J.; Conley, W.; Hung, R.; Yamada, S.; Patterson, K.; Somervell, M.; Trinque, B.; Tran, H. V.; Cho, S.; Chiba, T.; Lin, S-H.; Jamieson, A.; Johnson, H.; Vander Heyden, T.; Willson, C. G. *J. Vac. Sci. Technol. B.* **2000**, *18*, 3396-3401.

(38) Kraus, C. A.; Brown, E. H. *J. Am. Chem. Soc.* **1929**, *51*, 2690-2696.

(39) Knunyants, I. L.; Zeifman, Y. V.; Lushnikova, T. V.; Rokhlin, E. M.; Abduganiev, Y. G.; Utebaev, U. *J. Fluorine Chem.* **1975**, *6*, 227-241.

CHAPTER 3

Metal-catalyzed Addition Polymers of Fluorinated Tricyclononenes for Advanced Lithographic Applications

Metal-catalyzed Addition Polymers of Fluorinated Tricyclononenes for Advanced Lithographic Applications

Abstract Fluorinated tricyclo[4.2.1.$0^{2,5}$]non-7-ene-3-carboxylic acid esters are shown to undergo metal-catalyzed addition polymerization. The resulting homopolymers offer enhanced transparencies at 157 nm relative to conventional ester-functionalized polynorbornenes as determined by variable angle spectroscopic ellipsometry (VASE). To demonstrate their utility in the development of photoresists for 157 nm lithography, a fluorinated ester-functionalized tricyclononene is copolymerized with a hexafluorocarbinol-functionalized norbornene to produce an imageable photoresist copolymer. This copolymer exhibits significantly improved transparency relative to its non-fluorinated norbornene analogue. The preliminary lithographic imaging performance of the tricyclononene-based resists is compared to that of other addition copolymer resists. All resists based on carboxylic acid ester solubility switches require the use of a dissolution inhibitor to control their characteristic swelling behavior during development. The higher transparency and absence of swelling behavior of *t*-butoxycarbonyl-protected hexafluorocarbinol-based resists result in high resolution patterns. These results indicate that protected hexafluorocarbinols are the preferred solubility switching motif for 157 nm photoresists based on norbornene addition polymers.

Introduction

Specialized, alicyclic fluoropolymers are the focus of intense research as the semiconductor industry attempts to develop the functional photoresists required to enable the timely introduction of 157 nm optical lithography, as outlined in the International Technical Roadmap for Semiconductors (ITRS) timeline.[1,2] A prominent concern for 157 nm lithography is the feasibility of employing a practical resist thickness (> 200 nm), which requires a photoresist with a low absorption coefficient.[3] In order to fulfill this requirement while retaining optimal

imaging properties, a critical balance of several, often competing, material properties, such as transparency, etch resistance, glass transition temperature, thermal stability, and dissolution behavior, must be achieved. Metal-catalyzed addition polymers of norbornene, based on such monomers as the norbornene *t*-butyl ester (NBTBE, **3.1**, Figure 3.1), were developed for use at 193 nm, with the carbon-rich and heteroatom-deficient norbornane backbone structures proving to be suitable replacements for the heavily absorbing, etch-resistant aromatics used in previous generations of photoresists. Unfortunately, like the majority of the polar functionalities (esters, carbonates, alcohols, and anhydrides) used in resist chemistry,[4] the high absorbance of ester-functionalized monomers such as **3.1** prevents their use at 157 nm.

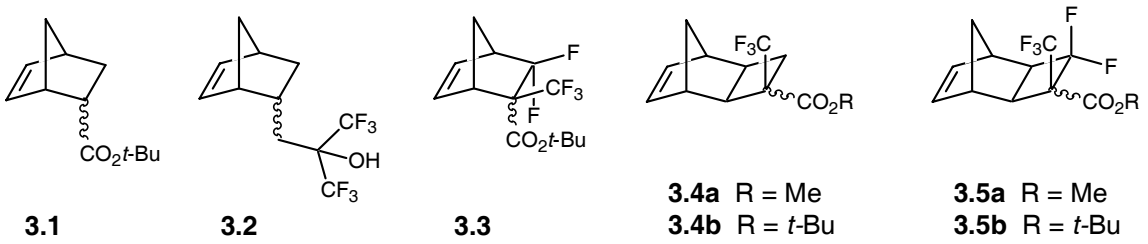

Figure 3.1. Norbornene-type monomers for 157 nm photoresists

Through computational[5] and experimental[6] efforts, it was discovered that the incorporation of fluorinated substituents dramatically reduces the absorption of various structures at 157 nm. For example, the hexafluoroisopropanol-functionalized norbornene (NBHFA, **3.2**) was found to be highly transparent.[6] In addition, due to the inductive effects of the two trifluoromethyl groups, the acidity of the this type of fluorinated alcohol is similar to phenol,[7] allowing this polar monomer to replace the highly absorbing phenolic structures used in previous generations of resists. The incorporation of an α-trifluoromethyl group was found to significantly reduce the absorption of carboxylic acid esters.[6] Systematic experimental[8] and computational[9] studies on the effect of fluorination on the transparency of norbornene indicate that substitution at the 2 position is more beneficial than at the 7 position and disubstitution is more effective than

monosubstitution. With these design principles in hand, the fluorinated monomer **3.3** was subsequently designed as an ideal replacement for the highly absorbing norbornene **3.1**. Unfortunately, norbornene monomers of this type with geminal electron-withdrawing ester and trifluoromethyl substituents were found to be unsuitable for polymerization with common nickel and palladium catalysts.[10] The addition of an α-trifluoromethyl group in **3.3**, while addressing the transparency problem, hinders the polymerization. Thus, alternative approaches towards a polymerizeable monomer incorporating these transparent esters were investigated.

Recently, we synthesized a series of fluorinated ester-functionalized tricyclo[4.2.1.$0^{2,5}$]non-7-ene (TCN) monomers (**3.4** and **3.5**).[11] By moving the sterically bulky, geminal electron-withdrawing functionalities an additional carbon away from the double bond onto the cyclobutane ring (which is exclusively in the exo configuration), we hoped to improve the reactivity of the tricyclononene monomers towards metal-catalyzed addition polymerization. Initial gas phase transparency measurements of saturated TCN compounds revealed their enhanced transparencies at 157 nm relative to non-fluorinated norbornane analogues. While the use of TCN chemistry in photoresists is a potential solution to the polymerization difficulties of the partially fluorinated norbornenes mentioned previously, confirmation of the enhanced transparency and polymerization activity is required. Herein, we report the synthesis of ester-functionalized TCN homopolymers and copolymers for thin film transparency measurements. The initial imaging performance of a TCN-based photoresist is compared to other norbornene addition polymer resists under development.

Results and Discussion

Synthesis of TCN Homopolymers The most common late transition metal catalyst systems used to polymerize norbornene systems by an addition mechanism are based on nickel[12] and palladium.[13-15] To produce model polymers, monomers **3.1**, **3.2**, **3.4**, and **3.5** were polymerized using cationic palladium allyl hexafluoroantimonate catalyst reported by Risse,[14] selected for its ready availability, ease of preparation, and tolerance to polar functionalities. Polymerization

proceeded at room temperature with quantitative disappearance of the monomer after 24-36 hours by ^{1}H NMR. While the reaction is considerably slower than the polymerization of norbornene, it is comparable to the polymerization of norbornenes possessing polar substituents.[14,15] Indeed, due to the nearly identical olefin structure, the behavior of TCN monomers is similar to that of norbornene monomers. For example, we have observed that TCN monomers undergo facile radical copolymerization with maleic anhydride to produce alternating copolymers,[16] analogous to the functionalized norbornene-maleic anhydride copolymers[17] developed for 193 nm lithography.

During polymerization of monomers containing *t*-butyl esters (such as **3.1** and **3.4b**), catalytic deprotection of the *t*-butyl esters was observed (with the generation of isobutylene and carboxylic acid observed by ^{1}H NMR), resulting in precipitation of the deprotected polymers. Unlike our experiences with a (η_6-tolyl)nickel(perfluorophenyl)$_2$ catalyst, some acid is apparently formed during polymerization using the cationic palladium catalyst, presumably as a result of chain transfer reactions. This formation of $HSbF_6$, a very strong acid, is disastrous. This premature deprotection presented a large problem because selective reprotection of some acidic functionalities with acid-labile protecting groups (for solubility switching) in the presence of other polar functionalities (for adhesion, dissolution properties, etc.) is not a trivial process on multi-component polymers. This problem was solved through the introduction of sterically hindered, polymer-bound 2,6-di-*t*-butyl pyridine as "proton sponge" to neutralize any acid that is produced. This hindered amine does not effectively bind to the active catalyst, so the rate of polymerization is not significantly affected. In addition, the proton sponge beads can be easily filtered away from the reaction media, providing a convenient way to eliminate any residual highly absorbing, basic pyridine species which could interfere with resist performance.

In order to mimic the low molecular weights (3-8 kDa) of the successful poly(norbornene-*co*-maleic anhydride) alternating copolymers developed for 193 nm, a method to control the polymer molecular weight must be employed, particularly in the case of the highly

active, yet slow initiating (η_6-tolyl)nickel(perfluorophenyl)$_2$ catalyst. All efforts to reduce the molecular weight of the nickel-catalyzed norbornene addition polymers through the use of chain transfer agents such as 1-hexene (to promote β-hydride elimination[18]) or increased catalyst loadings (up to 10 mol%) met with little success.[19] While the addition of 1-hexene was unable to reduce the molecular weight to the level desired, use of catalyst loadings in excess of 5 mol% was successful in producing addition polymers with molecular weights below 10,000.[20] While this is an expensive solution to the problem, it is sufficient to produce quantities of material for resist evaluation. If metal-catalyzed addition polymers are to be commercialized, levels of residual metal contamination must be brought down to less than 20 parts per billion. That, however, is an issue which will have to be addressed by resist suppliers. All of the polymers discussed in this work were prepared with a cationic allyl palladium catalyst using the procedure shown in Figure 3.2.

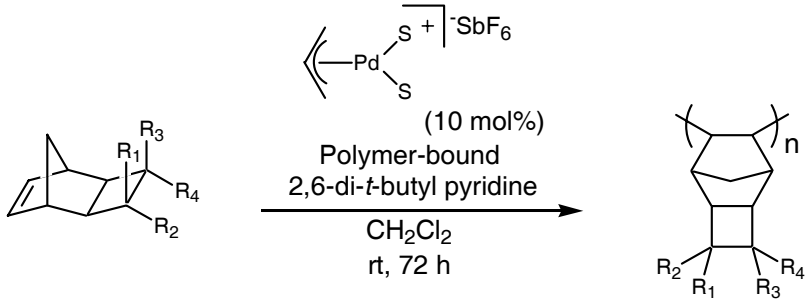

Figure 3.2. Palladium-catalyzed addition polymerization

Polymerization of fluorinated TCN monomers **3.4a** and **3.5a** afforded good yields of TCN homopolymers **3.8** and **3.9**, in stark contrast to the trace yields[10] achieved with norbornene monomers like **3.3** under identical conditions. The facts that polymerization proceeds in the presence of basic pyridine moieties and the observed unreactivity of TCN monomers towards radical initiators at moderate temperatures[17] rule out any cationic or radical polymerization mechanism. The lack of double bonds (as observed by ^{1}H NMR) and the high glass transition

temperatures of TCN polymers confirm the 2,3-addition polymer structure. Furthermore, the moderate molecular weights and polydispersity indices (1.7 < PDI < 2.7) of the polymers are typical of polymerizations with palladium catalysts.[13-15] It should be noted that the fluorinated TCN compound **3.4a** was also readily polymerized by nickel systems such as Ni(tolyl)(perfluorophenyl)$_2$.

VASE Analysis of TCN Homopolymers Removal of the palladium from the polymer chains by treatment with hydrogen followed by filtration and multiple precipitations produced polymers sufficiently clean for analysis by variable angle spectroscopic ellipsometry. The VASE spectra agree with the trends observed in the VUV spectra (Figure 3.3), although the reduction in absorbance afforded by additional fluorine substituents seems to be larger when measured by VASE. The homopolymer of NBTBE (**3.6**) has an absorbance at 157 nm of 6.02 μm^{-1}, compared to the homopolymer of NBHFA (**3.7**) which is around 1.14 μm^{-1}. In any copolymer of these two

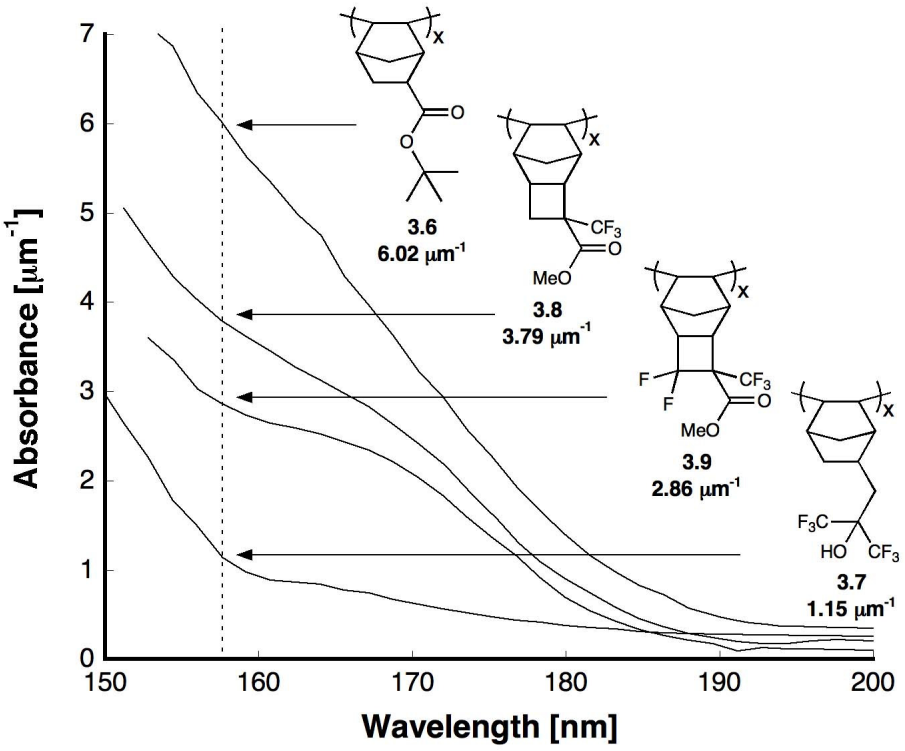

Figure 3.3. VASE spectra of TCN homopolymers

monomers, even small amounts of the highly absorbing ester-containing monomer **3.1** will raise the overall absorbance of the polymer considerably. In comparison, the TCN homopolymer **3.8** possesses an absorbance coefficient of 3.79 μm^{-1}at 157 nm. The addition of the trifluoromethyl group alpha to the ester increases the transparency of the material by approximately 2 orders of magnitude. The further incorporation of fluorine in TCN **3.5a** serves to increase the transparency of the homopolymer (**3.9**) by another order of magnitude (α_{10} = 2.86 μm^{-1} at 157 nm).

These thin film measurements of transparency support the gas-phase measurements previously reported. In fact, the thin film measurements indicate the benefits of increased fluorination are greater than the gas-phase VUV measurements indicate. Using these fluorinated TCN monomers, polymers with identical ester content and higher transparency or identical transparency and higher ester content, relative to copolymers of NTBE (**3.1**), can be synthesized. The higher transparency of these materials offers the possibility of ester-containing norbornene-type addition polymers as single layer resists. Towards this end, the synthesis and copolymerization of a number of fluorinated TCN monomers with *t*-butyl ester functionalities to produce imageable resist materials is reported here.[20] However, given the potential benefits of the TCN framework in 157 nm photolithography, exploration of other potential pathways to produce photoresist polymers from a wide range of TCN monomers via free radical, ring-opening metathesis (ROMP), and addition polymerization have been undertaken.[22]

Synthesis of TCN Resist Copolymers The extremely high transparency (1.15 μm^{-1}) and excellent dissolution behavior of polyNBHFA (**3.7**) provide a suitable base material which can be tailored by the incorporation of various functionalized monomers. The ester-functionalized resist **3.10** (Figure 3.4) was the first norbornene addition polymer resist synthesized for 157 nm lithography. While the high absorbance of the ester results in only moderate transparency for the copolymer, it offers sufficient performance for it to have been commercialized for preliminary tool testing while more transparent resists are developed. Therefore, it serves as a good

benchmark for evaluating other norbornene addition polymer-based photoresists. Replacement of the heavily absorbing NBTBE (**3.1**) with the more transparent tricyclononene **3.4b** affords the TCN-based resist **3.11.** Comparison of the lithographic performance of **3.10** and **3.11** will allow the effect of additional transparency on the resist performance to be evaluated. Finally, these resists will be compared to the partially protected hexafluorocarbinol-based resist **3.12**. Copolymer **3.12** is a 157 nm analogue of the partially protected poly(hydroxystyrene) resists[22] such as APEX-E used at 248 nm. A complete list of polymers studied along with their absorption coefficients and molecular weights are given in Table 3.1.[11,20]

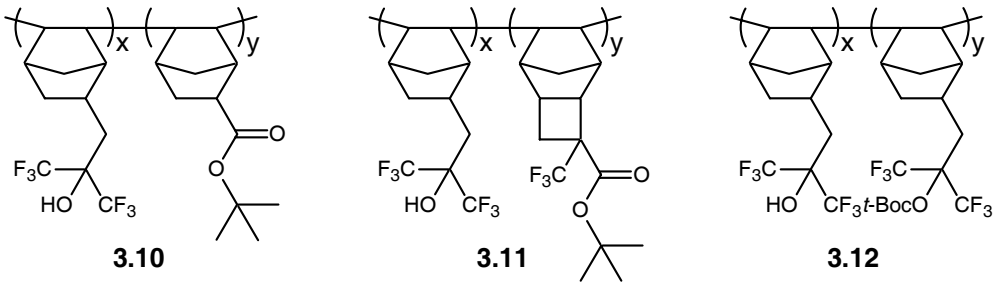

Figure 3.4. Metal-catalyzed addition copolymers for 157 nm resist applications

Table 3.1. Absorption coefficients and molecular weights of polymers studied[11,20]

Polymer	x	y	M_n [g/mol]	PDI	α_{10}^{157nm} [μm^{-1}]	α_{10}^{193nm} [μm^{-1}]	α_{10}^{248nm} [μm^{-1}]
3.6			5380	1.79	6.02	0.39	0.10
3.7			8150	2.11	1.15	0.27	0.20
3.8			66300	2.11	3.79	0.18	0.03
3.9			7200	2.58	2.86	0.12	0.02
3.10a	65	35	3150	3.38	2.74	0.02	0.03
3.10b	80	20	-	-	2.28	0.26	0.04
3.11a	74	26	13800	2.19	1.97	< 0.01	0.05
3.11b	83	17	5200	2.78	1.67	< 0.01	0.02
3.12	67	33	-	-	2.17	0.49	0.11
3.13			1590	1.45	3.62	0.22	0.06

Synthesis and Characterization of TCN-based Resists Copolymers (**3.11a** and **3.11b**) from the more readily accessible *t*-butyl ester-functionalized TCN monomer **3.4b** were synthesized for initial imaging studies.[20] The more transparent and lithographically useful TCN monomer **3.5b** has been scaled up, but was unable to be evaluated prior to the dismantling of the 157 nm exposure tool at SEMATECH. Copolymerization of **3.4b** and **3.2** afforded copolymers **3.11a/b** with compositions that closely mirrored the respective feed ratios. That these compositions are obtained at modest yields suggest they are the result of nearly identical inherent reactivities and not simply a result of full conversion. This allows for control of the copolymer composition by controlling the feed ratio. The nearly identical reactivities of NBHFA (**3.2**) and TCN **3.4b** illustrate the effectiveness of the additional cyclobutane ring in relieving the steric and electronic impacts of increased fluorination on the polymerization activity of the TCN monomer.

As expected, the more fluorinated TCN copolymer **3.11b** exhibits greatly enhanced transparency relative to the NBTBE-based copolymer **3.10b** with nearly identical ester content (Figure 3.5). While the difference of the vacuum ultraviolet spectra measured by variable angle spectroscopic ellipsometry does not seem extraordinary at first glance, replacing only ~ 20% of the polymer with a more transparent monomer results in a polymer that is ~53% more transparent (for a 300 nm thick film). Back of the envelope calculations suggest a copolymer with the more transparent **3.5b** (with the same 83/17 composition) should have an absorbance of ~1.45 μm^{-1} and exhibit ~78 % more transparency for a 300 nm thick film relative to **3.10b**.

Lithographic Performance of TCN-based Resists Initial lithographic evaluation of the TCN-based resist **3.11b** revealed the presence of significant swelling in the developer (A, Figure 3.6).[20] This is similar to the behavior encountered with **3.10** (C, Figure 3.6) and seems to be characteristic of ester-functionalized norbornene addition polymers.[23] Likely, it is the presence of some readily ionizable carboxylic acid groups attached to the rigid polymer backbone which induces the swelling. It is clear that simple reduction of the resist molecular weight is insufficient to alleviate this swelling behavior. Alternatively, the addition of a dissolution inhibitor (DI) can

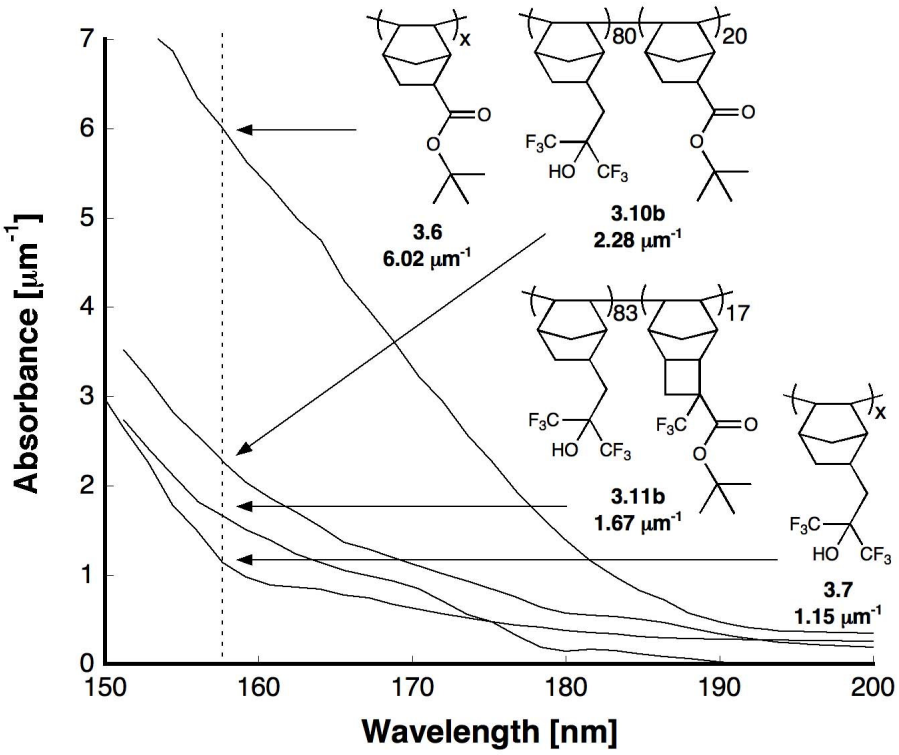

Figure 3.5. VASE spectrum of TCN-based photoresist copolymer **3.11b**

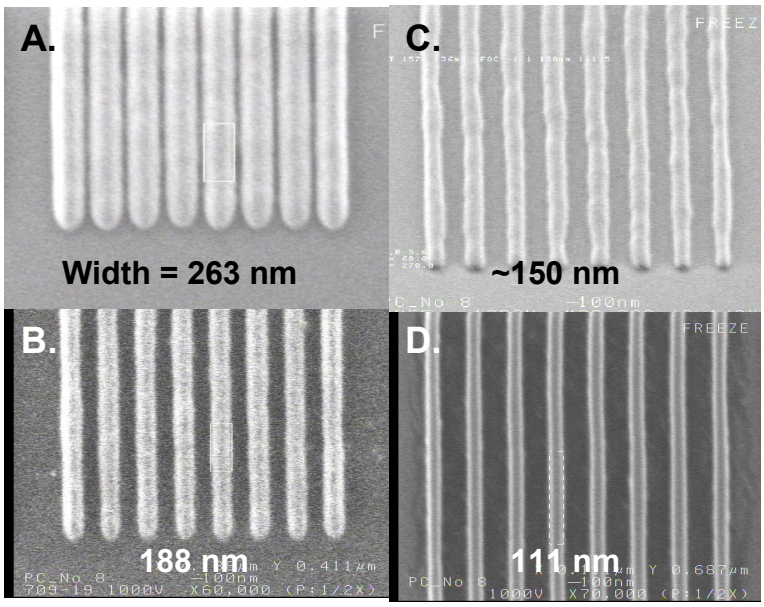

Figure 3.6. Scanning electron micrograph images ester-functionalized copolymers A. **3.11b** B. 50/50 blend of **3.11a** with **3.13** C. **3.10b** D. 70/30 blend of **3.10a** with **3.13** Note evidence of swelling and increase line edge roughness without **3.13**.

be used to control the dissolution rate eliminate swelling behavior of resist polymers during development.[24] Presumably, these DIs sequester the carboxylic acid groups in the unexposed regions with intermolecular hydrogen bonds and reduce their availability to react with the developer. Fortunately, addition of moderate amounts of the fluorinated dissolution inhibitor **3.13** (Figure 3.8) was successful in alleviating this swelling behavior (B, Figure 3.6). Initial lithographic results with **3.11b**/**3.13** system revealed its capability for high resolution imaging (Figure 3.7).[20]

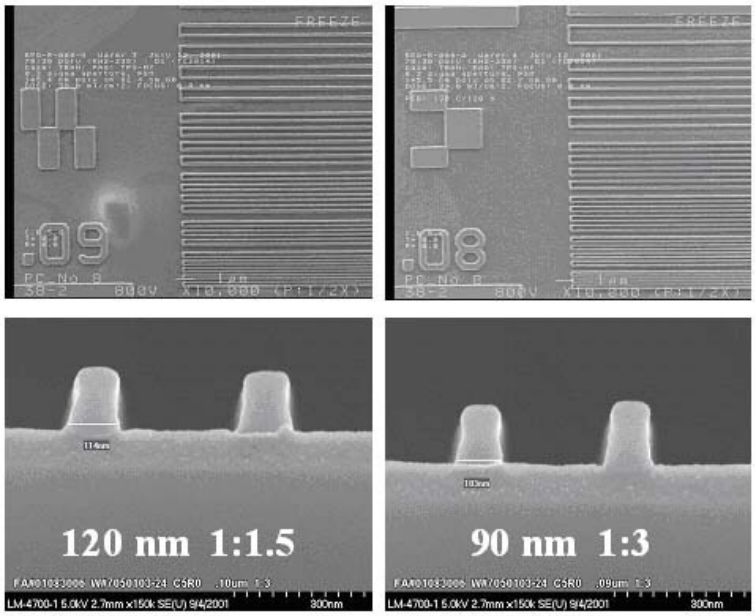

Formulation: 70/30 blend of **3.11b** with **3.11**, 6 wt% TPS-Nf, 0.3 wt% TBAH in PGMEA

Conditions: 157 nm exposure (0.6 NA-0.3σ, 39.0 mJ/cm^2), phase shift mask, 146 nm thick resist on 82nm antireflective layer (AR19), 140 °C-60s PAB, 130 °C-90s PEB, 20s 0.26N TMAH development

Figure 3.7. Scanning electron micrographs of images from TCN copolymer **3.11b**

Additional efforts toward optimization of the lithographic imaging performance of this TCN/dissolution inhibitor system would result in significantly better results. Copolymers incorporating the more transparent TCN monomer **3.5b** would be expected to offer improved

imaging performance. However, one of the biggest factors in the imaging performance of these ester-functionalized resists is the transparency of the dissolution inhibitor which can account for as much as 50% of the material in some formulations. The VUV spectrum of the fluorinated dissolution inhibitor **3.13** used in these lithographic evaluations is shown in Figure 3.8.[20]

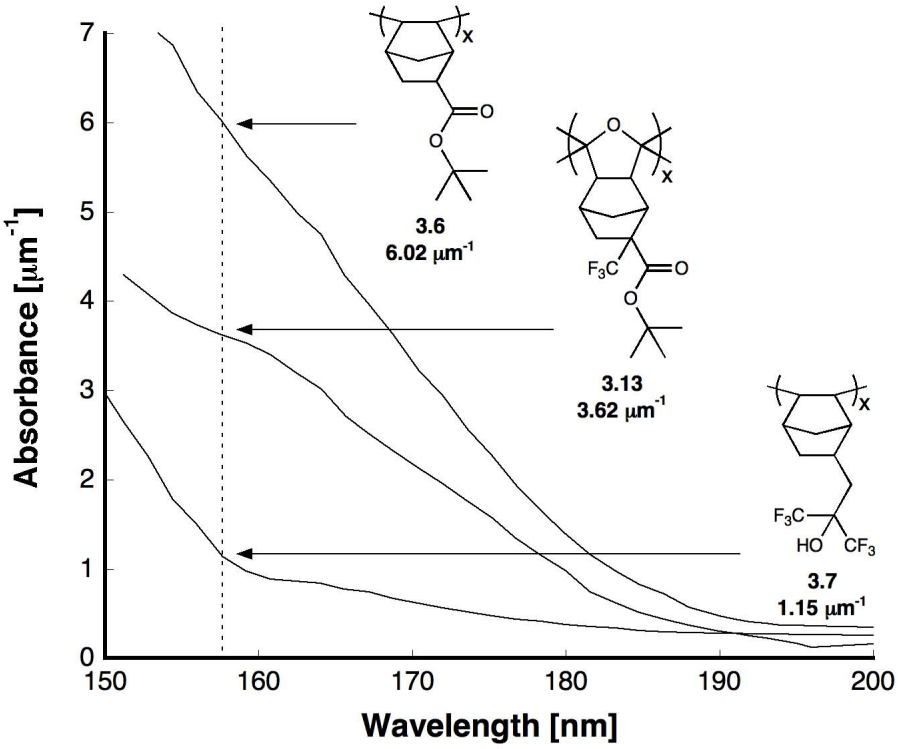

Figure 3.8. VASE spectrum of dissolution inhibitor **3.13**[20]

While the low molecular weight (x < 6) ketal carbon monoxide oligomers **3.13** serve as an effective dissolution inhibitor, its absorption coefficient is 3.6 μm^{-1} at 157 nm (Figure 3.8) – significantly higher than any of the ester-functionalized resists.[25] The presence of such a highly absorbing dissolution inhibitor decreases the transparency and lithographic performance of the photoresist polymer substantially. It also masks the true effect of the increased transparency of the TCN component on the imaging properties. Since this work was completed, a number of

groups have reported a number of more transparent dissolution inhibitors for use at 157 nm that would significantly improve the initial imaging results shown here.[26]

Partially Protected Hexafluorocarbinol-based Resists As mentioned previously, partial protection of poly(NBHFA) homopolymer **3.7** affords copolymer **3.12**, a 157 nm analogue of the partially protected poly(hydroxystyrene) copolymers (APEX-E)[22] used at 248 nm. The t-butoxycarbonyl protecting group increases the absorbance of the resultant polymer, albeit not as dramatically as the comparable use of NBTBE. Resists formulated from **3.12** afforded high resolution images without the use of any dissolution inhibitor despite its higher absorbance than the TCN copolymer **3.11b**.[20] While the transparencies of **3.10a** and **3.12** are very similar, the developed images obtained using these materials are very different due to the swelling behavior exhibited by carboxylic acid ester-based resists. These results indicate that solubility switches based on protected hexafluorocarbinols are superior for 157 nm photoresists based on norbornene addition polymers.

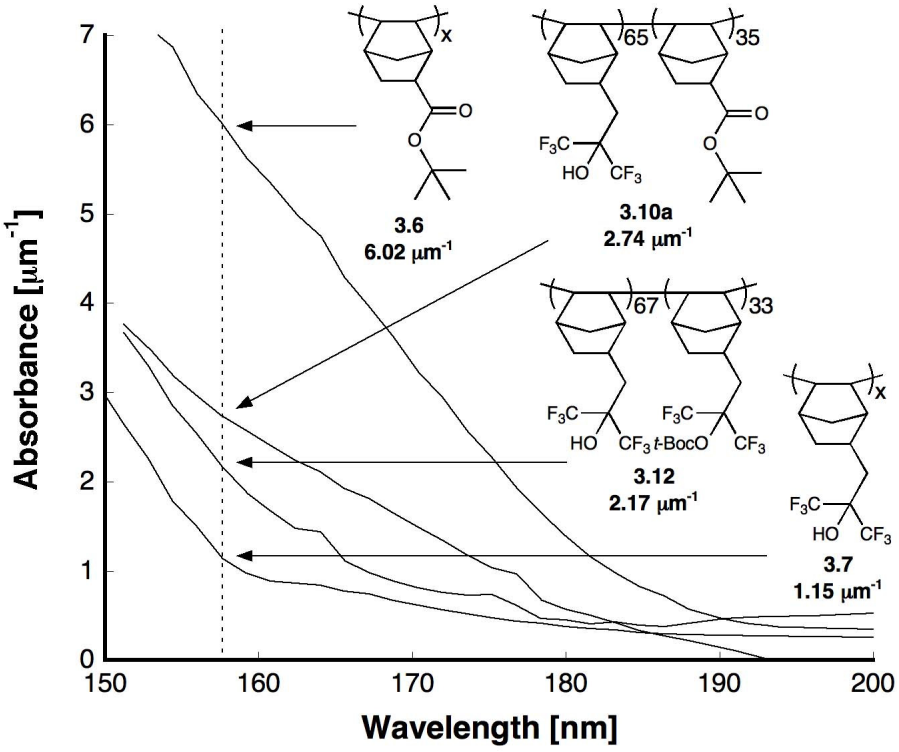

Figure 3.9. Absorbances of hexafluorocarbinol and carboxylic acid ester-based resists[20]

Conclusions

While fluorinated geminally disubstituted norbornenyl esters were unable to be polymerized via metal-catalyzed addition polymerization, fluorinated tricyclononenes were readily polymerized to afford ester-functionalized polymers with enhanced transparency at 157 nm relative to their non-fluorinated norbornene analogues. The exo configuration of cyclobutane ring of the tricyclononene framework allows it to serve as a scaffold capable of bearing fluorinated substituents while protecting the olefin from the steric and electronic affects of these groups. Copolymerization of a fluorinated tricyclononene with a hexafluorocarbinol-functionalized norbornene afforded photoresist copolymers with compositions nearly identical to the feed ratio. While this tricyclononene-based photoresist offered improved transparency relative to its less fluorinated norbornene analogue, both systems exhibited swelling behavior during development due to their carboxylic acid ester solubility switching functionalities. When a fluorinated dissolution inhibitor was incorporated into the formulation to control this swelling, promising lithographic images were obtained. A partially protected hexafluorocarbinol-based resist, while less transparent than the tricyclononene resist, offers good imaging performance due to its lack of swelling. These results illustrate the remarkable influence of the solubility switch chemistry on the dissolution behavior and imaging performance of the resist polymers. Specifically, they indicate that a hexafluorocarbinol-based solubility switch is the preferred design motif for high performance addition polymer resists for 157 nm. Further developments in transparent ester-functionalized norbornene-like monomers (such as the tricyclononene monomers described here) must be accompanied by the development of extremely transparent dissolution inhibitors. Additionally, these studies suggest the most promising pathway toward a successful 157 nm photoresist based on norbornene-addition polymers is the development of hexafluorocarbinol-functionalized norbornene or norbornene-like monomers with increased fluorine contents to afford an absorbance below 0.70 μm^{-1}.

Experimental

Materials: All manipulations and polymerizations with air-sensitive materials were carried out in an N_2-filled drybox or using standard Schlenk techniques. Argon was purified by passage through columns of BASF RS-11 (Chemalog) and Linde 4-Å[36] molecular sieves. Dichloromethane was rigorously degassed in 18 L reservoirs and passed through two sequential purification columns consisting of activated alumina. All starting materials were procured from Aldrich except 1,1,1-trifluoro-2-(trifluoromethyl)pent-4-en-2-ol (AZ Clariant), triphenylsulfonium nonaflate (AZ Clariant), 1,4-bis(2-hydroxy-hexafluoroisopropyl)benzene (Oakwood), and 2-(trifluoromethyl)acrylic acid (Honeywell and Central Glass Co.) and used as received, unless noted otherwise. Poly(NBHFA-*co*-NBTBE) (Composition: 80/20) (**3.10b**) was generously provided by Ralph Dammel and AZ-Clariant. The syntheses of monomers **3.1**, **3.2**, and **3.4b** and polymers **3.6**, **3.7**, **3.10a**, **3.11a/b**, **3.12**, and **3.13** have been performed by colleagues at the University of Texas, Austin. [20] Select data are reproduced here only for comparison.

Instruments and Equipment: Nuclear magnetic resonance (NMR) spectra were obtained using either a Bruker AMX300, Varian *Unity Plus 300*, or Varian *Mercury 300* spectrometer (^{1}H: 300 MHz, ^{13}C: 75 MHz, ^{19}F: 282 MHz). Shifts for NMR spectra are reported in ppm relative to TMS (for ^{19}F, $CFCl_3$ unless otherwise noted) or to the chemical shift of the solvent. Infrared spectra were recorded on a Nicolet *Avatar 360* IR spectrometer. Mass spectra were measured on a Finnigan *MAT TSQ-700* spectrometer. Molecular weights (M_n) and polydispersity indices (PDI) were measured from THF solutions using a Viscotek GPC equipped with a set of two 5 mm crosslinked polystyrene columns (linear mix and 100 Å) from American Polymer Standards and are reported relative to polystyrene standards. Select samples were analyzed by SEC using a GPC apparatus equipped with two PLgel 5 μm mixed-C columns (Polymer Labs) connected in series with a DAWN EOS multi-angle laser light scattering (MALLS) detector and an Optilab DSP digital refractometer (both from Wyatt Technology). No calibration standards were used and *dn/dc* values were obtained for each injection by assuming 100% mass elution from the

columns. Polymers containing acidic functional groups were pre-treated with either diazomethane or iodomethane/DBU before GPC measurement, unless noted otherwise. Differential scanning calorimetry (DSC) measurements and thermal gravimetric analysis (TGA) were performed on a Perkin Elmer *Series-7* thermal analysis system. Gas chromatographs were recorded on a Hewlett Packard *5890 Series II* with an *HP-5* (crosslinked 5% PH ME siloxane) capillary column and flame ionization detector (FID).

Vacuum UV Spectroscopy: VUV spectra of polymer films were calculated from measurements made with a J.A. Woollam *VU301* variable angle spectroscopic ellipsometer (VASE) and/or measured with the Acton *CAMS-507* spectrophotometer. The films were cast on either silicon wafers (VASE) or calcium fluoride disks (Acton) from solutions in propylene glycol methyl ether acetate (PGMEA) or cyclohexanone and baked at 100-130°C for at least 5 minutes prior to analysis. All absorbance data reported are in base 10.

Imaging: All imaging work was performed on an Exitech 157 nm small field (1.5 x 1.5 mm^2) mini-stepper (0.6 NA) using either a binary mask (σ 0.7) or phase-shift mask (σ 0.3) at International SEMATECH in Austin, TX. Scanning electron micrographs were collected on a JEOL *JWS-7550*, and cross-sectional data were collected on a Hitachi *4500* microscope. Coating, baking, and development of resist films were performed using an FSI *Polaris 2000* track. Thickness measurements were made on a Prometrix interferometer. A typical resist formulation was prepared by mixing the polymer with 6 wt% (relative to polymer) photoacid generator (triphenylsulfonium nonaflate) and 0.3 wt% tetrabutylammonium hydroxide (TBAH) as the base to control acid diffusion and reduce T-topping. Dissolution inhibitors were mixed with the polymer to the desired ratio. The entire mixture was diluted in PGMEA to provide a viscosity that provides resist thicknesses of approximately 100-200 nm after spinning the resist at 2500 rpm onto a silicon wafer that had been previously coated with ~80 nm BARC (bottom anti-reflective coating, Shipley AR19). The post-apply bake was 140°C for 60 sec and the post-exposure bake

was 130°C for 90 sec, unless stated otherwise. The exposed resists were developed in the industry-standard 0.26 *N* tetramethylammonium hydroxide (TMAH) developer.

Methyl 3-(trifluoromethyl)tricyclo[4.2.1.0^{2,5}]non-7-ene-3-carboxylate (TCNCF$_3$ME 3.4a). Quadricyclane (1.5 equiv., 4.25 g, 0.046 mol) and methyl (2-trifluoromethyl)acrylate[6a] (1 equiv., 4.55 g, 0.30 mol) were reacted according to the general procedure mentioned above to produce, after Kugelrohr vacuum distillation, 6.78 g (0.028 mol) of colorless liquid. Yield: 94%. Isomer composition: 32 % syn, 68 % anti. ^{1}H NMR ($CDCl_3$, 300 MHz, ppm): 6.1-5.9 (m, 4H, H-7+H-8, syn+anti), 3.80 (s, 3H, COOC*H*$_3$, syn), 3.78 (s, 3H, COOC*H*$_3$, anti), 3.06 (s, 1H, H-1, syn), 2.99 (s, 1H, H-1, anti), 2.82 (s, 1H, H-6, syn), 2.74 (s, 1H, H-6, anti), 2.68 (ddd, *J* = 3.0, 7.5, 13.2 Hz, 1H, anti), 2.5-1.9 (7 H), 1.48-1.24 (4 H). ^{13}C NMR ($CDCl_3$, 75 MHz, ppm): δ 171.16 (d, *J* = 2.9 Hz, *C*OOMe, syn), 168.85 (d, *J* = 2.4 Hz, *C*OOMe, anti), 136.74 (olefin C, anti), 136.62 (olefin C, syn), 135.24 (olefin C, syn), 135.06 (olefin C, anti), 126.32 (q, *J* = 280 Hz, CF_3, anti), 125.16 (q, *J* = 281 Hz, CF_3, syn), 53.30 (COO*C*H3, syn), 52.81 (COO*C*H$_3$, anti), 49.56 (q, *J* = 28.6 Hz, quat. C, C-3, syn), 49.40 (q, *J* = 26.5 Hz, quat. C, C-3, anti), 44.50 (CH, C-6, anti) 44.18 (CH, C-6, syn), 44.15(CH, C-2, syn), 42.86 (CH, C-1, syn), 42.50 (CH, C-1, anti), 41.95 (m, *J* = 2.0 Hz, CH, C-2 anti), 41.14 (m, CH_2, C-9, anti), 40.71 (CH_2, C-9, syn), 32.98 (CH, C-5, syn), 32.83 (CH, C-5, anti), 26.07 (d, *J* = 2.4 Hz, CH_2, C-4, anti), 25.93 (d, *J* = 1.9 Hz, CH_2, C-4, syn). ^{19}F NMR ($CDCl_3$, 282 MHz, ppm) (referenced to external C_6F_6 standard at -166.717 ppm): δ -66.25 (s, 3F, -CF_3, syn), -75.13 (s, 3F, -CF_3,, anti). IR (KBr, cm^{-1}): 3060 (alkene), 2970, 2892, 1742 (C=O), 1473, 1436, 1333, 1322, 1275, 1225, 1163, 1132, 1087, 712, 671. HRMS-EI (*m/z*): $[M]^+$ calcd for $C_{12}H_{14}F_3O_2$, 246.0868; found, 246.0868.

***tert*-Butyl 3-(trifluoromethyl)tricyclo[4.2.1.0^{2,5}]non-7-ene-3-carboxylate (TCNCF$_3$TBE, 3.4b).**[20] To a 300 mL Parr pressure reactor equipped with a stir bar were added quadricyclane (20.0 g, 217 mmol) and *tert*-butyl 2-(trifluoromethyl)acrylate (**9**, 46.0 g, 238 mmol). The pressure reactor was sealed, and the reaction mixture was stirred overnight at 100°C. The crude

product was allowed to cool to room temperature and fractionally distilled under vacuum. The product was collected at 90-94°C / 6 mm Hg as a clear oil (52.0 g, 83%). ^{1}H NMR ($CDCl_3$, 300 MHz, ppm): δ 1.50 (s, 9H, t-Bu), 1.25-3.02 (m, 8H, aliphatic), 5.95-6.05 (m, 2H, CH=CH). ^{19}F NMR ($CDCl_3$, 282 MHz, ppm): δ -65.0, -74.0. IR (NaCl, cm^{-1}): 3050, 2975, 1736 (C=O), 1475, 1372, 1316, 1280 (C-F), 1255, 1157, 1127, 840. HRMS-CI (*m/z*): $[M + H]^+$ calcd for $C_{15}H_{17}F_3O_2$, 289.141; found, 289.142.

Methyl 4,4-difluoro-3-(trifluoromethyl)tricyclo-[4.2.1.0^{2,5}]non-7-ene-3-carboxylate (TCNF$_2$CF$_3$ME, 3.5a). To a 300 mL Parr pressure reactor equipped with a magnetic stir bar were added quadricyclane (1.5 g, 16.3 mmol) and methyl 3,3-difluoro-2-(trifluoromethyl)acrylate (3.9 g, 20.4 mmol). The pressure vessel was sealed, and the reaction mixture was stirred at 100°C for 72 hours. After cooling to room temperature, the residue was purified by fractional vacuum distillation (39-40°C / 0.30 mm Hg) to yield a clear oil (1.0 g, 22%). In a subsequent synthesis, it was found that if the reaction was allowed to sit at room temperature for 14 days after the initial heating, the isolated yield increased to 73%. Isomer composition: 49% syn, 51% anti. ^{1}H NMR ($CDCl_3$, 300 MHz, ppm): δ 6.27 (dd, *J* = 2.7, 5.7 Hz, olefin H, 1H, anti), 6.05-6.15 (m, olefin H, 3H, 2 syn+1 anti), 3.87 (s, COOC*H*$_3$, 3H, anti), 3.86 (s, COOC*H*$_3$, 3H, syn), 3.53 (s, 1H, H-1, syn), 3.22 (2H, H-1, H-6, anti), 3.13 (s, 1H, H-6, syn), 2.84-2.75 (m, 1H, H-5, anti), 2.75-2.6 (m, 1H, H-5, syn), 2.39-2.31 (m, 1H, H-2, syn), 2.10 (d, *J* = 10.2 Hz, 1H, H-2, anti), 1.50-1.30 (m, 4H, H-9 syn, H-9 anti, syn+anti). ^{13}C NMR (C_6D_6, 75 MHz, ppm): 165.11 (COOMe, syn), 162.91 (COOMe, anti), 139.62 (olefin C, anti), 137.82 (olefin C, syn), 136.93 (olefin C, syn), 136.77 (olefin C, anti), 123.97, (q, J = 283 Hz, CF_3, syn), 123.68 (q, J = 280 Hz, CF_3, anti), 116.72 (t, *J* = 292 Hz, C-5), 114.09, (t, *J* = 296 Hz, C-5), 53.32 (COO*C*H$_3$, anti), 52.64 (COO*C*H$_3$, syn), 50.70 (dd, *J* = 19.2, 26 Hz, CH, C-5, anti), 50.36 (t, *J* =23 Hz, CH, C-5, syn), 43.71 (CH, C-1, anti), 43.26 (CH, C-1, syn), 43.11 (dd, *J* = 4.4, 8.2 Hz, CH_2, C-9, anti), 42.82 (d, *J* = 6.6 Hz, CH_2, C-9, syn), 42.08 (CH, C-6, anti), 41.29 (t, *J* = 2.3 Hz, CH, C-6, syn), 37.21(dd, J

= 4.9, 12 Hz, CH, C-2, anti), 36.90 (m, CH, C-2, syn). ^{19}F NMR (Acetone, 282 MHz, ppm): δ – 61.67 (d, *J* = 6.7 Hz, 3F, CF_3, anti), -68.36 (d, *J* = 2.0 Hz, 3F, CF_3, syn), -85.70 (dm, *J* = 211 Hz, 1F, F-4 syn, anti), -97.15 (dm, *J* = 217 Hz, 1F, F-4 anti, syn), -106.87 (d, *J* = 217 Hz, 1F, F-4 syn, syn), -113.94 (d, *J* = 211 Hz, 1F, F-4 anti, anti). IR (NaCl, cm^{-1}): 3058 (alkene), 2991, 2909, 1752 (C=O), 1429, 1317, 1219, 1045, 897, 794, 697. HRMS-CI (*m/z*): $[M + H]^+$ calcd for $C_{12}H_{12}F_5O_2$, 283.0757; found, 283.0755.

General Polymerization Procedure: To a 20ml vial equipped with a stir bar were added allyl palladium chloride dimer (13.0 mg, 0.032 mmol) and silver hexafluoroantimonate (28 mg, 0.064 mmol) in a dry box. Dichloromethane (5 mL) was added and the mixture was stirred at room temperature for 20 minutes. The mixture was filtered through a 0.45 μm PTFE syringe filter into a 25 mL round-bottom flask containing a solution of tricyclononene monomer (3.25 mmol, [M]/[C]=50:1) in dichloromethane (10 mL). For resist evaluation, higher catalyst loadings ([M]/[C] = 10) were used to ensure only low molecular weight polymer (< 10,000 g/mol) was formed. For monomers with *t*-butyl ester functionalities, the resulting solution was stirred for 10 min at room temperature and then transferred to a 25 mL round-bottom flask containing polymer-bound 2,6-di-*t*-butyl-pyridine (1 mg/mg catalyst). The reaction mixture was stirred at room temperature for 96 hours, then filtered through a 0.45 μm PTFE syringe filter to remove the polymer-bound base, concentrated *in vacuo*, and precipitated into hexanes (100 mL). The crude polymer was dissolved in ethyl acetate (50 mL), and stirred vigorously under a hydrogen atmosphere overnight. The solution was allowed to sit, unstirred, for another hour, at which time a black solid (Pd) aggregated and precipitated. The black solid was removed by filtration through celite. The filtrate was treated with activated carbon and stirred for 3 hours. The activated carbon was removed by filtration through celite, and the resulting filtrate was washed with saturated $NaHCO_3$, water, and brine, dried with $MgSO_4$, filtered, concentrated *in vacuo* at 50°C, and precipitated into hexanes. Filtration provided the product as a white powder.

Poly(NBTBE) (3.6).[20] GPC: M_n = 5380; PDI = 1.79. α_{10}^{157nm} = 6.02 μm^{-1}. α_{10}^{193nm} = 0.39 μm^{-1}. α_{10}^{248nm} = 0.10 μm^{-1}.

Poly(NBHFA) (3.7).[20] GPC: M_n = 3,860; PDI= 2.11. α_{10}^{157nm} = 1.15 μm^{-1}. α_{10}^{193nm} = 0.27 μm^{-1}.. α_{10}^{248nm} = 0.20 μm^{-1}.

Poly(TCNCF$_3$ME) (3.8). Methyl 3-(trifluoromethyl)tricyclo[4.2.1.0^{2,5}]non-7-ene-3-carboxylate (**3.4a**) was polymerized by the general procedure mentioned previously ([M]/[C] = 50:1) to produce a 79 % yield of white polymeric powder. ^{1}H NMR (CD_2Cl_2, 300 MHz, ppm): δ 4.20-3.30 (br s, COOC*H*$_3$), 0.50-3.20 (br m, aliphatic). GPC (GPC): M_n = 66,300, PDI = 2.11. α_{10}^{157nm} = 3.79 μm^{-1}. α_{10}^{193nm} = 0.18 μm^{-1}. α_{10}^{248nm} = 0.03 μm^{-1}.

Poly(TCNF$_2$CF$_3$ME) (3.9). Methyl 4,4-difluoro-3-(trifluoromethyl)tricyclo-[4.2.1.0^{2,5}]non-7-ene-3-carboxylate (**3.5a**) was polymerized by the general procedure mentioned previously ([M]/[C] = 10:1) to produce a 50% yield of white polymeric powder. GPC: M_n = 7,200, PDI = 2.58. α_{10}^{157nm} = 2.86 μm^{-1}. α_{10}^{193nm} = 0.12 μm^{-1}. α_{10}^{248nm} = 0.02 μm^{-1}.

Poly(NBHFA-*co*-NBTBE) (3.10a).[20] Composition as determined by TGA: NBHFA/ NBTBE = 65/35. α_{10}^{157nm} = 2.74 μm^{-1}. α_{10}^{193nm} = 0.02 μm^{-1}. α_{10}^{248nm} = 0.03 μm^{-1}.

Poly(NBHFA-*co*-NBTBE) (3.10b).[20] Courtesy of Ralph Dammel and AZ-Clariant. NBHFA/ NBTBE = 80/20. α_{10}^{157nm} = 2.28 μm^{-1}. α_{10}^{193nm} = 0.26 μm^{-1}. α_{10}^{248nm} = 0.04 μm^{-1}.

Poly(NBHFA-*co*-TCNCF$_3$TBE) (3.11).[20] For **3.11a**, Composition as determined by TGA: NBHFA/TCNCF$_3$TBE = 74/26. α_{10}^{157nm} = 1.97 μm^{-1}. α_{10}^{193nm} < 0.01 μm^{-1}. α_{10}^{248nm} = 0.05 μm^{-1}. For **3.11b**, Composition as determined by TGA: NBHFA/TCNCF$_3$TBE = 83/17. α_{10}^{157nm} = 1.67 μm^{-1}. α_{10}^{193nm} < 0.01 μm^{-1}. α_{10}^{248nm} = 0.02 μm^{-1}.

Poly(NBHFA-*co*-NBHFABOC) (3.12).[20] Composition as determined by TGA: NBHFA/NBHFABOC = 67/33. α_{10}^{157nm} = 2.17 μm^{-1}. α_{10}^{193nm} = 0.49 μm^{-1}. α_{10}^{248nm} = 0.11 μm^{-1}.

Poly(NBCF$_3$TBE-*co*-carbon monoxide) (3.13).[20] GPC: M_n = 1590; PDI = 1.45. α_{10}^{157nm} = 3.62 μm^{-1}. α_{10}^{193nm} = 0.22 μm^{-1}. α_{10}^{248nm} = 0.06 μm^{-1}.

References and Notes

(1) *International Technology Roadmap for Semiconductors, 2000 Update*, SRC, http://public.itrs.net/Files/2000UpdateFinal/ORTC2000final.pdf.

(2) Patterson, K.; Somervell, M.; Willson, C. G. *Solid State Technol.* **2000**, *43(3)*, 41-48.

(3) (a). Bloomstein, T. M.; Rothschild, M.; Kunz, R. R.; Hardy, D. E.; Goodman, R. B.; Palmacci, S. T. *J. Vac. Sci. Technol. B* **1998**, *16*, 3154-3157. (b). Rothschild, M.; Bloomstein, T. M.; Curtin, J. E.; Downs, D. K.; Fedynyshyn, T. H.; Hardy, D. E.; Kunz, R. R.; Liberman, V.; Sedlacek, J. H. C.; Uttaro, R. S.; Bates, A. K.; Van Peski, C. *J. Vac. Sci. Technol. B* **1999**, *17*, 3262-3266.

(4) (a). Okoroanyanwu, U.; Shimokawa, T.; Byers, J.; Willson, C. G. *Chem. Mater.* **1998**, *10*, 3319-27. (b). Okoroanyanwu, U.; Byers, J.; Shimokawa, T.; Willson, C. G. *Chem. Mater.* **1998**, *10*, 3328-3333. (c). Okoroanyanwu, U.; Shimokawa, T.; Byers, J.; Willson, C. G. *J. Molec. Catal. A* **1998**, *133*, 93-114. (d). Varanasi, P. R.; Jordhamo, G.; Lawson, M. C.; Chen, R.; Brunsvold, W. R.; Hughes, T.; Keller, R.; Khojasteh, M.; Li, W.; Allen, R. D.; Ito, H.; Opitz, J.; Truong, H.; Wallow, T. *Proc. SPIE* **2000**, *3999*, 1157-1162. (e). Allen, R. D.; Opitz, J.; Wallow, T.; DiPietro, R. A.; Hofer, D. C.; Jayaraman, S.; Hullihan, K. A.; Rhodes, B. L.; Shick, R. A. *Proc. SPIE* **1998**, *3333*, 463-471.

(5) (a). Matsuzawa, N. N.; Mori, S.; Yano, E.; Okasaki, S.; Ishitani, A.; Dixon, D. A. *Proc. SPIE*, **2000**, *3999*, 375-384. (b). Toriumi, M.; Satou, I.; Itani, T. *J. Vac. Sci. Technol. B* **2000**, *18*, 3328-3331.

(6) (a). Chiba, T.; Hung, R. J.; Yamada, S.; Trinque, B.; Yamachika, M.; Brodsky, C.; Patterson, K.; Vander Heyden, A.; Jamison, A.; Lin, S. H.; Somervell, M.; Byers, J.; Conley, W.; Willson, C. G. *J. Photopolymer Sci. Technol.* **2000**, *13*, 657-664. (b). Brodsky, C.; Byers, J.; Conley, W.; Hung, R.; Yamada, S.; Patterson, K.; Somervell, M.;

Trinque, B.; Tran, H. V.; Cho, S.; Chiba, T.; Lin, S-H.; Jamieson, A.; Johnson, H.; Vander Heyden, T.; Willson, C. G. *J. Vac. Sci. Technol. B.* **2000**, *18*, 3396-3401.

(7) Grandler, J. R.; Jencks, W. P. *J. Am. Chem. Soc.* **1982**, *104*, 1937-1951.

(8) (a). Trinque, B. C.; Chambers, C. R.; Osborn, B. P.; Callahan, R. P.; Lee, G. S. Kusumoto, S.; Sanders, D. P.; Grubbs, R. H.; Conley, W. E.; Willson, C. G. *J. Fluor. Chem.* **2003**, *122*, 17-26. (b). Trinque, B. C.; Osborn, B. P.; Chambers, C. R.; Hsieh, Y.-T.; Corry, S.; Chiba, T.; Hung, R. J.; Tran, H. V.; Zimmerman, P.; Miller, D.; Conley, W.; Wilson, C. G. *Proc. SPIE* **2002**, *4690*, 58-68.

(9) For calculations of the VUV spectra of fluorinated norbornenes, see: (a). Dixon, D. A.; Matsuzawa, N. N.; Ishitani, A.; Uda, T. *Phys. Stat. Sol B* **2001**, *226*, 69-77. (b). Matsuzawa, N. N.; Ishitani, A.; Dixon, D. A.; Uda, T. *Proc. SPIE* **2001**, *4345*, 396-405. (c). Yamazaki, T.; Itani, T. *Jpn. J. Appl. Phys.* **2003**, *42*, 3881-3884.

(10) No homopolymer of methyl 2-(trifluoromethyl)-norborn-5-ene-2 carboxylate was isolated after attempted polymerization with palladium or nickel catalysts. In copolymerizations with the hexafluoroisopropyl alcohol norbornene **2.2**, the geminally di-substituted norbornene was incorporated in significantly lower than stoichiometric amounts and low (< 10%) overall yields were observed. (a). Hung, R. J.; Tran, H. V.; Trinque, B. C.; Chiba, T.; Yamada, S.; Sanders, D.; Connor, E. F.; Grubbs, R. H.; Klopp, J. M.; Frechet, J. M. J.; Thomas, B. H.; Shafer, G. J.; DesMarteau, D. D.; Conley, W.; Willson, C. G. *Proc. SPIE* **2001**, *4345*, 385-395. (b). Tran, H. V.; Hung, R. J.; Chiba, T.; Yamada, S.; Mrozek, T.; Hsieh, Y-T.; Chambers, C. R.; Osborn, B. P.; Trinque, B. C.; Pinnow, M. J.; Sanders, D. P.; Connor, E. F.; Grubbs, R. H.; Conley, W.; MacDonald, S. A.; Willson, C. G. *J. Photopolym. Sci. Technol.* **2001**, *14*, 669-674.

(11) Sanders, D. P.; Connor, E. F.; Grubbs, R. H.; Hung, R. J.; Osborn, B. P.; Chiba, T.; MacDonald, S. A.; Willson, C. G.; Conley, W. *Macromolecules* **2003**, *36*, 1534-1542.

(12) (a). Barnes, D. A.; Benedikt, G. M.; Goodall, B. L.; Huang, S. S.; Kalamarides, H. A.; Lenhard, S.; McIntosh, L. H., III.; Selvy, K. T.; Shick, R. A.; Rhodes, L. F. *Macromolecules* **2003**, *36*, 2623-2632. (b). Park, K. H.; Twieg, R. J.; Ravikiran, R.; Rhodes, L. F.; Shick, R. A.; Yankelevich, D.; Knoesen, A. *Macromolecules* **2004**, *37*, 5163-5178. (c). Lin, S. T; Narske, R. N.; Klabunde, K. J. *Organometallics* **1985**, *4*, 571-574.

(13) (a). Sen, A.; Lai, T.-L. *Organometallics* **1982**, *1*, 415-417. (b). Sen, A.; Lai, T-W; Thomas, R. R. *J. Organomet. Chem.* **1988**, *358*, 567. (c). Mehler, C.; Risse, W. *Makromol. Chem. Rapid. Commun.* **1991**, *12*, 255-259. (d). Mehler, C.; Risse, W. *Macromolecules* **1992**, *12*, 4226-4228. (e). Seehof, N.; Mehler, C.; Breunig, S.; Risse, W. *J. Molec. Catal.* **1992**, *76*, 219-228. (f). Lipian, J.; Mimna, R. A.; Fondran, J. C.; Yandulov, D.; Shick, R. A.; Goodall, B. L.; Rhodes, L. F.; Huffman, J. C. *Macromolecules* **2002**, *35*, 8969-8977.

(14) (a). Breunig, S.; Risse, W. *Makromol. Chem.* **1992**, *193*, 2915-2927. (b). Mehler, C.: Risse, W. *Makromol. Chem., Rapid Commun*. **1992**, *13*, 455-459. (c). Reinmuth, A.; Mathew, J. P.; Melia, J; Risse, W. *Macromol. Rapid Commun*. **1996**, *17*, 173-180. (d). Mathew, J. P.; Reinmuth, A.; Melia, J; Swords, N.; Risse, W. *Macromolecules* **1996**, *39*, 2755-2763.

(15) (a). Hennis, A. D.; Polley, J. D.; Long, G. S.; Sen, A.; Yandulov, D.; Lipian, J.; Benedikt, G. M.; Rhodes, L. F.; Huffman, J. *Organometallics* **2001**, *20*, 2802-2812. (b). Goodall, B. L.; Barnes, D. A.; Benedikt, G. M.; McIntosh, L. H.; Rhodes, L. F. *Polym. Mat. Sci. Eng.* **1997**, *76*, 56-57.

(16) Copolymerization of *tert*-butyl tricyclo[4.2.1.$0^{2,5}$]non-7-ene-3-carboxylate with maleic anhydride using AIBN as an initiator ([M]/[I] = 25) as described in Ref. 4a (Willson et al.) produced a while solid polymer with M_n (GPC-MALLS) = 2,480, PDI = 1.3 in 21% yield. Under these same conditions, homopolymerization of the TCN *t*-butyl ester was not observed, as much higher temperatures and initiator concentrations are required for the

radical homopolymerization of norbornene-type monomers to proceed as noted in Ref. 4a and Cirvello, J. V.; Shim, S-Y. *Chem. Mater.* **1996**, *8*, 376-381.

(17) (a). Houlihan, F. M.; Wallow, T. I.; Nalamasu, O.; Reichmanis, E. *Macromolecules* **1997**, *30*, 6517-6524. (b). Reichmanis, E.; Nalamasu, O.; Houlihan, F. M.; Wallow, T. I.; Timko, A. G.; Cirelli, R. A.; Dabbagh, G.; Hutton, R. S.; Novembre, A. E.; Smith, B. W. *J. Vac. Sci, Technol. B* **1997**, *5,* 2528-2533. (c). Nalamasu, O.; Houlihan, F. M.; Cirelli, R. A.; Timko, A. G.; Watson, G. P.; Hutton, R. S.; Gabor, A.; Medina, A.; Slater, S. *J. Vac. Sci, Technol. B* **1998**, *16*, 3716-21. (d). Byers, J.; Patterson, K.; Cho, S.; McCallum, M.; Willson, C. G. *J. Photopolym. Sci. Technol.* **1998**, *11*, 465-474. (e). Douki, K.; Kajita, T.; Shimokawa, T. *Proc. SPIE* **2000**, *3999*, 1128-1135. (f). Park, J.-H.; Kim, J.-Y.; Seo, D.-C.; Park, S.-Y.; Lee, H.; Kim, S.-J.; Jung, J.-C.; Baik, K.-H. *Proc. SPIE* **2000**, *3999*, 1163-1170.

(18) Goodall, B. L.; Benedikt, G. M.; McIntosh, L. H.; Barns, D. A. *U. S. Patent* 5468819, **1995**.

(19) Yamada, S. *Ph. D. Dissertation* University of Texas, Austin, **2000**.

(20) Tran, H. V.; Hung, R. J.; Chiba, T.; Yamada, S.; Mrozek, T.; Hsieh, Y.-T.; Chambers, C. R.; Osborn, B. P.; Trinque, B. C.; Pinnow, M. J.; MacDonald, S. A.; Willson, C. G.; Sanders, D. P.; Connor, E. F.; Grubbs, R. H.; Conley, W. *Macromolecules* **2002**, *35*, 6539-6549.

(21) (a). Osborn, B. P. *Ph.D. Dissertation* University of Texas, Austin, **2004**. (b). http://willson.cm.utexas.edu/Research/Sub_Files/157/index.htm.

(22) For reviews of the development of chemically amplified resists, see: (a). Willson, C. G.; Ito, H.; Frechet, J. M. J.; Tessier, T. G.; Houlihian, F. M. *J. Electrochem. Soc.* **1986**, *133*, 181-187. (b). Reichmanis, E.; Houlihan, F. M.; Nalamasu, O.; Neenan, T. X. *Chem. Mater.* **1991**, *3*, 394-407. (c). MacDonald, S. A.; Willson, C. G.; Frechet, J. M. *Acc. Chem. Res.* **1994**, *27*, 151-158. (d). Ito, J. *IBM J. Res. Dev.* **1997**, *41*, 69-80. (e). Stewart, M. D.;

Patterson, K.; Somervell, M. H.; Willson, C. G. *J. Phys. Org. Chem.* **2000**, *13*, 767-774. (f). Ito, H. *J. Polym. Sci. A: Polym. Chem.* **2003**, *41*, 3863-3870.

(23) Ito, H. *IBM. J. Res. Dev.* **2001**, *45*, 683-695.

(24) Ito, H.; Allen, R. D.; Opitz, J.; Wallow, T. I.; Truong, H. D.; Hofer, D. C.; Varanasi, P. R.; Jordhamo, G. M.; Jayaraman, S.; Vicari, R. *Proc. SPIE* **2000**, *3999*, 2-12.

(25) (a). Hung, R. J.; Tran, H. V.; Trinque, B. C.; Chiba, T.; Yamada, S.; Sanders, D.; Connor, E. F.; Grubbs, R. H.; Klopp, J. M.; Frechet, J. M. J.; Thomas, B. H.; Shafer, G. J.; DesMarteau, D. D.; Conley, W.; Willson, C. G. *Proc. SPIE* **2001**, *4345*, 385-395. (b). Trinque, B. C.; Chiba, T.; Hung, R. J.; Chambers, C. R.; Pinnow, M. J.; Osborn, B. P.; Tran, H. V.; Wunderlich, J.; Hsieh, Y.-T.; Thomas, B. H.; Shafer, G.; DesMarteau, D. D.; Conley, W.; Willson, C. G. *J. Vac. Sci. Technol. B* **2002**, *20*, 531-536.

(26) (a). Conley, W.; Miller, D.; Chambers, C.; Osborn, B.; Hung, R. J.; Tran, H. V.; Trinque, B. C.; Pinnow, M.; Chiba, T.; MacDonald, S.; Zimmerman, P.; Dammel, R.; Romano, A.; Willson, C. G. *Proc. SPIE* **2002**, *4690*, 69-75. (b). Conley, W.; Miller, D.; Chambers, C.; Trinque, B. C.; Osborn, B.; Chiba, T.; Zimmerman, P.; Dammel, R.; Romano, A.; Willson, C. G. *J. Photopolym. Sci. Technol.* **2002**, *15*, 613-618. (c). Fresco, Z. M.; Bensel, N.; Suez, I.; Backer, S. A.; Frechet, J. M. J.; Conley, W. *J. Photopolym. Sci. Technol.* **2003**, *16*, 27-36.

CHAPTER 4

Development of Fluorinated Oxatricyclononene Monomers and Oxetane Acetal Structures for 157 nm Lithography

Development of Fluorinated Oxatricyclononene Monomers and Oxetane Acetal Structures for 157 nm Lithography

Abstract Fluorinated 3-oxatricyclo[4.2.1.$0^{2,5}$]non-7-enes, readily obtained via the thermal cycloaddition of trifluoromethyl ketones with quadricyclane, are oxetane-functionalized norbornene monomers potentially amenable to a variety of polymerization pathways to afford new materials for deep ultraviolet lithography. A Lewis acid-catalyzed Wagner-Meerwein rearrangement of the oxetane-functionalized monomers produces a new series of fluorinated alicyclic monomers, 4-oxatricyclo[4.3.$0^{1,6}$.$0^{3,7}$]non-8-enes. This high yielding, 2-step synthesis affords a unique class of highly fluorinated, alicyclic monomers potentially useful to increase etch resistance and mechanical properties in advanced photoresist materials. These novel highly fluorinated structures exhibit high transparency indicating their suitability for use in a number of deep ultraviolet photolithographic applications. Oxetane acetal structures are shown to be highly transparent at 157 nm while being significantly more susceptible to acid-catalyzed ring-opening. Initial studies of a model 2-methoxy-3-oxa-tricyclononane which opens quantitatively to a hexafluorocarbinol-substituted norcamphor derivative are presented.

Introduction

The unique combination of transparency,[1] acidity,[2] and excellent dissolution behavior[3] imparted by hexafluorocarbinols to photoresist polymers has made them the dominant design motif for 157 nm photoresists.[4-8] While most heavily investigated for use in 157 nm lithography, hexafluorocarbinols are being back-integrated into resists for 193 nm and 193 nm immersion lithography. The vast majority of chemically-amplified positive tone photoresists being investigated for 193 nm, 193 nm immersion, and 157 nm lithography (such as the one shown in Figure 4.1) employ a latent acidic functionality with a photoacid-cleavable protecting group.[9] After exposure to deep ultraviolet (UV) radiation, the protecting group is cleaved catalytically by

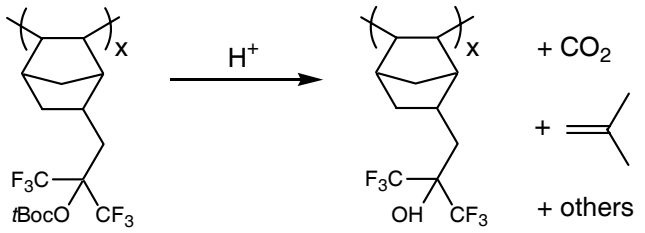

Figure 4.1. 157 nm photoresist with outgassing products

a photogenerated acid, releasing a number of volatile fragments which can outgas from the photoresist film and contaminate optical elements and produce distortions in the imaged features.[10] These issues have prompted the development of low-outgassing or mass-persistent photoresists based on the acid-catalyzed ring-opening of small and medium-sized lactones.[11] Negative tone resists also solve this outgassing problem, however, no negative tone resists based on fluorinated oxiranes or oxetanes suitable for 157nm lithography have been reported. 2,2-Bis(trifluoromethyl) oxetane has been shown to ring-open under acidic conditions in the presence of water or other nucleophiles to produce hexafluorocarbinol-functionalized compounds.[12] We imagined using an olefin-containing annulated oxetane (shown in Figure 4.2) which would remain intact during metal-catalyzed addition or ring-opening metathesis polymerization, yet ring-open under the superacidic conditions of imaging to produce either crosslinked networks (negative tone resists) or possibly hexafluorocarbinol-functionalized polymers (positive tone resists).

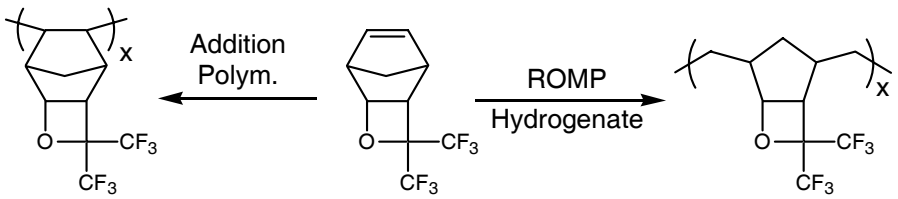

Figure 4.2. Oxetane-functionalized monomer and polymers

A number of 3-oxa-tricyclo[4.2.1.$0^{2,5}$]non-7-enes similar to the desired monomer have been reported in the literature to be synthesized via the cycloaddition of quadricyclane (**4.1**) with activated carbonyl compounds.[13] With non-activated ketones, photochemical or very high pressure techniques are required. The resultant norbornene-like annulated oxetanes are exclusively exo in configuration, which is ideal for metal-catalyzed polymerization. Given our experience with using quadricyclane cycloadditions with fluorinated olefins to synthesize tricyclo[4.2.1.$0^{2,5}$]non-7-ene monomers for use in 157 nm photoresists,[14] we sought to expand this methodology to include fluorinated ketones such as hexafluoroacetone to produce fluorinated 3-oxa-tricyclo[4.2.1.$0^{2,5}$]non-7-enes.[15]

Results and Discussion

Monomer Synthesis After condensation of hexafluoroacetone at -78 °C into a Fisher-Porter bottle containing quadricyclane, warming of the mixture to 0 °C resulted in a violent exotherm. This behavior is a marked contrast to quadricyclane cycloadditions with fluorinated olefins which only proceed upon extended heating.[14] On the other hand, this behavior is not so surprising in

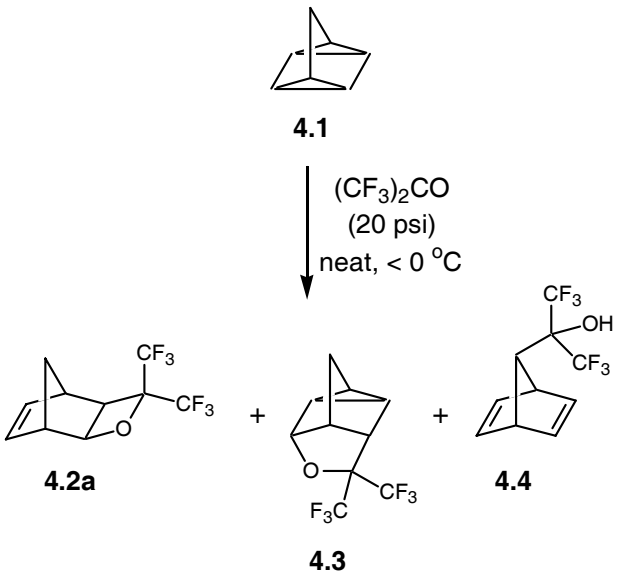

Figure 4.3. Synthesis of 3-oxa-tricyclo[4.2.1.$0^{2,5}$]non-7-enes

light of the ability of hexafluoroacetone to serve as an excellent dienophile in Diels-Alder reactions.[16,17] Subsequent analysis of the product mixture revealed three major products (Figure 4.3). The major product was the desired 3-oxatricyclononene (**4.2a**). The oxetane was determined to be exclusively in the exo configuration by examination of the ^{1}H coupling of the C-2 endo proton and comparison with the known 4,4-diphenyl-3-oxa-tricyclo[4.2.1.0^{2,5}]non-7-ene.[18] The second product was a result of a homo-endo type cycloaddition with norbornadiene (either present as an impurity in **4.1** or formed via thermal isomerization during the reaction) leading to compound **4.3**.[19] Modification of the reaction procedure to maintain a reaction temperature below 0 °C eliminated the formation of **4.3**, allowing the use of technical grade quadricyclane without affecting conversions to **4.2a**. Interestingly, the 7-substituted norbornadiene **4.4** was also isolated in small yields (< 1%) during column chromatography. Our preliminary efforts to increase yields of **4.4** in order to examine its optical transparency or potential materials applications have met with little success so far.

Table 4.1 presents the scope of this reaction with a variety of fluorinated ketones. One trifluoromethyl group is sufficient activation for the cycloaddition to proceed; however, higher reaction temperatures are required for the less activated ketones. While these less fluorinated oxatricyclononenes are not sufficiently transparent for use at 157 nm, their aliphatic groups provide excellent handles for ^{1}H NMR NOE experiments.

Table 4.1. Synthesis of 3-oxa-tricyclo[4.2.1.0^{2,5}]non-7-enes

Compound	R_1	R_2	Temp. (°C)	Time (h)	Syn:Anti	Isolated Yield (%)
4.2a	CF_3	CF_3	0	4	-	71
4.2b	Ph	CF_3	90	64	71:28	51
4.2c	CH_2Br	CF_3	60	16	58:42	81
4.2d*	Ph	Ph	rt	16	-	15

* Reaction performed photochemically (see experimental section)

Upon drying **4.2a** over 4 Å molecular sieves in preparation for metal-catalyzed polymerization, a new compound was observed to slowly form. Heating a dichloromethane solution of **4.2a** over flame-activated molecular sieves overnight resulted in complete isomerization of **4.2a** to 5,5-bis(trifluoromethyl)-4-oxa-tricyclo[4.3.$0^{1,6}$.$0^{3,7}$]non-8-ene (**4.5a**) (Figure 4.4). Suspecting the Lewis-acidic nature of the molecular sieves to be responsible, a number of Lewis acids including BF_3, $AlCl_3$, $FeCl_3$, $SnCl_4$ were all found to affect quantitative rearrangement.[20] Structural confirmation was achieved by osmium-catalyzed dihydroxylation of the olefin **4.5a** to produce the crystalline diol **4.6** whose x-ray crystal structure is shown in Figure 4.5.[21] This isomerization behavior is remarkably different than non-fluorinated 3-oxatricyclo[4.2.1.$0^{2,5}$]non-7-enes which retrocyclize to produce unsaturated aldehydes upon exposure to Lewis acids or rhodium complexes (lower pathway, Figure 4.4).[22] The destabilization of the partial positive charge by the highly electron-withdrawing trifluoromethyl groups disfavors this pathway and favors cleavage of the C2-O3 bond to form a non-classical norbornenyl cation which undergoes a Wagner-Meerwein rearrangement. Intramolecular quenching of the cation by the Lewis acid coordinated alkoxide produces **4.5a**. The large relief of ring strain by ring expansion of a strained oxetane to an unstrained tetrahydrofuran provides for a

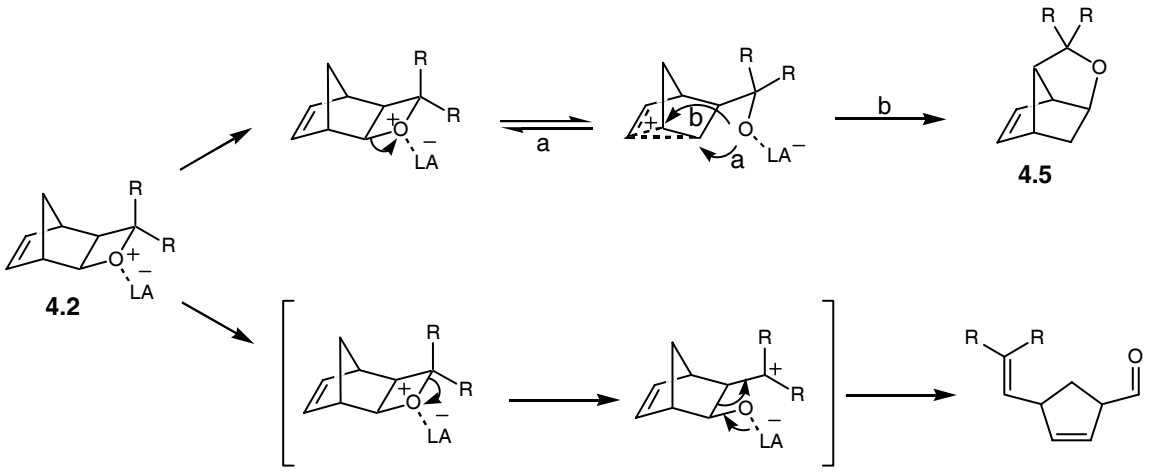

Figure 4.4. Lewis acid-catalyzed isomerizations of 3-oxatricyclononenes

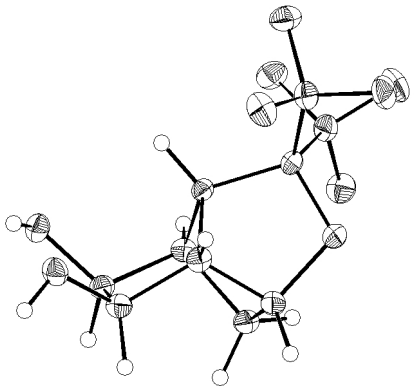

Figure 4.5. X-ray crystallographic structure of **4.6**

Table 4.2. Synthesis of 4-oxa-tricyclo[4.3.0^{1,6}.0^{3,7}]non-8-enes

4-Oxa-TCN	Parent 3-Oxa-TCN	Lewis acid	Temp. (°C)	Time (h)	Endo:Exo	Isolated Yield (%)
4.5a	**4.2a**	BF_3•OEt_2	rt	6	-	97
4.5a	**4.2a**	4Å MS	40	14	-	90
4.5b	**4.2b**	BF_3•OEt_2	40	21	71:28	76
4.5b	**4.2b**	4Å MS	40	24	71:28	96
4.5c	**4.2c**	BF_3•OEt_2	40	16	52:48*	82
4.5c	**4.2c**	4Å MS	40	16	58:42	98

***** Using **4.2c** with syn:anti ratio 52:48

rapid and irreversible reaction.[23-25]

All fluorinated 3-oxatricyclonenes (**4.2**) underwent clean isomerization to their respective 4-oxatricyclononenes (**4.5**) without polymerization (Table 4.2). ^{1}H NMR NOE experiments confirm that the 4-*anti*-substituent in the oxetane **4.2** always ends up in the endo-configuration in **4.5** after isomerization (Figure 4.6), in agreement with the mechanism shown in Figure 4.4. The necessity of only one trifluoromethyl group for the cycloaddition and subsequent isomerization allows for versatile derivatization of these compounds by simply using a functionalized trifluoromethyl ketone. Since this work was originally intended to develop materials for 157 nm lithography, only the highly fluorinated compounds **4.2a** and **4.5a** are examined further; however,

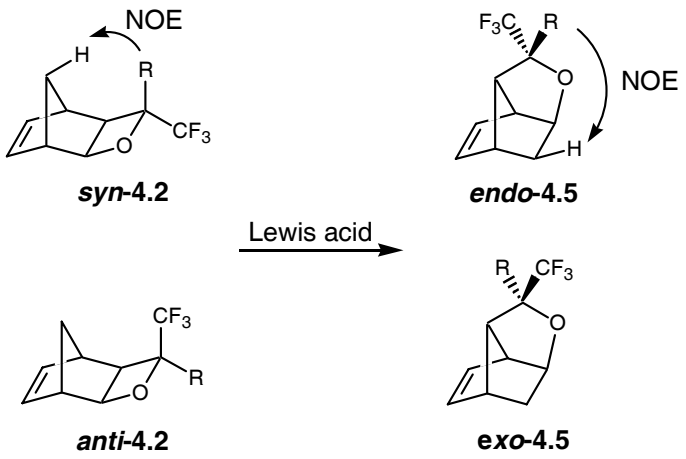

Figure 4.6. Stereochemistry of isomerization products

this methodology provides rapid and facile construction of a new class of fluorinated polycyclic olefins for use as building blocks for other materials and small molecules.

Optical Properties In order to examine the transparency of these fluorinated oxatricyclononenes, compounds **4.2a** and **4.5a** were hydrogenated over palladium on carbon to produce the oxatricyclononanes **4.7** and **4.8**, respectively. 4-Oxatricyclononane **4.8** was also synthesized in quantitative yield via exposure of 3-oxatricyclononane **4.7** to the Lewis acidic conditions used to isomerize **4.2a**. Their vacuum ultraviolet (VUV) spectra are shown in Figure 4.7. Surprisingly, despite the presence of the oxetane oxygen and the lack of fluorination directly on the norbornane skeleton, both oxatricyclononanes display high transparency at 157 nm. 3-Oxatricyclononane **4.7** is one of the most transparent norbornanes examined to date. These promising results prompted us to explore polymerization of these structures to provide confirmation of this high transparency.

Reactivity of Oxetane Ring The oxetane ring in **4.2a** is remarkably stable. Lithium aluminum hydride, lithium triethylborohydride, and lithium tri-*t*-butoxyalumium hydride/triethylborane were all ineffective at opening the oxetane to any useful extent. The oxetane ring proved slightly easier to open under acidic conditions. Reaction with stoichiometric

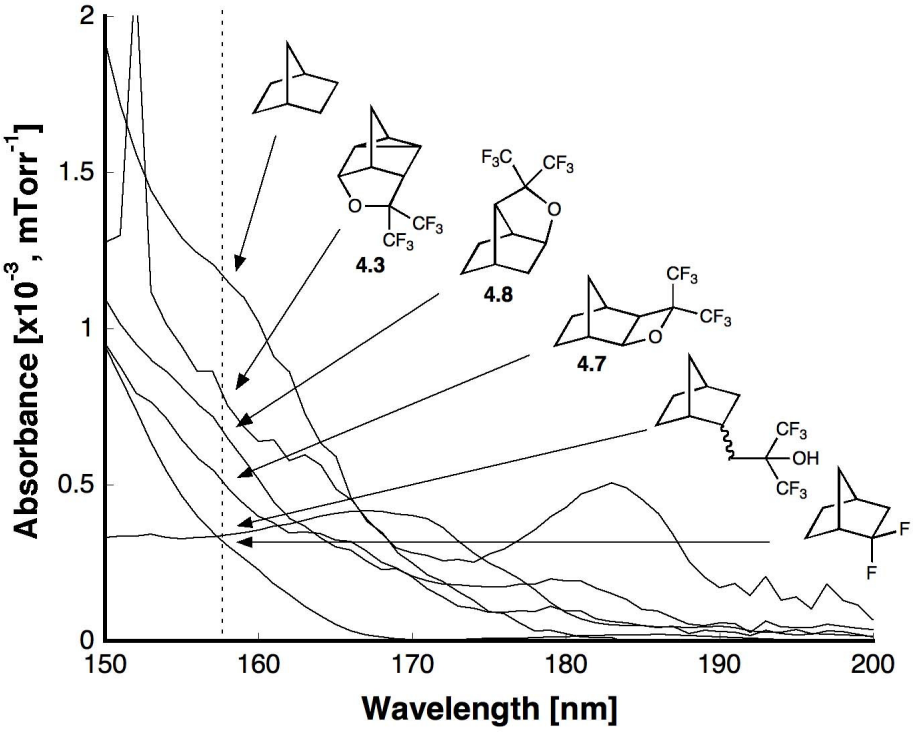

Figure 4.7. Vacuum ultraviolet spectra of oxatricyclononanes

amounts of trifluoroacetic acid afforded conversion to three hexafluorocarbinol-containing products: two nortricyclane structures with trifluoroacetate groups and one trifluoroacetate-free norbornene. Methanolysis resulted in the production of moderate yields of non-olefin ring-opened products (Figure 4.8).

Unfortunately, the saturated oxatricyclononane **4.7** is strongly resistant to ring opening under acidic conditions. Attempted methanolysis with sulfuric acid resulted in only trace reaction after 56 hours of reflux. Reaction with catalytic amounts of triflic acid afforded isomerization to **4.5a**, while reaction with stoichiometric amounts of triflic acid afforded ring-opened products. This is in marked contrast to 2,2-bis(trifluoromethyl)oxetane which ring-opens to afford monomeric and dimeric diols when heated with sulfuric acid for 1 hour.[26] Clearly, the annulated

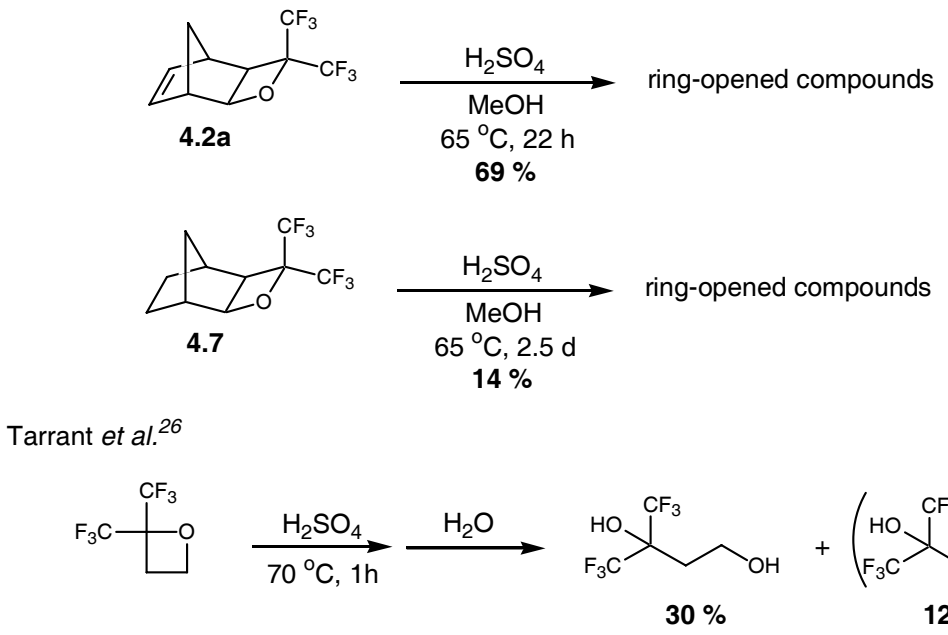

Figure 4.8. Acid-catalyzed ring-opening of **4.2a** and **4.7**

structure affords the oxetane ring a significant amount of stability, presumably by blocking nucleophilic attack which would have to occur from the endo side of the norbornene ring.

Therefore, ring-opening must proceed by an E1-process which is extremely slow and can result in isomerization to **4.5a**. In order for these structures to be useful as an active functionality in a photoresist, either the bulk of the annulating structure must be reduced to allow more room for nucleophilic attack on the oxetane (perhaps by using ring-opening metathesis), or the E1 process must be accelerated by stabilizing the resultant positive charge. While the ring-opening metathesis approach will be explored in Chapter 5, we explore the second option in this chapter by taking a look at oxetane acetal structures.

Model Oxetane Acetal Structures While hexafluoroacetone reacts with olefins containing an allylic hydrogen via an ene reaction at elevated temperatures to afford homoallylic hexafluorocarbinols,[27] it reacts with vinyl ethers under mild conditions to produce oxetane acetals.[28] These fluorinated oxetane acetals have been shown to open readily under acidic conditions to afford unsaturated hexafluorocarbinols[28] or β-hydroxy aldehydes[26,29]. Although the

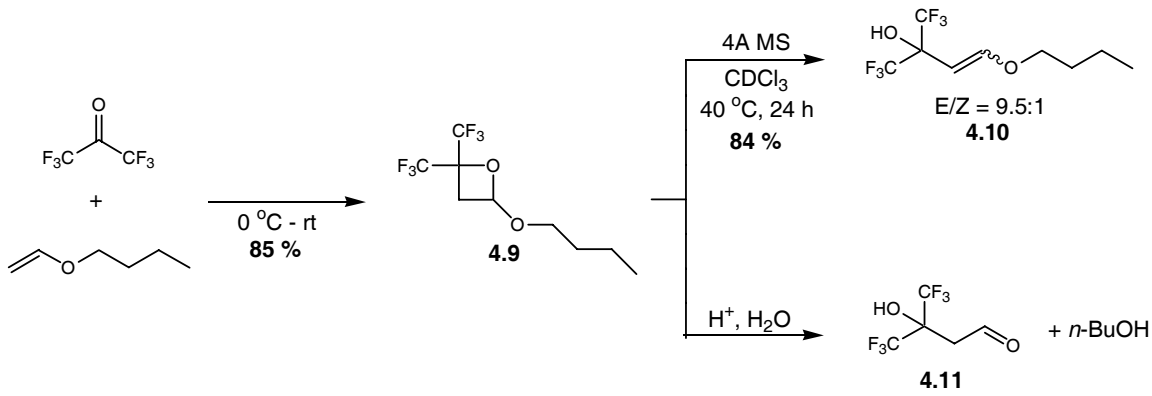

Figure 4.9. Model oxetane acetal synthesis

oxetane acetal structure is significantly more acid-labile, the effect of the additional oxygen on the absorbance of the structure could increase the absorption at 157 nm.

In order to examine the transparency of the oxetane acetal structure, 4-butoxy-2,2-bis(trifluoromethyl)-oxetane was synthesized by treatment of *n*-butyl vinyl ether with hexafluoroacetone (Figure 4.9). Quantitative cycloaddition occurred at 0 °C to afford high yields of oxetane acetal **4.9** after distillation. When the oxetane acetal was heated in the presence of a Lewis acid or sulfuric acid in the absence of water, the predominant ring-opened product is the unsaturated hexafluorocarbinol **4.10**; however, when water is present, aldehyde **4.11** and decomposition products such as the α,β-unsaturated aldehyde[26,29] are the major products in agreement with the literature. These reactions confirmed the high sensitivity of the fluorinated oxetane acetal structure to acidic conditions.

In order to evaluate the potential impact of the oxetane acetal structure on the transparency at 157 nm, the vacuum ultraviolet spectrum of **4.9** was measured and is shown in Figure 4.10. Remarkably, the oxetane acetal structure is extremely transparent despite the hydrocarbon tail and the additional oxygen. It appears to have slightly better transparency than hexafluoroisopropanol.

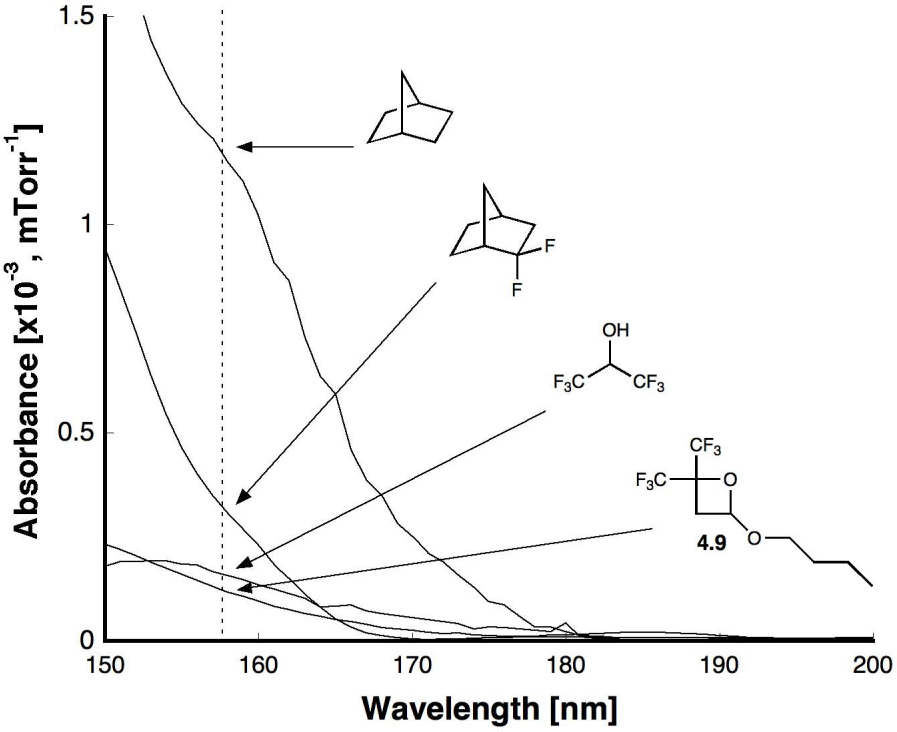

Figure 4.10. Vacuum ultraviolet spectrum of oxetane acetal **4.9**

With these results in hand, we set out to design an oxetane-acetal framework capable of being polymerized. The polymer portion may be connected to the oxetane acetal through 3 different locations: the alkoxy portion of the enol ether, the vinyl portion of the enol ether, or the perfluorinated ketone. An oxetane acetal connected to a polymer backbone through the alkoxy portion would release the hexafluorocarbinol as the volatile aldehyde during deprotection. This is disadvantageous because a non-acidic alcohol is now bound to the polymer backbone which is not base soluble, and the volatile aldehyde and its by-products pose a serious contamination problem to the lens optics. Of the two remaining routes, functionalization of heavily fluorinated ketones is the significantly more difficult endeavor. The most straightforward approach would be to attach the oxetane acetal to the polymer backbone through the olefinic group.

Seeking to maintain the norbornene framework for its high etch resistance and its ability to polymerize via a number of radical and metal-catalyzed pathways, the model 2-alkoxy-3-oxa-

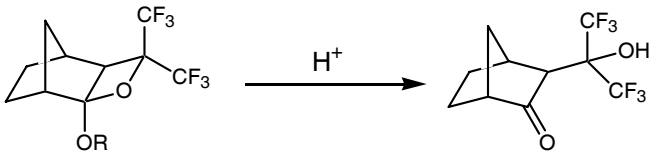

4.12 **4.13**

Figure 4.11. Model 2-alkoxy-3-oxatricyclononane system

tricyclo[4.2.1.$0^{2,5}$]nonane **4.12** was devised (Figure 4.11). This structure combines the alicyclic structure of the 3-oxatricyclononanes shown discussed previously with the acid labile oxetane acetal structure. Upon exposure to acid, it is expected to ring-open to form the hexafluorocarbinol-functionalized norcamphor **4.13**. Hexafluorocarbinol **4.13** has previously been synthesized by the Frechet group for use as a dissolution inhibitor for 157 nm lithography.[30] In addition, synthesis of an unsaturated version capable of being polymerized should be relatively straightforward. However, the combination of the oxetane acetal with the strained oxatricyclononene framework may lead to excessive sensitivity to acid. Fortunately, Kirby *et al.* have shown that incorporation of fluorine on the alkoxy portion of oxetane acetal (from 2,2,2-trifluoroethanol) slows the rate of ring-opening by 3 orders of magnitude.[31] This additional fluorination should also help increase transparency even further.

Synthesis of the non-fluorinated oxetane acetal **4.12a** proceeded in a straightforward manner starting from norcamphor (Figure 4.12). The dimethyl acetal of norcamphor was first converted to the methyl enol ether **4.15a**.[32] Exposure of **4.15a** to hexafluoroacetone afforded the oxetane acetal **4.12a** in good yields. Unfortunately, we were unable to produce the fluorinated enol ether **4.15b** from the fluorinated ketal **4.14b** with the same methodology (likely due to the lower electron density on the oxygens reducing their affinity for the aluminum trichloride). Performing the reaction at higher temperatures or with boron trifluoride diethyl etherate were similarly ineffective. Reaction with trimethylsilyl triflate/diisopropylethylamine, another common method to produce enol ethers from ketals,[33] was also ineffective. It is likely that

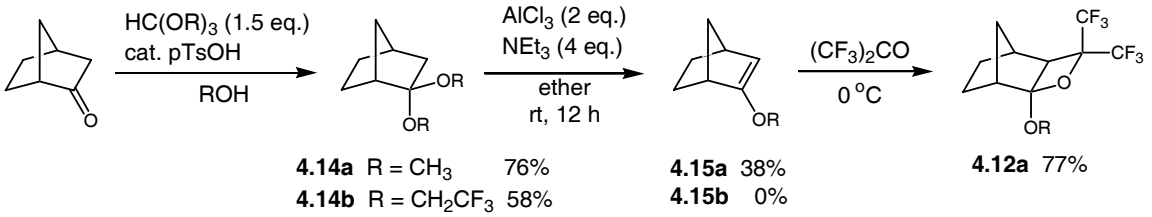

Figure 4.12. Synthesis of model 2-alkoxy-3-oxa-tricyclononanes

thermal cracking[34] of **4.14b** is required to generate the fluorinated enol ether.

Exposure of oxetane acetal **4.12a** to acidic conditions resulted in its quantitative hydrolysis to **4.13** under moderate conditions (Figure 4.13). The identity of the product was confirmed by independent synthesis from the silyl enol ether **4.16**. After reaction of trimethylsilyl enol ether **4.16** with hexafluoroacetone, three products were observed. The TMS-protected carbinol **4.17**, the deprotected carbinol **4.13,** and what is assigned to be the 2-siloxy-3-oxa-tricyclo[4.2.1.$0^{2,5}$]nonane **4.18** in a 1.9:1.3:1.0 ratio. Rearrangement products and other

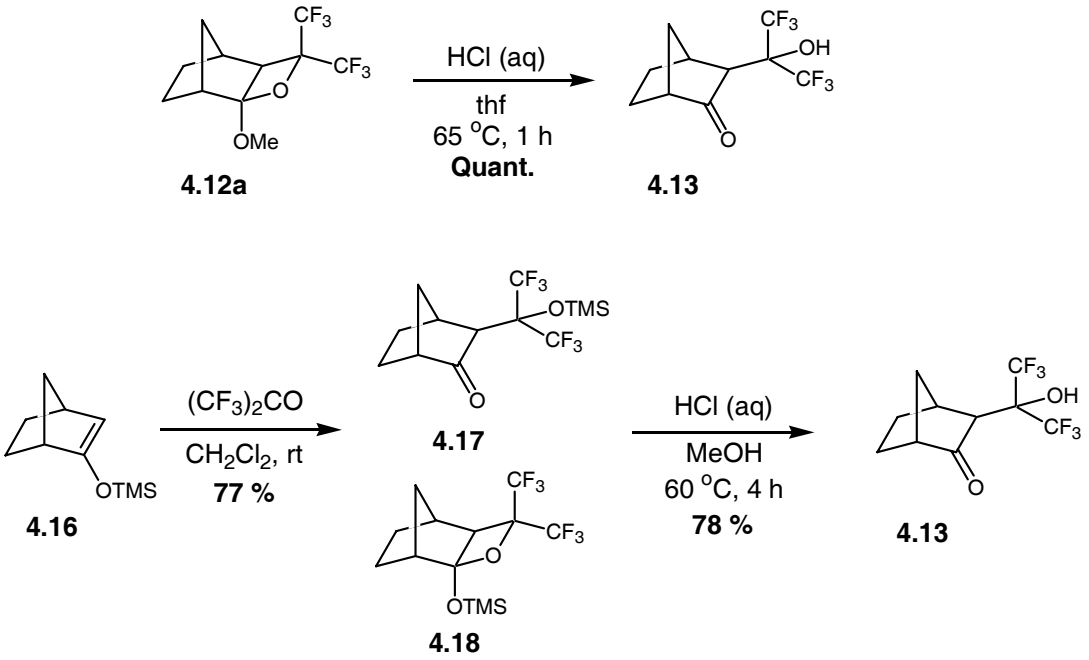

Figure 4.13. Acid-catalyzed ring-opening of model 2-alkoxy-3-oxa-tricyclononane

alkylations can be ruled out by the fact that the three component mixture reduces exclusively to **4.13** under hydrolytic conditions. This oxetane acetal formation is unusual, considering the reaction of silyl enol ethers with hexafluoroacetone usually results only in alkylation with silyl transfer to the oxygen.[35]

Unfortunately, the non-fluorinated oxetane acetal **4.12** has limited stability unless it is stored in the presence of a base such as potassium carbonate. Without a stabilizer, the oxetane acetal converts to **4.13** over the course of a few days, even when stored in the refrigerator. An oxetane acetal this sensitive would be unlikely to survive long term storage in a formulated resist or the baking processes involved in resist processing. However, the fluorinated oxetane acetal bears the promise of increased transparency and more importantly, an increased activation energy for ring-opening.

Conclusions

A wide variety of 3-oxa-tricyclo[4.2.1.$0^{2,5}$]non-7-enes have been synthesized in high yields via the thermal cycloaddition of quadricyclane with trifluoromethyl ketones. Lewis acid catalyzed rearrangement of these oxetane-functionalized monomers provides easy access to a valuable new class of fluorinated, alicyclic, norbornene-like monomers, 4-oxa-tricyclo[4.3.$0^{1,6}$.$0^{3,7}$]non-8-enes. Both frameworks exhibit good transparency at 193 nm and 157 nm and may be potentially employed in free-radical and metal-catalyzed addition and ring-opening metathesis polymerizations. Such structures could be used in conventional photoresists in place of norbornene to impart transparency and etch resistance or increase thermal and mechanical properties. The high stability of saturated 3-oxatricyclononanes towards acid-catalyzed ring-opening has caused us to explore more labile oxetane acetal structures. While a model oxetane acetal structure exhibits favorable transparency at 157nm, and a model 2-methoxy-3-oxa-tricyclononane opens quantitatively to a hexafluorocarbinol-substituted norcamphor derivative, such oxetane acetals are perhaps too sensitive to acid-catalyzed ring-

opening. Future work into more fluorinated oxetane acetal structures may prove to provide latent hexafluorocarbinols with high transparency and the right activation energy for ring-opening.

Experimental

Materials: All air sensitive manipulations and polymerizations were carried out in an N_2-filled drybox or using standard Schlenk techniques. All solvents were rigorously degassed in 18 L reservoirs and passed through two sequential purification columns consisting of activated alumina.[36] All starting materials were procured from Aldrich except 3-bromo-1,1,1-trifluoroacetone and trifluoroacetophenone (Avocado). Quadricyclane[37] was a gift from Exciton, Inc., Dayton, Ohio and was made available through a Phase II SBIR project that has been sponsored by the Propulsion Directorate of the U.S. Air Force Research Laboratory, AFRL/PR. **WARNING: Quadricyclane has extraordinary toxicity for a hydrocarbon.**[38] Just as with the fluorinated ketones used in this paper, standard chemical safety precautions should be taken to avoid inhalation of quadricyclane vapors. 2,2-Difluoronorbornane was synthesized by colleagues in the Willson group (University of Texas, Austin). All liquid reagents used for vacuum UV measurements were distilled from appropriate drying agents, thoroughly degassed by freeze, pump, thaw cycles and sealed in glass ampoules under vacuum.

Methods: Nuclear magnetic resonance (NMR) spectra were obtained using either a Bruker AMX300, Varian *Unity Plus 300*, Varian *Gemini 300*, or Varian *Mercury 300* spectrometer (^{1}H: 300 MHz, ^{13}C: 75 MHz, ^{19}F: 282 MHz). Shifts for NMR spectra are reported in ppm relative to TMS (for ^{19}F, internal C_6F_6 (~ 0.5 %) at -162.2 ppm[39]) or to the chemical shift of the residual proteo solvent.

X-ray Crystallography: X-ray crystallographic analysis on **4.6** was performed by the California Institute of Technology X-ray crystallography facility. See Appendix B for experimental procedure, labeled drawings, table of atomic coordinated, complete bond distances and angles, and anisotropic displacement parameters. Crystallographic data for compound **4.6** have been

deposited at the CCDC, 12 Union Road, Cambridge CB2 1EZ, UK, and copies can be obtained on request, free of charge, by quoting the publication citation and the deposition number 203516.

Vacuum UV Spectroscopy: Gas phase VUV measurements were made on an Acton *CAMS-507* spectrophotometer fitted with a custom-made gas cell attachment. The details of the cell design and implementation have been described previously.[1b]

4,4-Bis(trifluoromethyl)-3-oxa-tricyclo[4.2.1.0^{2,5}]non-7-ene (4.2a). Quadricyclane (10.2 mL, 10.0 g, 109 mmol) was added to an oven-dried 100 mL Fisher-Porter bottle and degassed via 3 sequential freeze-pump-thaw cycles. After cooling the reaction vessel to 0 °C, the system was exposed to 20 psi of hexafluoroacetone under rapid stirring. After the hexafluoroacetone was consumed over the course of a few minutes, the system was repressurized with hexafluoroacetone. This was repeated until no observable pressure decrease was observed after 20 minutes. Excess hexafluoroacetone was carefully vented through concentrated sodium hydroxide solution. The colorless liquid was purified via silica gel flash column chromatography (20:1 pentane/ether) to produce a colorless liquid. Alternatively, hexafluorocarbinol-containing impurities (such as **4.5**) may be washed away with saturated potassium carbonate solution followed by vacuum distillation (79 °C, 30 Torr). Yield: 71%. ^{1}H NMR ($CDCl_3$, 300 MHz, ppm): δ 6.31 (dd, *J* = 5.7, 3.3 Hz), 5.91 (dd, *J* = 5.7, 3.3 Hz), 4.74 (d, *J* = 3.6 Hz), 3.23 (s), 3.20 (s), 2.59 (d, *J* = 4.8 Hz), 2.40 (d, *J* = 9.6 Hz), 1.59 (d, *J* = 9.6 Hz). ^{19}F NMR ($CDCl_3$, 282 MHz, ppm): δ -69.09 (q, *J* = 10.6 Hz), -78.68 (q, *J* = 10.6 Hz). ^{13}C NMR ($CDCl_3$, 75 MHz, ppm): 140.84, 132.56, 123.87 (q, *J* = 286 Hz), 121.94 (q, *J* = 286 Hz), 84.33, 80.40 (m), 45.32, 42.24, 42.00, 41.69 (q, *J* = 4.60 Hz). HRMS-[GC-EI+] (m/z): [M•]+ calc'd for $C_{10}H_8F_6O$, 258.0479; found, 258.0481.

4-Phenyl-4-trifluoromethyl-3-oxa-tricyclo[4.2.1.0^{2,5}]non-7-ene (4.2b). Quadricyclane (0.831 g, 9.02 mmol) and 2,2,2-trifluoroacetophenone (1.52 mL, 1.88 g, 10.8 mmol) were added to a flame dried 50 mL thick-walled Schlenk tube and degassed via 3 sequential freeze-pump-thaw

cycles. The reaction vessel was sealed under argon and heated at 90 °C for 17 hours. The yellowish liquid was purified via silica gel flash column chromatography (20:1 pentane/ether) to produce a colorless liquid. Yield: 1.16 g (51%). Isomer composition: 73% syn, 27% anti. ^{1}H NMR ($CDCl_3$, 300 MHz, ppm): δ 7.64(dd, *J* = 1.8, 0.9 Hz, 2H, anti), 7.5-7.3(m, 6H), 6.30 (dd, *J* = 5.4, 3.0 Hz, 1H, anti), 6.22 (dd, *J* = 5.7, 3.3 Hz, 1H, syn), 5.91(dd, *J* = 5.7, 3.3 Hz, 1H, syn), 5.83 (dd, *J* = 5.7, 3.3 Hz, 1H, anti), 4.76 (d, *J* = 4.8 Hz, 1H, syn), 4.47 (dd, *J* = 4.8, 2.1 Hz, 1H, anti), 3.34 (s, 1H, anti), 3.19 (d, *J* = 1.5 Hz, 1H, anti), 3.07 (t, *J* = 1.5 Hz, 1H, anti), 2.90-2.82 (m, 2H, syn), 2.75 (d, *J* = 9.3 Hz, 1H, anti, 2.51 (d, *J* = 4.8 Hz, 1H, anti), 1.62 (d, *J* = 9.3 Hz, 2H, syn), 1.20 (d, *J* = 9.6 Hz, 2H, anti). ^{19}F NMR ($CDCl_3$, 282 MHz, ppm): δ -72.58 (s, anti), -82.26 (s, syn) .^{13}C NMR ($CDCl_3$, 75 MHz, ppm): 141.35, 139.82, 139.20, 134.29, 132.98, 132.22, 128.55, 128.38, 128.14, 126.54, 126.47, 125.59 (q, *J* = 285 Hz, syn), 123.90 (q, *J* = 285 Hz, anti), 82.00, 81.42, 48.86, 45.68, 45.20, 42.68, 42.53 (m), 41.92, 41.61, 41.16. HRMS-[GC-EI+] (m/z): [M•]+ calc'd for $C_{15}H_{13}F_3O$, 266.0919; found, 266.0920.

4-Bromomethyl-4-trifluoromethyl-3-oxa-tricyclo[4.2.1.0^{2,5}]non-7-ene (4.2c). Quadricyclane (2.23 mL, 2.19 g, 23.8 mmol) and 1,1,1-trifluoro-3-bromoacetone (2.72 mL, 5.00 g, 26.2 mmol) were added to a flame dried 50 mL thick-walled Schlenk tube and degassed via 3 sequential freeze-pump-thaw cycles. The reaction vessel was sealed under argon and heated at 60 °C for 16 hours. The yellowish liquid was purified via silica gel flash column chromatography (30:1 pentane/ether) to produce a colorless liquid. Yield: 5.50 g (82 %) Isomer composition: 58 % syn, 44% anti. ^{1}H NMR ($CDCl_3$, 300 MHz, ppm): 6.31 (dd, *J* = 5.4, 3.3 Hz, 1H, anti), 6.27(dd, *J* = 5.4, 3.3 Hz, 1H, syn), 5.92 (dd, *J* = 5.4, 3.3 Hz, 1H, syn), 5.88 (dd, *J* = 5.4, 3.3 Hz, 1H, anti), 4.62 (d, *J* = 4.5 Hz, 1H, syn), 4.59 (d, *J* = 4.8 Hz, 1H, anti), 3.81 (d, *J* = 11.1 Hz, 1H, anti), 3.67 (dm, *J* = 11.1 Hz, 1H, anti), 3.61 (s, 2H, syn), 3.17(s, 2H), 3.13 (s, 2H), 2.50 (d, *J* = 5.1 Hz, 2H), 2.46 (d, *J* = 9.9 Hz, 1H, anti), 2.12 (d, *J* =9.3 Hz, 1H, syn), 1.65(d, *J* = 9.3 Hz, 1H, syn), 1.53 (d, *J* 9.9 Hz, 1H, anti). ^{19}F NMR ($CDCl_3$, 282 MHz, ppm): δ -69.23 (s, anti), -80.43 (s, syn). ^{13}C NMR

($CDCl_3$, 75 MHz, ppm): 141.26 (anti), 139.83 (syn), 132.76 (syn), 132.20 (anti), 125.78 (q, *J* = 287 Hz, syn), 81.79 (anti), 81.78 (syn), 80.02 (m, anti), 78.82 (m, syn), 45.51 (anti), 45.15 (anti), 44.95 (syn), 42.34 (syn), 42.26 (anti), 41.61 (m, anti), 40.95 (syn), 40.54 (syn), 32.93 (d, J = 3.1 Hz, anti), 24.21 (d, J = 1.5 Hz, syn). HRMS-[GC-EI+] (m/z): [M•]+ calc'd for $C_{10}H_{10}F_3OBr$ 281.9866,; found, 281.9867.

4,4-Diphenyl-3-oxa-tricyclo[4.2.1.0^{2,5}]non-7-ene (4.2d). Norbornadiene (2.70 mL, 2.30 g, 25.0 mmol) and benzophenone (3.04 g, 16.7 mmol) in 500 mL benzene were added to a photochemical reaction vessel and degassed via sparging with nitrogen. The reaction vessel was irradiated for 16 hours with a Hanovia 400W medium pressure Hg lamp. The yellowish liquid was purified by recrystallization from ether 2x to yield white crystals. Yield: 0.69 g (15%). Spectra agree with previous reports.[18] ^{1}H NMR (CD_2Cl_2, 300 MHz, ppm): δ 7.56 (dt, *J* = 8.4, 1.5 Hz, 2H), 7.4-7.25 (m, 6H), 7.19 (tm, J = 6.9 Hz, 2H), 6.22 (dd, *J* = 5.7, 3.0 Hz, 1H), 5.89 (dd, *J* = 5.7, 3.0 Hz, 1H), 4.57 (dm, *J* = 5.4 Hz, 1H), 3.03 (m, 2H), 2.87 (dt, *J* = 5.1 1.5 Hz, 1H), 1.78 (d, *J* = 9.0 Hz, 1H), 1.20 (dt, *J* = 9.3, 1.5 Hz, 1H). ^{13}C NMR (CD_2Cl_2, 75 MHz, ppm):149.15, 144.72, 139.70, 133.24, 128.82, 128.56, 127.08, 126.83, 125.17, 124.96, 84.84, 79.44, 49.41, 46.14, 42.65, 42.11. HRMS-[GC-EI+] (m/z): [M•]+ calc'd for $C_{20}H_{18}O$, 274.1358; found, 274.1359.

4,4-Bis(trifluoromethyl)-3-oxa-tetracyclo[7.1.0.0^{2,6}.0^{5,9}]nonane (4.3). Norbornadiene (4.7 mL, 4.0 g, 43 mmol) was added to an oven dried 100 mL Fisher-Porter bottle and degassed via 3 sequential freeze-pump-thaw cycles. Hexafluoroacetone was condensed into the vessel at -78 °C. The reaction vessel was closed under argon and slowly warmed to room temperature. The reaction was heated at 90 °C for 24 hours. Excess hexafluoroacetone was carefully vented through concentrated sodium hydroxide solution. The colorless liquid was purified via silica gel flash column chromatography (40:1 hexane/ethyl acetate) to produce a colorless liquid. Yield: 2.4 g(22%). ^{1}H NMR ($CDCl_3$, 300 MHz, ppm): δ 4.58 (s, 1H), 2.80 (s,1H), 2.53 (s, 1H), 1.70 (d, *J* = 1.8 Hz, 2H), 1.57 (t, *J* = 5.2 Hz, 1H), 1.45 (d, *J* = 4.8 Hz, 2H). ^{19}F NMR ($CDCl_3$, 282 MHz,

ppm): δ -68.88 (q, *J* = 11.2 Hz), -75.15 (q, *J* = 10.5 Hz). ^{13}C NMR ($CDCl_3$, 75 MHz, ppm): 123.51 (q, *J* = 286 Hz), 122.92 (q, *J* = 286 Hz), 87.22, 84.02 (m), 48.54, 40.95 (q, *J* = 4.0 Hz), 28.63, 16.10, 15.87, 12.63. HRMS-[GC-EI+] (m/z): [M•]+ calc'd for $C_{10}H_8F_6O$, 258.0479; found, 258.0484.

2-(Bicyclo[2.2.1]hepta-2,5-dien-7-yl)-1,1,1,3,3,3-hexafluoro-propan-2-ol (4.4). Column chromatography (20:1 pentane/ether) of the crude reaction mixture of **4.2a** afforded **4.5** as a colorless oil. Yield: < 1 %. ^{1}H NMR ($CDCl_3$, 300 MHz, ppm): δ 7.02 (t, *J* = 2.1 Hz, 2H), 6.96 (t, *J* = 2.1 Hz, 2H), 4.34 (s, 1H), 3.86 (s, 2H), 3.05 (s, H). ^{19}F NMR ($CDCl_3$, 282 MHz, ppm): δ -76.81 (s). ^{13}C NMR ($CDCl_3$, 75 MHz, ppm): δ 146.11, 142.72, 122.92 (q, *J* = 289 Hz), 78.29, 51.74. HRMS-[EI-GC] (m/z): [M•]+ calc'd for $C_{10}H_8F_6O$, 258.0468; found, 258.0479.

General procedure for Lewis acid catalyzed isomerization of 3-oxa-tricyclo[4.2.1.0^{2,5}]non-7-enes:

Method A. Boron trifluoride diethyl etherate: 3-Oxa-tricyclo[4.2.1.0^{2,5}]non-7-ene (**4.2**) (1.9 mmol) was added to a flame dried 100 mL round bottom flask with 10 mL anhydrous dichloromethane [0.2M]. Boron trifluoride diethyl etherate (0.19 mmol, 0.1 eq.) was added via syringe at 0 °C and the reaction was slowly warmed to room temperature and stirred for 6-18 hours. The boron trifluoride was quenched with excess anhydrous triethylamine. The dichloromethane was removed *in vacuo* and the crude reaction mixture was purified via silica gel flash column chromatography (20:1 pentane/ether) to afford clean **4.5**.

Method B. Flame activated molecular sieves: 3-Oxa-tricyclo[4.2.1.0^{2,5}]non-7-ene (**4.2**) (1.9 mmol) in 10 mL anhydrous dichloromethane [0.2M] was added to a flame dried 100 mL round bottom flask with flame activated 4Å molecular sieves (Advanced Specialty Gas Corp, rods). The reaction was heated at 40 °C until isomerization was complete. Filtration of the reaction mixture through a 0.45 μm PTFE syringe filter to remove cloudiness followed by removal of the solvent in vacuo afforded **4.5** in excellent yields.

5,5-Bis(trifluoromethyl)-4-oxa-tricyclo[4.3.0^{1,6}.0^{3,7}]non-8-ene (4.5a). *Method A:* Reaction of 4,4-bis(trifluoromethyl)-3-oxa-tricyclo[4.2.1.0^{2,5}]non-7-ene (**4.2a**) (9.68 g, 37.5 mmol) afforded 9.42 g (97%) of **4.5a**. *Method B:* Reaction of 4,4-bis(trifluoromethyl)-3-oxa-tricyclo[4.2.1.0^{2,5}]non-7-ene (**4.2a**) (1.03 g, 3.9 mmol) afforded 0.92 g (90%) of **4.5a**. ^{1}H NMR ($CDCl_3$, 300 MHz, ppm): δ 6.45 (dd, *J* = 6.0, 3.3 Hz), 5.84 (dd, *J* = 5.4, 3.3 Hz), 4.48 (s), 3.56 9(s), 2.99 (m), 2.93 (s), 2.16 (dd, *J* = 12.6, 4.8 Hz), 1.09 (dm, *J* = 12.6 Hz). ^{19}F NMR ($CDCl_3$, 282 MHz, ppm): δ -69.72 (q, *J* = 12.5 Hz), -74.97 (q, *J* = 11.8 Hz). ^{13}C NMR ($CDCl_3$, 75 MHz, ppm): δ 124.51, 127.72, 123.24 (q, *J* = 288 Hz), 122.73 (q, *J* = 288 Hz), 81.140 (m), 78.13, 64.99, 52.58 (m), 41.93, 36.29 (m). HRMS-[EI+GC] (m/z): [M•]+ calc'd for $C_{10}H_8F_6O$, 258.0479; found, 258.0487.

5-Phenyl-5-trifluoromethyl-4-oxa-tricyclo[4.3.0^{1,6}.0^{3,7}]non-8-ene (4.5b). *Method A:* Reaction of 4-phenyl-4-trifluoromethyl-3-oxa-tricyclo[4.2.1.0^{2,5}]non-7-ene (**4.2b**) (0.250 g, 0.84 mol) afforded 0.19 (76%) of **4.5a**. *Method B:* Reaction of 4-phenyl-4-trifluoromethyl-3-oxa-tricyclo[4.2.1.0^{2,5}]non-7-ene (**4.2b**) (0.250 g, 0.94 mol) afforded 0.24 g (96%) of **5a**. Composition: 71% endo, 28% exo. ^{1}H NMR ($CDCl_3$, 300 MHz, ppm): δ 8.0-7.0 (m, aromatic, 10H), 6.43 (ddd, *J* = 5.7, 3.3, 0.9 Hz, 1H, exo), 6.26 (ddd, *J* = 5.7, 3.3, 0.96 Hz, 1H, endo), 5.91 (ddd, *J* = 5.7, 3.3, 1.2 Hz, 1H, endo), 5.73 (ddd, *J* = 5.7, 3.3, 0.9 Hz, 1H, exo), 4.50 (m, 1H, exo), 4.43 (t, *J* = 3.0 Hz, 1H, endo), 3.57 (m, 1H, endo), 3.32 (m, 1H, endo), 3.17 (m, 1H, exo), 3.04 (m, 1H, exo), 2.88 (m, 1H, exo), 2.56 (m, 1H, endo), 2.29 (dd, *J* = 12.6, 4.8 Hz, 1H, exo), 1.52 (dd, *J* = 12.6, 4.8 Hz, 1H, endo), 1.12 (dm, *J* = 12.6 Hz, exo), 0.87 (ddd, *J* = 12.6, 3.6, 1.8 Hz, 1H, endo). ^{19}F NMR ($CDCl_3$, 282 MHz, ppm): δ -72.78 (s, exo), -77.02 (s, endo). ^{13}C NMR ($CDCl_3$, 75 MHz, ppm): 142.87, 140.50, 139.57, 136.07, 128.93, 128.42, 128.38, 128.22, 127.83, 126.48, 125.41 (q, *J* = 285 Hz, exo), 124.60 (q, *J* = 284 Hz, endo), 81.76 (m), 81.13 (m), 77.34, 76.59, 69.32, 67.25, 52.61, 52.11 (m), 42.28, 36.71 (m). HRMS-[GC-EI+] (m/z): [M•]+ calc'd for $C_{15}H_{13}F_3O$, 266.0919; found, 266.0926.

5-Bromomethyl-5-trifluoromethyl-4-oxa-tricyclo[4.3.0^{1,6}.0^{3,7}]non-8-ene (4.5c). *Method A:* Reaction of 4-bromomethyl-4-trifluoromethyl-3-oxa-tricyclo[4.2.1.0^{2,5}]non-7-ene (**2c**) (1.11, 3.92 mmol) afforded 0.913 g (82%) of **4.5a**. *Method B:* Reaction of 4-bromomethyl-4-trifluoromethyl-3-oxa-tricyclo[4.2.1.0^{2,5}]non-7-ene (**4.2c**) (1.20 g, 4.24 mmol) 4-phenyl-4-trifluoromethyl-3-oxa-tricyclo[4.2.1.0^{2,5}]non-7-ene (**4.2b**) (0.50 g, 1.9 mol) afforded 1.17 g (98%) of **5a**. Composition: 58% endo, 42% exo. ^{1}H NMR ($CDCl_3$, 300 MHz, ppm): δ 6.44 (dd, *J* = 6.0, 3.0 Hz, 1H, exo), 6.38 (dd, *J* = 6.0, 3.0 Hz, 1H, endo), 5.88 (dd, *J* = 6.0, 3.0 Hz, 1H, endo), 5.83 (dd, *J* = 6.0, 3.0 Hz, 1H, exo), 4.41 (d, *J* = 3.3 Hz, 1H, endo), 4.40 (d, *J* = 3.0 Hz, 1H, exo), 3.61 (d, *J* = 11.4 Hz, 1H, endo), 3.49 (m, 1H, endo), 3.46 (d, *J* = 11.4 Hz, 1H, endo), 3.45 (dm, *J* = 11.7 Hz, 1H, exo), 3.36 (dm, *J* = 11.4 Hz, 1H, exo), 3.29 (m, 1H, exo), 3.11 (m, 1H, endo), 3.00 (m, 3H,) 2.13 (dd, *J* = 12.6, 4.5 Hz, 1H, exo), 1.90 (dd, *J* = 12.9, 4.5 Hz, 1H, endo), 1.18 (dq, *J* = 12.9, 1.8 Hz, 1H, endo), 1.00 (dm, *J* = 12.6 Hz, 1H, exo). ^{19}F NMR ($CDCl_3$, 282 MHz, ppm): δ -70.46 (s, exo), -75.44 (s, endo). ^{13}C NMR ($CDCl_3$, 75 MHz, ppm): 143.41, 141.12, 128.81, 127.40, 125.28 (q, *J* = 287 Hz), 124.74 (q, *J* = 287 Hz), 79.13 (m), 78.21 (d, 2.0 Hz), 77.48 (d, J = 2.0 Hz) 66.44, 66.25, 52.48 (m), 41.80, 40.84, 36.68, 35.82, 31.33, 28.14. HRMS-[GC-EI+] (m/z): [M•]+ calc'd for $C_{10}H_{10}F_3OBr$, 281.9867; found, 281.9873.

5,5-Bis(trifluoromethyl)-4-oxa-tricyclo[4.3.0^{1,6}.0^{3,7}]nonane-8,9-diol (4.6). To a solution of **4.5a** (0.53 g, 2.1 mmol) and *n*-methyl morpholine oxide (0.29 g, 2.5 mmol) in 20 mL tetrahydrofuran/water (9;1) was added osmium tetroxide (2.5 wt% solution in *t*-butanol, 257 μL, 0.02 mmol). The reaction was stirred at room temperature for 30 minutes, after which TLC indicated consumption of **4.5a** was complete. Silica gel chromatography (1:2 pentane/ether) afforded **4.6** as a white crystalline solid. Slow recrystallization from hexanes/ether produced crystals suitable for x-ray crystallographic analysis. Yield: 0.300g (49 %). ^{1}H NMR (Acetone-d_6, 300 MHz, ppm): δ 4.51 (m, 2H), 4.35 (d, *J* = 6.6 Hz, 1H), 3.94 (t, *J* = 6.0 Hz, 1H), 3.88 (m, 1H), 3.19 (s, 1H), 2.72 (m, 1H), 2.43 (dm, *J* = 7.5 Hz, 1H), 1.74 (dd, *J* = 14.1, 6.3 Hz, 1H), 1.06 (d, J = 14.1 Hz, 1H). ^{19}F NMR (Acetone-d_6, 282 MHz, ppm): δ -70.66 (q, *J* = 11.9 Hz), -75.32 (q, *J* =

11.9 Hz). ^{13}C NMR (Acetone-d_6, 75 MHz, ppm): δ 124.34 (q, *J* = 288 Hz), 123.76 (q, *J* = 288 Hz), 84.44 (m), 81.58, 74.99, 66.97, 55.54 (m), 48.09, 43.80, 30.08. HRMS-[FAB-gly] (m/z): [M + H]+ calc'd for $C_{10}H_{11}F_6O_3$, 293.0612; found, 293.0609.

4,4-Bis(trifluoromethyl)-3-oxa-tricyclo[4.2.1.0^{2,5}]nonane (4.7). 4,4-Bis(trifluoromethyl)-3-oxa-tricyclo[4.2.1.0^{2,5}]non-7-ene (**4.2a**) (0.97 g, 3.8 mmol) and palladium on carbon (10 wt% Pd, 150 mg) were added to a 100 mL round bottom flask with 15 mL diethyl ether. The solution was degassed via 3 freeze-pump-thaw cycles. After attaching a balloon of hydrogen, the reaction was stirred overnight at room temperature. Subsequent filtration through a 0.45 μm PTFE filter and removal of the solvent in vacuo afforded **4.7** as a colorless liquid. Yield: 0.98g (100 %). ^{1}H NMR (CD_2Cl_2, 300 MHz, ppm): δ 4.99 (dd, *J* = 3.0, 1.2 Hz, 1H), 2.71 (d, *J* = 4.5 Hz, 1H), 2.61 (s, 1H), 2.52 (d, *J* = 11.1 Hz, 1H), 2.44 (m, 1H), 1.7-1.5 (m, 2H), 1.44 (d, *J* = 11.1 Hz, 1H), 1.08 (m 1H), 0.93 (m, 1H). ^{19}F NMR (CD_2Cl_2, 282 MHz, ppm): δ -70.39 (m), -79.50 (m). ^{13}C NMR (CD_2Cl_2, 75 MHz, ppm): 124.06 (q, *J* = 288 Hz), 122.20 (q, *J* = 288 Hz), 89.03 46.27, 39.39, 36.50, 33.33 (m), 28.86, 22.18. HRMS- (m/z): [M•]+ calc'd for $C_{10}H_{10}F_6O$, 260.0636; found, 260.0632.

5,5-Bis(trifluoromethyl)-4-oxa-tricyclo[4.3.0^{1,6}.0^{3,7}]nonane (4.8). 5,5-Bis(trifluoromethyl)-4-oxa-tricyclo[4.3.0.0^{3,7}]non-8-ene (**4.5a**) (0.75 g, 2.9 mmol) and palladium on carbon (10 wt% Pd, 150 mg) were added to a 100 mL round bottom flask with 50 mL diethyl ether. The solution was degassed via three freeze-pump-thaw cycles. After attaching a balloon of hydrogen, the reaction was stirred for 12 hours at room temperature. Subsequent filtration through a 0.45 μm PTFE filter and removal of the solvent in vacuo afforded **4.8** as a colorless liquid. Yield; 0.75g (100 %). ^{1}H NMR (CD_2Cl_2, 300 MHz, ppm): δ 4.41 (s, 1H), 2.85 (dd, *J* = 3.0, 1.5 Hz, 1H), 2.56 (s, 1H), 2.41 (dd, *J* = 3.9, 1.8 Hz, 1H), (dd, *J* = 13.8, 5.4 Hz, 1H), 1.75-1.60 (m, 2H), 1.5-1.35 (m, 2H), 1.18 (dm, *J* = 12.3 Hz, 1H). ^{19}F NMR ($CDCl_3$, 282 MHz, ppm): δ -70.39 (q, *J* = 11.9 Hz), -75.05 (q, *J* = 11.9 Hz). ^{13}C NMR ($CDCl_3$, 75 MHz, ppm): 123.87 (q, *J* = 287 Hz), 123.26 (q, *J* =

287 Hz), 84.46, 51.03, 47.09 (m), 37.04, 33.93 (m), 32.19, 18.84. HRMS-[GC-EI+] (m/z): [M•]+ calc'd for $C_{10}H_{10}F_6O$, 260.0636; found, 260.0640.

4-Butoxy-2,2-bis-trifluoromethyl-oxetane (4.9). *n*-Butyl vinyl ether (3.0 g mL, 3.0 mmol) was added to an oven dried 100 mL Fisher-Porter bottle and degassed via three sequential freeze-pump-thaw cycles. The vessel was pressurized with 20 psi of hexafluoroacetone at 0 °C while rapidly stirring. When the pressure fell to < 5 psi, an additional 20 psi of hexafluoroacetone was added. This procedure was repeated until the pressure did not decrease after 20 minutes. Excess hexafluoroacetone was carefully vented through concentrated sodium hydroxide solution. NMR analysis showed quantitative conversion to product. The colorless liquid was unstable to silica gel flash column chromatography, so Kugelrohr distillation (rt, 20 mTorr) was used to afford a colorless liquid. The product was stored over potassium carbonate. Yield: 6.6 g (85 %). ^{1}H NMR ($CDCl_3$, 300 MHz, ppm): δ 5.59 (t, *J* = 5.0 Hz, 1H), 3.79 (m, 1H), 3.56 (m, 1H), 3.07 (dd, *J* = 5.7, 13.5 Hz, 1H), 2.83 ddd, *J* = 1.5, 4.5, 13.5 Hz, 1H), 1.61 (m, 2H), 1.40 (m, 2H), 0.94 (t, *J* = 7.5 Hz, 3H). Spectrum agrees with previously reported compound (see Ref. 28a). ^{19}F NMR ($CDCl_3$, 282 MHz, ppm): δ -79.08 (m), -79.20 (m). ^{13}C NMR ($CDCl_3$, 75 MHz, ppm): 122.98 (q, *J* = 282 Hz), 121.62 (q, *J* = 282 Hz), 102.12, 76.14, 69.73, 32.33, 31.73, 19.22, 13.82. HRMS-[GC-EI+] (m/z): [M•]+ calc'd for $C_9H_{12}F_6O_2$, 266.0741; found, 266.0750.

4-Butoxy-1,1,1-trifluoro-2-trifluoromethyl-but-3-en-2-ol (4.10). 4-Butoxy-2,2-bis-trifluoromethyl-oxetane (**4.9**). (0.02 g, 0.08 mmol) in 1 mL $CDCl_3$ was added to an NMR tube with flame activated 4Å molecular sieves (3.0 g mL, 3.0 mmol) and heated for 24 hours at 40 °C. NMR analysis indicated the formation of 4 major products: 85% 4-Butoxy-1,1,1-trifluoro-2-trifluoromethyl-but-3-en-2-ol (4.x) (E/Z = 9.5:1), 3% aldehyde-containing species, and 13% of an unidentified compound. ***E*-4.10x:** ^{1}H NMR ($CDCl_3$, 300 MHz, ppm): δ 6.95 (d, *J* = 12.6 Hz, 1H), 4.82 (d, *J* = 12.6 Hz, 1H), 3.78 (t, *J* = 6.6 Hz, 2H), 2.86 (s, 1H), 1.68 (m, 2H), 1.40 (m, 2H), 0.96 (t, *J* = 7.2 Hz, 3H). ^{19}F NMR ($CDCl_3$, 282 MHz, ppm): δ -79.30 (m). ^{13}C NMR ($CDCl_3$, 75

MHz, ppm): 154.24, 124.38, 91.82, 70.01, 30.98, 19.02, 13.73. Spectrum agrees with previously reported compound (see Ref. 28a). ***Z*-4.10x:** ^{1}H NMR ($CDCl_3$, 300 MHz, ppm): δ 6.45 (d, *J* = 6.6 Hz, 1H), 4.59 (d, *J* = 7.2 Hz, 1H), 3.95 (t, *J* = 6.6 Hz, 2H), 3.05 (s, 1H), 1.67 (m, 2H), 1.40 m, 2H), 0.94 (t, *J* = 7.2 Hz, 3H). ^{19}F NMR ($CDCl_3$, 282 MHz, ppm): δ -79.12 (m). HRMS-[GC-EI+] (m/z): [M•]+ calc'd for $C_9H_{12}F_6O_2$, 266.0741; found, 266.0748.

2-Methoxy-4,4-bis-trifluoromethyl-3-oxa-tricyclo[4.2.1.0^{2,5}]nonane (4.12a). To a dry pressure reaction vessel was added 2-methoxy-norborn-2-ene (1.74 g, 14 mmol) and deoxygenated at –78 °C. The vessel was warmed to 0 °C and hexafluoroacetone was added to 20 psi. When the vessel pressure decreased to 5 psi, hexafluoroacetone was added to 20 psi and this procedure repeated until the pressure remained at 5 psi for 30 minutes. A vacuum line was used to remove remaining hexafluoroacetone to afford a yellow oil which was added to ether and successively washed with 0.5M sodium hydroxide solution, saturated potassium carbonate solution, and brine. The ether phase was dried over anhydrous potassium carbonate and distilled at 55 °C and 10 mTorr. ^{1}H NMR ($CDCl_3$, 300 MHz, ppm): δ 3.37 (s, 3H), 2.63 (m, 2H), 2.57 (s, 1H), 1.8-1.2 (m, 6H). ^{13}C NMR ($CDCl_3$, 75 MHz, ppm): 122.56 (q, *J* = 287 Hz), 51.94, 50.51, 39.64, 37.06, 34.78 (m), 27.75, 23.06. ^{19}F NMR ($CDCl_3$, 282 MHz, ppm): δ –67.00 (q, *J* = 12.0 Hz), -76.91 (q, *J* = 11.2 Hz). HRMS-[GC-EI+] (m/z): [M•]+ calc'd for $C_{11}H_{12}F_6O_2$, 290.0741; found, 290.0749.

3-(2,2,2-Trifluoro-1-hydroxy-1-trifluoromethyl-ethyl)-bicyclo[2.2.1]heptan-2-one (4.13). To a solution of 2-methoxy-4,4-bis-trifluromethyl-3-oxa-tricyclo[4.2.1.0^{2,5}]nonane (200 mg, 0.69 mmol) in 15 mL tetrahydrofuran was added 14 mL (0.042 mmol) of 10% hydrochloric acid. The mixture was stirred over an oil bath at 65 °C for 1 hour, and then cooled to room temperature. The mixture was diluted with 50 mL ether, extracted with ether three times, washed with sodium bicarbonate solution, and washed in water. The organic layers were dried over sodium sulfate and concentrated by rotary evaporation to yield 1.128 g clear liquid. ^{1}H NMR ($CDCl_3$, 300 MHz, ppm): δ 6.31 (s, 1H), 2.95 (s, 1H), 2.75 (d, *J* = 3.3 Hz, 1H), 2.41 (d, *J* = 3.3 Hz, 1H), 2.12 (d, *J* =

11.4 Hz, 1H), 2.1-1.95 (m, 2H), 1.7-1.5 (m, 3H). ^{19}F NMR ($CDCl_3$, 282 MHz, ppm): δ -72.92 (q, J = 9.3 Hz), -77.38 (q, J = 9.9 Hz). ^{13}C NMR ($CDCl_3$, 75 MHz, ppm): 123.26 (q, J = 286 Hz), 122.10 (q, J = 286 Hz), 50.18, 48.44, 36.84, 35.74, 30.63, 23.14. HRMS-[GC-EI+] (m/z): [M•]+ calc'd for $C_{10}H_{10}F_6O_2$, 276.0585; found, 276.0585.

2,2-Dimethoxynorbornane (4.14a). To a flask containing norcamphor (5.0 g, 45.4 mmol) and p-toluenesulfonic acid monohydrate (125 mg, 0.657 mmol) was added 25 mL dry methanol by cannula, followed by addition of dry trimethyl orthoformate (7.22 g, 68.1 mmol) by syringe. The solution was refluxed overnight at 65 °C and quenched with 30 mL of 10% potassium hydroxide solution. The product was extracted with 40% pentane in dichloromethane solution and dried with potassium carbonate. Distillation at 450 mTorr pressure yielded 5.76 g (81%) 2, 2-dimethoxynorbornane. ^{1}H NMR ($CDCl_3$, 300 MHz, ppm): δ 3.17 (s, 3H), 3.15 (s, 3H), 2.35 (m, 1 H), 2.24 (m, 1H), 1.8-1.2 (m, 6H). Spectrum agrees with literature: San Filippo J., Jr.; Anderson, G. M. *J. Org. Chem.* **1974**, *39*, 473-477. Wiberg, K. B.; Cunningham, W.C., Jr. *J. Org Chem.* **1990**, *55*, 679-684.

2,2-Bis-(2,2,2-trifluoroethoxy)norbornane (4.14b). To a flask containing norcamphor (g (45.4 mmol) and *p*-toluenesulfonic acid monohydrate (124 mg, 0.66 mmol) was added 2,2,2-trifluoroethanol (30 mL, 400 mmol) with a syringe. The flask was attached to a reverse Dean-Stark trap containing activated molecular sieves. The mixture was refluxed at 85 °C overnight. A solution of 30 mL of 10% potassium hydroxide in water was added, followed by extraction with 40% pentane in dichloromethane. The extracts were washed with water and brine, and then dried with potassium carbonate. ^{1}H NMR ($CDCl_3$, 300 MHz, ppm): δ 3.9-3.7 (m, 4H), 2.36 (d, J = 3.3, 1H), 2.30 (s, 1H), 1.7-1.2 (m, 8H). ^{13}C NMR ($CDCl_3$, 75 MHz, ppm): 124.29 (q, J = 277 Hz), 124.10 (q, J = 277 Hz), 112.31, 61.44 (q, J = 35 Hz), 59.56 (q, J = 35 Hz), 43.65, 41.17, 37.3, 36.23, 28.53, 21.72. ^{19}F NMR ($CDCl_3$, 282 MHz, ppm): δ -74.34 (t, J = 8.9 Hz), -74.47 (q, J = 8.1 Hz). HRMS-[GC-EI+] (m/z): [M•]+ calc'd for $C_{11}H_{14}F_6O_2$, 292.0898; found, 292.0895.

2-Methoxy-norborn-2-ene (4.15a). To a dry flask containing aluminum trichloride (8.5 g, 64 mmol) was added 75 mL anhydrous ether by cannula, followed by addition of triethylamine (12.9 g, 128 mmol) by syringe. After stirring at room temperature for one hour, a solution of 2,2-dimethoxynorbornane (5.0 g, 32 mmol) in 5 mL ether was added via a cannula. The reaction mixture was stirred in a cold water bath overnight, and then stirred with 150 mL of 5N sodium hydroxide solution. The mixture was extracted with ether and dried over potassium carbonate. The oily residue was distilled to yield 3.42 g of 2-methoxy-2-norbonene. ^{1}H NMR ($CDCl_3$, 300 MHz, ppm): δ 4.54 (d, *J* = 3.3 Hz, 1H), 3.50 (s, 3H), 2.82 (s, 1 H), 2.68 (s, 1H), 1.8-1.6 (m, 2H), 1.49 (m, 2H), 1.19 (m, 2H). ^{13}C NMR (CD_2Cl_2, 75 MHz, ppm):167.48, 99.07, 56.20, 47.30, 44.04, 40.87, 28.39, 24.98. Spectra agree with literature (see Ref 32).

Bicyclo[2.2.1]hept-2-en-2-yloxy)trimethyl silane (4.16). To a flask was added norcamphor (3.0 g, 27.2 mmol), 25 mL of n-pentane, triethylamine (3.44 g, 34.0 mmol), and trimethylsilyl chloride (3.70 g, 34.0 mmol). To this flask was slowly added a mixture of sodium iodide (5.11 g, 34.0 mmol) in 45 mL of acetonitrile. The reaction mixture was stirred overnight at room temperature. The pentane layer was removed by cannula, then the mixture extracted with dry n-pentane. Anhydrous potassium carbonate was added to the extracts, and then filtered. The dried solution was concentrated and distilled to 4.42 g (89.1%) of product. ^{1}H NMR ($CDCl_3$, 300 MHz, ppm): δ 4.70 (d, *J* = 2.7 Hz, 1H), 2.77 (m, 1H), 2.57 (m, 1H), 1.68 (m, 2H), 1.48 (dm, *J* = 8.1 Hz, 1H), 2.12 (m, 2H), 1.04 (dd, *J* = 1.8, 7.2 Hz, 2H), 0.20 (m, 9H). Spectrum matches literature: Cazeau, P.; Duboudin, F.; Moulines, F.; Babot, O.; Dunogues, J. *Tetrahedron* **1987**, *43*, 2075-2083.

3-[2,2,2-Trifluoro-1-trifluoromethyl-1-(trimethylsilanyloxyl)-ethyl]-bicyclo[2.2.1]heptan-2-one (4.17). A modified version of the synthetic procedure of Burger and Helmreich was used. To a pressure reaction vessel was added a solution of bicyclo[2.2.1]hept-2-en-2-yloxy)trimethyl silane (2.0 g, 10.9 mmol) in 10 mL of dichloromethane. A regulator was attached and the system degassed. Hexafluoroacetone was added to reach a pressure of 20 psi, and added each time the pressure dropped. When the pressure remained constant for 10 minutes, the reaction was

quenched with 30 mL of ice water. The reaction mixture was extracted with dichloromethane, and the organic extracts were washed with first water and then brine. The extracts were dried over magnesium sulfate and concentrated, then dried over potassium carbonate and concentrated to recover 2.94 g (77.4%) of a 1.9:1.3:1.0 mixture of **4.17**:**4.13**:**4.18**. 3-[2,2,2-Trifluoro-1-trifluoromethyl-1-(trimethylsilanyloxyl)-ethyl]-bicyclo[2.2.1]heptan-2-one (**4.17**): ^{1}H NMR ($CDCl_3$, 300 MHz, ppm): δ 2.95 (s, 1H), 2.62 (s, 1H), 2.30 (d, J = 3.3 Hz, 1H), 2.0-1.2 (m, 6H), 0.23 (m, 9H). ^{19}F NMR ($CDCl_3$, 282 MHz, ppm): δ -72.91 (q, 3H), -73.36 (q, 3H). 2-trimethylsiloxy-4,4-bis-trifluoromethyl-3-oxa-tricyclo[4.2.1.0^{2,5}]nonane (**4.18**): ^{1}H NMR ($CDCl_3$, 300 MHz, ppm): δ 2.53 (s, 1H), 2.30 (d, J = 3.3 Hz, 1H), 2.14(s, 1H), 2.11 (s, 1H), 2.0-1.2 (m, 6H), 0.21 (m, 9H). ^{19}F NMR ($CDCl_3$, 282 MHz, ppm): δ -67.38 (q, 3H), -76.82 (q, 3H).

References and Notes

(1) (a). Patterson, K.; Yamachika, M.; Hung, R. J.; Brodsky, C. J.; Yamada, S.; Somervell, M. H.; Osborn, B.; Hall, D.; Dukovic, G.; Byers, J.; Conley, W.; Willson, C. G. *Proc. SPIE* **2000**, *3999*, 365-374. (b). Brodsky, C.; Byers, J.; Conley, W.; Hung, R.; Yamada, S.; Patterson, K.; Somervell, M.; Trinque, B.; Tran, H. V.; Cho, S.; Chiba, T.; Lin, S-H.; Jamieson, A.; Johnson, H.; Vander Heyden, T.; Willson, C. G. *J. Vac. Sci. Technol.* B **2000**, *18*, 3396-3401.

(2) Gandler, J. R.; Jencks, W. P. *J. Am. Chem. Soc.* **1982**, *104*, 1937-51.

(3) (a). Ito, H. *IBM J. Res. Dev.* **2001**, *45*, 683-695. (b). Hoskins, T.; Chung, W. J.; Agrawal, A.; Ludovice, P. J.; Henderson, C. L.; Seger, L. D.; Rhodes, L. F.; Shick, R. A. *Macromolecules* **2004**, *37*, 4512-4518.

(4) (a). Trinque, B. C.; Chambers, C. R.; Osborn, B. P.; Callahan, R. P.; Lee, G. S.; Kusumoto, S.; Sanders, D. P.; Grubbs, R. H.; Conley, W. E.; Willson, C. G. *J. Fluor. Chem.* **2003**, *122*, 17-26. (b). Tran, H. V.; Hung, R. J.; Chiba, T.; Yamada, S.; Mrozek, T.; Hsieh, Y-T.; Chambers, C. R.; Osborn, B. P.; Trinque, B. C.; Pinnow, M. J.; MacDonald, S. A.; Willson,

C. G.; Sanders, D. P.; Connor, E. F.; Grubbs, R. H.; Conley, W. *Macromolecules* **2002**, *35*, 6539-6549. (c). Willson, C. G.; Trinque, B. C.; Osborn, B. P.; Chambers, C. R.; Hsieh, Y-T.; Chiba, T.; Zimmerman, P.; Miller, D.; Conley, W. *J. Photopolym. Sci. Technol.* **2002**, *15*, 583-590. (d). Tran, H. V.; Hung, R. J.; Chiba, T.; Yamada, S.; Mrozek, T.; Hsieh, Y-T.; Chambers, C. R.; Osborn, B. P.; Trinque, B. C.; Pinnow, M. J.; Sanders, D. P.; Connor, E. F.; Grubbs, R. H.; Conley, W.; MacDonald, S. A.; Willson, C. G. *J. Photopolym. Sci. Technol.* **2001**, *14*, 669-674. (e). Chiba, T.; Hung, R. J.; Yamada, S.; Trinque, B.; Yamachika, M.; Brodsky, C.; Patterson, K.; Vander Heyden, A.; Jamison, A.; Lin, S-H.; Somervell, M.; Byers, J.; Conley, W; Willson, C. G. *J. Photopolym. Sci. Technol.* **2000**, *13*, 657-664.

(5) (a). Ito, H.; Wallraff, G. M.; Brock, P. J.; Fender, N.; T., Hoa D.; Breyta, G.; Miller, D. C.; Sherwood, M. H.; Allen, R. D. *Proc. SPIE* **2001**, *4345*, 273-284. (b). Trinque, B. C.; Chiba, T.; Hung, R. J.; Chambers, C. R.; Pinnow, M. J.; Osborn, B. P.; Tran, H. V.; Wunderlich, J.; Hsieh, Y-T.; Thomas, B. H.; Shafer, G.; DesMarteau, D. D.; Conley, W.; Willson, C. G. *J. Vac. Sci. & Technol. B*. **2002**, *20*, 531-536. (c). Trinque, B. C.; Osborn, B. P.; Chambers, C. R.; Hsieh, Y-T.; Corry, S. B.; Chiba, T.; Hung, Raymond J-P.; Tran, H. V.; Zimmerman, P.; Miller, D.; Conley, W.; Willson, C. G. *Proc. SPIE* **2002**, *4690*, 58-68.

(6) (a). Kodama, S.; Kaneko, I.; Takebe, Y.; Okada, S.; Kawaguchi, Y.; Shida, N.; Ishikawa, S.; Toriumi, M.; Itani, T. *Proc. SPIE* **2002**, *4690*, 76-83. (b). Irie, S.; Ishikawa, S.; Hagiwara, T.; Yamazaki, T.; Furukawa, T.; Itani, T.; Kawaguchi, Y.; Kodama, S.; Yokokoji, O.; Kaneko, I.; Takebe, Y.; Okada, S. *Jap. J. Appl. Phys. Pt. 1*. **2003**, *42*(6B), 3743-3747.

(7) (a). Feiring, A. E.; Crawford, M.; Feldman, J.; Farnham, W. B.; Feldman, J.; French, R. H.; Leffew, K. W.; Petrov, V. A.; Schadt, F. L., III; Whelanad, R.C.; Zumsteg, F. C. *J. Fluorine Chem.* **2003**, *122*, 11-16. (b). Toriumi, M.; Ishikawa, T.; Kodani, T.; Koh, M.;

Moriya, T.; Araki, T.; Aoyama, H.; Yamashita, T.; Yamazaki, T.; Itani, T.; *J. Photopolym. Sci. Technol.* **2003**, *16*, 607-614. (c). Sharif, I.; DesMarteau, D.; Ford, L.; Shafer, G. J.; Thomas, B.; Conley, W.; Zimmerman, P.; Miller, D.; Lee, G. S.; Chambers, C. R.; Trinque, B. C.; Chiba, T.; Osborn, B. P.; Willson, C. G. *Proc. SPIE* **2003**, *5039*, 33-42.

(8) (a). Bae, Y. C.; Douki, K.; Yu, T.; Dai, J.; Schmaljohann, D.; Koerner, H.; Ober, C. K.; Conley, W. *Chem. Mater.* **2002**, *14*, 1306-1313. (b). Schmaljohann, D.; Young, C. B.; Dai, J.; Weibel, G. L.; Hamad, A. H.; Ober, C. K. *J. Photopolym. Sci. Technol.* **2000**, *13*, 451-458.

(9) (a). Stewart, M. D.; Patterson, K.; Sommervell, M. H.; Willson, C. G. *J. Phys. Org. Chem.* **2000**, *13*, 767-774. (b). Ito, H. *IBM J. Res. Dev.* **2000**, *44*, 119-130. (b). MacDonald, S. A.; Willson, C. G.; Frechet, J. M. J. *Acc. Chem. Res.* **1994**, *27*, 151-158.

(10) (a). Bloomstein, T. M.; Sedlacek, Jan H. C.; Palmacci, Stephen T.; Hardy, D. E.; Liberman, V.; Rothschild, M. *Proc. SPIE* **2003**, *5040*, 650-661. (b). Rothschild, M.; Bloomstein, T. M.; Fedynyshyn, T. H.; Liberman, V.; Mowers, W.; Sinta, R.; Switkes, M.; Grenville, A.; Orvek, K. *J. Fluorine Chem.* **2003**, *122*, 3-10. (c). Matsui, Y.; Umeda, S.; Seki, S.; Tagawa, S.; Ishikawa, S.; Itani, T. *Jap. J. Appl. Phys., Pt. 1*. **2003**, *42*(6B), 3894-3899. (d). Hien, S.; Angood, S.; Ashworth, D.; Basset, S.; Bloomstein, T. M.; Dean, K. R.; Kunz, R. R.; Miller, D. A.; Patel, S.; Rich, G. *Proc. SPIE* **2001**, *4345*, 439-447. (e). Fedynyshyn, T. H.; Kunz, R. R.; Sinta, R. F.; Goodman, R. B.; Doran, S. P. *J. Vac. Sci. Technol.* B **2000**, *18*, 3332-3339. (f). Cefalas, A. C.; Sarantopoulou, E.; Gogolides, E.; Argitis, P. *Microelectronic Eng.* **2000**, *53*, 123-126.

(11) (a). Pinnow, M. J.; Noyes, B. F., III; Tran, H. V.; Tattersall, P. I.; Cho, S.; Klopp, J. M.; Bensel, N.; Frechet, J. M. J.; Sanders, D. P.; Grubbs, R. H.; Willson, C. Grant. *PMSE Prepr.* ***2002***, *87*, 403-404. (b). Klopp, J. M.; Bensel, N.; Fresco, Z. M.; Frechet, J. M. J. *Chem. Comm.* **2002**, *24*, 2956-2957. (c). Kim, J-B.; Lee, J-J. *Polymer* **2002**, *43*, 1963-1967.

(12) Tarrant, P.; Bull, R. N. *J. Fluorine Chem.* **1988**, *40*, 201-215.

(13) (a). Papadopoulos, M.; Jost, R.; Jenner, G. *J. Chem. Soc., Chem. Comm.* **1983**, *5*, 221-222. (b). Papadopoulos, M.; Jenner, G. *Nouv. J. Chim.* **1984**, *8*, 729-732. (c). Jenner, G.; Papadopoulos, M. *Tetrahedron Lett.* **1985**, *26*, 725-726. (d). Jenner, G.; Papadopoulos, M. *Physica* **1986**, *139-140*, 729-731.

(14) Sanders, D. P.; Connor, E. F.; Grubbs, R. H.; Hung, R. J.; Osborn, B. P.; Chiba, T.; MacDonald, S. A.; Willson, C. G.; Conley, W. *Macromolecules* **2003**, *36*, 1534-1542.

(15) Recently, DuPont independently published the cycloaddition of fluorinated ketones with quadricyclane. (a). Petrov, V. A.; Davidson, F.; Smart, B. E. *J. Fluor. Chem.* **2004**, *125*, 1543-1552. (b). Feiring, A. E.; Schadt, F. L., III.; Petrov, V. A.; Smart, B. E.; Farnham, W. B. *PCT Int. Appl. WO 2004/014960*, **2004**.

(16) Patterson, V. A. *J. Org. Chem.* **1969**, *34*, 3650-3651.

(17) Hexafluoroacetone readily undergoes a Diels-Alder reaction with cyclopentadiene; however, the resulting adduct retrocyclizes at room temperature. (a). Linn, W. J. *J. Org. Chem.* **1964**, *29*, 3111-3114. (b). Martynov, B. I., Lantseva, L. T.; Dyatkin, B. L. *Zhurnal Organicheskoi Khimii* **1975**, *11*, 2282-2285.

(18) (a). Gorman, A. A.; Leyland, R. L. *Tetrahedron Lett.* **1972**, *52*, 5345-5348. (b). Kubota, T.; Shima, K.; Sakurai, H. *Chem. Lett.* **1972**, *5*, 343-346. (c). Barwise, A. J. G.; Gorman, A. A.; Leyland, R. L.; Parekh, C. T.; Smith, P. G. *Tetrahedron* **1980**, *36*, 397-407.

(19) Homo-endo adduct **4.3a** was independently synthesized in modest yield via the extended heating of norbornadiene in the presence of hexafluoroacetone (see experimental section).

(20) UV irradiation, weak Bronsted acidic conditions (acetic acid), and elevated temperatures were ineffective in accelerating the formation of the new compound.

(21) Compound **4.5a** displays the opposite regiochemistry of compounds formed via photochemical reactions of aromatic ketones with norbornadiene (such as 4,4-diphenyl-5-

oxa-tricyclo[4.3.$0^{1,6}$.$0^{3,7}$]non-8-ene) in which the oxygen is attached to the single carbon bridge.[17]

(22) Adames, G.; Bibby, C.; Grigg, R. *J. Chem. Soc., Chem. Commun.* **1972**, *8*, 491-492.

(23) Lewis acid-catalyzed ring expansions of oxetanes have been reported in the literature. Carless, H. A. J.; Trivedi, H. S.; *J. Chem. Soc., Chem. Comm.* **1979**, *8*, 382-383.

(24) A similar ring expansion has been reported in the literature for norbornene oxide,[25] although the conversion of an epoxide to an oxetane is less energetically favorable. Kas'jan, L. A.; Gnedenko, L. Y.; Galafeeva, M. F.; Kornilov, M. Y.; Krasutsky, P. A.; Averina, N. V.; Zefirov, N. S. *Tetrahedron Lett.* **1986**, *27*, 2921-2922.

(25) Similar Lewis-acid catalyzed rearrangements are likely responsible for the formation of other 4-oxatricyclo[4.3.$0^{1,6}$.$0^{3,7}$]non-8-enes (a). von Hans Fritz, C. D. W.; Winkler, T. *Helv. Chim. Acta* **1975**, *58*, 1345-1357. (b). Becherer, J.; Hauel, N.; Hoffmann, R. W. *Justus Liebigs Ann. Chem.* **1978**, *2*, 312-19.

(26) Tarrant, P.; Bull, R. N. *J. Fluor. Chem.* **1998**, *40*, 201-215.

(27) (a). Pattison, V. A. *J. Org. Chem.* 1969, *34*, 3650-3651. (b). Gambaryan, N. P.; Rokhlin, E. M.; Zeifman, Y. V.; Ching-Yun, C.; Knunyants, I. L. *Angew. Chem. Int. Ed.* **1966**, *5*, 947-956.

(28) (a). Gambaryan, N. P.; Simonyan, L. A.; Petrovskii, P. V. *Bull. Acad. Sci. USSR Div. Chem. Sci. (Engl. Transl.)* **1967**, 886-888. (b). Karakhanov, E. A.; Lysenko, S. V.; Kovaleva, N. F.; Brezhnev, L. Yu.; Glukhovtsev, V. G.; Karakhanov, R. A. *Moscow Universitet. A.* **1982**, *23*, 159-163.

(29) (a). Patton, J. R. *Ph.D. Dissertation* University of Florida, **1974**. (b). Davis, H. R. *US Pat. 3,169,610*, **1964**.

(30) Fresco, Z. M.; Bensel, N.; Suez, I.; Backer, S. A.; Frechet, J. M. J.; Conley, W. *J. Photopolym. Sci. Technol* **2003**, *16*, 27-36.

(31) Kirby, A. J.; Ryder, H.; Matasa, V. *J. Chem. Soc. Perkin Trans. 2* **1990**, *5*, 825-831.

(32) Barbot, F.; Miginiac, P. *Helvetica Chimica Acta* **1979**, *62*, 1451-1457.

(33) Gassman, P. G.; Burns, S. J.; Pfister, K. B. *J. Org. Chem.* **1993**, *58*, 1449-1457.

(34) Jefford, C. W.; Rimbault, C. G. *J. Am. Chem. Soc.* **1978**, *100*, 6437-6445.

(35) Burger, K.; Helmreich, B. *J. Prakt. Chem.* **1992**, *334*, 219-226.

(36) Pangborn, A. B.; Giardello, M. A.; Grubbs, R. H.; Rosen, R. K. Trimmers, F. J. *Organometallics* **1996**, *15*, 1518-1520.

(37) Quadricyclane (tetracyclo[3.2.0.$0^{2,7}$.$0^{4,6}$]heptane) can be synthesized photochemically from norbornadiene. (a). Hammond, G. S.; Turro, N. J.; Fischer, A. *J. Am. Chem. Soc.* **1961**, *83*, 4674-4675. (b). Hammond, G. S.; Wyatt, P.; DeBoer, C. D.; Turro, N. J. *J. Am. Chem. Soc.* **1964**, *86*, 2532-2533. (c). Smith, C. D.; Taggi, A. J.; Meinwald, J. *Org. Synth.* **1971**, *51*, 133-138. (d). Alberici, F.; Cassar, L.; Monti, F.; Neri, C.; Nodarai, N. *US Pat. 5076813*, **1991**.

(38) Kinkead, E. R.; Wolfe, R. E.; Salins, S. A.; Grabau, J. H. Report (1993), (Order No. AD-A272694). CAN 123:190700.

(39) Everett, T. S. In *ACS Monograph*, vol. 187(*Chemistry of Organic Fluorine Compounds II*), American Chemical Society: Washington, D.C. **1995**, pp. 1037-1086.

CHAPTER 5

Metal-catalyzed Addition and Ring-opening Metathesis Polymers of Fluorinated Oxatricyclononenes for Advanced Lithographic Applications

Metal-catalyzed Addition and Ring-opening Metathesis Polymers of Fluorinated Oxatricyclononenes for Advanced Lithographic Applications

Abstract Fluorinated 3-oxatricyclo[4.2.1.$0^{2,5}$]non-7-enes serve as oxetane-functionalized norbornene monomers amenable to metal-catalyzed addition or ring-opening metathesis polymerization to afford new materials for deep ultraviolet lithography. 4-Oxatricyclo[4.3.$0^{1,6}$.$0^{3,7}$]non-8-enes, the Lewis acid-catalyzed rearrangement products of the 3-oxatricyclononenes, exhibit high transparency and good etch resistance indicating their suitability for use in a number of advanced photolithographic applications. Most importantly, the rigid alicyclic structure of 3,3-bis(trifluoromethyl)-4-oxatricyclononene affords a ROMP polymer with a glass transition temperature (T_g) in excess of 230 °C, indicating its potential to provide greatly needed T_g enhancement in ROMP-based photoresist copolymers for deep UV lithography. While residual unsaturation dramatically affects absorption at 193 nm, small amounts of unsaturation have little effect at 157 nm. Molecular weights of these fluorinated norbornene-like polymers can only be efficiently controlled kinetically with the terminal olefin chain transfer agents unlike polynorbornene. Finally, although oxatricyclononene addition polymers image poorly due to the high stability of the oxetane ring, low molecular weight oxatricyclononene ROMP copolymers bear promise as crosslinking agents in negative tone resist formulations. Ring-opening of the norbornene framework during polymerization allows for more facile nucleophilic attack on the oxetane ring and, therefore, higher crosslinking activity.

Introduction

The unique combination of transparency,[1] acidity,[2] and excellent dissolution behavior[3] imparted by hexafluorocarbinols to photoresist polymers has made them the dominant design motif for 157 nm photoresists.[4-8] While originally investigated for 157 nm lithography, hexafluorocarbinols are being back-integrated into resists for 193 nm and 193 nm immersion

lithography. The vast majority of chemically-amplified positive tone photoresists being investigated for 193 nm, 193 nm immersion, and 157 nm lithography (such as the one shown in Figure 5.1) employ a latent acidic functionality with a photoacid-cleavable protecting group.[9] After exposure to deep ultraviolet (UV) radiation, the protecting group is cleaved catalytically by a photogenerated acid, releasing a number of volatile fragments which can outgas from the photoresist film and contaminate optical elements and produce distortions in the imaged features.[10] These issues have prompted the development of low-outgassing or mass-persistent photoresists based on the acid-catalyzed ring-opening of small and medium-sized lactones.[11]

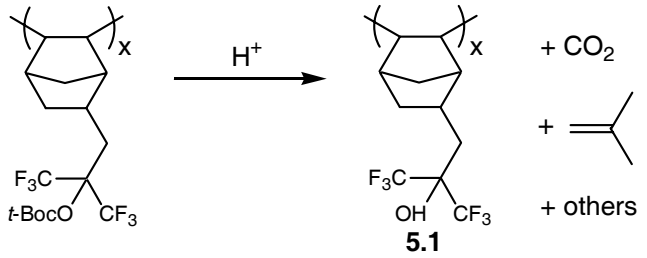

Figure 5.1. 157 nm photoresist with outgassing products

Negative tone resists also have the potential to solve this outgassing problem, however, no negative tone resists based on fluorinated oxiranes or oxetanes suitable for 157nm lithography have been reported. 2,2-Bis(trifluoromethyl) oxetane has been shown to ring-open under acidic conditions in the presence of water or other nucleophiles to produce hexafluorocarbinol-functionalized compounds.[12] We imagined using the olefin-containing annulated oxetane **5.2** (shown in Figure 5.2) which would remain intact during metal-catalyzed addition or ring-opening metathesis polymerization, yet ring-open under the superacidic conditions of imaging to produce either crosslinked networks (negative tone resists) or possibly hexafluoroalcohol-functionalized polymers (positive tone resists).

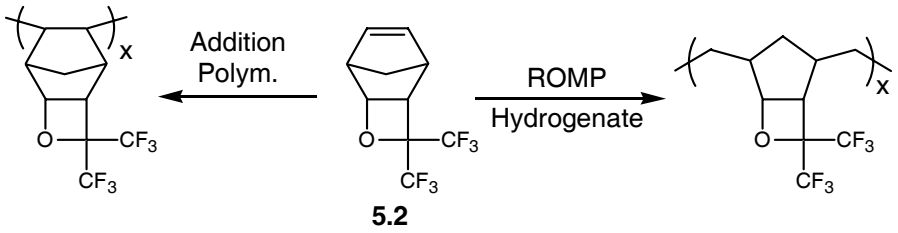

Figure 5.2. Oxetane-functionalized monomer and polymers

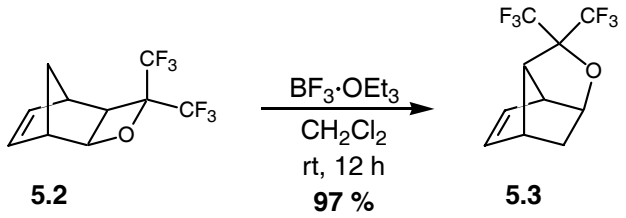

Figure 5.3. Lewis acid-catalyzed rearrangement of **5.2**

Previously, we have reported the synthesis of number of 3-oxa-tricyclo[4.2.1.$0^{2,5}$]non-7-enes via the cycloaddition of quadricyclane with activated carbonyl compounds.[13] The resultant norbornene-like annulated oxetanes are exclusively exo in configuration, which is ideal for metal-catalyzed polymerization. The 3-oxa-tricyclononenes undergo a Lewis acid-catalyzed Wagner-Meerwein rearrangement to cleanly produce 4-oxa-tricyclo[4.3.$0^{1,6}$.$0^{3,7}$]non-8-enes in high yield as shown in Figure 5.3.[13] These two classes of oxatricyclononene monomers exhibit high transparency in the deep ultraviolet spectral region, indicating their potential for use in advanced photolithographic applications. Here, we report the polymerization of the bis(trifluoromethyl) 3- and 4-oxa-tricyclononene monomers (**5.2** and **5.3**, respectively) via metal-catalyzed addition and ring-opening metathesis pathways to produce new materials for deep ultraviolet lithography.

Results and Discussion

Addition Polymerization Of the large number of metal catalysts capable of performing addition polymerization of norbornenes, the cationic palladium allyl and neutral η^6-tolyl-bis(perfluorophenyl) nickel catalysts were chosen for their ability to efficiently polymerize

tricyclononene compounds.[4b,14-17] Given the propensity of **5.2** to undergo Lewis acid-catalyzed rerarrangement, the stability of **5.2** to a variety of metal complexes $[Pd(COD)(Cl)]_2$, $[Rh(cyclooctene)_2(Cl)]_2$, and inorganic salts ($NaBF_4$, $NaSbF_6$, $AgBF_4$, $AgSbF_6$) in dichloromethane at 40 °C for 18 hours was examined. Oxetane **5.2** proved to be inert to all except $AgSbF_6$, in which case, predominantly isomerization to **5.3** was observed. Despite these generally encouraging results, initial polymerization attempts resulted in failure. No reaction was observed with the neutral nickel catalyst and immediate gelation and precipitation was observed with the cationic palladium allyl hexafluoroantimonate catalyst. Fortunately, this side reaction of the oxetane could be avoided by switching to the tetrafluoroborate counteranion. With the cationic palladium allyl tetrafluoroborate catalyst, moderate yields of polymer **5.4** were achieved after a few days at room temperature (Figure 5.4). Examination of the resultant polymer by NMR indicated two prominent structures, both that of the 3-oxatricyclononene **5.2** (< 20%) and of the 4-oxatricyclononane **5.3** (> 80%). This was confirmed by spectral comparison of polymer **5.5** synthesized independently from **5.3**. Following the polymerization via NMR allowed observation of the competing isomerization of monomer **5.2** to **5.3** during the polymerization. Therefore, it is reasoned that the resultant polymers have a gradient structure, initially being rich in oxetane and

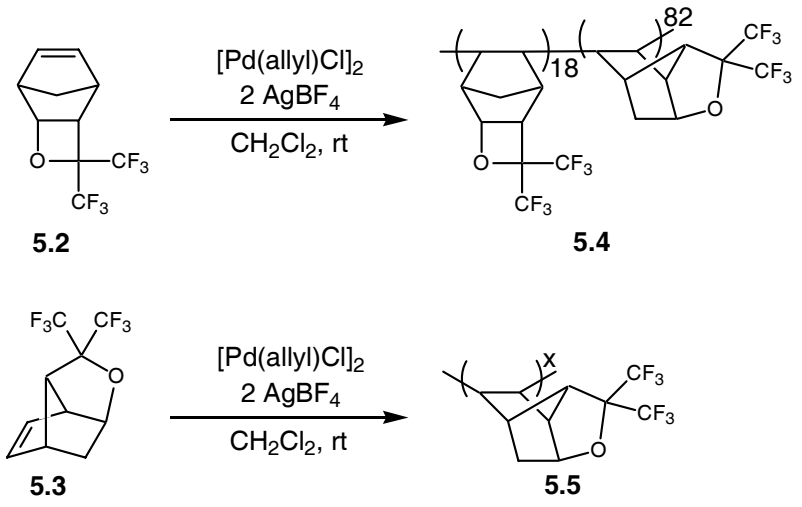

Figure 5.4. Addition polymerization of oxatricyclononenes

ending in tetrahydrofuranyl-rich sequences.

Copolymerization of **5.2** with 2-bicyclo[2.2.1]hept-5-en-2-ylmethyl-1,1,1,3,3,3-hexafluoro-propan-2-ol (NBHFA, **5.6**) afforded polymer **5.7** with a composition of 70% **5.6**, 20% **5.2**, and 10% **5.3**. While incorporation of the 4-oxatricyclononane structure offers the likely benefit of increased etch resistance, a random incorporation via copolymerization of **5.2** and **5.3** rather than the gradient incorporation would be advantageous. In addition to the evaluating neutral nickel-based addition catalysts, the use of bulky and electron-donating phosphines such as tricyclohexylphosphine to lower the cationic character of the palladium center[17] and slow/eliminate this isomerization side reaction is being explored.

Optical Properties of Addition Polymers Variable angle spectroscopic ellipsometry (VASE) spectra of polymers **5.4** and **5.5** are shown in Figure 5.5. Two features are readily apparent. First, the homopolymer **5.5** shows low absorption at 157 nm (1.46 μm^{-1}) and 193 nm

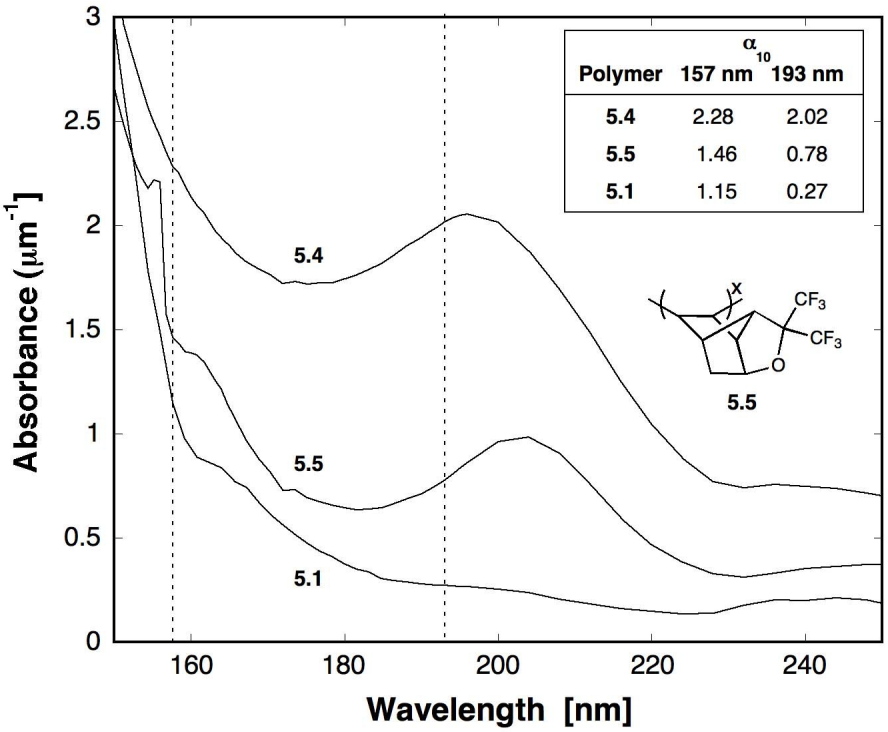

Figure 5.5. VASE spectra of oxatricyclononene addition polymers

(0.78 μm^{-1}). This is similar to the performance shown by the early batches of poly(NBHFA) **5.1**, which upon optimization afforded the spectrum shown in Figure 5.5. Secondly, the copolymer **5.4** has a surprisingly high absorbance at 157 and 193 nm (2.28 and 2.02 μm^{-1}, respectively). The cause of this high absorbance is being investigated; however, it is presumed that some nortricyclane structures are formed which can absorb in these regions.

To examine the potential etch resistance of these oxatricyclononene-based materials, polymer **5.5** was subjected to a standard silicon oxide etch process as shown in Figure 5.6. While the oxide etch process is the most demanding etch process experienced by the resist, polymer **5.5** exhibited promising etch resistance (2.3 times slower than the base silicon oxide etch rate), comparing favorably to the optimized commercial resists Shipley UV-210 and UV-6. Better performance is expected under the more mild polysilicon etch conditions. These results suggest the potential for **5.3** and its derivatives to be used as transparent, etch-resistant comonomers in

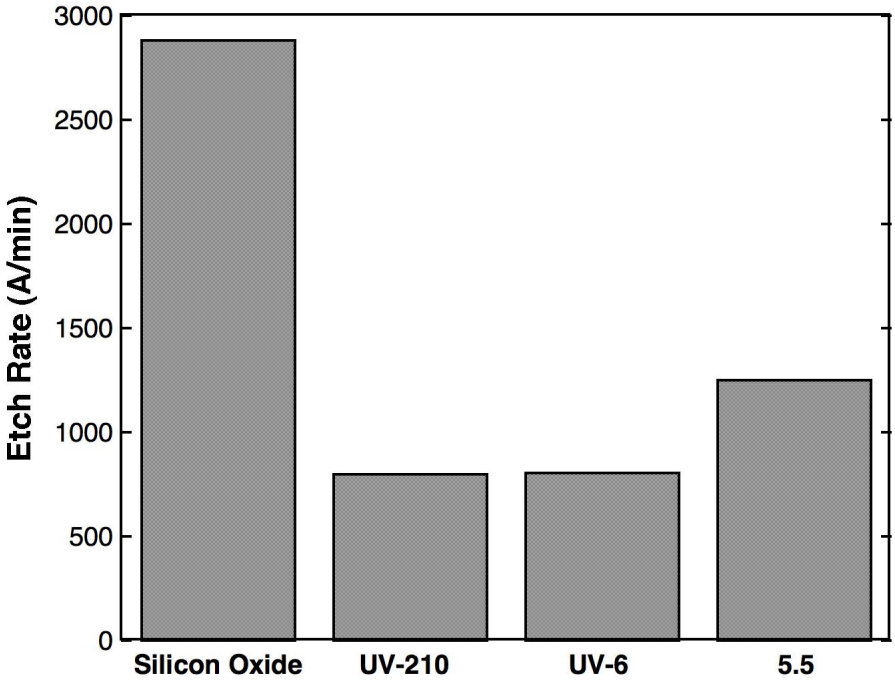

Figure 5.6. Oxide etch resistance of **5.5**

conventional metal-catalyzed or radically polymerized norbornene-based resists or, if the olefin is hydrated, as pendant groups in fluorinated cyclopolymer and tetrafluoroethylene copolymer resists in place of norbornyl or isobornyl groups.

Lithographic Performance of Oxatricyclononene Resists Two oxatricyclononene addition polymers were examined for their lithographic performance at 157 nm. Polymer **5.4** was blended with the more transparent base polymer, poly(NBHFA) **5.1,** (5% **5.4**, 95% **5.1**) (93.7% total) and combined with a standard amount of 6% triphenylsulfonium nonaflate photoacid generator and 0.03% tetra-*n*-butyl ammonium hydroxide in PGMEA. Irradiation at 157nm using a binary mask afforded poor positive tone images (Figure 5.7). The terpolymer **5.7** (70% NBHFA **5.6**, 20% oxetane **5.2**, 10% **5.3**) also provided similar positive tone images. The norbornene framework and bulky electron-withdrawing trifluoromethyl groups in addition polymers of **5.2**, while imparting significant stability and transparency to the oxetane, prevents

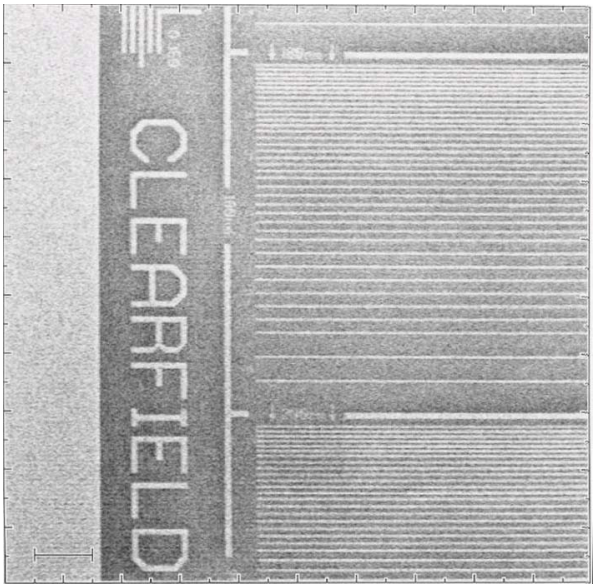

Imaging conditions: 93.7% polymer (95% **5.1**, 5% **5.4**), 6% triphenylsulfonium nonaflate, 0.03% tetrabutyl ammonium hydroxide Dose: ~ 47 mJ/cm^2; Focus: ~0.35; NA: 0.85; σ: 0.7; Binary mask.

Figure 5.7. Imaging of oxatricyclononene addition polymers

reaction of the oxetane to form crosslinked networks. However, it is this same stability that makes the oxetane ring very difficult to open.[18] It is unclear whether the large exposure dose required to achieve clearing of the exposed regions is due to the slow ring-opening of the oxetane to form hexafluorocarbinol species or whether the image we see is a result of dissolution inhibition due to the large amount of PAG.

It is obvious from these results that any ring-opening is too slow to be useful. The norbornene framework forces attacking nucleophiles to approach from the hindered endo face of the structure, forcing any ring-opening reaction to proceed by a slow E1-type mechanism, which can also lead to isomerization rather than ring-opening. In order to increase the reactivity of these annulated oxetanes, a potential reduction in the steric hindrance around the oxetane could be realized by polymerizing **5.2** via ring-opening metathesis. The resultant ring-opened structure (see Figure 5.2) should be more accessible to attack by nucleophilic species.

Ring-Opening Metathesis Polymerization The high activity and low Lewis acidity of ruthenium-based olefin metathesis catalysts catalysts (Figure 5.8, **5.8**-**5.10**)[19] should allow for the efficient polymerization of **5.2** without the isomerization problems encountered in the synthesis of addition polymers. In addition, the number of efficient chain transfer methodologies[20] available to control the molecular weight of norbornene ROMP polymers offers the possibility of using much lower catalyst loadings relative to metal-catalyzed addition polymerizations while producing more controlled molecular weights and molecular weight distributions. This is a

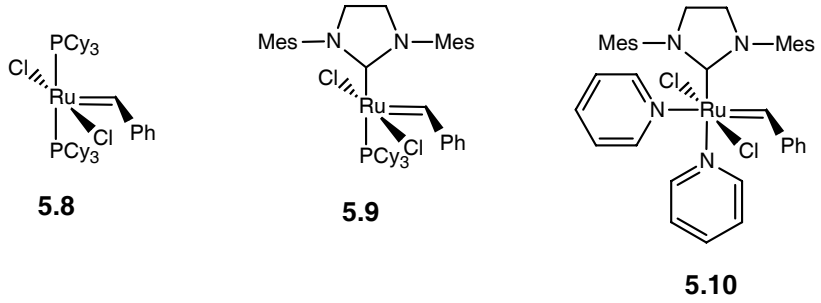

5.8 **5.9** **5.10**

Figure 5.8. Olefin metathesis catalysts

distinct advantage when it comes to catalyst removal, given the need for extremely low residual metal contamination in commercial resists.[21]

While ROMP-based resists have been previously explored for 193 nm lithography,[22] a number of shortcomings, including generally low glass transition temperatures, phase incompatibility with common photoacid generators (PAGs), poor dissolution behavior with standard developer concentrations, and swelling during development, have prevented them from being adopted commercially. The necessary hydrogenation of the unsaturated backbone of ROMP polymers unfortunately results in a significant lowering of the glass transition temperature. For example, the glass transition temperature of the hexafluorocarbinol-functionalized ROMP polymer **5.11** shown in Figure 5.9 – one of the first ROMP polymers explored for use at 157 nm – suffers a significant decrease from 115 °C to the less useful 85 °C after hydrogenation.[23] A common route to achieve higher glass transition temperatures is to use norbornene-like monomers with additional cyclic units. Unfortunately, the increase in glass transition temperature gained by the incorporation of additional simple annulated rings onto norbornene has been shown to be relatively independent of ring-size and shows only moderate effect.[24] The additional hydrocarbon units also make dissolution into an aqueous base developer more difficult.

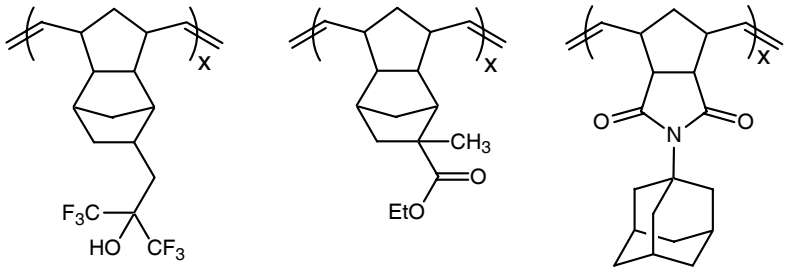

5.11 T_g = 115 °C

5.12 T_g = 160 °C

5.13 T_g = 271 °C

Figure 5.9. Effect of structure on glass transition temperatures of ROMP polymers

Other approaches towards increasing the glass transition temperature include incorporation of hydrogen bonding carboxylic acid groups[22] or bulky polar functionalities such as esters (**5.12**)[25] or maleimides (**5.13**).[26] Unfortunately, free carboxylic acid dramatically increases the background dissolution rate and the esters and maleimide functionalities are not transparent at 157nm. After several unsuccessful attempts to bulk up the ethylene linkages of the ROMP polymer backbone, we decided to investigate making the cyclopentane backbone unit more rigid and bulky via incorporation of a bridging group. Methyl tricyclo[4.3.$0^{1,6}$.$0^{3,7}$]non-8-ene-2-carboxylate (**5.14**), originally synthesized by our laboratory as part of the effort to synthesize the natural product (±)-Δ9(12)-capnellene,[27] seemed to be an ideal model system (Figure 5.10). However, the presence of the nearly identical core structure in **5.3** prompted us to initially explore the ring-opening polymerization of **5.3** as a possible transparent, high Tg ROMP structure suitable for use in 193 nm and 157 nm photoresist polymers.

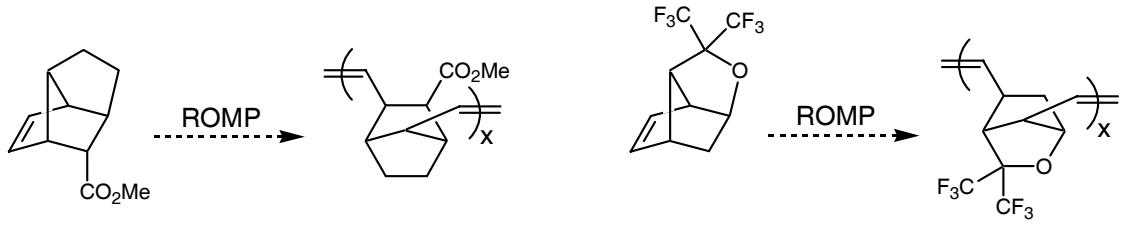

Figure 5.10. Potential routes to high T_g ROMP polymers

Ring-opening Metathesis Polymerization of 5.3 Surprisingly, after reaction of 100 equivalents of **5.3** with the highly active bispyridine catalyst **5.10** in dichloromethane at room temperature for 12 hours, no polymer formation was observed (Entry 1, Table 5.1). Given the high ring strain of norbornene monomers, these conditions [0.4 M] are well above the critical concentration and ring-opening metathesis should proceed to very high conversions.[28] However, NMR experiments indicated only ~3% conversion of **5.3**. No conversion was detected in NMR

Table 5.1. Ring-opening metathesis polymerization of **5.3**

Entry	Monomer	Catalyst	[M]/[C]	Conc. [M]	Time (h)	M_n (kDa)	PDI	Isolated Yield (%)
1	**5.3**	**5.10**	100:1	0.4	12	-	-	~3
2	**5.3**	**5.10**	100:1	1.0	12	18.5	1.30	45
3	**5.3**	**5.10**	100:1	3.0	12	27.0	1.14	79
4	**5.3**	**5.10**	100:1	neat	12	70.2	1.29	66
5	**5.3**	**5.9**	100:1	3.2	12	193.6	1.32	99
6	**5.3**	**5.8**	100:1	3.2	12	38.2	1.14	91
6	**5.3**	**5.8**	100:1	3.2	12	38.2	1.14	91
7	**5.3**	**5.10**	100:1	3.2	12	24.5	1.09	80
8[a]	**5.3**	**5.10**	100:1	3.2	6	20.5	1.05	59
9	**5.2**	**5.10**	100:1	0.2	6	32.4	1.04	99
10	**5.2** + **5.3** (1:1)	**5.10**	100:1	0.8	24	22.2	1.08	71

[a] Reaction performed at 0 °C

experiments with catalysts **5.8** or **5.9**. For low ring-strain olefins such as cyclopentane, neat conditions are generally required to achieve significant molecular weight polymer.[28,29] When the polymerization of **5.3** with the bispyridine catalyst **5.10** was performed neat, the reaction mixture gelled after 1-2 hours at room temperature (Entry 4, Table 5.1). The resultant polymer **5.16** was insoluble in dichloromethane or chloroform, but is readily soluble in more polar solvents such as tetrahydrofuran. Gel permeation chromatography indicated a surprisingly high molecular weight polymer, given the relatively slow polymerization and extremely rapid initiation rate of **5.10**.[30] This is most likely the result of the low solubility of **5.10** in neat **5.3** (i.e., only a small amount of catalyst is soluble, thereby artificially increasing the effective monomer to catalyst ratio). The addition of a small amount of dicholoromethane to pre-dissolve the catalyst before injecting the monomer afforded much narrower molecular weight distributions and more controlled molecular weights. Catalyst **5.9** (the slowest initiating catalyst) produces high molecular weight polymer with a PDI ~1.32 (Entry 6, Table 5.1) while catalyst **5.10** which initiates more than a million times faster[30] produces controlled molecular weight polymers with a narrow PDI of 1.09.[31,32]

Effects of Bulky Alicyclic Framework We were delighted to discover that the ROMP polymer **5.16** possessed extremely high glass transition temperatures (~233 °C). Comparison with the much lower T_g of ROMP polymer **5.17** (~128 °C) from monomer **5.2** illustrates the effectiveness of the additional bridging structure in increasing the glass transition temperature of norbornene-based ROMP polymers. Unfortunately, we were unable to achieve hydrogenation of more than 50% of the backbone olefins of **5.16**. The combination of poor solubility due to the high degree of fluorination and polymer rigidity coupled with the steric hindrance around the backbone olefins prevented high degrees of hydrogenation of polymer **5.16** despite our screening a number of solvents and reaction temperatures.

Control of Molecular Weight via Chain Transfer While catalyst control of molecular weight is effective in the case of rapidly initiating catalyst **5.10**, use of chain transfer to control molecular weight and lower the required catalyst loadings would be advantageous. We expected the use of chain transfer to control the ROMP of **5.3** to be more complicated than with highly reactive monomers such as norbornene. The hindered backbone olefins in ROMP polymer **5.16** are potentially more resistant towards the efficient secondary metathesis required in thermodynamic chain transfer processes[20].

Initially, *trans*-3-hexene was selected as a chain transfer agent (CTA). Attempts to control the molecular weight kinetically (Entries 1-6, Table 5.2 and Figure 5.10) were moderately effective. Molecular weights were consistently higher than expected and the effectiveness of the CTA decreased as the [CTA]:[monomer] ratio increased. Production of molecular weights in the 5-10 kDa range was not possible. A more active chain-transfer agent, 1,4-diacetoxy-*cis*-2-butene (DACB), which was demonstrated as an effective CTA for the ROMP of norbornene,[20b] was even less effective than 3-hexene. The reduced yields at higher chain transfer agent loadings may be due to the increased formation of very low molecular weight, non-isolable oligomers via ring-opening cross-metathesis.

Given the failure of the kinetic chain transfer approach to produce good control of molecular weight, the thermodynamic chain transfer methodology was examined. Polymerization of norbornene with catalyst **5.9** in the presence of DCAB at 55 °C was demonstrated to afford polynorbornene with a molecular weight determined by the monomer to chain transfer agent ratio.[20b] High molecular weight polynorbornene can also be reduced to lower molecular weights via this approach. The more sterically hindered olefins of polynorbornene necessitate the use of second generation catalysts such as **5.9** and elevated temperatures to allow for the efficient secondary metathesis necessary to redistribute the chain ends and achieve the equilibrium distribution. Unfortunately, this approach (Entries 10-12 and 13-15, Table 5.1 and Figure 5.11) met with equal difficulty. Catalyst **5.9** afforded very low yields of polymer (< 10%). Use of the

Table 5.2. Effect of chain transfer agents on ROMP of **5.3**[a]

Entry	CTA[b]	[M]/[CTA]	M_n(theor.) (kDa)	M_n(expt.) (kDa)	PDI	Isolated Yield (%)
1	-		258	304.1	1.80	71
2	A	100:1	23.5	118.6	1.56	67
3	A	50:1	12.3	83.7	1.53	65
4	A	25:1	6.3	56.3	1.54	67
5	A	12.5:1	3.2	35.6	1.50	56
6	A	6.25:1	1.6	25.6	1.39	37
7	B	50:1	12.3	141.2	1.51	71
8	B	12.5:1	3.2	81.8	1.60	64
9	B	6.25:1	1.6	51.3	1.74	56
10[c]	B	50:1	12.3	79.0	1.33	28
11[c]	B	12.5:1	3.2	50.8	1.64	22
12[c]	B	6.25:1	1.6	21.0	1.38	8.0
13[d]	-	100:1	23.5	63.3	1.58	5.5
14[d]	B	50:1	12.3	46.1	1.72	6.9
15[d]	B	25:1	6.3	38.3	1.80	6.3

[a] All reactions performed using 0.1 mol% catalyst **5.10** in CH_2Cl_2 [1.5 M] at room temperature for 12 h.
[b] Chain transfer agents: (A) *trans*-3-hexene and (B) 1,4-diacetoxy-*cis*-2-butene
[c] Reaction performed in 1,2-dichloroethane at 55 °C for 16 h
[d] Reaction performed with 0.1 mol% catalyst **5.9** in 1,2-dichloroethane at 55 °C for 16 h

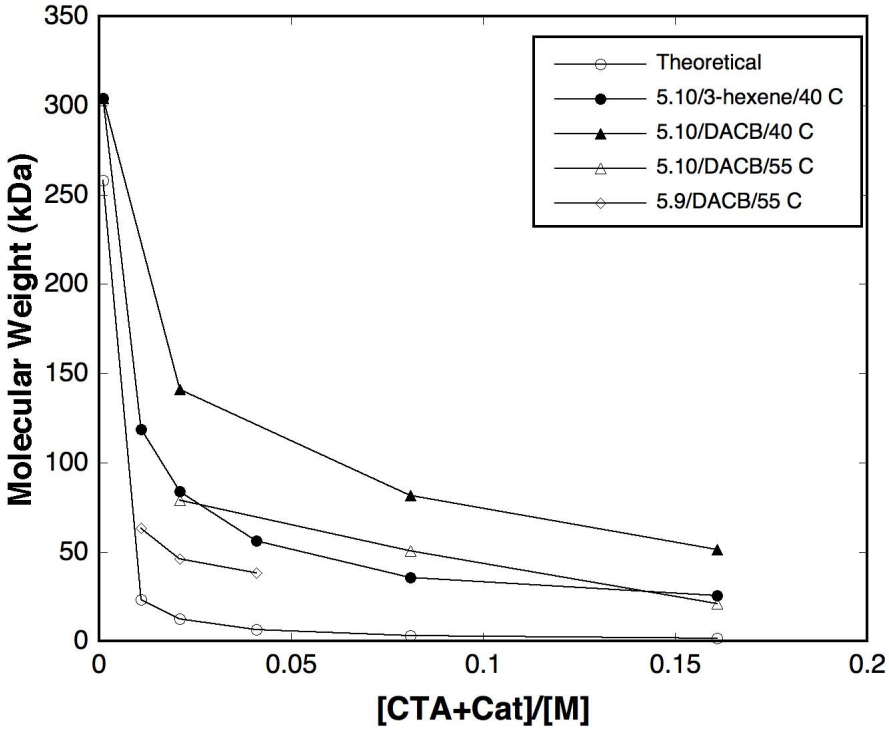

Figure 5.11. Effect of chain transfer on ROMP of **5.3**

more rapidly initiating catalyst **5.10** which can effectively polymerize **5.3** at this concentration, afforded higher yields (<30%) of polymer, but exhibited less molecular weight control than **5.9**, probably due to its lower stability. However, molecular weight control was increased relative to the same reaction performed at 40 °C.

Optimization of Chain Transfer Conditions In order to determine optimal conditions to control the molecular weight of these polymers, the effects of chain transfer agent, temperature, and catalyst choice on molecular weight must be evaluated; however, no direct comparison of chain transfer performance of a number of first and second-generation ruthenium metathesis catalysts has been reported in the literature. Second-generation ruthenium metathesis catalysts have been shown to perform secondary metathesis reactions on the olefinic backbone of poly(norbornene), affording thermodynamic control of molecular weight via the use of chain transfer agents.[20] The molecular weights of a number of polynorbornenes synthesized using three

Table 5.3. Effects of CTA purity and catalyst on molecular weight of polynorbornene

1,4-diacetoxy-*cis*-2-butene	5.9		5.18		5.10	
	M_n (kDa)	PDI	M_n (kDa)	PDI	M_n (kDa)	PDI
Undistilled	176.1	2.25	16.6	1.46	20.1	2.95
Distilled	24.9	7.90*	15.9	1.46	9.4	1.51

Conditions: 1.25M in 1,2-dichloroethane, 55 °C, 12 h. [M]/[C]= 1000:1, [M]/[CTA] = 25:1
(* Bimodal distribution)

second-generation catalysts and 1,4-diacetoxy-*cis*-2-butene chain transfer agent are shown in Table 5.3. Catalyst **5.9** afforded extremely high molecular weight insoluble material immediately upon addition of monomer. Even after 12 hours, insoluble material remained. The phosphine-free catalyst **5.18** ($(H_2Imes)(Cl)_2Ru$ (=CHC_6H_4(*o*-O-*i*-Pr)), which initiates faster than **5.9**, did not form insoluble material and afforded polynorbornene with a molecular weight about 7 times higher than the monomer to catalyst ratio should afford. While catalysts **5.9** and **5.18** have significantly more stability than the bispyridine catalyst **5.10**, the very high initiation rate of **5.10** afforded reasonable control of the molecular weight. However, the molecular weight distribution was much broader than expected. Subsequent inspection of the 1,4-diacetoxy-*cis*-2-butene chain transfer agent revealed it to contain a number of olefinic and aldehyde impurities. The presence of these impurities would likely have a large impact on the performance of the bispyridine catalyst. Distillation of the CTA from calcium hydride afforded a reduction in the contaminants; however, a number of impurities were still present. The use of the distilled chain transfer agent afforded a dramatic improvement in molecular weight control for catalysts **5.9** and **5.10**. The performance of catalyst **5.18** was unaffected by purity of the chain transfer agent. Catalyst **5.10** afforded the best control of the molecular weight. Since the initial molecular weights are controlled kinetically, the use of a rapidly initiating catalyst is beneficial to prevent the formation of insoluble material. In addition, despite the lower stability of **5.10**, its polymerization of a high-strain monomer like norbornene is faster than decomposition reactions; therefore, its higher rate

of initiation[30] results in better control of the molecular weight than the more stable, slower initiating **5.9**. The molecular weight distributions are narrower than previous reports (PDI=2.0)[20] due to the shorter reaction times; however, these reaction times are perhaps more representative of common usage of these catalysts.

Previous polymerizations of **5.2** with *trans*-3-hexene resulted in poor molecular weight control (M_n(expt'l) = 69.9 kDa, PDI = 1.77, M_n(theor.) = 5.2 kDa). Subjection of the isolated polymer to metathesis conditions with the undistilled 1,4-diacetoxy-*cis*-2-butene ([monomer equiv.]/[CTA] = 20:1) CTA for 24 hours at 55 °C afforded no reduction in molecular weight (M_n= 5.2 kDa, PDI = 1.71). Despite the presence of impurities, the good performance of this olefin in cross-metathesis reactions makes the total lack of reactivity in this case raise serious question marks about the ability of second-generation catalysts to perform secondary metathesis reactions on the more hindered olefins in these poly(2-oxatricyclononenene)s. All previous reported attempts to control the molecular weights of polynorbornene via this thermodynamic approach were performed on unsubstituted norbornene. The additional steric hindrance and the different solution conformations induced by the presence of the fluorinated substituents would be expected to influence the reactivity of the backbone olefins.

In order to examine the effects of fluorinated substituents on the molecular weight control using chain transfer agents, polymerizations of the hexafluorocarbinol-functional norbornene **5.6** with several catalysts and chain transfer agents were performed, the results of which are

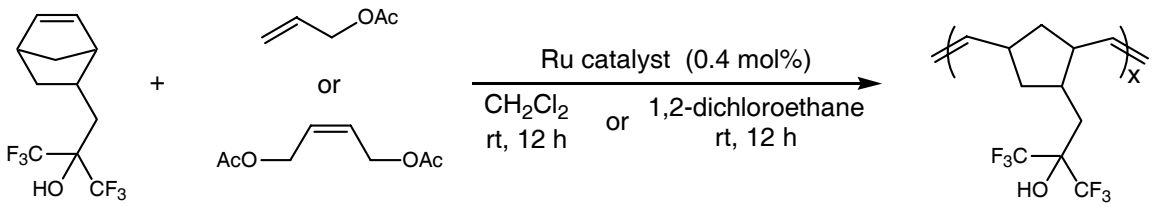

Figure 5.12. Molecular weight control during polymerization of **5.6**

Table 5.4. Control of molecular weight of polymer **5.1** via chain transfer

Catalyst	Temp. (°C), solvent	[M]/ [CTA]	M_n (calc.) rel. to PS[a]	1,4-Diacetoxy-*cis*-2-butene		Allyl Acetate	
				M_n (Da)	PDI	M_n (Da)	PDI
	rt, CH_2Cl_2	10:1	4960	20560*	1.48	6990[b]	1.61
5.8	rt, CH_2Cl_2	5:1	2480			4000[b]	1.53
	rt, CH_2Cl_2	1:1	495			1310*	1.46
	rt, CH_2Cl_2	10:1	4960			20650	1.66
5.9	rt, CH_2Cl_2	5:1	2480			17110[b]	1.84
	rt, CH_2Cl_2	1:1	495			4840[b]	1.85
	rt, CH_2Cl_2	10:1	4960			28200[b]	1.50
	rt, CH_2Cl_2	5:1	2480			24800	1.65
5.10	rt, CH_2Cl_2	1:1	496			7900[b]	2.12
	55, 1,2-DCE	10:1	4960	10240	1.47	13900	1.68
	55, 1,2-DCE	1:1	495	13270	1.64		
	rt, 1,2-DCE	10:1	4960			13980	1.72
5.18	55, 1,2-DCE	10:1	4960	33300	1.59	12660	1.70
	55, 1,2-DCE	1:1	495	16130	1.94		

[a] Calculated molecular weight corrected to reflect value vs. polystyrene (see text)
M_n(calc.) = M_0 x [M]/[C] x 1.81. Does not include endgroups
[b] Monomer and CTA mixed with catalyst solution at -40 °C and allowed to warm to rt
All molecular weights are reported relative to polystyrene

presented in Table 5.4 and Figure 5.12. Under thermodynamic conditions (55 °C, 1,2-dichloroethane), catalyst **5.10** exhibited identical performance with both CTAs; however, catalyst **5.18** showed slightly better molecular weight control with allyl acetate. Unfortunately, the molecular weights are much larger than the theoretical values (without correction). Under kinetic control with the bisphosphine catalyst **5.8**, the use of the terminal olefin chain transfer agent (allyl acetate) afforded significantly better molecular weight control. These results indicate that the molecular weight of polymer **5.1** appears to be primarily controlled kinetically. Since terminal olefins are more reactive than internal olefins, allyl acetate is the preferred CTA in these

polymerizations. Allyl acetate also has none of the purity concerns of 1,4-diacetoxy-*cis*-2-butene. Room temperature polymerizations with second generation catalysts **5.9** and **5.10** were unable to produce low molecular weight material (M_n < 5 kDa), even with stoichiometric loadings of chain transfer agent. The first-generation, bisphosphine catalyst **5.8** was able to control the molecular weight down to the oligomer level. GPC analysis clearly shows the production of monomeric, dimeric, and other oligomeric species. The apparent molecular weight difference between the successive oligomeric fractions was ~495 g/mol relative to polystyrene. The calculated theoretical molecular weights in Table 5.4 are corrected by a factor of 1.81 (495/274) to account for the relative molecular weight values determined by gel permeation chromatography. The ability of the first generation catalysts to kinetically control molecular weight more efficiently is somewhat surprising, given the higher activity of the bispyridine catalyst **5.10**. However, these molecular weight results reflect not the initiation rates, but more likely, the relative reaction rates of the respective catalysts with high-strain, bulky norbornenes and terminal olefins. This relative rate of reaction appears to be more competitive with the first generation catalyst. It should be noted that these results are also highly monomer dependent. Polymerization of **5.2** with the second-generation bispyridine catalyst **5.10** and allyl acetate affords good molecular weight control below 5000 Da. Therefore, it must be reiterated that selection of the most active catalyst or fastest initiating catalyst will not always produce the best results and each system should be evaluated independently.

Copolymerization of 5.3 While the high glass transition temperature was extremely desirable, the high concentrations required for significant monomer conversion and the inability to fully hydrogenate these polymers posed significant challenges. Given the norbornene-like structure of **5.3**, its reluctance to polymerize was puzzling. ROMP of **5.3** with an excess of acyclic olefin such as *t*-butyl acrylate or *trans*-3-hexene revealed only low to moderate conversions to ring-opened product, whereas under the same conditions, **5.2** ring-opened quantitatively. These results indicated that the primary issue was not ring strain, but coordination

to, and reaction of **5.3** with the catalyst, especially if the catalyst had already initiated to form a very bulky alkylidene. If this was indeed the case, a less sterically bulky comonomer should be able to coordinate and undergo metathesis to form a more accessible ruthenium alkylidene capable of coordinating and reacting with another monomer of **5.3**. Similar rationales have been used to explain the alternating ROMP copolymerizations of norbornenes in certain systems.[33] Indeed, when a less bulky monomer such as cyclooctene or norbornene was introduced with **5.3** to a dichloromethane solution of **5.10** at concentrations where **5.3** by itself would not homopolymerize [0.4 M], significant conversions of **5.3** were observed via ^{19}F NMR (55% and 20%, respectively). This provided evidence that monomers such as **5.3** could be copolymerized at reasonable concentrations and opened up the possibility of synthesizing alternating copolymer structures.

Copolymerization of Oxatricyclononenes The ring-opening polymerization of **5.2** (Entry 9, Table 5.1) provides good yields of the oxetane-functionalized polymer **5.18** (Figure 5.13). ROMP polymer **5.17** was hydrogenated under standard conditions to produce the saturated

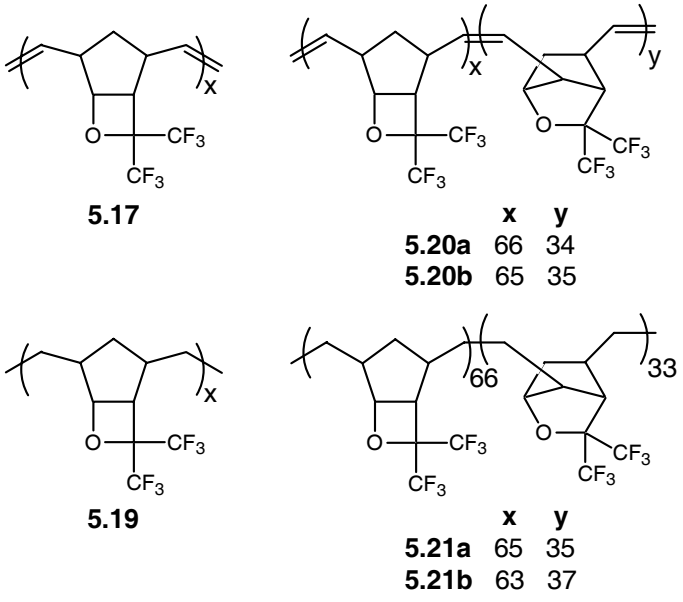

Figure 5.13. ROMP of oxatricyclononenes

polymer **5.19**. No evidence of ring-opening or oxetane isomerization after either polymerization or hydrogenation was observed via ^{19}F NMR. Unfortunately, as expected, the glass transition temperature of polymer **5.17** (128 °C) was reduced to ~99 °C after hydrogenation. However, it is sufficiently high that incorporation of 30-50% of **5.3** via copolymerization should boost the T_g into a useful range of 120 °C.

Given the inability to adequately hydrogenate polymer **5.16**, copolymerization incorporation ratios of **5.3** lower than 50% seemed desirable to avoid the formation of sequences of **5.3** which would be difficult to hydrogenate. Copolymerization of a 1:1 mixture of **5.2** and **5.3** resulted in copolymer **5.20** with an incorporation ratio of 66:34 (Figure 5.12 and Entry 10, Table 5.1). This is highly reproducible within experimental error and reflects the lower reactivity of **5.3** relative to **5.2**. The second-generation catalyst **5.10** was used exclusively in these polymerizations due to the ease of separation of catalyst from the polymer via precipitation into methanol. Unlike the other catalysts investigated, catalyst **5.10** and its Fischer carbene (the product of quenching the polymerization) are highly soluble in methanol. In addition, their brilliant green color affords simple visual determination of the number of precipitations required to remove the catalyst. Trace metals analysis of a hydrogenated copolymer **5.21** prepared initially using 1 mol% **5.10** via inductively coupled plasma mass spectroscopy revealed the initial metal content (3804 ppm) had been reduced to 130 ppm. While this level is significantly higher than would be acceptable to the semiconductor industry, it is important to note that the initial catalyst concentration used in this example was 2-3 orders of magnitude larger than would be required for a process using chain transfer to control molecular weight. In addition, this removal of 96.6% of the ruthenium was achieved without the use of any special metal scavenging techniques.

Unlike the partial hydrogenation of the ROMP homopolymer **5.16**, hydrogenation of the less hindered backbone in copolymer **5.20** proceeded to significantly higher conversions. However, the polymers **5.21a** and **5.21b** still contain roughly 5-10% residual unsaturation.[34]

Nevertheless, polymer **5.21a** exhibits a T_g of 120 °C in good agreement with the expected value calculated from via the Flory-Fox equation. This result confirms the ability of **5.3** to serve as glass transition temperature enchancing comonomers in ROMP polymerizations.

Transparency of Oxatricyclononene ROMP Polymers The deep UV spectra of hydrogenated 4-oxatricyclononene copolymers **5.21a** and **5.21b** were measured by variable angle spectroscopic ellipsometry (VASE) and are shown in Figure 5.14. Copolymer **5.21b**, despite showing a fairly strong absorption at 193 nm due to the residual unsaturation (~ 8%), exhibits promisingly low absorbance (1.34 μm^{-1}) at 157 nm. While the effect of the higher degree of hydrogenation of the 3-oxatricyclononene polymer **5.19** (~ 98%) on the absorbance at 193 nm is substantial, the transparency at 157 nm is barely affected. The olefinic absorption band centered at 190 nm, therefore, appears to be a larger concern for applications in 193 nm and 193 nm immersion lithography. However, when extremely large amounts of unsaturation are left in the

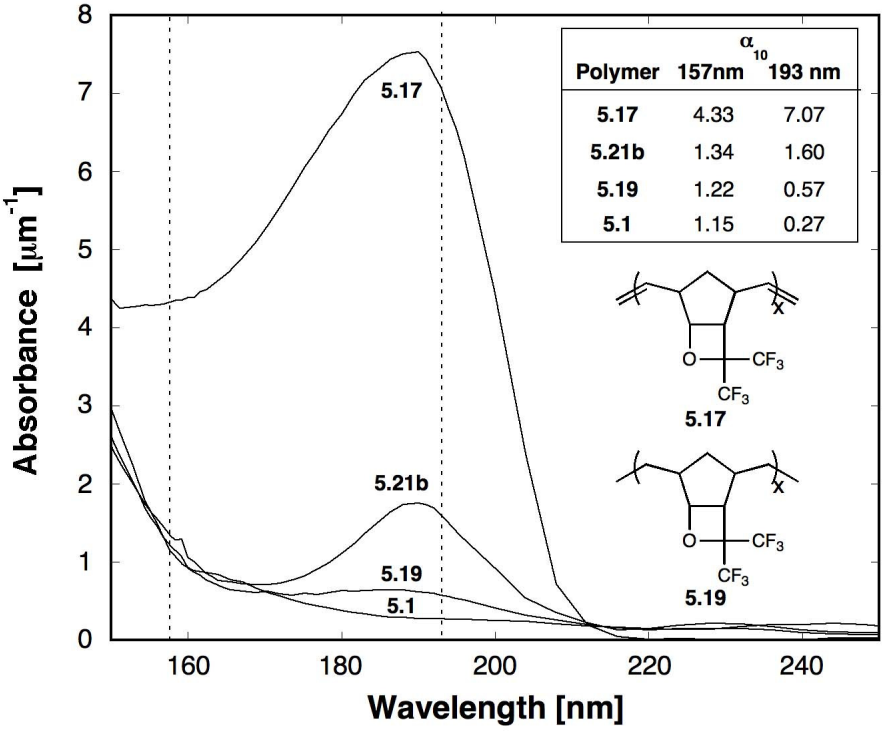

Figure 5.14. VASE of oxatricyclononene ROMP polymers

polymer such as in the case of the non-hydrogenated polymer **5.17,** the absorbance at 157 nm becomes unacceptably high.

These initial fluorinated ring-opening metathesis polymers already offer similar transparency to one of the most transparent norbornene addition polymers. Optimization of the polymer hydrogenation and purification conditions is expected to produce further gains in transparency. For example, although copolymer **5.21a** appears to have more residual unsaturation than **5.21b** (9.1% v. 7.7%) via ^{1}H NMR, it is significantly less absorbing at 193 nm (Figure 5.15). It seems unlikely that a 2% compositional difference would account for this. The major difference between these copolymers is that **5.21a** underwent a second hydrogenation using hydrogen and palladium on carbon. Although the palladium-catalyzed hydrogenation was unable to reduce the degree of unsaturation by more than 1%, apparently, the hydrogenation conditions were effective in removing some highly absorbing species that are not readily identifiable by NMR.

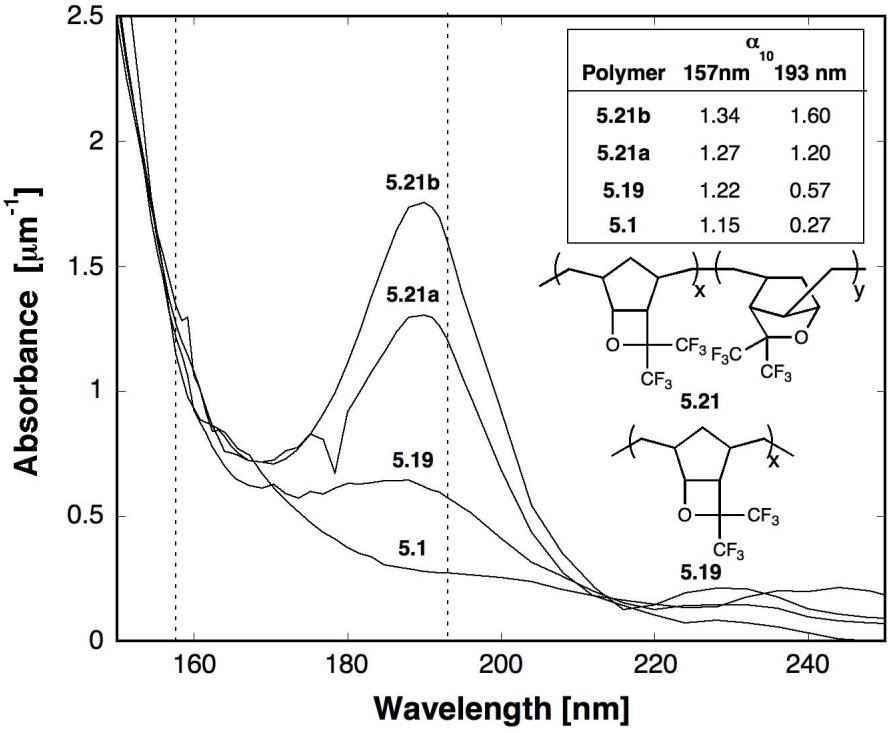

Figure 5.15. VASE of oxatricyclononene ROMP polymers

Computational studies have suggested that cylcopentane structures are more transparent than norbornane structures and much more transparent than tricylcododecane structures.[35] All of our efforts to prepare ROMP polymers of hexafluorocarbinol-functionalized tetracyclododecenes resulted in polymers with absorbances of ~ 3 μm^{-1} or greater, indicating there is a significant absorbance penalty for adding the additional cyclic unit. However, by comparing the addition polymer **5.1** with polymers **5.19** and **5.21**, it can be seen that there is very little difference in the transparency of these vastly different frameworks. Although polymer **5.1** has an additional CH_2 per repeat unit, it is the longer runs of adjacent methylenes (such as the ethylene unit in the ROMP polymers) that are predicted to absorb at 157 nm.[35] Therefore, the transparency at 157 nm for these polymers is dictated more by the overall levels and distribution of fluorination (i.e. two CF_3 groups) than the alicyclic backbone structure. In the end, higher levels of fluorination are required to achieve the transparencies required for 157 nm photoresists (~ 0.7 μm^{-1}).

Lithographic Performance of ROMP-based Oxatricyclononene Resists: In order to evaluate their potential as negative tone photoresists, polymer **5.21a** was imaged under standard lithographic conditions; however, the polymer did not clear in the unexposed areas. No clearing was observed in the exposed regions either, even at an extremely high exposure dose (~100 mJ/cm^2). The oxetane is not opening in the presence of the photoacid to produce hexafluorocarbinol groups which would render the polymer soluble in the exposed regions. Meanwhile, the base polymer is too hydrophobic to dissolve in the aqueous developer in the unexposed regions. Polymer **5.21a** was subsequently blended with polyNBHFA **5.1** (10:90, respectively) to afford a more base soluble composition. Here, the oxetane polymer **5.21a** is intended to act as a crosslinking agent to react with the hexafluorocarbinols of **5.1** in the exposed regions. Initial exposure results without a mask show clear negative tone behavior at ~32 mJ/cm^2 Figure 5.16).

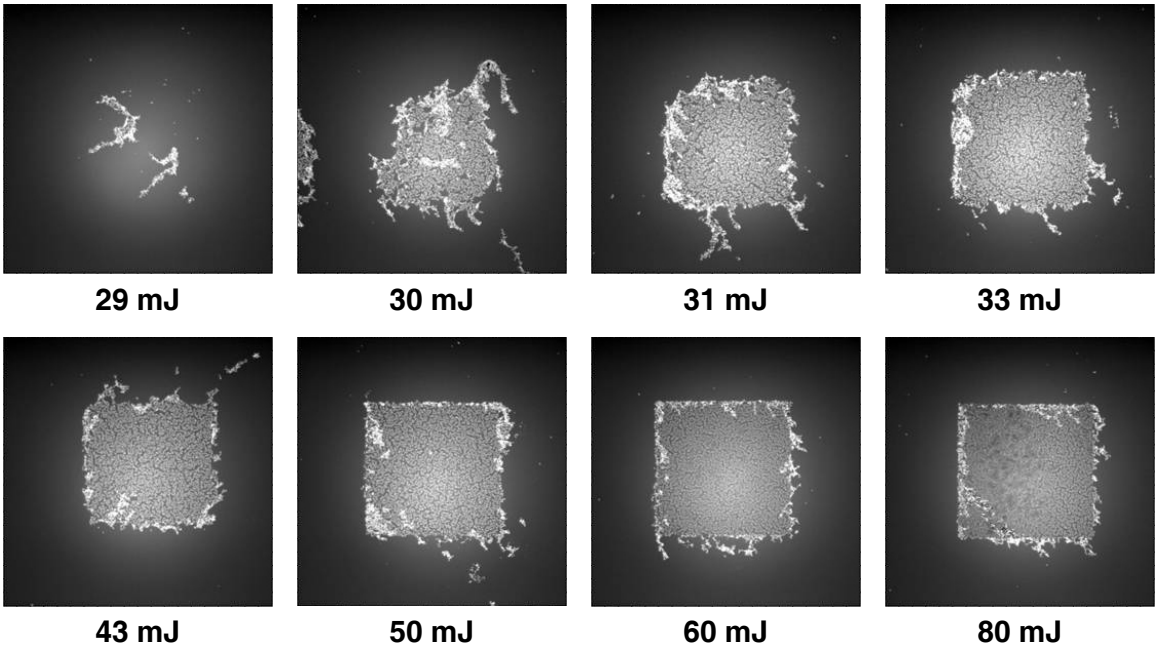

Figure 5.16. Negative tone behavior of blend of **5.1**/**5.21a** (90:10) as a function of exposure dose

However, when a mask was used, no discernable pattern was formed, only swelling and cracking. The solubility of **5.21** is clearly not high enough to afford development of fine features. Therefore, to resolve this hydophobicity concern, the oxetane monomer **5.2** was copolymerized with **5.6** to afford oligomeric copolymers using the terminal olefin chain transfer strategy mentioned above. Previous attempts to copolymerize **5.2** with hexafluorocarbinol-functional tetracyclododecenes resulted in polymers which crosslinked enough during storage to form insoluble gels when attempted to be redissolved. This problem can be mediated by reducing the molecular weight of the material by more than an order of magnitude. Lower molecular weight materials require a larger number of crosslinking reactions to generate insoluble material. However, when blended into a base-stabilized resist formulation with polyNBHFA (**5.1**), only a few crosslinks are required to form an insoluble, crosslinked material.

Copolymerization of **5.2** with **5.6** using allyl acetate as a CTA with the bisphosphine catalyst **6.1** afforded near quantitative yields of low molecular weight copolymers **5.22a/b**(M_n < 5 kDa). The incorporation ratio is identical to the feed ratio within experimental error. Initial

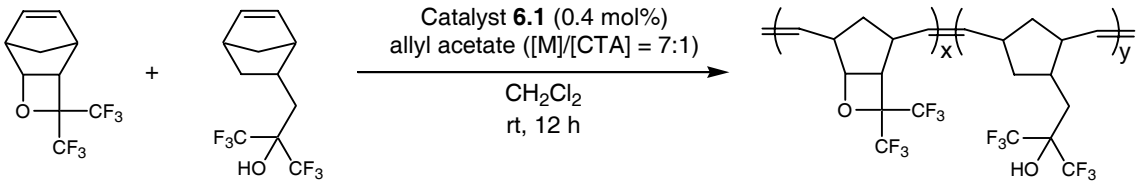

	Feed		Polymer			
	x	y	x	y	M_n	PDI
5.22a	50	50	54	46	4030	1.40
5.22b	33	66	33	66	4090	1.47

Figure 5.17. Low-molecular weight copolymers for crosslinking agents

imaging experiments are underway to evaluate the lithographic utility of these oligomeric cross-linking agents. Incorporation of a more nucleophilic alcohol to the base polymer (such the primary alcohol of norborn-5-en-2-yl methanol) is expected to improve crosslinking considerably.

Conclusions

Fluorinated oxatricyclononenes offer good transparency at 193 nm and 157 nm and may be employed in either metal-catalyzed addition or ring-opening metathesis polymerizations. Palladium-catalyzed addition polymerization of 3-oxatricyclonene proceeded with a simultaneous isomerization reaction to produce gradient copolymers. Oxatricyclononene-based addition polymer resists showed positive-tone behavior rather than negative tone behavior due to the stability of the norbornene-annulated framework. The 4-oxatricyclononene **5.2** provides transparent addition polymers with high etch-resistance and ROMP polymers with high glass transition temperatures. Such structures could be used in conventional photoresists in place of norbornene to impart transparency and etch resistance or in ROMP polymers as a valuable comonomer to increase glass transition temperatures. Polymer molecular weights were most readily controlled using kinetic molecular weight control using terminal olefin chain transfer agents such as allyl acetate. Secondary metathesis on the hindered backbone olefins of these functionalized norbornenes occurs too slowly (if at all) to afford useful molecular weight control.

The second-generation ruthenium bispyridine catalyst **5.10** affords the best combination of activity, molecular weight control, and ease of removal. While ROMP copolymers of 3-oxatricyclononenes proved too hydrophobic to dissolve in common aqueous developers, they have been shown to exhibit negative tone behavior when blended with polyNBHFA **5.1**. The reduction in steric hindrance around the oxetane ring via opening the norbornene framework during metathesis affords higher crosslinking activity. Work is continuing to explore alternative approaches towards utilizing these promising functionalities in deep ultraviolet resist materials, including low molecular weight copolymers with NBHFA **5.1** for transparent crosslinking agents in negative tone resist formulations.

Experimental

Materials: All air sensitive manipulations and polymerizations were carried out in an N_2-filled drybox or using standard Schlenk techniques. All solvents were rigorously degassed in 18 L reservoirs and passed through two sequential purification columns consisting of activated alumina.[36] All starting materials were procured from Aldrich except quadricyclane (Exciton, Inc.), 3-(bicyclo[2.2.1]hept-5-en-2-yl)-1,1,1-trifluoro-2-(trifluoromethyl)propan-2-ol (NBHFA, **5.6**) and polyNBHFA (**5.1**) (courtesy of the Willson Lab, University of Texas, Austin). Quadricyclane was a gift from Exciton, Inc., Dayton, Ohio, and was made available through a Phase II SBIR project that has been sponsored by the Propulsion Directorate of the U.S. Air Force Research Laboratory, AFRL/PR. **(WARNING: Quadricyclane has extraordinary toxicity for a hydrocarbon.)**[37] Just as with the fluorinated ketones used in this paper, standard chemical safety precautions should be taken to avoid inhalation of quadricyclane vapors. Ruthenium olefin metathesis catalysts **5.8**, **5.9**, and **5.18** were obtained from Materia, Inc. Catalyst **5.10** was synthesized according to the literature.[38]

Methods: Nuclear magnetic resonance (NMR) spectra were obtained using either a Bruker AMX300, Varian *Unity Plus 300*, or a Varian *Gemini 300*, or Varian *Mercury 300* spectrometer (^{1}H: 300 MHz, ^{13}C: 75 MHz, ^{19}F: 282 MHz). Shifts for NMR spectra are reported in ppm relative

to TMS (for ^{19}F, internal C_6F_6 (~ 0.5 %) at -162.2 ppm) or to the chemical shift of the residual proteo solvent. Molecular weights (M_n) and polydispersity indices (PDI) were measured from THF solutions by size exclusion chromatography (SEC) using a GPC apparatus equipped with two PLgel 5 μm mixed-C columns (Polymer Labs) connected in series with a DAWN EOS multi-angle laser light scattering (MALLS) detector and an Optilab DSP digital refractometer (both from Wyatt Technology). All molecular weight values are given relative to polystyrene standards. When no calibration standards were used, *dn/dc* values were obtained for each injection by assuming 100% mass elution from the columns. Differential scanning calorimetry (DSC) measurements were performed on either a Perkin Elmer *Series-7* or *Pyris* thermal analysis system. Trace metals analysis via inductively coupled plasma mass spectroscopy (ICP-MS) was performed by Desert Analytics, Tucson, Az.

Vacuum UV Spectroscopy*:* VUV spectra of polymer films were calculated from measurements made with a J. A. Woollam *VU301* variable angle spectroscopic ellipsometer (VASE) and/or measured with the Acton *CAMS-507* spectrophotometer. The films were cast on either silicon wafers (VASE) or calcium fluoride disks (Acton) from solutions in propylene glycol methyl ether acetate (PGMEA) or cyclohexanone and baked at 100-130°C for at least 5 minutes prior to analysis. All absorbance data reported are in base 10.

Silicon oxide etch: Reactive ion etching (RIE) experiments were performed using a Tel Unity2 DRM. The polymer sample was spin-coated on a hexamethyldisilazane-primed silicon substrate and baked at 90 °C for 90 seconds to afford a polymer coating with final thickness of approximately 150 nm. The blanket etch rate for the material was determined by pre- and post-etch thickness measurements using a non-polymerizing Ar/C4F8 oxide etch process. Tool conditions used for the experiment are as follows: 1500 W / 40 mT / 200 sccm Ar / 50 sccm CO / 10 sccm C4F8 / 5 sccm O2 / 40 C

Lithographic Imaging: All imaging work was performed on an Exitech 157 nm small field (1.5 x 1.5 mm^2) mini-stepper (0.6 NA) using either a binary mask (σ 0.7) or phase-shift mask (σ 0.3) at International SEMATECH in Austin, TX. Scanning electron micrographs were collected on a JEOL *JWS-7550*, and cross-sectional data were collected on a Hitachi *4500* microscope. Coating, baking, and development of resist films were performed using an FSI *Polaris 2000* track. Thickness measurements were made on a Prometrix interferometer. A typical resist formulation was prepared by mixing the polymer with 6 wt% (relative to polymer) photoacid generator (triphenylsulfonium nonaflate) and 0.3 wt% tetrabutylammonium hydroxide (TBAH) as the base to control acid diffusion and reduce T-topping. Dissolution inhibitors were mixed with the polymer to the desired ratio. The entire mixture was diluted in PGMEA to provide a viscosity that provides resist thicknesses of approximately 100-200 nm after spinning the resist at 2500 rpm onto a silicon wafer that had been previously coated with ~80 nm BARC (bottom anti-reflective coating, Shipley AR19). The post-apply bake was 140°C for 60 seconds and the post-exposure bake was 130°C for 90 seconds, unless stated otherwise. The exposed resists were developed in the industry-standard 0.26 *N* tetramethylammonium hydroxide (TMAH) developer.

Synthesis and Compounds:

Poly(2-bicyclo[2.2.1]hept-5-en-2-ylmethyl-1,1,1,3,3,3-hexafluoro-propan-2-ol)[4b] (5.1). M_n = 3.86 kDa. PDI = 2.11. $\alpha_{10}^{157nm} = 1.15\ \mu m^{-1}$. $\alpha_{10}^{193nm} = 0.27\ \mu m^{-1}$. $\alpha_{10}^{248nm} = 0.20\ \mu m^{-1}$.

4,4-Bis(trifluoromethyl)-3-oxa-tricyclo[4.2.1.$0^{2,5}$]non-7-ene (5.2).[13] Quadricyclane[39](10.2 mL, 10.0 g, 109 mmol) was added to an oven-dried 100 mL Fisher-Porter bottle and degassed via 3 sequential freeze-pump-thaw cycles. After cooling the reaction vessel to 0 °C, the system was exposed to 20 psi of hexafluoroacetone under rapid stirring. After the hexafluoroacetone was consumed over the course of a few minutes, the system was repressurized with hexafluoroacetone. This was repeated until the no observable pressure decrease was observed after 20 minutes. Excess hexafluoroacetone was carefully vented through concentrated sodium

hydroxide solution. The colorless liquid was purified via silica gel flash column chromatography (20:1 pentane/ether) to produce a colorless liquid. Alternatively, hexafluorocarbinol-containing impurities may be washed away with saturated potassium carbonate solution followed by vacuum distillation (79 °C, 30 Torr). Yield: 71%. ^{1}H NMR ($CDCl_3$, 300 MHz, ppm): δ 6.31 (dd, *J* = 5.7, 3.3 Hz), 5.91 (dd, *J* = 5.7, 3.3 Hz), 4.74 (d, *J* = 3.6 Hz), 3.23 (s), 3.20 (s), 2.59 (d, *J* = 4.8 Hz), 2.40 (d, *J* = 9.6 Hz), 1.59 (d, *J* = 9.6 Hz). ^{19}F NMR ($CDCl_3$, 282 MHz, ppm): δ -69.09 (q), -78.68 (q). ^{13}C NMR ($CDCl_3$, 75 MHz, ppm): 140.84, 132.56, 123.87 (q, *J* = 286 Hz), 121.94 (q, *J* = 286 Hz), 84.33, 80.40 (m), 45.32, 42.24, 42.00, 41.69 (q, *J* = 4.60 Hz). HRMS-[GC-EI+] (m/z): [M•]+ calc'd for $C_{10}H_8F_6O$, 258.0479; found, 258.0481.

5,5-Bis(trifluoromethyl)-4-oxa-tricyclo[4.3.0^{1,6}.0^{3,7}]non-8-ene (5.3).[13] 3-Oxa-tricyclo[4.2.1.0^{2,5}]non-7-ene (5.1) (9.68 g, 37.5 mmol) was added to a flame dried 100 mL round bottom flask with 50 mL anhydrous dichloromethane [0.2M]. Boron trifluoride diethyl etherate (3.75 mmol, 0.1 eq.) was added via syringe at 0 °C and the reaction was slowly warmed to room temperature and stirred for 12 hours. The boron trifluoride was quenched with excess anhydrous triethylamine. The dichloromethane was stripped and the crude reaction mixture was purified via silica gel flash column chromatography (20:1 pentane/ether) to afford 9.42 g (97%) of 5.2 as a colorless liquid. ^{1}H NMR ($CDCl_3$, 300 MHz, ppm): δ 6.45 (dd, *J* = 6.0, 3.3 Hz), 5.84 (dd, *J* = 5.4, 3.3 Hz), 4.48 (s), 3.56 9(s), 2.99 (m), 2.93 (s), 2.16 (dd, *J* = 12.6, 4.8 Hz), 1.09 (dm, *J* = 12.6 Hz). ^{19}F NMR ($CDCl_3$, 282 MHz, ppm): δ -69.72 (q, *J* = 12.6 Hz), -74.97 (q, *J* = 12.16 Hz). ^{13}C NMR ($CDCl_3$, 75 MHz, ppm): δ 124.51, 127.72, 123.24 (q, *J* = 288 Hz), 122.73 (q, *J* = 288 Hz), 81.140 (m), 78.13, 64.99, 52.58 (m), 41.93, 36.29 (m). HRMS-[EI+GC] (m/z): [M•]+ calc'd for $C_{10}H_8F_6O$, 258.0479; found, 258.0487.

General Addition Polymerization Procedure: To a 20ml vial equipped with a stir bar were added allyl palladium chloride dimer (49.6 mg, 0.136 mmol) and silver tetrafluoroborate (52.8 mg, 0.271 mmol) in a dry box. Dichloromethane (5 mL) was added and the mixture was stirred

at room temperature for 20 minutes. The mixture was filtered through a 0.45 μm PTFE syringe filter into a 25 mL round-bottom flask containing a solution of oxatricyclononene monomer (0.70 g, 2.71 mmol, [M]/[C]=10:1) in dichloromethane (10 mL). The reaction mixture was stirred at room temperature for 96 hours then filtered through a 0. 45 μm PTFE syringe filter to remove the polymer-bound base, concentrated *in vacuo*, and precipitated into methanol (100 mL). The crude polymer was dissolved in ethyl acetate (50 mL) and stirred vigorously under a hydrogen atmosphere overnight. The solution was then allowed to sit for another hour to allow the palladium(0) to coagulate and precipitate. The black solid was removed by filtration through celite. The filtrate was concentrated and precipitated into methanol. Filtration provided the product as a white powder.

Poly[(4,4-bis(trifluoromethyl)-3-oxa-tricyclo[4.2.1.0^{2,5}]non-7-ene)-co-(5,5-bis(trifluoromethyl)-4-oxa-tricyclo[4.3.0.0^{3,7}]non-8-ene)] (5.4). Catalyst: Allyl palladium chloride dimer/$AgBF_4$. [M]/[C] = 20:1. Conditions: dichloromethane, rt, 5 d. Polymer composition: 18% **5.2**. 82% **5.3**. ^{1}H NMR (CD_2Cl_2, 300 MHz, ppm): δ 6.6-5.4 (0.25H), 5.3-4.0 (1.0 H), 3.6-0.6 (6.7H). ^{19}F NMR (CD_2Cl_2, 282 MHz, ppm): δ -68- -69 (0.9F), -69 - -72 (12.7F), -72 - -73 (1F), -73 - -77 (11.37), -79 - -81 (m, 3F). α_{10}^{157nm} = 2.28 μm^{-1}. α_{10}^{193nm} = 2.02 μm^{-1}. α_{10}^{248nm} = 0.71 μm^{-1}.

Poly(5,5-bis(trifluoromethyl)-4-oxa-tricyclo[4.3.0^{1,6}.0^{3,7}]non-8-ene) (5.5). Catalyst: Allyl palladium chloride dimer/$AgBF_4$. [M]/[C] = 20:1. Conditions: dichloromethane, rt, 8 d. ^{1}H NMR (Acetone-d_6, 300 MHz, ppm): δ 4.9-4.3 (m. aliphatic), 3.6-1.0 (m, aliphatic). ^{19}F NMR (Acetone-d_6, 282 MHz, ppm): δ -67.62 (m, 3F),-72.66 (m, 3F). M_n = 1.75 kDa. PDI = 1.23. α_{10}^{157nm} = 1.46 μm^{-1}. α_{10}^{193nm} = 0.78 μm^{-1}. α_{10}^{248nm} = 0.37 μm^{-1}.

Poly[2-bicyclo[2.2.1]hept-5-en-2-ylmethyl-1,1,1,3,3,3-hexafluoro-propan-2-ol)-co-(4,4-bis(trifluoromethyl)-3-oxa-tricyclo[4.2.1.0^{2,5}]non-7-ene)-co-(5,5-bis(trifluoromethyl)-4-oxa-tricyclo[4.3.0.0^{3,7}]non-8-ene)] (5.7). Reaction performed by Brian Osborn, Willson research

group, University of Texas, Austin. Catalyst: allyl palladium chloride dimer/$NaSbF_6$. [M]/[C] = 9:1. 1 eq. polymer-bound 2,6-di-*t*-butyl pyridine per eq. catalyst. Conditions: dichloromethane, rt, 3 d. Feed ratio: 66:33 **5.2**:**5:6**. Polymer composition: 70:20:10 **5.6**:**5.2**:**5.3**. Yield: 24 %. Polymer composition: 70% NBHFA (**5.6**), 20% **5.2**, 10% **5.3**.

General Ring-Opening Metathesis Polymerization Procedure: To a 50 mL round-bottom flask with Teflon stirbar and teflon-coated septa cap was added the ruthenium catalyst (56 mg, .077 mmol, 0.01 eq.). The flask was purged with argon and anhydrous dichloromethane was injected. Upon dissolution of the catalyst, monomer (3.86 mmol) was injected and allowed to stir at room temperature. The reaction was quenched by the addition of more than 50 equivalents (relative to catalyst) of ethyl vinyl ether and allowed to stir at room temperature for 1 hour. The dichloromethane was removed *in vacuo* and the crude polymer dissolved in a minimal amount of ethyl acetate. The polymer was precipitated into methanol, centrifuged, and rinsed with methanol. After 2-3 precipitation cycles, the colorless polymer was dried under vacuum (10 mTorr) to afford a white polymeric solid. Note in all copolymers there is ~ 1% of an unknown fluorinated structure. It is assumed that this is the result of a ruthenium-catalyzed olefin isomerization.

For screening of chain transfer conditions, the scale was significantly reduced with 100-200 mg of monomer and the reactions were performed in 5 dram vials with teflon septa caps.

Poly(5,5-bis(trifluoromethyl)-4-oxa-tricyclo[4.3.0.0^{3,7}]non-8-ene) (5.16). Catalyst: **5.10** (1 mol%). CTA: 1,4-diacetoxy-*cis*-2-butene [M]/[CTA] = 50:1. Conditions: Dichloromethane, rt, 24 h. Yield: 71%. ^{1}H NMR (Acetone-d_6, 300 MHz, ppm): δ 6.0-5.5 (m, 2H), 4.61 (m, 1H), 3.31 (m, 1H), 2.89 (m, 2H), 2.25 (m, 1H), 2.00 (m, 1 H). ^{19}F NMR (Acetone-d_6, 282 MHz, ppm): δ -66.80 (s, 3F), -71.06 (s, 3F). M_n = 83.0 kDa. PDI = 1.07. T_g = 233°C.

Poly(4,4-bis(trifluoromethyl)-3-oxa-tricyclo[4.2.1.0^{2,5}]non-7-ene) (5.17). Catalyst: **5.10** (0.2 mol%). CTA: allyl acetate [M]/[CTA] = 5:1. Conditions: dichloromethane, rt, 12 h. Yield: 67%. ^{1}H NMR ($CDCl_3$, 300 MHz, ppm): δ 5.8-5.4.9 (m, 2H), 4.8-4.55 (m, 0.1H), 4.52 (m, 0.1H), 3.62

(m, 0.4H), 3.45-2.9 (m, 1.4H), 2.42 (m, 0.6H), 1.44 (m, 0.6H). ^{19}F NMR ($CDCl_3$, 282 MHz, ppm): δ -72.0 - -73.5 (m, 3F), -79.55 (m, 3F). M_n = 3.1k kDa. PDI = 1.38.

For thermal analysis: M_n = 91.6 kDa, PDI = 1.43, T_g = 128 °C.

Poly[(4,4-bis(trifluoromethyl)-3-oxa-tricyclo[4.2.1.0^{2,5}]non-7-ene)-co-(5,5-bis(trifluoromethyl)-4-oxa-tricyclo[4.3.0.0^{3,7}]non-8-ene)] (5.20).

(5.20a). Catalyst: **5.10** (1 mol%). Conditions: 1,2-dichloroethane, 55 °C, 24 h. Feed ratio: 50:50 **5.2**:**5:3**. Polymer composition: 66:34 **5.2**:**5.3**. Yield: 71%. ^{1}H NMR ($CDCl_3$, 300 MHz, ppm): δ. ^{19}F NMR ($CDCl_3$, 282 MHz, ppm): δ -68.23 (m, 1.74F), -69.76 (m, 0.06F), -72- -73.2 (m, 2.94), -73.53 (m, 1.86F), -75.08 (m, 0.09F), -79.81 (m, 3F). M_n = 22.2 kDa. PDI = 1.08. T_g = 154 °C.

(5.20b). Catalyst: **5.10** (2 mol%). Conditions: dichloromethane, rt, 16h. Feed ratio: 50:50 **5.2**:**5:3**. Polymer composition: 65:35 **5.2**:**5.3**. Yield: 72%. ^{1}H NMR ($CDCl_3$, 300 MHz, ppm): δ. 6.0-5.3 (3H), 5.3-5.0 (1H), 4.8-4.55 (0.64H), 3.8-3.57 (0.60H), 3.55-3.3 (2.44H), 3.2-2.8 (1.7H), 2.6-2.2 (1.6H), 2.2-1.8 (1H), 1.8-1.5 (1.1H). ^{19}F NMR ($CDCl_3$, 282 MHz, ppm): δ -68.15 (m, 1.74F), -69.70 (m, 0.06F), -72.4- -73.2 (m, 2.94F), -73.38 (m, 1.86F), -75.01 (m, 0.09F), -79.69 (m, 3F). M_n = 12.1 kDa. PDI = 1.10.

Poly[(4,4-bis(trifluoromethyl)-3-oxa-tricyclo[4.2.1.0^{2,5}]non-7-ene)-co-(2-bicyclo[2.2.1]hept-5-en-2-ylmethyl-1,1,1,3,3,3-hexafluoro-propan-2-ol) (5.22).

(5.22a). Catalyst: **5.8** (0.8 mol%). Conditions: CH_2Cl_2, rt, 24 h. CTA: allyl acetate ([M]/[C] = 7:1). Feed ratio: 50:50 **5.2**:**5:6**. Polymer composition: 55:45 **5.2**:**5.6**. Yield: 99%. ^{1}H NMR ($CDCl_3$, 300 MHz, ppm): δ 6.6-6.4 (m, 1H), 6.0-5.7 (m, 0.7H), 5.7-5.3 (m, 6H), 5.3-4.9 (m, 3H), 4.7-4.4 (m, 1H), 3.8-3.5 (m, 0.4H), 3.5-3.2 (m, 3.4H), 3.2-1.0 (25H). ^{19}F NMR ($CDCl_3$, 282 MHz, ppm): δ -72.24 (m, 2.6F), --76 - -79 (m, 4.7H), -79.56 (m, 3F). M_n = 4.2 kDa. PDI = 1.35.

(5.22b). Catalyst: **5.8** (0.8 mol%). Conditions: CH_2Cl_2, rt, 24 h. CTA: allyl acetate ([M]/[C] = 7:1). Feed ratio: 33:66 **5.2**:**5:6**. Polymer composition: 33:66 **5.2**:**5.6**. Yield: 99%. ^{1}H NMR ($CDCl_3$, 300 MHz, ppm): δ 6.6-6.4 (m, 1H), 6.0-4.9 (m, 6H), 4.7-4.4 (m, 0.7H), 3.8-3.5 (m,

0.4H), 3.5-3.2 (m, 1.5H), 3.2-1.0 (18H). ^{19}F NMR ($CDCl_3$, 282 MHz, ppm): δ -72.32 (m, 2.3F), --76 - -79 (m, 8.6H), -79.56 (m, 3F). M_n = 4.2 kDa. PDI = 1.35.

General Hydrogenation Procedure for Ring-Opening Metathesis Polymers: In a flame-dried, 100 mL 2-neck round bottom flask equipped with a Teflon stirbar and reflux condenser, *p*-tosylhydrazide (5 eq.) was added. ROMP polymer was dissolved in 25 mL of propylene glycol methyl ether acetate (PGMEA) and added to the flask, followed by tri-*n*-propylamine (7 eq.). The mixture was degassed via 3 freeze-pump-thaw cycles. The reaction was heated to 130 °C under argon at which point, gas evolution began. After 4 hours, a second portion of *p*-tosylhydrazide was added and the reaction allowed to stir for 6 hours. Upon completion, the reaction was cooled to room temperature, taken up in ethyl acetate, washed with 0.1 N HCl solution, $NaHCO_3$ solution, and brine. The organic layer was dried over sodium sulfate, filtered, and concentrated. Repeated precipitation into methanol, centrifugation, and washing with methanol produced colorless polymer which was dried overnight to produce a white polymeric solid.

Poly(4,4-bis(trifluoromethyl)-3-oxa-tricyclo[4.2.1.0^{2,5}]non-7-ene) (5.19). Starting polymer: M_n = 20.2k, PDI = 1.25. Conditions: Hydrogenated according to general procedure. 86% hydrogenation, 79% yield. Second hydrogenation: 98% hydrogenation, 79% yield. Yield: 62%. Yield: 53 %. ^{1}H NMR ($CDCl_3$, 300 MHz, ppm): δ. 5.39 (m, 0.03H), 5.03 (1H), 4.1-4.0 (0.2H), 3.75-3.5 (0.04H), 3.4-3.2 (1H), 2.75-2.5 (1H), 2.5-2.2 (2H), 1.6-1.4 (4H), 1.4-1.2 (1H) ^{19}F NMR ($CDCl_3$, 282 MHz, ppm): -72.54 (m, 3 F), -79.73 (m, 3F). M_n = 20.2 kDa. PDI = 1.25. α_{10}^{157nm} = 1.22 μm^{-1} α_{10}^{193nm} = 0.57 μm^{-1}. α_{10}^{248nm} = 0.07μm^{-1}.

For thermal analysis: M_n = 208.3 kDa. PDI = 1.52. T_g = 99 °C.

Poly[(4,4-bis(trifluoromethyl)-3-oxa-tricyclo[4.2.1.0^{2,5}]non-7-ene)-co-(5,5-bis(trifluoromethyl)-4-oxa-tricyclo[4.3.0.0^{3,7}]non-8-ene)] (5.21).

(5.21a). Conditions: Hydrogenated according to general procedure. 90% hydrogenation, 72% yield. Second hydrogenation H_2 (1 atm), Pd/C (10 wt % Pd), rt, 9h: 90.8% hydrogenation, 84% yield. Yield: 60%. Polymer composition: 65:35 **5.2**:**5.3**. ^{1}H NMR ($CDCl_3$, 300 MHz, ppm): δ 6.0-5.3 (0.44H), 5.2-5.0 (1H), 4.8-4.4 (0.54H), 3.8-3.10 (1.5H), 3.1-2.75 (1H), 2.75-2.5 (1.4H), 2.5-2.3 (2H), 2.2-2.0 (1.7H), 1.95-1.3 (6H). ^{19}F NMR ($CDCl_3$, 282 MHz, ppm): -68.02 (m, 1.68F), -70.4 (m, 0.03F), -72 - -74.0 (m, 4.8F), -75.1m, 0.02F), -79.98 (m, 3F). M_n = 25.0 kDa. PDI = 1.08. T_g = 120 °C . α_{10}^{157nm} = 1.27 μm^{-1} α_{10}^{193nm} = 1.20 μm^{-1}. α_{10}^{248nm} < 0.01 μm^{-1}.

(5.21b). Conditions: Hydrogenated according to general procedure. 78% hydrogenation, 59% yield. Second hydrogenation: 92.3% hydrogenation, 81% yield. Total yield: 48%. Polymer composition: 63:37 **5.2**:**5.3**. ^{1}H NMR ($CDCl_3$, 300 MHz, ppm): δ 6.0-5.3 (0.19H), 5.15-5.0 (1H), 4.8-4.4 (0.66H), 3.4-3.2 (1H), 3.0-2.8 (1H), 2.8-2.55 (1.5H), 2.5-2.3 (2H), 2.2-2.0 (2H), 2-1.35 (7 H), 1.35-1.0 (1.5H) ^{19}F NMR ($CDCl_3$, 282 MHz, ppm): δ -67.90 (m, 1.83F), -70.34 (m, 0.03F), -72- -74 (m, 4.95F), -74.94 (m, 0.06F), -79.79 (m, 3F). M_n = 14.2 kDa. PDI = 1.09. α_{10}^{157nm} = 1.34 μm^{-1} α_{10}^{193nm} = 1.60 μm^{-1}. α_{10}^{248nm} = 0.09 μm^{-1}.

Trace metals analysis: Polymer composition: 68:33 **5.2**:**5.3**. M_n = 19.9 kDa, PDI = 1.11. %Ru (ICP-MS) = 0.013%.

References and Notes

(1) (a). Patterson, K.; Yamachika, M.; Hung, R. J.; Brodsky, C. J.; Yamada, S.; Somervell, M. H.; Osborn, B.; Hall, D.; Dukovic, G.; Byers, J.; Conley, W.; Willson, C. G. *Proc. SPIE* **2000**, *3999*, 365-374. (b). Brodsky, C.; Byers, J.; Conley, W.; Hung, R.; Yamada, S.; Patterson, K.; Somervell, M.; Trinque, B.; Tran, H. V.; Cho, S.; Chiba, T.; Lin, S-H.; Jamieson, A.; Johnson, H.; Vander Heyden, T.; Willson, C. G. *J. Vac. Sci. Technol.* B **2000**, *18*, 3396-3401.

(2) Gandler, J. R.; Jencks, W. P. *J. Am. Chem. Soc.* **1982**, *104*, 1937-1951.

(3) (a). Ito, H. *IBM J. Res. Dev.* **2001**, *45*, 683-695. (b). Hoskins, T.; Chung, W. J.; Agrawal, A.; Ludovice, P. J.; Henderson, C. L.; Seger, L. D.; Rhodes, L. F.; Schick, R. A. *Macromolecules* **2004**, *37*, 4512-4518.

(4) (a). Trinque, B. C.; Chambers, C. R.; Osborn, B. P.; Callahan, R. P.; Lee, G. S.; Kusumoto, S.; Sanders, D. P.; Grubbs, R. H.; Conley, W. E.; Willson, C. G. *J. Fluor. Chem.* **2003**, *122*, 17-26. (b). Tran, H. V.; Hung, R. J.; Chiba, T.; Yamada, S.; Mrozek, T.; Hsieh, Y-T.; Chambers, C. R.; Osborn, B. P.; Trinque, B. C.; Pinnow, M. J.; MacDonald, S. A.; Willson, C. G.; Sanders, D. P.; Connor, E. F.; Grubbs, R. H.; Conley, W. *Macromolecules* **2002**, *35*, 6539-6549. (c). Willson, C. G.; Trinque, B. C.; Osborn, B. P.; Chambers, C. R.; Hsieh, Y-T.; Chiba, T.; Zimmerman, P.; Miller, D.; Conley, W. *J. Photopolym. Sci. Technol.* **2002**, *15*, 583-590. (d). Tran, H. V.; Hung, R. J.; Chiba, T.; Yamada, S.; Mrozek, T.; Hsieh, Y-T.; Chambers, C. R.; Osborn, B. P.; Trinque, B. C.; Pinnow, M. J.; Sanders, D. P.; Connor, E. F.; Grubbs, R. H.; Conley, W.; MacDonald, S. A.; Willson, C. G. *J. Photopolym. Sci. Technol.* **2001**, *14*, 669-674. (e). Chiba, T.; Hung, R. J.; Yamada, S.; Trinque, B.; Yamachika, M.; Brodsky, C.; Patterson, K.; Vander Heyden, A.; Jamison, A.; Lin, S-H.; Somervell, M.; Byers, J.; Conley, W; Willson, C. G. *J. Photopolym. Sci. Technol.* **2000**, *13*, 657-664.

(5) (a). Ito, H.; Wallraff, G. M.; Brock, P. J.; Fender, N.; T., Hoa D.; Breyta, G.; Miller, D. C.; Sherwood, M. H.; Allen, R. D. *Proc. SPIE* **2001**, *4345*, 273-284. (b). Trinque, B. C.; Chiba, T.; Hung, R. J.; Chambers, C. R.; Pinnow, M. J.; Osborn, B. P.; Tran, H. V.; Wunderlich, J.; Hsieh, Y-T.; Thomas, B. H.; Shafer, G.; DesMarteau, D. D.; Conley, W.; Willson, C. G. *J. Vac. Sci. & Technol. B*. **2002**, *20*, 531-536. (c). Trinque, B. C.; Osborn, B. P.; Chambers, C. R.; Hsieh, Y-T.; Corry, S. B.; Chiba, T.; Hung, Raymond J-P.; Tran, H. V.; Zimmerman, P.; Miller, D.; Conley, W.; Willson, C. G. *Proc. SPIE* **2002**, *4690*, 58-68.

(6) (a). Kodama, S.; Kaneko, I.; Takebe, Y.; Okada, S.; Kawaguchi, Y.; Shida, N.; Ishikawa, S.; Toriumi, M.; Itani, T. *Proc. SPIE* **2002**, *4690*, 76-83. (b). Irie, S.; Ishikawa, S.; Hagiwara, T.; Yamazaki, T.; Furukawa, T.; Itani, T.; Kawaguchi, Y.; Kodama, S.; Yokokoji, O.; Kaneko, I.; Takebe, Y.; Okada, S. *Jap. J. Appl. Phys. Pt. 1*. **2003**, *42*(6B), 3743-3747.

(7) (a). Feiring, A. E.; Crawford, M.; Feldman, J.; Farnham, W. B.; Feldman, J.; French, R. H.; Leffew, K. W.; Petrov, V. A.; Schadt, F. L., III; Wheland, R.C.; Zumsteg, F. C. *J. Fluorine Chem.* **2003**, *122*, 11-16. (b). Toriumi, M.; Ishikawa, T.; Kodani, T.; Koh, M.; Moriya, T.; Araki, T.; Aoyama, H.; Yamashita, T.; Yamazaki, T.; Itani, T.; *J. Photopolym. Sci. Technol.* **2003**, *16*, 607-614. (c). Sharif, I.; DesMarteau, D.; Ford, L.; Shafer, G. J.; Thomas, B.; Conley, W.; Zimmerman, P.; Miller, D.; Lee, G. S.; Chambers, C. R.; Trinque, B. C.; Chiba, T.; Osborn, B. P.; Willson, C. G. *Proc. SPIE* **2003**, *5039*, 33-42.

(8) (a). Bae, Y. C.; Douki, K.; Yu, T.; Dai, J.; Schmaljohann, D.; Koerner, H.; Ober, C. K.; Conley, W. *Chem. Mater.* **2002**, *14*, 1306-1313. (b). Schmaljohann, D.; Young, C. B.; Dai, J.; Weibel, G. L.; Hamad, A. H.; Ober, C. K. *J. Photopolym. Sci. Technol.* **2000**, *13*, 451-458.

(9) (a). Stewart, M. D.; Patterson, K.; Sommervell, M. H.; Willson, C. G. *J. Phys. Org. Chem.* **2000**, *13*, 767-774. (b). Ito, H. *IBM J. Res. Dev.* **2000**, *44*, 119-130. (b). MacDonald, S. A.; Willson, C. G.; Frechet, J. M. J. *Acc. Chem. Res.* **1994**, *27*, 151-158.

(10) (a). Bloomstein, T. M.; Sedlacek, Jan H. C.; Palmacci, Stephen T.; Hardy, D. E.; Liberman, V.; Rothschild, M. *Proc. SPIE* **2003**, *5040*, 650-661. (b). Rothschild, M.; Bloomstein, T. M.; Fedynyshyn, T. H.; Liberman, V.; Mowers, W.; Sinta, R.; Switkes, M.; Grenville, A.; Orvek, K. *J. Fluorine Chem.* **2003**, *122*, 3-10. (c). Matsui, Y.; Umeda, S.; Seki, S.; Tagawa, S.; Ishikawa, S.; Itani, T. *Jap. J. Appl. Phys., Pt. 1*. **2003**, *42*(6B), 3894-3899. (d). Hien, S.; Angood, S.; Ashworth, D.; Basset, S.; Bloomstein, T. M.; Dean, K. R.; Kunz, R. R.; Miller, D. A.; Patel, S.; Rich, G.. *Proc. SPIE* **2001**, *4345*, 439-447. (e). Fedynyshyn,

T. H.; Kunz, R. R.; Sinta, R. F.; Goodman, R. B.; Doran, S. P. *J. Vac. Sci. Technol.* B **2000**, *18*, 3332-3339. (f). Cefalas, A. C.; Sarantopoulou, E.; Gogolides, E.; Argitis, P. *Microelectronic Eng.* **2000**, *53*, 123-126.

(11) (a). Pinnow, M. J.; Noyes, B. F., III; Tran, H. V.; Tattersall, P. I.; Cho, S.; Klopp, J. M.; Bensel, N.; Frechet, J. M. J.; Sanders, D. P.; Grubbs, R. H.; Willson, C. Grant. *PMSE Prepr.* **2002**, *87*, 403-404. (b). Klopp, J. M.; Bensel, N.; Fresco, Z. M.; Frechet, J. M. J. *Chem. Comm.* **2002**, *24*, 2956-2957. (c). Kim, J-B.; Lee, J-J. *Polymer* **2002**, *43*, 1963-1967.

(12) Tarrant, P.; Bull, R. N. *J. Fluorine Chem.* **1988**, *40*, 201-215.

(13) (a). Sanders, D. P. *Chapter 4 - Ph. D. Thesis*, California Institute of Technology, **2004**. (b). Sanders, D. P.; Osborn, B. P.; Willson, C. G.; Grubbs, R.H. Manuscript in preparation, **2004**.

(14) Sanders, D. P.; Connor, E. F.; Grubbs, R. H.; Hung, R. J.; Osborn, B. P.; Chiba, T.; MacDonald, S. A.; Willson, C. G.; Conley, W. *Macromolecules* **2003**, *36*, 1534-1542.

(15) Mathew, J. P.; Reinmuth, A.; Melia, J.; Swords, N.; Risse, W. *Macromolecules* **1996**, *29*, 2755-2763.

(16) Barnes, D. A.; Benedikt, G. M.; Goodall, B. L.; Huang, S. S.; Kalamarides, H. A.; Lenhard, S.; McIntosh, L. H., III; Selvy, K. T.; Schick, R. A.; Rhodes, L. F. *Macromolecules* **2003**, *36*, 2623-2632.

(17) (a). Lipian, J.; Mimna, R. A.; Fondran, J. C.; Yandulov, D.; Shick, R. A.; Goodall, B. L.; Rhodes, L. F.; Huffman, J. C. *Macromolecules* **2002**, *35*, 8969-8977. (b). Hennis, A. D.; Polley, J. D.; Long, G. S.; Sen, A.; Yandulov, D.; Lipian, J.; Benedikt, G. M.; Rhodes, L. F.; Huffman, J. *Organometallics* **2001**, *20*, 2802-2812.

(18) Sulfuric acid-catalyzed methanolysis of oxetane **5.2** proceeded in 69% of ring-opened compounds after 22 hours. Ring-opening of the saturated version was significantly slower (14% after 2.5 days). Depending upon reaction conditions, reaction of saturated **5.2** with

triflic acid in benzene resulted in either stoichiometric ring-opening or catalytic isomerization to saturated version of **5.3**.

(19) (a). Nguyen, S. T.; Trnka, T. M. In *Handbook of Olefin Metathesis*, vol. 1: Wiley-VCH: Weinheim, **2003**; pp. 61- 85. (b). Frenzel, U.; Nuyken, O. *J. Polym. Sci. A. Polym. Chem.* **2002**, *40*, 2895-2916. (c). Trnka, T. M.; Grubbs, R. H. *Acc. Chem. Res.* **2001**, *34*, 18-29. (d). Buchmeiser, M. R. *Chem. Rev.* **2000**, *100*, 1565-1604. (e). Bielawski, C. W.; Grubbs, R. H. *Angew. Chem. Int. Ed.* **2000**, *39*, 2903-2906.

(20) (a). Bielawski, C. W.; Hillmyer, M. A. In *Handbook of Olefin Metathesis*, vol. 3: Wiley-VCH: Weinheim, **2003**; pp. 255- 282. (b). Bielawski, C. W.; Benitez, D.; Morita, T.; Grubbs, R. H. *Macromolecules* **2001**, *34*, 8610-8618. (c). Katayama, H.; Fukuse, Y.; Nobuto, Y.; Akamatsu, K.; Ozawa, F. *Macromolecules* **2003**, *36*, 7020-7026.

(21) Reichmanis, E.; Nalamasu, O.; Houlihan, F. M. *Acc. Chem. Res.* **1999**, *32*, 659-667.

(22) (a). Okoroanyanwu, U.; Shimokawa, T.; Byers, J.; Willson, C. G. *Chem. Mat.* 1998, *10*, 3319-3327. (b). Patterson, K. W. *Ph.D. Dissertation,* University of Texas-Austin, **2000**. (c). Suwa, M.; Iwasawa, H.; Kajita, T.; Yamamoto, M.; Iwanaga, S-I. *Proc. SPIE* **1998**, *3333*, 26-31. (d). Meyer, U.; Kern, W.; Hummel, K.; Stelzer, F. *Eur. Polym. J.* **1999**, *35*, 69-76.

(23) Sanders, D. P.; Osborn, B. P. Unpublished results.

(24) Preishuber-Pflugl, P.; Eder, E.; Stelzer, F.; Reisiniger, H.; Mulhaupt, R.; Forsyth, J.; Perena, J. M. *Macromol. Chem. Phys.* **2001**, *202*, 1130-1137.

(25) Otsuki, T.; Goto, K.; Komiya, Z. *J. Polymer Sci. A Polym. Chem.* **2000**, *38*, 4661-4668.

(26) Contreras, A. P.; Cerda, A. M.; Tlenkopatchev, M. A. *Macromol. Chem. Phys.* **2002**, *203*, 1811-1818.

(27) (a). Stille, J. R.; Grubbs, R. H. *J. Org. Chem*. **1989**, *54*, 434-444. (b). Stille, J. R.; Grubbs, R. H. *J. Org. Chem.* **1990**, *55*, 843-862.

(28) Ivin, K. J. *Makromol. Chem., Macrmol. Symp.* **1991**, *42/43*, 1-14.

(29) Hejl, A.; Scherman, O. A.; Grubbs, R. H. *Macromolecules* **2005**, accepted.

(30) Love, J. A.; Morgan, J. P.; Trnka, T. M.; Grubbs, R. H. *Angew. Chem. Int. Ed.* **2002**, *41*, 4035-4037.

(31) (a). Slugovc, C.; Demel, S.; Stelzer, F. *Chem. Commun.* **2002**, 2572-2573. (b). Choi, T. L.; Grubbs, R. H. *Angew. Chem Int. Ed.* **2003**, *42*, 1743-1746. (c). Slugovc, C.; Riegler, S.; Haynn, G.; Saf, R.; Stelzer, F. *Macromol. Rapid Commun.* **2003**, *24*, 435-439.

(32) It should be noted that these PDIs are significantly narrower that those of norbornene polymerized at room temperature with these catalysts.[31b] The inability of the ruthenium catalyst to readily react with the more hindered backbone olefins of **5.16** at these temperatures limits chain transfer and provides for a more controlled polymerization. Even lower PDIs (1.05) can be achieved with catalyst **5.10** by lowering the reaction temperature to 0 °C (see Entry 8, Table 3).

(33) (a). Ilker, M. F.; Coughlin, E. B. *Macromolecules* **2002**, *35*, 54-58. (b). Al Samak, B.; Carvill, A. G.; Hamilton, J. G.; Rooney, J. J.; Thompson, J. M. *Chem. Commun.* **1997**, 2057-2058.

(34) It is unknown whether this reluctance to hydrogenate is due to adjacent units of **5.2** or olefin isomerization to very sterically hindered trisubstituted olefins which may be occurring during either polymerization or hydrogenation. In certain cases, copolymers polymerized at a lower temperature (room temperature) in order to limit any ruthenium-catalyzed olefin isomerization proved to hydrogenate more completely (>98%). Additional work is ongoing to understand and resolve this difficulty.

(35) Dixon, D. A.; Matsuzawa, N. N.; Ishitani, A.; Uda, T. *Phys. Stat. Sol B* **2001**, *226*, 69-77. (b). Matsuzawa, N. N.; Ishitani, A.; Dixon, D. A.; Uda, T. *Proc. SPIE* **2001**, *4345*, 396-405. (c). Yamazaki, T.; Itani, T. *Jpn. J. Appl. Phys.* **2003**, *42*, 3881-3884.

(36) Pangborn, A. B.; Giardello, M. A.; Grubbs, R. H.; Rosen, R. K. Trimmers, F. J. *Organometallics* **1996**, *15*, 1518-1520.

(37) Kinkead, E. R.; Wolfe, R. E.; Salins, S. A.; Grabau, J. H. Report (**1993**), (Order No. AD-A272694). CAN 123:190700.

(38) Sanford, M. S.; Love, J. A.; Grubbs, R. H. *Organometallics* **2001**, *20*, 5314-5318.

(39) Quadricyclane (tetracyclo[3.2.0.$0^{2,7}$.$0^{4,6}$]heptane) can be synthesized photochemically from norbornadiene. (a). Hammond, G. S.; Turro, N. J.; Fischer, A. *J. Am. Chem. Soc.* **1961**, *83*, 4674-4675. (b). Hammond, G. S.; Wyatt, P.; DeBoer, C. D.; Turro, N. J. *J. Am. Chem. Soc.* **1964**, *86*, 2532-2533. (c). Smith, C. D.; Taggi, A. J.; Meinwald, J. *Org. Synth.* **1971**, *51*, 133-138. (d). Alberici, F.; Cassar, L.; Monti, F.; Neri, C.; Nodarai, N. *US Pat. 5076813*, **1991**.

CHAPTER 6

Multifunctional Monomers and Materials for Advanced Lithographic Applications via Olefin Metathesis

Multifunctional Monomers and Materials for Advanced Lithographic Applications via Olefin Metathesis

Abstract Well-defined ruthenium olefin metathesis catalysts display the high reactivity and functional group tolerance required for the synthesis of new monomers and materials for deep ultraviolet lithography. Ring-opening metathesis polymerization of hexafluorocarbinol-functionalized tetracyclododecene monomers affords polymers which, after hydrogenation, are highly transparent at 193 nm, provided the acidic alcohol is protected prior to polymerization. However, these same ROMP polymers continue to exhibit inherently high absorbance (~3.0 μm^{-1}) at 157 nm despite our best efforts. Ruthenium-catalyzed cross-metathesis can serve as a mild and convenient route to the production of hexafluorocarbinol-functionalized products which would ordinarily be synthesized via alkylations of highly toxic hexafluoroacetone. The presence of the acidic fluoroalcohol leads to uncharacteristically low E/Z ratios in certain instances. Further investigation into the origin of this low stereoselectivity resulted in the discovery that additives such as acetic acid can be effective in eliminating problematic olefin migration side-reactions. An example of the benefits of the cross-metathesis approach is the 2-step synthesis of norbornene monomers with both ester and hexafluorocarbinol functionalities. Gas-phase ultraviolet spectroscopy reveals that these difunctional norbornane structures have extraordinarily high transparency at 157 nm. The intramolecularly hydrogen-bound functionalities of these structures are expected to impart modified dissolution properties (including reduced swelling behavior) to advanced resist materials for deep ultraviolet lithography.

Introduction

The development of selectively fluorinated monomers and materials for deep ultraviolet lithographic applications has been widely explored due to the high transparency of fluorinated materials at 157 nm.[1] A wide variety of fluorinated backbone structures have been explored,

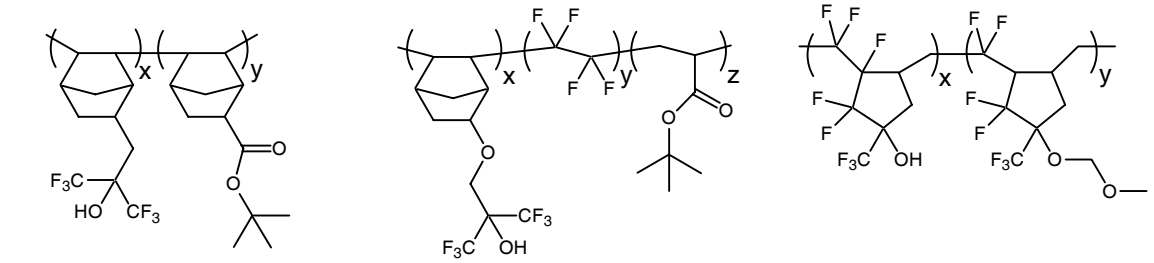

Figure 6.1. Fluoropolymers for use as photoresists at 157 nm

including metal-catalyzed norbornene and tricyclononene addition polymers,[2] free-radical copolymers of fluorinated acrylates and methacrylates,[3] free-radical copolymers of tetrafluoroethylene with functionalized olefins,[4] and free-radical cycloaliphatic polymers,[5] some of which are shown in Figure 6.1. The key development, however, was the discovery of the remarkable transparency[1,6] and dissolution properties[7] imparted by the use of highly fluorinated alcohols, particularly hexafluorocarbinols. The pKa of heavily fluorinated alcohols is comparable to phenols due to the strong inductive stabilization of their conjugate bases.[8] Unlike carboxylic acid ester-based materials, hexafluorocarbinol-functionalized resists offer the unique combination of extremely high transparency with ideal dissolution behavior (and a notable lack of swelling[7] in the developing solution which has been a particular problem with ester-functionalized norbornene-type addition polymers).

Free-radical polymerization processes have dominated resist development efforts due to their advantages of low cost, synthetic ease, and, most importantly, the lack of residual metallic contaminants which are difficult to remove and may detrimentally affect subsequent device performance/lifetime. However, the unique problems associated with developing materials with high transparency at 157 nm while maintaining good mechanical properties has caused many research labs to examine fluorinated norbornene monomers. While a tremendous variety of norbornene and norbornene-like monomers are readily accessible via cycloaddition processes

with functionalized olefins,[9] norbornene-type monomers do not homopolymerize efficiently via radical processes[10] and must be copolymerized with electron-deficient olefins such as tetrafluoroethylene.[4] Norbornene-type monomers are, however, readily polymerized via a number of metal-catalyzed pathways including addition (coordination) polymerization and ring-opening metathesis polymerization.[9] A particular challenge of employing metal catalysis to synthesize resist materials for 157 nm is the large number of polar and relatively acidic functionalities which must be tolerated by the metal catalysts. This requirement of high functional group tolerance rules out the use of oxophilic early transition metal catalysts and favors the use of late-transition metal catalysts. Specifically, neutral nickel[11] and cationic palladium[12] catalysts have been widely used for the synthesis of norbornene addition polymers and ruthenium catalysts[13] have been employed for the synthesis of ring-opening metathesis polymers.

The high activity and functional group tolerance of ruthenium-based olefin metathesis catalysts such as **6.1** and **6.2** (Figure 6.2) makes them particularly attractive in the synthesis of the highly functionalized monomers and polymers useful for lithographic applications.[13] While removal of metallic contaminants from polymeric materials to the parts per billion level required by the semiconductor industry is extraordinarily difficult, removal of metallic species from low molecular weight monomeric species capable of being purified by distillation or sublimation is

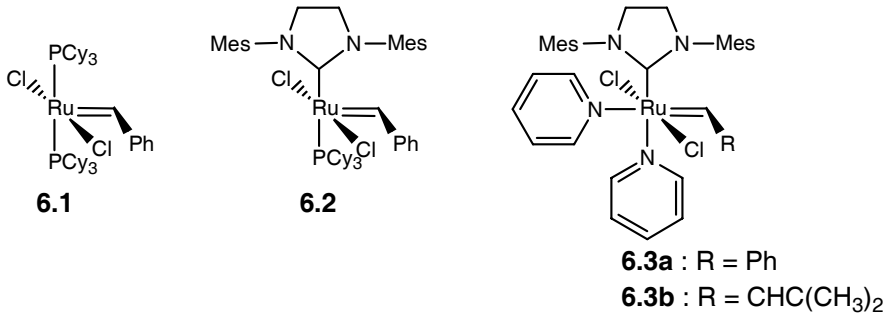

Figure 6.2. Ruthenium olefin metathesis catalysts

trivial. Therefore, application of transition metal catalysis towards monomer synthesis rather than polymer synthesis may be a more practical way to take advantage of the unique chemical transformations performed by these catalysts. In this work, various applications of ruthenium-catalyzed olefin metathesis are explored in the construction of multiply functionalized monomers and low molecular weight materials for use in deep ultraviolet lithography, with a particular focus on hexafluorocarbinol-functionalized compounds.

Results and Discussion

ROMP of Hexafluorocarbinol-containing Monomers Ring-opening metathesis polymerization (ROMP) of norbornene-type monomers had been explored during the development of 193 nm resists.[14] ROMP of 8-functionalized tetracyclo[4.4.$0^{1,6}$.$1^{2,5}$.$1^{7,10}$]dodec-3-ene (TCD) monomers using various metathesis catalysts yielded photoresist materials of only moderate utility. High loadings of free carboxylic acid-containing monomer were required for the resulting materials to have glass transition temperatures above 120 °C. These polymers exhibited undesirable swelling behavior and were not fully phase compatible with a large number of standard photoacid generators. TCD monomer **6.4a** is a byproduct of the Diels-Alder reaction used to produce the most widely used hexafluorocarbinol-functionalized norbornene. In spite of the failure of previous ROMP polymers as resist materials, the ability to turn this waste stream into a potentially high value-added material via olefin metathesis is particularly attractive.

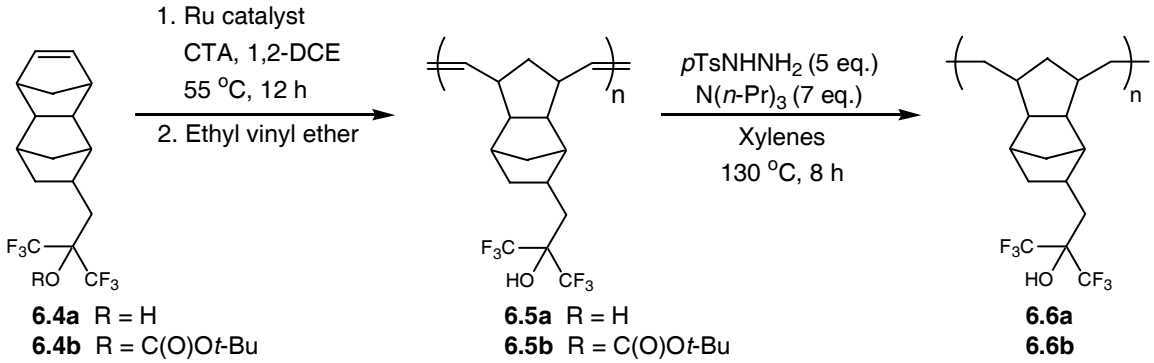

Figure 6.3. ROMP of hexafluorocarbinol-functionalized TCD monomers

ROMP of **6.4a** with catalyst **6.2a** in the presence of chain transfer agent afforded excellent yields of a brownish polymer (Figure 6.3). Standard chain transfer protocols called for the use of a symmetric internal olefinic chain transfer agent (CTA) such as 1,4-diacetoxy-*cis*-2-butene or *trans*-3- hexene and high reaction temperatures (55 °C, 16-24 h).[15] However, the secondary metathesis reactions which efficiently redistribute the chain lengths to the statistically determined value (DP = [M]/[CTA]) in the polymerization of norbornene are not as facile with the more hindered backbone olefins in the TCD ROMP polymer. As a result, molecular weights were consistently much higher than expected. With these bulkier TCD monomers, molecular weights were only able to be controlled kinetically through the use of either catalyst control (using a rapidly initiating catalyst such as **6.3a/b**) or the use of a terminal olefin chain transfer agent such as allyl acetate.[16] Unfortunately, the glass transition temperatures of polymer **6.5a** is only moderate (~115 °C) and falls further to ~ 85 °C after hydrogenation.[16] The large amount of color remaining in these polymers after reaction is equally problematic. The transparency of the hydrogenated polymer **6.6a** as measured by variable angle scanning ellipsometry (VASE) is fairly high as shown in Figure 6.4. A large number of copolymers of **6.4a** with various functionalized norbornene monomers were synthesized; however, all had unacceptable absorbance at (~ 3.5 μm^{-1}).[16] ROMP polymers consistently show higher, unacceptable absorbance at 157 nm relative to radical and metal-catalyzed addition polymers made from the same. The relative contributions of residual catalyst, hydrogenation by-products, polymer end groups, and the actual saturated ring-opened TCD structure to this higher absorbance are unknown. As a result, a conscientious effort to produce an ultra-clean "ideal" sample was attempted.

One difficulty in obtaining clean polymer is the inability to cleanly precipitate polymer **6.5a** into common solvents due to its amphiphilic nature. The acidic alcohols confer solubility in polar solvents such as methanol while the lipophilic backbone prevents the polymer from precipitating cleanly out of hexanes or pentanes. While the polymer is insoluble in aqueous

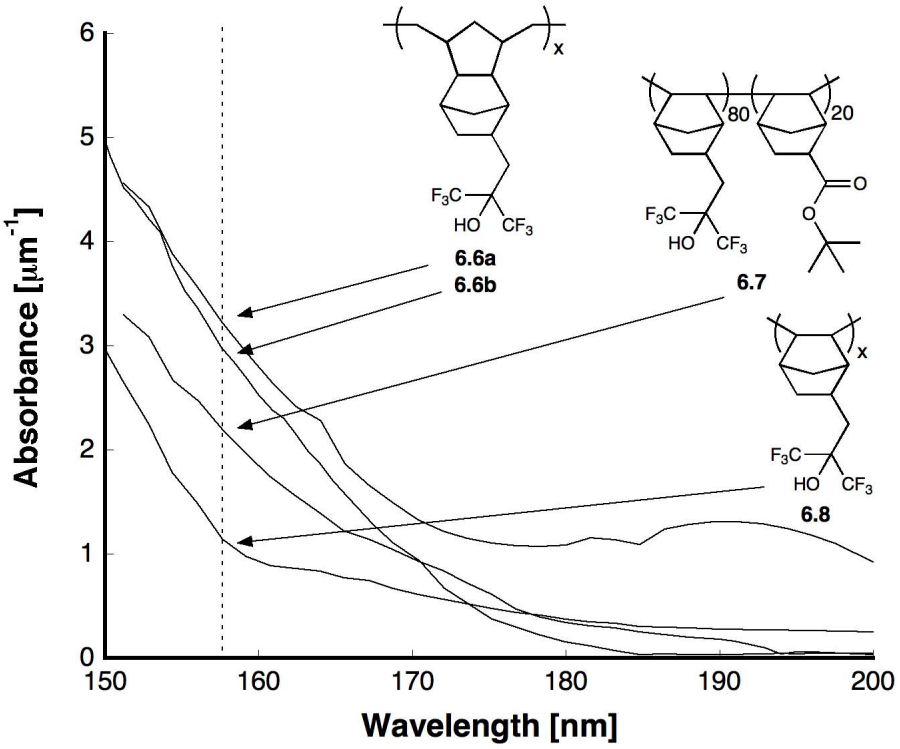

Figure 6.4. VASE spectra of metal-catalyzed polymers with hexafluorocarbinols

solutions, the monomer and catalyst by-products are also insoluble and the resulting polymer is particularly difficult to dry completely. A number of various techniques stated in the literature[17,18] for efficient removal of ruthenium metathesis catalyst by-products were attempted in order to clean up the brown polymer obtained after precipitation. The acidity of the fluorinated alcohols caused the polymer to stick excessively to a silica gel plug, resulting in large losses of material. The bound polymer could only be eluted with pure dichloromethane or ethyl acetate with little reduction in coloration. Attempts were made to exchange a water soluble phosphine ligand onto the residual catalyst to enable aqueous extraction according to the procedure of Maynard *et al*.[18] After extended exchange periods with excess of the water soluble phosphine, no color was observed to migrate to the aqueous extraction layer. Performing the ligand exchange directly after polymerization under inert conditions was also ineffective. Dialysis in methanol using regenerated cellulose dialysis tubes (500 molecular weight cutoff) was effective at

removing residual monomer; however, little reduction in coloration was observed. Extended heating in the presence of a hydrogen atmosphere or hydrochloric acid solution was similarly ineffective and only served to exacerbate the problem. Clearly, either the catalyst or a catalyst decomposition product must be interacting with the acidic hexafluorocarbinols (perhaps forming polymer-bound metal alkoxides) given the colorless ROMP polymers typically obtained using monomers like 4,4-bis(trifluoromethyl)-3-oxa-tricyclo[4.2.1.$0^{2,5}$]non-7-ene and catalyst **6.3a**.[19]

In order to observe the effect of the acidic hexafluorocarbinol, the alcohol of **6.4a** was protected with a *t*-butoxy carbonyl protecting group. The protected monomer **6.4b** was polymerized with the dimethylvinyl carbene catalyst **6.3b**. Fortunately, the *t*-Boc protected polymer **6.5b** precipitated cleanly from methanol, affording a nearly colorless polymer. Hydrogenation of **6.5b** resulted in the colorless saturated polymer **6.6b**, whose VASE spectrum is shown in Figure 6.4. While the transparency at 193 nm is greatly enhanced (1.28 μm^{-1} to 0.04 μm^{-1}), the improvement at 157 nm is less significant (3.23 μm^{-1} to 2.98 μm^{-1}). Several important conclusions can be made from these results. First, in agreement with theoretical calculations, the ring-opened TCD structure is considerably more absorbing than the norbornene addition structure.[20] Second, while the overall performance of the catalyst is unaffected by the presence of the hexafluorocarbinols, the presence of such acidic species results in entrapment of catalyst or catalyst decomposition products and highly colored polymers. Finally, ROMP-based polymers such as **6.6b** with their extremely high transparency at 193 nm are potentially attractive for use with 193 nm or 193 nm immersion lithography.

Other Approaches Toward High T_g Metathesis-based Structures One of the characteristic problems with ROMP materials is their moderate to low glass transition temperatures (T_g).[21] These are the result of the flexible ethylene linkage formed during hydrogenation of these materials. Traditionally, the solution has been to use higher cyclopentadiene analogs (such as TCD monomers); however, the increase in T_g is roughly independent of the nature of the

additional cyclic structure.[22] In addition, expansion of the hydrocarbon backbone has the additional effect of reducing the solubility of the resulting structure in aqueous developing solutions. Previously, we showed that rigidifying the cyclopentane backbone structure with a bridging unit was sufficient to dramatically increase the resultant ROMP polymer's T_g.[19] However, a more direct approach would be to increase the barriers to rotation around the ethylene bridge via the incorporation of a methyl group on the bridgehead carbon or the olefinic carbon.

The methyl-functionalized norbornene carboxylic acid methyl ester **6.9** was readily synthesized via the Diels-Alder reaction of methyl cyclopentadiene and methyl acrylate. Attempts at ROMP of **6.9** using catalyst **6.2** resulted in no isolable polymer. The use of higher temperatures or the faster initiating catalyst **6.3a** was also unsuccessful. Purification of the monomer via fractional distillation or column chromatography also proved to be ineffective. Monitoring of the reaction by NMR shows initiation of the catalyst and formation of very small amounts of ring-opened material, but no substantial consumption of monomer. This was

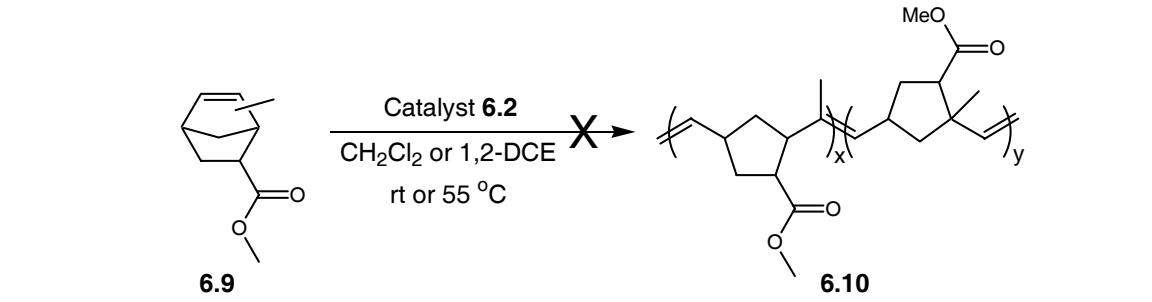

Work by Dr. Emmanuelle Despagnet-Ayoub

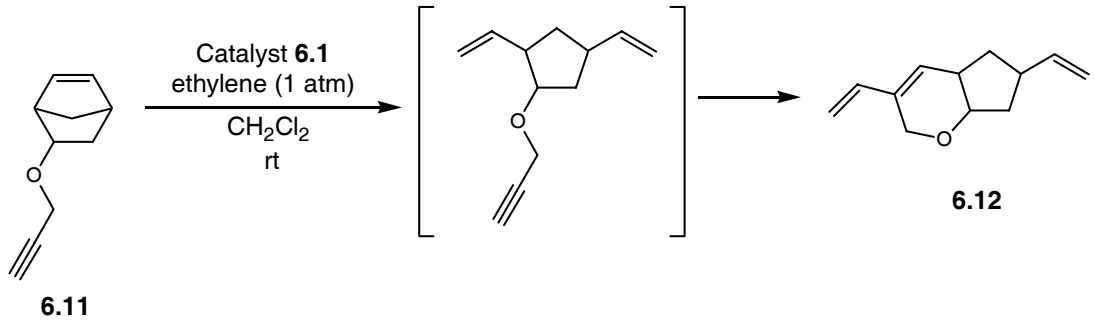

Figure 6.5. Other approaches toward high T_g metathesis structures

unexpected since the ROMP of 1-methyl norbornene with catalyst **6.1** has been reported in the literature.[23] Also, Morgan *et al.* observed the successful ring-opening cross-metathesis of the exo isomer of the dimethyl ester of 1-methyl nadic anhydride, while the endo isomers and the trisubstituted olefin isomers were unreactive but did not decompose the catalyst.[24] Additional work is needed to further elucidate this behavior.

Acyclic diene metathesis (ADMET)[25] polymerization is a potentially useful polymerization methodology since it simplifies the chemical design considerations. Instead of carefully placing steric bulk on an existing norbornene framework, an ADMET approach simply calls for the presence of two terminal olefins on an arbitrary functionalized structure. Given the ability of enyne cascade metathesis reactions to produce polycyclic structures,[26] we imagined the synthesis of an asymmetric polycyclic structure starting from the propargyl ether-functionalized norbornene **6.11**. For use as a lithographic material, polar functional groups could be placed at the 3-position. Following the procedure of North *et al.*,[27] ring-opening metathesis of **6.11** with catalyst **6.1** in the presence of ethylene followed by in-situ ring-closing enyne metathesis upon removal of the ethylene afforded the polycyclic triene **6.12**. Unfortunately, no polymer formation was observed when **6.12** was subjected to ADMET conditions with catalyst **6.**2. Primarily, metathetical dimerization at the terminal olefin was observed while the less reactive terminal dienes were left unreacted. While second generation metathesis catalysts such as **6.2** have been shown to perform cross-metathesis on terminal dienes, the additional sterics imparted by the polycyclic structures are sufficient to prevent the efficient cross-coupling metathesis reactions required for high conversions and significant molecular weight development. Other groups have attempted to design polycyclic structures with pendant allyl ethers suitable for polymerization via ADMET.[28] The lack of polymer formation in these reactions was likely due to the in-situ isomerization of the allyl ether to a crotyl ether capable of reacting with and deactivating the catalyst.[29] These longer tethers would also likely have a more detrimental impact on the T_g than

the polycyclic core would have a positive impact. As a result, ADMET currently seems to be an ineffective approach to produce high T_g materials.

Cross-Metathesis in Resist Material Development The use of olefin cross-metathesis (CM) in the synthesis of monomers suitable for polymerization by conventional means appeared to be a practical way to employ metathesis without concern for glass transition temperatures or the difficult removal of residual metal contamination from hard-to-purify polymeric materials. A number of carboxylic acid ester-functionalized norbornene addition polymers such as **6.7** exhibit substantial swelling problems in aqueous developer solutions.[2b,7] Polyfunctional dissolution inhibitors[30] such as those shown in Figure 6.6 are required to alleviate this swelling behavior. Characteristic of these dissolution inhibitors is the presence of multiple protected hexafluorocarbinol groups. These functionalities are typically synthesized via alkylation of the extremely toxic hexafluoroacetone. With the recent commercial availability of a variety of olefin-functionalized hexafluorocarbinols (such as **6.13** and **6.14**), olefin cross-metathesis could potentially serve as a convenient synthetic methodology for the introduction of hexafluorocarbinols.

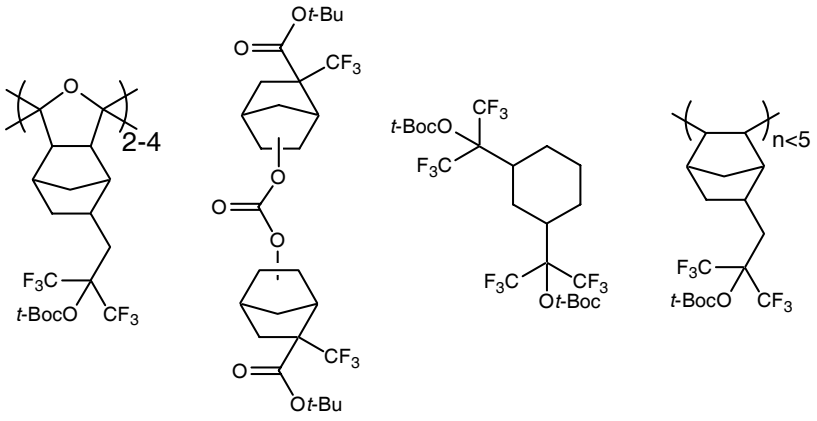

Figure 6.6. Dissolution inhibitors for use at 157 nm

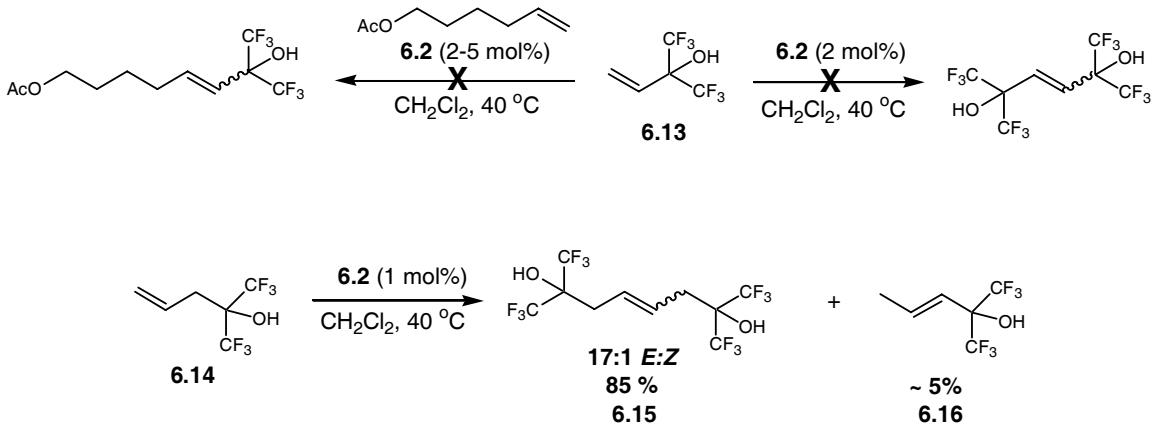

Figure 6.7. Cross-metathesis of hexafluorocarbinol-functionalized olefins

Cross-Metathesis of Hexafluorocarbinol-Functionalized Olefins The allylic hexafluorocarbinol **6.13** does not undergo cross-metathesis with either 5-hexenyl acetate or self-metathesis (Figure 6.7). This is perhaps not surprising given the additional detrimental effects of the increased steric hindrance and reduced electron density on the olefin due to the fluorine substituents in **6.13** to the already low reactivity of the non-fluorinated 1,1-dimethyl-prop-2-ene-1-ol.[31] However, the homoallylic alcohol **6.14**, in which the steric and electronic influences of the trifluoromethyl groups are further removed from the olefin, displays high cross-metathesis activity. High yields of self-metathesis product **6.15** can be obtained with good trans selectivity. The remaining hexafluorocarbinol species were isolated as the starting material and the isomerization product *E*-1,1,1-trifluoro-2-trifluoromethyl-pent-3-ene-2-ol (**6.16**), which is inert to olefin metathesis.

Cursory examination of olefins **6.14** and **6.15** show them to be potential analogues of two commonly used ROMP chain transfer agents: allyl acetate and 1,4-diacetoxy-*cis*-2-butene.[15] While ROMP of TCD monomer **6.4a** afforded a polymer potentially useful at 193 nm, use of olefins **6.14** or **6.15** in the ring-opening cross metathesis (ROCM) of **6.4a** would result in polyfunctional monomeric or oligomeric structures reminiscent of the dissolution inhibitors shown in Figure 6.6. Initial experiments showed that the internal olefin of **6.15** is insufficiently

reactive to compete with ROMP, leading to high molecular weight material. Conversely, the terminal olefin **6.14**, when used in super-stoichiometric amounts, affords good yields of oligomeric ROCM products and dimer **6.15,** which can be separated by column chromatography and recovered.

Development of Difunctional Monomers The homoallylic alcohol **6.14** is primarily used in a Diels-Alder reaction with cyclopentadiene to produce a hexafluorocarbinol-functionalized norbornene.[2e] While 1,2-disubstituted olefins are typically less reactive in Diels-Alder processes, if olefin **6.15** could undergo cycloaddition, perhaps at higher temperatures or pressures, it would constitute a facile route to monomers with multiple hexafluorocarbinol groups. Since dissolution inhibitors presumably act by sequestering ionizable functionalities with intermolecular hydrogen bonds,[30] incorporation of a hydrogen bond acceptor or donor on the same monomer as the solubility switch could allow for an *intra*molecular dissolution inhibition effect, leading to a reduction of swelling behavior and modification of dissolution behavior. A few model polymers are shown in Figure 6.8. Since **6.14** is a good CM substrate, olefin cross-metathesis is an ideal route to the difunctional olefins necessary to synthesize the respective norbornene monomers. As a result of this strategy, both functionalities in the commercial resist **6.7** could be incorporated into a single monomer.

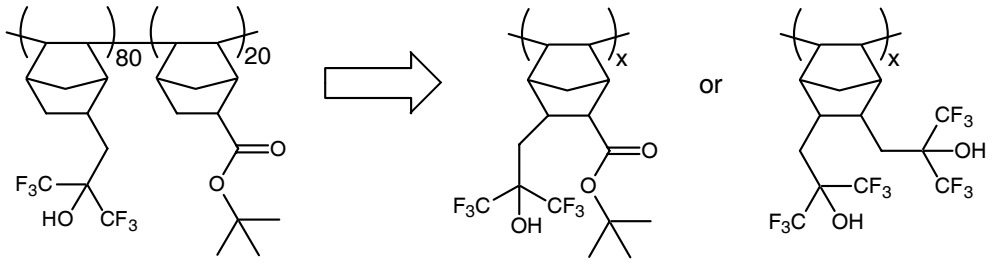

Figure 6.8. Polymers from multifunctional monomers

The Diels-Alder reaction of diol **6.15** with cyclopentadiene was attempted as shown in Figure 6.9. Only very low yields of the di(hexafluorocarbinol)norbornene **6.17** was isolated. The product was contaminated with small amounts of higher cyclopentadiene adducts. Since the internal olefin of **6.15** does not have the steric problems which cause the allylic alcohol **6.13** to be unreactive towards cycloaddition with cyclopentadiene, increasing the dienophilicity of the olefin with an ester-substituent should be sufficient to achieve useful cycloaddition yields. Fortunately, the cross-metathesis of α,β-unsaturated carbonyl compounds such as acrylates with terminal olefins can be performed with high product and stereoselectivity using second-generation catalysts such as **6.2**.[32]

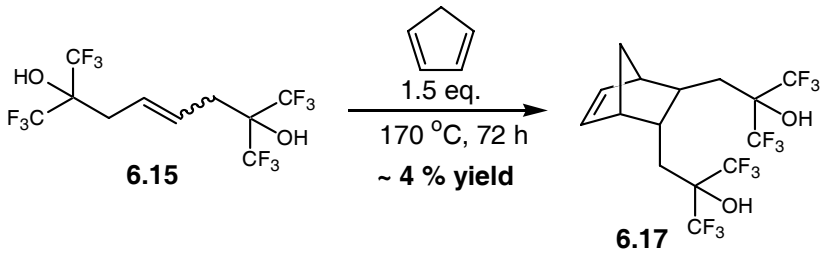

Figure 6.9. Diels-Alder synthesis of difunctional monomer

Cross-metathesis of the homoallylic alcohol **6.15** with methyl acrylate afforded the hexafluorocarbinol-substituted unsaturated ester **6.18** in good yield (Figure 6.10). While cross-metathesis of α,β-unsaturated carbonyl compounds with α-olefins using catalyst **6.2** typically results in product distributions with high trans content (E/Z > 20:1),[31,32] cross-metathesis with **6.14** resulted in an uncharacteristically low E/Z ratio of 2.5:1. Cross-metathesis with *t*-butyl acrylate resulted higher yields of **6.18b** but similar E/Z ratios. Interestingly, the ^{1}H NMR resonance for the alcohol proton was strikingly different between the two isomers, with the Z-isomer being far downfield relative to the E-isomer. The two isomers were readily separable by column chromatography. While these two phenomena would seem to indicate the presence of

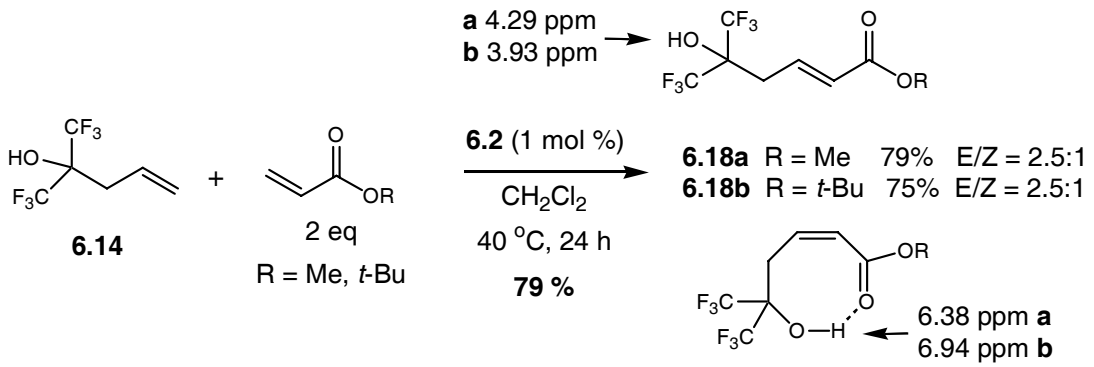

Figure 6.10. Synthesis of substituted crotonates via cross-metathesis

strong intramolecular hydrogen bonding in the Z-isomer, whether this is the root cause of the low E/Z ratio is unclear.

Investigations into Low E/Z Ratios In order to investigate the origin of the low E/Z ratios observed in cross-metathesis of **6.14** with acrylates, a number of fluorinated and non-fluorinated analogues of **6.14** were synthesized and subjected to cross-metathesis conditions with methyl acrylate using **6.2** (Table 6.1). While unprotected 3-pentenyl alcohol underwent facile isomerization to aldehyde products and resulted in poor CM yields, the *t*-butyldimethylsilyl-protected alcohol afforded the 5-(*t*-butyldimethylsilanyloxy)-pent-2-enoic acid methyl ester **6.19** with high E selectivity (Entry 1, Table 6.1). Similarly, CM with the non-fluorinated analogue of **6.14**, 2-methyl-pent-4-en-2-ol **6.20**, afforded the methyl-substituted product **6.21** with high E selectivity. Since isopropyl groups are more isosteric with trifluoromethyl groups,[33] the bis(isopropyl)-functionalized alcohol **6.22** was synthesized and found to again produce cross-product with high E content. Since equally bulky alcohols afford only trans product, steric hindrance by the trifluoromethyl groups in **6.18a** is not preventing secondary metathesis from isomerizing any cis isomers to the more stable trans isomer.

In order to examine the effect of the acidic alcohol, two protected versions of **6.14** were synthesized. Again, the protected alcohols afforded only trans products, although the yield with the *t*-butoxycarbonyl-protected alcohol was extremely low and no self-metathesis dimer of **6.26**

was observed by NMR. These results indicate the presence of the acidic hexafluorocarbinol is responsible for the low stereoselectivity of the reaction. However, it is not known what the dominant interaction is: intermolecular hydrogen bonding between the alcohol and the incoming acrylate during olefin binding and metallacycle formation, interaction between the dissociated basic phosphine and the acidic alcohol, or intramolecular interaction with the catalyst during metathesis.

Table 6.1. Investigation into the E/Z selectivity of cross-metathesis with **6.14**

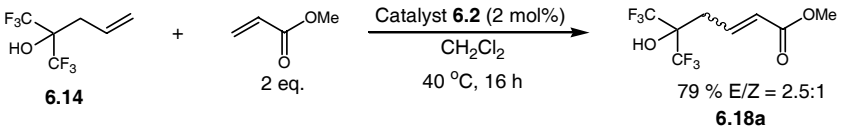

Entry	Substrate	Equiv. MA	Time (h)	Product	Yield (%)	E/Z
1	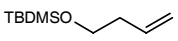	2	20	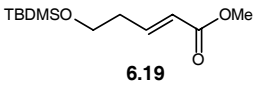 **6.19**	80*	20:1
2	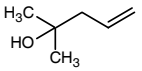 **6.20**	2	18	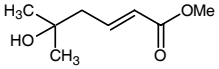 **6.21**	81	> 20:1
3	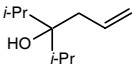 **6.22**	2	16	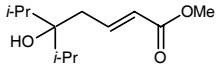 **6.23**	49	> 17:1
4	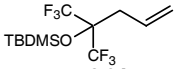 **6.24**	2	16	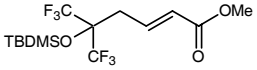 **6.25**	46	> 12:1
5	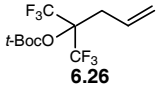 **6.26**	2	16	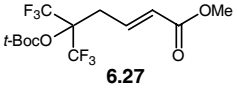 **6.27**	26	> 20:1
6	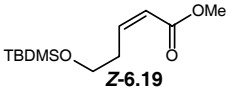 ***Z*-6.19**	1	20	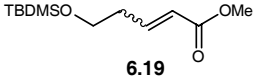 **6.19**		12:1
7	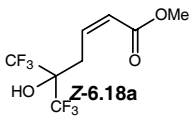 ***Z*-6.18a**	1	16	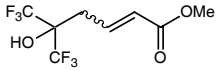 **6.18a**		1.6:1

Yields determined by NMR. *Isolated yield.

Although *E*-crotonates are thermodynamically more stable than *Z*-crotonates, it is not known whether the high trans selectivity in cross-metathesis with acrylates is a result of kinetic or thermodynamic preference. In order to test the ability of *cis*-α,β-unsaturated esters to undergo secondary metathesis-based isomerization to the trans isomer, ***Z*-6.19** was synthesized directly from the unsaturated lactone, 5,6-dihydro-pyran-2-one.[34] Reaction of ***Z*-6.19** directly with catalyst **6.2** resulted predominantly in the 2-bond migration of the double bond to form the more electron-rich silyl enol ether **6.28** (E:Z ~ 1.1). Addition of one equivalent of methyl acrylate relative to substrate reduced this isomerization to negligible levels. The E/Z of the resulting product was 12:1, indicating that the olefins of the α,β-unsaturated carbonyl compounds are able to undergo secondary metathesis albeit with more difficulty than regular aliphatic internal olefins. Resubjection of ***Z*-6.18a** (isolated from a 2.5:1 E/Z mixture by column chromatography) afforded **6.18a** with an E/Z ratio of ~1.6:1, consistent with the results from ***Z*-6.28**. These results support the E/Z ratios obtained in these CM reactions being the thermodynamic distributions with a strong intramolecular hydrogen bond in **6.18** responsible for the lower than expected E/Z ratio.

Prevention of Ruthenium-Catalyzed Olefin Isomerization The isomerization/migration of olefins during olefin metathesis is a side-reaction which lowers reaction yields and results in complex product mixtures which are often difficult to separate.[35] While the exact mechanism(s)[35,36] (metal-based hydride, π-allyl, or other pathways) responsible for this isomerization are unknown, recent results indicate that ruthenium hydride species formed by decomposition of the ruthenium metathesis catalysts can catalyze the migration of olefins under metathesis conditions.[37,38] Currently, to avoid olefin migration during the metathesis reaction, the reactions must be stopped as soon as high conversion is reached as further reaction leads only to product degradation via olefin isomerization.[39] This is a particular problem in the cross-metathesis of products such as insect pheromones where the product olefin will not be hydrogenated and the location of the olefin is critical for activity. The high efficiency of the 2-

bond isomerization of ***Z*-6.19** to the silyl enol ether **6.28** coupled with the extremely diagnostic signals associated with the starting *Z*-vinyl ester and the product *E*-vinyl ester and vinyl ether olefinic protons make this an excellent system for studying the isomerization process. This system is a good mimic of a metathesis reaction which has already reached full conversion while not being complicated by the presence of ruthenium methylidenes. Of particular interest was the reduction of olefin migration observed when an additional equivalent of methyl acrylate was added to the reaction mixture. This provided evidence that simple additives may be sufficient to prevent olefin isomerization in certain systems by either modifying the ruthenium decomposition process or by scavenging ruthenium hydrides before they can initiate isomerization.

The effect of a number of simple additives on the amount of olefin migration of ***Z*-6.19** is shown in Table 6.2. In place of the metathesis active methyl acylate, maleic anhydride was utilized and found to result only in catalyst deactivation. Nolan *et al.* observed that the amount of olefin isomerization is strongly solvent dependent and the addition of small amounts of tricyclohexylphosphine oxide eliminated the formation of isomerized products.[36b] Since less isomerization was observed in slightly acidic solvents such as 1,2-dichloroethane, we decided to examine the effects of acidic additives on the isomerization process. Previously, our group has shown that one of the decomposition pathways leading to hydride formation involves attack by the phosphine. The use of acidic additives was hoped to buffer the reaction and scavenge either the phosphine prior to hydride formation or react directly with any metal hydride directly. Alcohols with pK_as $\geq$ 9 had little effect; however, the more acidic acetic acid afforded excellent yields of ***E*-6.19** without any observable olefin migration. The higher efficiency of cis to trans isomerization using acetic acid in place of methyl acrylate is due to the rate acceleration due to phosphine scavenging and lower stability (i.e. higher decomposition rate) of ruthenium enoic carbenes formed by reaction with methyl acrylate. Morgan *et al.* have employed a large number of acidic and metallic phosphine scavengers and showed that acids with pK_as ~4-5 lead to optimal rate acceleration without decreasing catalyst lifetimes.[24,40] Our results indicate that simple

Table 6.2. Effect of additives on olefin migration

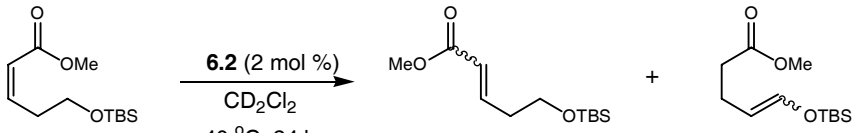

***Z*-6.19** [0.4 M] **6.19** **6.28**

Additive	^{1}H NMR Product Distribution	
None	19 % E/Z = 20:1	81% E/Z ~ 1:2
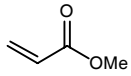	Quant. E/Z = 12:1	0 %
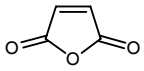	> 95 % E/Z ~ 1:10	0 %
CF_3CH_2OH	11% E/Z > 20:1	89 % E/Z ~ 1:2
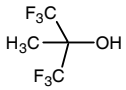	19 % E/Z > 20:1	81 % E/Z ~ 1:2
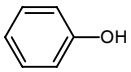	17 % E/Z > 20:1	83 % E/Z ~ 1:2
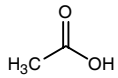	> 95 % E/Z > 20:1	0 %

carboxylic acids such as acetic and benzoic acids would be an ideal reaction additive for certain cross-metathesis reactions with **6.2** to eliminate olefin migration and afford shorter reaction times.

Unfortunately, in a few other cross-metathesis reaction systems, the presence of acetic acid was insufficient to shut down the olefin migration. Whether this failure is due to the additional presence ruthenium methylidene (and its decomposition by-products)[38] or the presence of an alternative isomerization pathway is unknown. However, our results have shown that simple additives can be highly effective at shutting down olefin migration processes, and screening of more effective inhibitors is ongoing.[41]

Synthesis of Difunctional Monomers The Diels-Alder reaction of ***E*-6.18** with cyclopentadiene afforded the difunctional monomer **6.29** in good yield, although the methyl ester

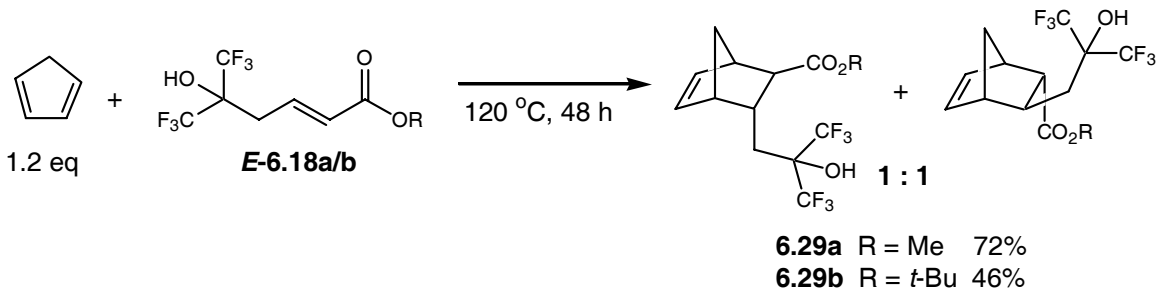

Figure 6.11. Diels-Alder synthesis of difunctional monomers

resulted in higher yields than the *t*-butyl ester. The more facile cycloaddition resulted in the formation of only a small amount (< 5%) of higher cyclopentadiene adducts. Consistent with the Diels-Alder reactions of *trans*-methyl crotonate,[42] no exo/endo selectivity was observed with ***E*-6.18**. ^{1}H NMR spectroscopy of **6.29** showed the presence of two distinct downfield hydroxyl resonances, indicating that the hydroxyl groups are participating in intramolecular hydrogen bonding interactions with the nearby ester groups in the chlorinated NMR solvent.

The *t*-butyl ester serves as an excellent solubility switch with which to observe the deprotection reaction, although virtually any acid-labile ester protecting group could be installed via cross-metathesis with the appropriately protected acrylic acid. Removal of the *t*-butyl protecting group was achieved via heating in the presence of *p*-toluene sulfonic acid to afford the carboxylic acids **6.30** (Figure 6.12). No lactonization was observed by NMR. The *anti*-configuration of the two functionalities and the low nucleophilicity of the tertiary hexafluorocarbinols effectively prevents any undesirable lactonization.

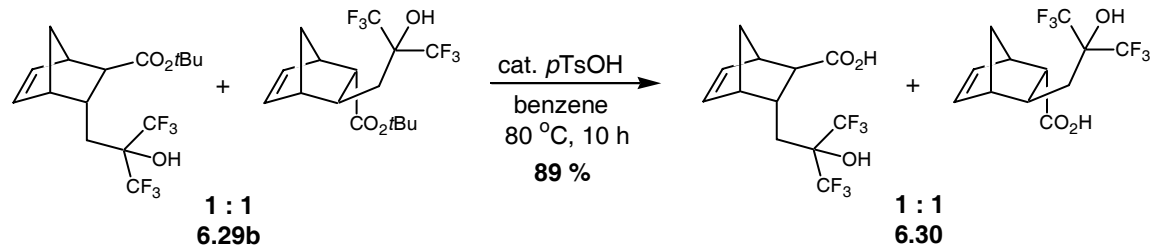

Figure 6.12. Acid-catalyzed deprotection of difunctional monomers

Given the high transparency of the norbornane hexafluorocarbinol **6.31** (1.15 μm^{-1}) relative to the norbornane methyl ester **6.32** (6.02 μm^{-1}), it was unclear just how transparent monomer **6.29** would be since it contains both heavily absorbing and highly transparent groups. Hydrogenation of **6.29a** and **6.29b** over Pd/C afforded clean production of the saturated compounds **6.33a** and **6.33b**, respectively. Their vacuum ultraviolet spectra are shown in Figure 6.13. The saturated difunctional monomers exhibit remarkable transparency at 157 nm. In fact, their absorbance is virtually identical to the mono-hexafluorocarbinol functionalized norbornane **6.31**.

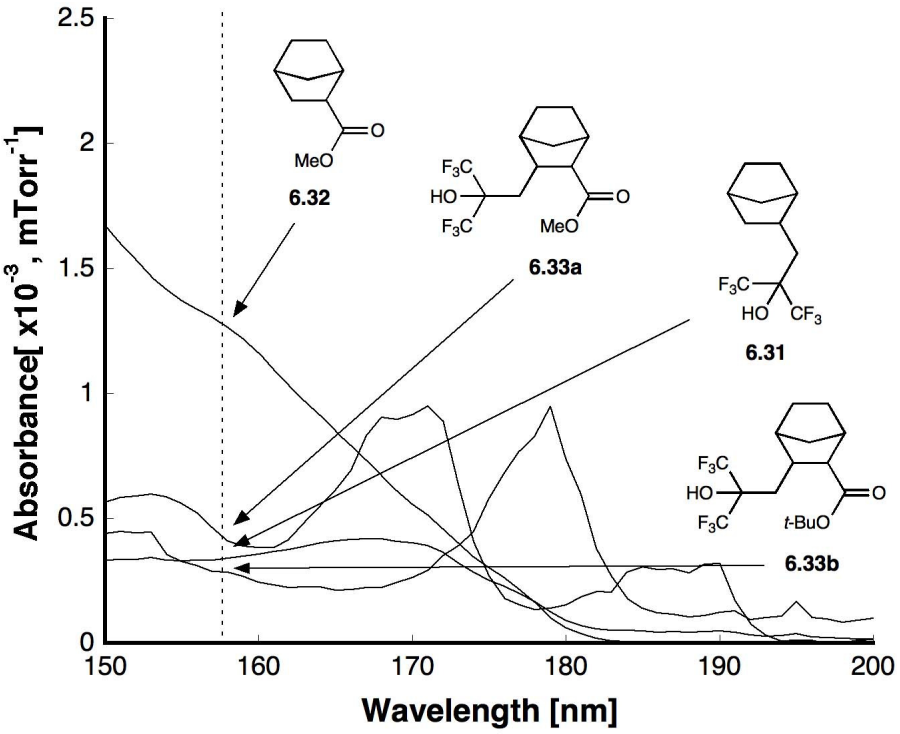

Figure 6.13. Vacuum UV spectra of difunctional norbornanes

While one must not be overzealous in drawing conclusions from this preliminary data, it seems clear that a significant red-shifting of the ester absorption band has occurred, similar to the results obtained via the incorporation of a trifluoromethyl group alpha to the ester group. The most likely explanation for this phenomenon is the intramolecular hydrogen-bonding of the polar

alcohol to the ester group. The magnitude of the red-shifting parallels the downfield shifting of the hexafluorocarbinol proton resonances in the ^{1}H NMR spectra upon proceeding from the methyl ester (δ = 6.17 and 5.42 ppm) to the *t*-butyl ester (δ = 6.77 and 5.96 ppm). For comparison, the hexafluorocarbinol proton appears at 2.78 ppm for the non-ester functionalized norbornene. It may be that the more bulky *t*-butyl ester is favoring a conformation more amenable to hydrogen bonding, thereby influencing the strength of the hydrogen bonding and the transparency. Because the low volatility of these difunctional monomers results in less than ideal gas phase spectra, syntheses of polymeric samples for VASE are being pursued to confirm these exciting results.

The syn versions of **6.29** would be potentially useful for negative tone resists if the lactonization were reasonably facile, or if the equilibrium lay on the side of the ring-opened product, the lactone versions could undergo acid-catalyzed hydrolysis to afford a mass-persistent solubility switch.[43] A ring-closing metathesis route toward the synthesis of the bis(trifluoromethyl)dihydropyranone **6.35** is shown in Figure 6.14. Esterification of the sodium

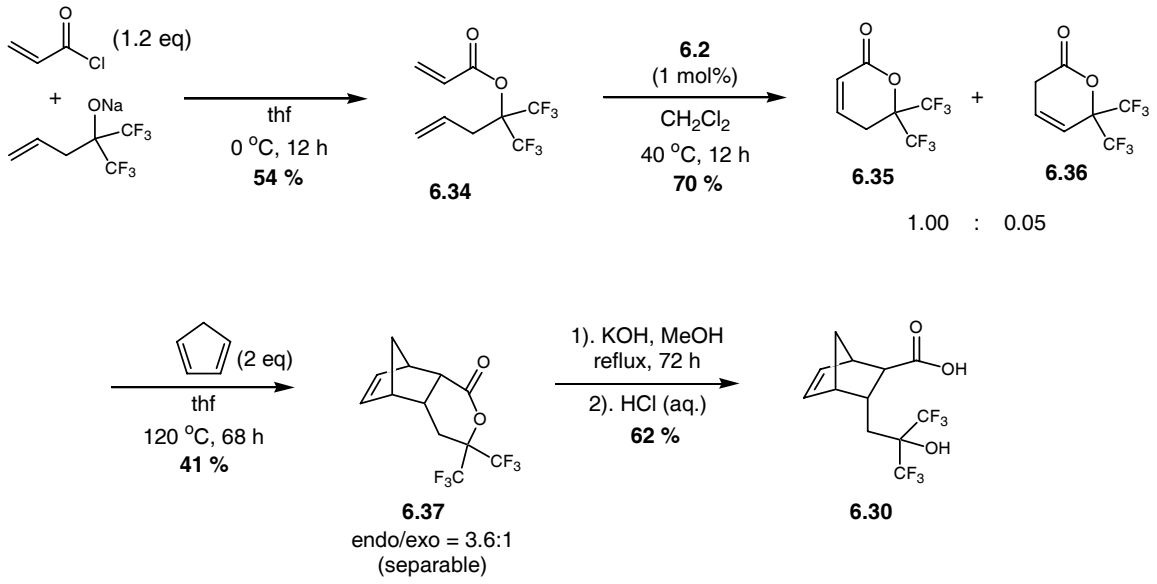

Figure 6.14. Synthesis of lactone-functionalized monomers

salt of **6.14** with acryoyl chloride afforded diene **6.34** in moderate yield. Ring-closing metathesis of **6.34** resulted in good yields of the bis(trifluoromethyl)dihydropyranone **6.35**; however, a small amount of the olefin migration product **6.36** was observed. Hydrolysis of lactone **6.35** with potassium hydroxide and protection of the methyl ester afforded **6.18a** in 47% yield, but only a 1:3 E/Z ratio. Given the loss of product due to isomerization, the unsaturated lactone **6.35** was reacted directly with cyclopentadiene to afford the norbornenyl lactone **6.37**. Although only moderate yields were achieved, it is likely that Lewis acid catalysis would be effective in boosting product yields and endo selectivity.[44] ***Endo*-6.37** was isolated cleanly by column chromatography with no contamination by ***exo*-6.37** or higher cyclopentadiene adducts. Base-catalyzed hydrolysis of ***endo*-6.37** resulted in the production of a single isomer of **6.30** in which the ester has been epimerized to the exo-configuration. Spectroscopic comparison to the isomeric mixture of **6.30** (Figure 6.12) confirmed the identity of the product.

Although these monomers are quite promising, it would be nice to find a route to these monomers which does not involve the relatively expensive ruthenium metathesis catalyst **6.2**. The oxidation of activated allylic carbons (such as in 3,6-dihydro-2H-pyran) to unsaturated lactones by pyridinium chlorochromate has been reported in the literature.[45] The bis-trifluoromethylated version of this dihydropyran is readily obtained via the Diels-Alder reaction of hexafluoroacetone with 1,3-butadiene.[46] With the synthesis of large quantities of **6.38** possible, screening of several oxidation catalysts was performed. Oxidation with pyridinium chlorochromate in a sealed tube afforded a moderate yield of the desired unsaturated lactone **6.35**. Unfortunately, this process was quite lengthy and required several additions of PCC and long reaction times at elevated temperatures.[45] Prolonged reaction at higher temperatures lead to two deleterious side reactions: the retro-Diels-Alder reaction of **6.38** and the 1,3-allylic rearrangement of the initial chromate adduct to form the dihydropyranone **6.39**.

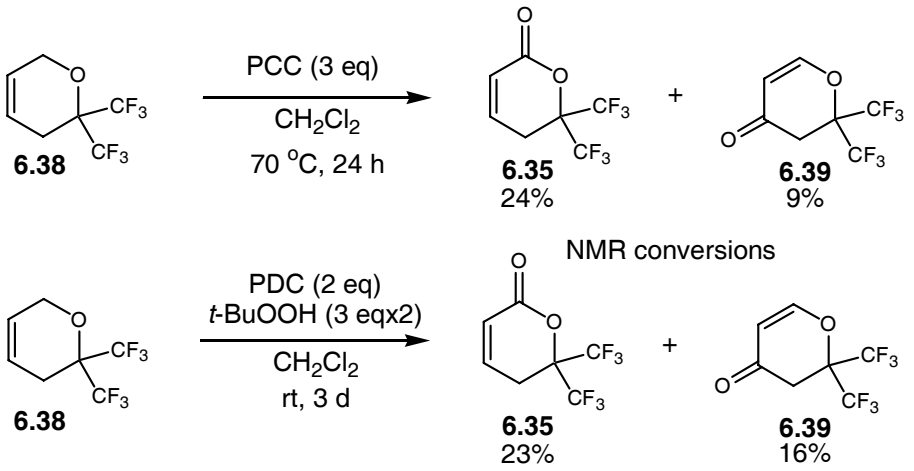

Figure 6.15. Alternative syntheses of fluorinated unsaturated lactones

Screening of several reaction conditions was unable to improve product yields. An alternative oxidant, selenium dioxide, was unreactive towards allylic oxidation of this substrate. However, the oxidation of 3,4-dihydro-2H-pyran with pyridinium dichromate/*t*-butyl hydroperoxide has been reported to produce the identical unsaturated lactone structures.[47] Subjection of **6.38** to these oxidation conditions afforded similar results to the PCC oxidations, albeit with slightly higher yields of the non-desired product **6.39**. Unfortunately, it seems the detrimental electron-withdrawing effects of the trifluoromethyl groups prevent the allylic position from being sufficiently activated towards oxidation. The resulting slow oxidation process allows for isomerization of the initial chromate oxidized species leading to a mixture of products.

Conclusions

Well-defined ruthenium olefin metathesis catalysts display the high reactivity and functional group tolerance required for the synthesis of new monomers and materials for deep ultraviolet lithography. Ring-opening metathesis polymerization of hexafluorocarbinol-functionalized tetracyclododecene monomers affords polymers which, after hydrogenation, are highly transparent at 193 nm, provided the acidic alcohol is protected prior to polymerization.

However, these same ROMP polymers continue to exhibit inherently high absorbance (~3.0 μm^{-1}) at 157 nm despite our best efforts. Alternative metathesis-based approaches to the synthesis of high T_g structures via ROMP of methyl-substituted norbornenes and ADMET of polycyclic structures were unsuccessful.

Ruthenium-catalyzed cross-metathesis can efficiently introduce hexafluorocarbinol groups onto a variety of olefin-containing substrates using readily available hexafluorocarbinol-functionalized olefins. The cross-metathesis approach serves as a mild and convenient route to products which would ordinarily be synthesized via alkylation of highly toxic hexafluoroacetone. Cross-metathesis of homoallylic hexafluorocarbinols with acrylates affords cross-products which exhibit uncharacteristically low E/Z ratios. The presence of the acidic alcohol is the key to the production of higher amounts of cis olefin in this system. *Cis*-α,β-unsaturated carbonyl compounds are subject to secondary metathesis-based isomerization to their trans isomers; however, olefin migration to form more electron-rich olefins was observed in certain instances. The addition of acetic acid to the reaction solution resulted in higher catalyst reactivity while eliminating olefin migration. Work is continuing in this area to further understand the nature of olefin migration and find more effective additives which can eliminate this migration in a general manner. An example of the benefits of the cross-metathesis approach to introduction of hexafluorocarbinol groups is the 2-step synthesis of norbornene monomers with both ester and hexafluorocarbinol functionalities. Gas-phase ultraviolet spectroscopy reveals that these difunctional norbornane structures have extraordinarily high transparency at 157 nm. Alternatively, ring-closing metathesis can be employed to synthesize unsaturated, trifluoromethylated lactones suitable for production of the same class of difunctional norbornenes. Work is continuing towards the polymerization of these structures in order to confirm their high transparency and examine their dissolution properties.

Experimental

Materials: All air sensitive manipulations and polymerizations were carried out in an N_2-filled drybox or using standard Schlenk techniques. All solvents were rigorously degassed in 18 L reservoirs and passed through two sequential purification columns consisting of activated alumina.[48] All starting materials were procured from Aldrich except 1,1,1-trifluoro-2-(trifluoromethyl)-pent-4-ene-2-ol (Oakwood), hexafluoroacetone (Oakwood), or unless otherwise mentioned. Compounds **6.4a**, **6.13**, **6.32**, and **6.31** and polymer **6.8** were generously donated or synthesized by the Willson Lab at the University of Texas, Austin. Photoresist **6.7** was generously donated by Ralph Dammel of AZ-Clariant. The norbornenyl propargyl ether **6.11** and the bicyclic triene **6.12** were synthesized by Dr. Emmanuelle Despagnet-Ayoub. Ruthenium olefin metathesis catalysts **6.1** and **6.2** were obtained from Materia, Inc. Catalysts **6.3a** and **6.3b** were synthesized according to the literature.[49] All liquid reagents used for vacuum UV measurements were distilled from appropriate drying agents, thoroughly degassed by freeze, pump, thaw cycles and sealed in glass ampoules under vacuum.

Methods: Nuclear magnetic resonance (NMR) spectra were obtained using a Varian *Mercury 300* spectrometer (^{1}H: 300 MHz, ^{13}C: 75 MHz, ^{19}F: 282 MHz). Shifts for NMR spectra are reported in ppm relative to TMS (for ^{19}F, internal C_6F_6 (~ 0.5 %) at -162.2 ppm) or to the chemical shift of the residual proteo solvent. Molecular weights (M_n) and polydispersity indices (PDI) were measured from THF solutions by size exclusion chromatography (SEC) using a GPC apparatus equipped with two PLgel 5 μm mixed-C columns (Polymer Labs) connected in series with a DAWN EOS multi-angle laser light scattering (MALLS) detector and an Optilab DSP digital refractometer (both from Wyatt Technology). All molecular weight values are given relative to polystyrene standards. When no calibration standards were used, *dn/dc* values were obtained for each injection by assuming 100% mass elution from the columns. All reported molecular weights are relative to polystyrene standards. Differential scanning calorimetry (DSC) measurements was performed on either a Perkin Elmer *Series-7* or *Pyris* thermal analysis system.

Vacuum UV Spectroscopy: Gas phase VUV measurements were made on an Acton *CAMS-507* spectrophotometer fitted with a custom-made gas cell attachment. The details of the cell design and implementation have been described previously.[1c] All liquid compounds for vacuum UV measurements were distilled from appropriate drying agents, thoroughly degassed by freeze, pump, thaw cycles and sealed in glass ampoules under vacuum.

Synthesis: **8-(1,1,1,3,3,3-Hexafluoro-2-t-butyldimethylsilanyloxy-propyl)-tetracyclo[4.4.0^{1,6}.1^{2,5}.1^{7,10}]dodec-3-ene (6.4b).** To a flame-dried 100 mL 2-neck flask was added sodium hydride (153 mg, 6.35 mmol, 1.1 eq.). 70 mL of dry degassed tetrahydrofuran was added via cannula. To the stirring suspension was added hexafluorocarbinol **6.4a** (2.0 g, 5.78 mmol, 1.0 eq.) slowly via syringe. After the evolution of gas had ceased (~ 5 minutes) the solution was stirred for 40 minutes at room temperature. A solution of di-*t*-butyl dicarbonate (1.39 g, 6.35 mmol, 1.1 eq.) in 5 mL of tetrahydrofuran was transferred to the reaction flask. The reaction immediately turned cloudy and was allowed to stir overnight. The reaction was then diluted with water and extracted into 250 mL of ether. The organic layer was washed with water until the washings were neutral. The organic layer was then washed with brine and dried over sodium sulfate. The ether was removed *in vacuo* to afford 1.88 g (73 %) of **6.4b** as a colorless liquid. R_f = 0.64 (20:1 hexane:ethyl acetate). Data tabulated for major isomer only: ^{1}H NMR ($CDCl_3$, 300 MHz, ppm): δ 6.05-5.95 (m, 2H), 2.85 (m, 2H), 2.3-2.2 (m, 2H), 2.03 (unresolved m, 2H), 1.52 (s, 9H), 1.4-1.2 (m, 4H), 0.64 (d, *J* = 10.5 Hz, 1H), 0.59 (dm, *J* = 10.8 Hz, 1H). ^{13}C NMR ($CDCl_3$, 75 MHz, ppm): δ 149.23, 136.19, 135.94, 84.80, 53.22, 49.27, 47.22, 46.87, 43.59, 41.34, 340.69, 9.48, 35.67, 35.20, 31.46, 29.57, 27.73. ^{19}F NMR ($CDCl_3$, 282 MHz, ppm): δ -71.9 - -72.3 (m, 6F).

General Ring-Opening Metathesis Polymerization Procedure: To a 20 mL vial with Teflon stirbar and teflon-coated septa cap was added the ruthenium catalyst. The vial was purged with argon and degassed, anhydrous dichloromethane or 1,2-dichloroethane was injected. Upon

dissolution of the catalyst, a solution of monomer was injected and allowed to stir at room temperature. The reaction was quenched by the addition of more than 50 equivalents (relative to catalyst) of ethyl vinyl ether and allowed to stir at room temperature for 1 hour. The solvent was removed *in vacuo* and the crude polymer dissolved in a minimal amount of ethyl acetate. The polymer was precipitated into methanol, centrifuged, and rinsed with methanol. After 2-3 precipitation cycles, the colorless polymer was dried under vacuum (10 mTorr) to afford a white polymeric solid.

Polymer 6.5a. 6.4b (3.0 g, 8.84 mmol, 1 eq.) was polymerized using catalyst **6.3a** (4.0 mg, 0.0047 mmol, [M]/[C] = 1875) using the general procedure detailed above with *trans*-3-hexene (24.7 mg, 0.29 mmol, [M]/[CTA] = 30:1) as a chain transfer agent. After 12 hours, the reaction was quenched accordingly and the ruthenium was attempted to be removed via exchange with a water-soluble phosphine (See reference 18). However, the polymer could only be filtered through a plug of silica using methanol, resulting in the loss of significant amounts of material and little reduction in coloration. Yield: 1.70 g (57%). ^{1}H NMR ($CDCl_3$, 300 MHz, ppm): δ 6.04 (s, 0.5 H), 5.50 (m, 2H), 3.6-2.6 (m, 5H), 2.6-0.5 (m, 10H). ^{19}F NMR ($CDCl_3$, 282 MHz, ppm): δ -76.0 - -79.8 (m, 6F). DSC: T_g = ~115 °C. SEC (GPC): M_n = 147.8 kDa. PDI = 2.1.

Polymer 6.5b. 6.4b (1.88g, 4.21 mmol, 1 eq.) was polymerized using catalyst **6.3b** (29.7 mg, 0.042 mmol, 0.01 eq.) using the general procedure detailed above without the use of a chain transfer agent. After 12 hours, the reaction was quenched accordingly and the solution concentrated, taken up in a minimal quantity of ethyl acetate and precipitated into methanol. The polymer was dried under high vacuum overnight to afford 1.59 g (85 %) of polymer **6.5b.** ^{1}H NMR ($CDCl_3$, 300 MHz, ppm): δ 5.6-5.4 (br s, 2H), 3.2-0.8 (15 H), 1.53 (s, 9H). ^{19}F NMR ($CDCl_3$, 282 MHz, ppm): δ -72.55 (s, 3F), -72.76 (s, 3F). SEC (GPC): M_n = 36.3 kDa. PDI = 1.18. DSC: T_g = 83 °C.

General Hydrogenation Procedure for Ring-Opening Metathesis Polymers: In a flame-dried, 100 mL 2-neck round bottom flask equipped with a Teflon stirbar and reflux condenser, *p*-tosylhydrazide (5 eq. per olefin eq.) was added. ROMP polymer dissolved in 25 mL xylenes was added, followed by tri-*n*-propylamine (7 eq. per olefin eq.). The mixture was degassed via 3 freeze-pump-thaw cycles. The reaction was heated to 130 °C under argon at which point gas evolution began. After 4 hours, a second portion of *p*-tosylhydrazide was added and the reaction was allowed to stir for 6 hours. Upon completion, the reaction was cooled to room temperature, taken up in ethyl acetate, washed with 0.1 N HCl solution, $NaHCO_3$ solution, and brine. The organic layer was dried over sodium sulfate, filtered, and concentrated. Repeated precipitation into methanol, centrifugation, and washing with methanol produced colorless polymer which was dried overnight to produce a white polymeric solid.

Polymer 6.6a. Polymer **6.5a** was hydrogenated using the general procedure detailed above by Brian Osborn (Wilson Group, University of Texas, Austin). DSC: T_g = 85 °C. SEC (GPC): M_n = 147.8 kDa. PDI = 2.01. $\alpha_{10}^{157nm} = 3.23\ \mu m^{-1}$. $\alpha_{10}^{193nm} = 1.28\ \mu m^{-1}$. $\alpha_{10}^{248nm} = 0.19\ \mu m^{-1}$.

Polymer 6.6b. Polymer **6.5b** (1.1g, 2.46 mmol, 1 eq.) was hydrogenated using the general procedure detailed above without the use of a chain transfer agent. After the standard workup, the polymer was evacuated to dryness, taken up in acetone and precipitated into hexanes. Upon stripping of the solvent, the polymer emerges as a white colorless polymer. The resultant polymer was submitted to dialysis conditions using a 500 molecular weight cut-off dialysis tube (Spectra/Por DispoDialyzer) in methanol for 24 hours, changing the solvent bath every 6 hours. The resulting methanol solution was evacuated to dryness and the polymer washed with hexanes. The polymer was transferred to a vial containing hexanes using acetone and then evacuated to dryness. The colorless tacky polymer was dried under high vacuum overnight to afford 0.59 g (53 %) of polymer **6.6b.** ^{1}H NMR ($CDCl_3$, 300 MHz, ppm): δ 3.1-2.8 (m), 2.4-0.6 (m). ^{19}F NMR

($CDCl_3$, 282 MHz, ppm): δ -76.2 - -78.6 (m, 6F). DSC: T_g = 83 °C. SEC (GPC): M_n = 46.1 kDa. PDI = 1.22. α_{10}^{157nm} = 2.98 μm^{-1}. α_{10}^{193nm} = 0.04 μm^{-1}. α_{10}^{248nm} = 0.02 μm^{-1}.

1/6-Methyl-bicyclo[2.2.1]hept-5-ene-2-carboxylic acid methyl ester (6.9). To a flame-dried, nitrogen cooled, 500 mL round bottom flask with dropping funnel and reflux condenser were added: 4-*t*-butyl catechol (0.20g, 1.3 mmol, 0.003 eq.) and methyl acrylate (35 mL, 387 mmol, 1 eq.). The addition funnel was charged with freshly cracked methyl cyclopentadiene (33 mL). The reaction was heated to 50 °C and the methyl cyclopentadiene added dropwise over 15 minutes. The reaction temperature was raised to 80 °C and heated for 2.5 hours. The reaction mixture was distilled under reduced pressure (water aspirator) with the main fraction being collected at 130 °C. 7.4 g of the distilled product was purified by column chromatography (95:5 hexane/ethyl acetate) to afford 7.12 g of **6.9** as a colorless liquid. R_f = 0.38 (95:5 hexane/ethyl acetate). 7 isomers observed by gc/ms. GC/MS: *m/z* = 166. Composition (in order of increased retention time). 0.6%:11.4%:21.8%:6.2%:29.2%:19.2%:11.7% Spectra agree with those of Mellor *et al*. *JCS Perkin Trans. II* **1974**, 26-31.

1,1,1,8,8,8-Hexafluoro-2,7-bis-trifluoromethyl-oct-4-ene-2,7-diol (6.15). Hexafluorocarbinol **6.14** (3.0 g, 14.4 mmol, 1 eq.) was added to a flame-dried 50 mL 2-neck, round bottom flask with a reflux condenser containing catalyst **6.2** (122 mg, 0.144 mmol, 0.01 eq.) in 30 mL of dry, degassed CH_2Cl_2. The reaction was heated at 40 °C with a slow nitrogen sparge for 24 hours. The reaction was concentrated and purified via silica gel column chromatography (90:10 hexane:ethyl acetate to 1:1 hexane:ethyl acetate) to afford 2.36 g (85%) of **6.15** as a water white liquid. R_f = 0.10 (90:10 hexane/ethyl acetate). E/Z = 17:1. ^{1}H NMR ($CDCl_3$, 300 MHz, ppm): δ 5.75 (t, 2H), 4.29 (br s, 2H), 2.76 (d, *J* = 5.1 Hz, 4H). ^{13}C NMR ($CDCl_3$, 75 MHz, ppm): δ 128.15, 123.10 (q, *J* = 288 Hz), 75.52 (m), 33.63. ^{19}F NMR ($CDCl_3$, 282 MHz, ppm): δ -76.97 (s, *E*), -77.15 (s, *Z*). HRMS-[GC-EI+] (m/z): [M•]+ calc'd for $C_{10}H_8F_{12}O_2$, 388.0332; found, 388.0341.

***E*-1,1,1-Trifluoro-2-trifluoromethyl-pent-3-en-2-ol (6.16).** ^{1}H NMR ($CDCl_3$, 300 MHz, ppm): δ 6.3-6.4(m, 1H), 5.60 (d, *J* = 15.9 Hz, 1H), 1.86 (dd, *J* = 1.5, 7.2 Hz, 3H). ^{19}F NMR ($CDCl_3$, 282 MHz, ppm): δ -78.10 (s).

1,1,1,3,3,3-Hexafluoro-2-[3-(3,3,3-trifluoro-2-hydroxy-2-trifluoromethyl-propyl)-bicyclo[2.2.1]hept-5-en-2-ylmethyl]-propan-2-ol (6.17). To a 20 mL thick-walled Schlenk tube were added freshly cracked cyclopentadiene (0.31 g, 4.69 mmol, 1.4 eq.). **6.15** (1.3 g, 3.35 mmol, 1 eq.), α,α,α-trifluorotoluene (2 mL), and hydroquinone (10 mg). The reaction mixture was degassed by 3 freeze-pump-thaw cycles and the vessel sealed under argon. The reaction was heated at 130 °C for 72 hours and cooled to room temperature. The reaction mixture was separated via silica gel column chromatography (80:20 hexane:ethyl acetate) to afford **6.17** (~ 4%) (R_f = 0.63, 70:30 hexane:ethyl acetate) with the recovery of 1.19 g (36%) of **6.15**. The product **6.17** coeluted with ~ 0.25 eq. of **6.15** and 0.60 eq. of the tetracyclododecene biscarbinol. **6.17.** ^{1}H NMR ($CDCl_3$, 300 MHz, ppm): δ 6.27 (dd, *J* = 2.7, 5.7 Hz, 1H), 6.08 (dd, *J* = 3.0, 5.7 Hz, 1H), 2.87 (s, 1H), 2.75 (s, 1H), 2.66 (s, 1H), 2.5-1.0 (7H). ^{19}F NMR ($CDCl_3$, 282 MHz, ppm): δ -75.82 (q, 3F), -76.31 (s, 3F), -78.28 (q, 3F), -78.44 (s, 3F). GC/MS: *m/z* = 453 [M-H], 435 [$M–H_2O$], 66 [cyclopentadiene].

6,6,6-Trifluoro-5-hydroxy-5-trifluoromethyl-hex-2-enoic acid methyl ester (6.18a). Hexafluorocarbinol **6.14** (2.0g, 9.6 mmol, 1 eq.) and methyl acrylate (1.73 mL, 19.2 mmol, 2 eq.) were added to a flame-dried 50 mL 2-neck, round bottom flask with a reflux condenser containing catalyst **6.2** (163mg, 0.192 mmol, 0.02 eq.) in 15 mL of dry, degassed CH_2Cl_2. The reaction was heated at 40 °C with a slow nitrogen sparge for 20 hours. The reaction was concentrated and purified via silica gel column chromatography (20:1 hexane:ethyl acetate to 85:15 hexane:ethyl acetate). Two fractions were collected: Fraction A (R_f = 0.29): 0.57 g (22%) of ***Z*-6.18a**. Fraction B (R_f = 0.19): 1.75 g of a 1:0.12 mix of ***E*-6.18a**:**6.15**.

***E*-6.18a.** ^{1}H NMR ($CDCl_3$, 300 MHz, ppm): δ 7.02 (dd, *J* = 7.8, 15.3 Hz, 1H), 6.01 (dd, *J* = 1.2, 15.9 Hz, 1H), 4.29 (br s, 1H), 3.76 (s, 3H), 2.86 (d, *J* = 7.8 Hz, 2H). ^{13}C NMR ($CDCl_3$, 75 MHz, ppm): δ 166.73, 139.05, 125.96, 52.29, 33.34. ^{19}F NMR ($CDCl_3$, 282 MHz, ppm): δ -77.01 (s).

***Z*-6.18a.** ^{1}H NMR ($CDCl_3$, 300 MHz, ppm): δ 6.38 (s, 2H), 6.35 (m, 1H), 6.22 (d, *J* = 11.4 Hz, 1H), 3.82 (s, 3H), 3.11 (d, *J* = 8.1 Hz, 2H). ^{13}C NMR ($CDCl_3$, 75 MHz, ppm): δ 169.36, 139.39, 125.69, 53.01, 29.41. ^{19}F NMR ($CDCl_3$, 282 MHz, ppm): δ -77.27 (s). HRMS-[EI+] (m/z): [M•]+ calc'd for $C_8H_8F_6O_3$, 266.0378; found, 266.0376.

6,6,6-Trifluoro-5-hydroxy-5-trifluoromethyl-hex-2-enoic acid *t*-butyl ester (6.18b).

Hexafluorocarbinol **6.14** (2.0g, 9.6 mmol, 1 eq.) and *t*-butyl acrylate (1.70 mL, 11.5 mmol, 1.2 eq.) were added to a flame-dried 50 mL 2-neck, round bottom flask with a reflux condenser containing catalyst **6.2** (81.6 mg, 0.096 mmol, 0.01 eq.) in 10 mL of dry, degassed CH_2Cl_2. The reaction was heated at 40 °C with a slow nitrogen sparge for 30 hours. The reaction was concentrated and purified via silica gel column chromatography (20:1 pentane:ether ramping to 85:15 pentane ether). Crude NMR indicated E/Z = 3.1:1 and 80% conversion. When the reaction was performed with 2 eq. of *t*-butyl acrylate the E/Z ratio was 2.5:1 at 75% conversion. Two fractions were collected: Fraction A (R_f = 0.42): 0.47 g (11%) of ***Z*-6.18b:6.15** (1:0.07). Fraction B (R_f = 0.2, 0.15): 1.75 g (64%) of ***E*-6.18b**.

***E*-6.18b.** ^{1}H NMR ($CDCl_3$, 300 MHz, ppm): δ 6.94 (dt, *J* = 7.5, 15.0 Hz, 1H), 5.94 (dt, *J* = 1.5, 14.1 Hz, 1H), 3.93 (s, 1H), 2.82 (d, *J* = 7.2 Hz, 2H), 1.49 (s, 9H). ^{13}C NMR ($CDCl_3$, 75 MHz, ppm): δ 166.03, 137.97, 127.83, 81.83, 33.00, 28.21. ^{19}F NMR ($CDCl_3$, 282 MHz, ppm): δ -76.73 (s). HRMS-[FAB+] (m/z): [M•]+ calc'd for $C_{11}H_{15}F_6O_3$, 309.0925; found, 309.0925.

***Z*-6.18b.** ^{1}H NMR ($CDCl_3$, 300 MHz, ppm): δ 6.94 (s, 1H), 6.21 (m, 1H), 6.14 (d, *J* = 11.4 Hz, 1H), 3.05 (d, *J* = 7.8 Hz, 2H), 1.51 (s, 9H). ^{19}F NMR ($CDCl_3$, 282 MHz, ppm): δ -77.24 (s).

General Procedure for E/Z Selectivity Studies: In a nitrogen filled drybox, catalyst **6.2** (5.2 mg, 0.0061 mmol, 0.02 eq.) was added to a screw-cap NMR tube along with 1 mL dry CD_2Cl_2. On

the benchtop, the unsaturated carbinol was added (0.31 mmol, 1 eq.) via syringe followed by methyl acrylate (55 μL, 0.61 mmol, 2 eq.). The NMR tube was heated on an oil bath at 40 °C for 16 hours. The product distribution was determined by NMR analysis of the olefin and allylic proton resonances.

5-(*t*-Butyldimethylsilanyloxy)-pent-2-enoic acid methyl ester (6.19). After 16 hours of reaction, silica gel chromatography afforded 80% isolated yield of **6.19** (E/Z > 20:1). Also isolated 10% yield 5-(t-butyldimethylsilanyloxy)-pent-4-enoic acid methyl ester (**6.28**) (E/Z = 1.00:1.03).

***E*-6.19.** ^{1}H NMR ($CDCl_3$, 300 MHz, ppm): δ 6.97 (dt, *J* = 7.2, 15.6 Hz, 1H), 5.88 (dt, *J* = 1.5, 15.6 Hz, 1H), 3.73 (s, 3H), 3.72 (t, *J* = 6.6 Hz, 2 H), 2.42(ddt, *J* = 1.5, 6.3 Hz, 7.2 Hz, 2H), 0.90 (s, 9H), 0.06 (s, 6H). ^{13}C NMR ($CDCl_3$, 75 MHz, ppm): δ 167.13, 146.43, 122.71, 61.74, 51.62, 35.94, 26.09, 18.50, -5.13. HRMS-[GC-EI+] (m/z): [M-H]+ calc'd for $C_{12}H_{23}O_3Si$, 243.1417; found, 243.1407.

6.28. ^{1}H NMR ($CDCl_3$, 300 MHz, ppm): δ 6.29 (dm, *J* = 12.0 Hz, 1H, *E*), 6.20(dt, *J* = 5.7 Hz, 1H, *Z*), 4.97 (dt, *J* = 7.5,12.0 Hz, 1H, *E*), 4.46(dt, *J* = 6.0, 6.0 Hz, 1H, *Z*), 3.67 (s, 3H, *E*), 3.66 (s, 3H, *Z*), 2.45-2.35 (m, 2H, *E*), 2.3-2.2 (m, 2H, *Z*), 0.93 (s, 9H, *E*), 0.91 (s, 9H, *Z*), 0.12 (s, 12H, *E/Z*). ^{13}C NMR ($CDCl_3$, 75 MHz, ppm): δ 174.16, 173.77, 141.61, 139.84, 109.51, 108.31, 51.67, 35.35, 34.35, 25.89, 25.83, 23.29, 19.62, 18.54, 18.48, -5.47, -5.59. HRMS-[GC-EI+] (m/z): [M•]+ calc'd for $C_{12}H_{24}O_3Si$, 244.1495; found, 244.1482.

2-Methyl-pent-4-en-2-ol (6.20). To a flame-dried 3 neck flask with stirbar was added 35 mL of 1M allyl magnesium bromide solution (in diethyl ether) (35 mmol, 1.2 eq.). The solution was cooled to 0 °C and dry acetone (2.13 mL, 1.68g) was added dropwise over 5 minutes. The reaction was allowed to warm to room temperature and stir for 7 hours. The reaction was then cooled to 0 °C and quenched with saturated ammonium chloride solution. The aqueous layer was extracted 3 times with ether. The organic layers were combined and washed with sodium

bicarbonate solution and brine. After drying over sodium sulfate, the solution was concentrated and purified directly by silica gel chromatography (3:2 pentane:ether) to afford 0.97g (26%) of **6.20** as a colorless liquid. R_f = 0.43 (70:30 ethyl acetate /hexane). ^{1}H NMR ($CDCl_3$, 300 MHz, ppm): 5.88 (ddt, J = 7.2, 9.9, 17.1 Hz, 1H), 5.2-5.1 (m, 2H), 2.27 (d, *J* = 7.5 Hz, 2 H), 1.52 (s, 1H), 1.23 (s, 6H). ^{13}C NMR ($CDCl_3$, 75 MHz, ppm): δ 134.42, 118.86, 70.52, 48.38, 29.27. HRMS-[GC-EI+] (m/z): [M•]+ calc'd for $C_6H_{12}O$, 100.0888; found, 100.0896.

5-Hydroxy-5-methyl-hex-2-enoic acid methyl ester (6.21). The product distribution after 16 hrs: 1.00 **6.21** (> 20:1 E/Z), 1.14 methyl acrylate, 0.72 **6.20**, 0.17 homodimer of **6.20**. *E*-isomer: ^{1}H NMR (CD_2Cl_2, 300 MHz, ppm): δ 7.01 (dt, *J* = 7.8, 15.6 Hz, 1H), 5.88 (dt, *J* = 1.5, 15.6 Hz, 1H), 3.71 (s, 3H), 2.37(dd, *J* = 1.5, 7.8 Hz, 2H). ^{13}C NMR (CD_2Cl_2, 75 MHz, ppm): δ 167.10, 145.74, 124.29, 70.94, 51.83, 46.89, 30.12, 29.76. HRMS-[GC-CI] (m/z): [M+H]+ calc'd for $C_8H_{15}O_3$, 159.1021; found, 159.1021.

3-Isopropyl-2-methyl-hex-5-en-3-ol (6.22). Compound **6.22** was prepared via the procedure of Masuyama *et al.*[50] The product was purified by silica gel chromatography (3:2 pentane:ether) to afford 4.77 g of a mixture of 1:0.33 **6.22**:diisopropyl ketone corresponding to 56 % yield. No further purification attempts were made. R_f = 0.21 (20:1 Hexane /ethyl acetate). ^{1}H NMR ($CDCl_3$, 300 MHz, ppm): δ 5.88 (m, 1H), 5.2-5.0 (m, 2H), 2.32 (dm, *J* = 7.5 Hz, 2H), 1.93 (m, 2H), 0.96 (t, *J* = 7.2 Hz, 12H). ^{13}C NMR ($CDCl_3$, 75 MHz, ppm): δ 135.32, 117.88, 76.98, 38.51, 34.40, 17.76, 17.52. HRMS-[GC-EI+] (m/z): [M-H]+ calc'd for $C_{10}H_{19}O$, 155.1436; found, 155.1435.

5-Hydroxy-5-isopropyl-6-methyl-hept-2-enoic acid methyl ester (6.23). The product distribution after 16 hrs: 1.33 **6.23** (17:1 E/Z), 1.75 methyl acrylate, 0.72 **6.22**, 0.32 homodimer of **6.22**. *E*-isomer: ^{1}H NMR (CD_2Cl_2, 300 MHz, ppm): δ 7.03 (dt, *J* = 7.8, 15.6 Hz, 1H), 5.85 (dm, *J* = 15.6 Hz, 1H), 3.70 (s, 3H), 2.44(dd, *J* = 1.8, 7.8 Hz, 2H), 1.39 (s, 1H), 0.95 (t, *J* = Hz, 12H).

Z-isomer: ^{1}H NMR (CD_2Cl_2, 300 MHz, ppm): δ 2.90-2.85 (dd, 1H). Homodimer: ^{1}H NMR (CD_2Cl_2, 300 MHz, ppm): δ 2.26 (m, 4H), 1.32 (s, 2H).

1,1,1-Trifluoro-2-(*t*-butyldimethylsilanyloxy-2-trifluoromethyl-pent-4-ene (6.24). To a flame-dried 50 mL 2-neck flask was added sodium hydride (0.38 g, 15.8 mmol, 1.1 eq.). 30 mL of dry degassed tetrahydrofuran was added via cannula. To the stirring suspension was added hexafluorocarbinol **6.14** (3.0 g, 14.4 mmol, 1.0 eq.) slowly via syringe. The solution was heated at 40 °C for 1 hour. The solution was cooled to 0 °C prior to a solution of t-butyldimethylsilyl chloride (2.39g, 15.8 mmol, 1.1 eq.) in 5 mL of tetrahydrofuran was added. The reaction was subsequently heated at 40 °C overnight. The solution was concentrated and purified directly by silica gel chromatography (50:1 pentane:ether) to afford 4.16 g (90%) of **6.24** as a colorless liquid. R_f = 0.91 (20:1 hexane ether). ^{1}H NMR ($CDCl_3$, 300 MHz, ppm): δ 5.95-5.75 (m, 1H), 5.25-5.15 (m, 2H), 2.70 (d, *J* = 7.2 Hz, 2H), 0.91 (s, 9H), 0.19 (s, 6H). ^{13}C NMR ($CDCl_3$, 75 MHz, ppm): δ 129.32, 123.18 (q, J = 289 Hz), 120.36, 37.23, 25.61, 18.87, -3.28. ^{19}F NMR ($CDCl_3$, 282 MHz, ppm): δ -75.55 (s).

5-(*t*-Butyldimethylsilanyloxy)-6,6,6-trifluoro-5-trifluoromethyl-hex-2-enoic acid methyl ester (6.25). Product distribution after 16 hours: 1.33 **6.25** (> 12:1 E/Z), 0.85 methyl acrylate, 1.00 **6.24**, < 0.15 homodimer of **6.24**. *E*-isomer: ^{1}H NMR ($CDCl_3$, 300 MHz, ppm): δ 6.97 (m, 1H), 5.96 (dt, *J* = 1.5, 15.6 Hz, 1H), 3.78 (s, 3H), 2.82(d, *J* = 7.5 Hz, 2H), 0.92 (s, 9H), 0.20 (s, 6H). ^{19}F NMR ($CDCl_3$, 282 MHz, ppm): δ -75.07 (s).

1,1,1-Trifluoro-2-*t*-butoxycarbonyloxy-2-trifluoromethyl-pent-4-ene (6.26). To a flame-dried 25 mL 2-neck flask was added sodium hydride (57 mg, 2.11 mmol, 1.1 eq.). 15 mL of dry degassed tetrahydrofuran was added via cannula. To the stirring suspension was added hexafluorocarbinol **6.14** (0.40 g, 1.92 mmol, 1.0 eq.) slowly via syringe. After the evolution of gas had ceased (~ 5 minutes) the solution turned clear. A solution of di-t-butyl dicarbonate (0.46 g, 2.11 mmol, 1.1 eq.) in 2 mL of tetrahydrofuran was transferred to the reaction flask. The

reaction immediately turned cloudy and was allowed to stir overnight. The reaction was then diluted with water and extracted into 200 mL of ether. The organic layer was washed with water until the washings were neutral. The organic layer was then washed with brine and dried over sodium sulfate. The solution was concentrated and purified directly by silica gel chromatography (20:1 pentane:ether) to afford 0.41g (70%) of **6.26** as a colorless liquid. R_f = 0.66 (20:1 hexane:ethyl acetate). ^{1}H NMR ($CDCl_3$, 300 MHz, ppm): δ 5.9-5.7 (m, 1H), 5.35-5.35 (m, 2H), 3.22 (d, *J* = 7.2 Hz, 2 H), 1.51 (s, 9H). ^{13}C NMR ($CDCl_3$, 75 MHz, ppm): δ 127.87, 122.05 (q, J = 267.4 Hz), 122.03, 84.93, 31.60, 27.68. ^{19}F NMR ($CDCl_3$, 282 MHz, ppm): δ -72.54 (s). HRMS-[GC-EI+] (m/z): [M•]+ calc'd for $C_{11}H_{14}F_6O_3$, 308.0847; found, 308.0845.

5-*t*-Butoxycarbonyloxy-6,6,6-trifluoro-5-trifluoromethyl-hex-2-enoic acid methyl ester (6.27). Product distribution after 16 hours: 0.35 **6.27** (> 20:1 E/Z), 1.25 methyl acrylate, 1.00 **6.26**. *E*-isomer: ^{1}H NMR (CD_2Cl_2, 300 MHz, ppm): δ 6.9-6.75 (m, 1H), 6.04 (dm, *J* =15.3 Hz, 1H), 3.73 (s, 3H), 2.44(d, *J* = 7.8 Hz, 2H), 1.50 (s, 9H). ^{19}F NMR ($CDCl_3$, 282 MHz, ppm): δ -72.86 (s).

***Z*-5-(*t*-Butyldimethylsilanyloxy)-pent-2-enoic acid methyl ester (*Z*-6.19).** ***Z*-6.19** in 44% yield from 5,6-dihydro-2H-pyran-2-one according to the procedure of Herold *et al*.[51] ^{1}H NMR ($CDCl_3$, 300 MHz, ppm): δ 6.36 (dt, *J* = 7.2, 11.7 Hz, 1H), 5.85 (dt, *J* =1.5, 11.7 Hz, 1H), 3.71 (s, 3H), 2.88 (ddt, *J* = 1.5, 6.0, 6.0 Hz, 2H), 0.89 (s, 9H), 0.06 (s, 6H). ^{13}C NMR ($CDCl_3$, 75 MHz, ppm): δ 166.97, 147.60, 120.59, 62.24, 51.23, 32.79, 26.10, 18.50, -5.53.

Isomerization of *Z*-6.19. After 16 hours of isomerization in the presence of 1 equivalent of methyl acrylate, NMR analysis indicated an E/Z ratio of 12:1.

Isomerization of *Z*-6.18a. After 16 hours of isomerization in the presence of 1 equivalent of methyl acrylate, NMR analysis indicated an E/Z ratio of 1.6:1.

General Procedure for Olefin Isomerization Studies: In a nitrogen filled drybox, catalyst **6.2** (3.4 mg, 0.004 mmol, 0.02 eq.) was added to a screw-cap vial with a teflon stirbar along with 1

mL dry CD_2Cl_2. On the benchtop, the additive (1 eq.) was added via syringe followed by substrate ***E*-6.19** (50 μL, 0.20 mmol, 1 eq.). The vial was heated on an oil bath at 40 °C for 16 hours. The product distribution was determined by NMR analysis of the olefin and allylic proton resonances.

Methyl 3-(3,3,3-trifluoro-2-hydroxy-2-trifluoromethyl-propyl)-bicyclo[2.2.1]hept-5-ene-2-carboxylic acid ester (6.29a). To a 10 mL thick-walled Schlenk tube were added ***E*-6.18a** (1.5 g, 5.6 mmol, 1.0 eq.), and MEHQ (10 mg) followed by freshly cracked cyclopentadiene (450 mg, 6.8 mmol, 1.2 eq.). The reaction mixture was degassed via 3 freeze-pump thaw cycles and the vessel sealed under argon. The reaction was stirred at room temperature for 2 days after which no reaction had taken place. The mixture was degassed again and heated at 80 °C for 48 hours, after which time the reaction was purified by silica gel column chromatography (10:1 hexane:ethyl acetate) to afford 1.12 g (72%) of **6.29a** as a 1.02:1.00 mixture of isomers (R_f = 0.38, 85:15 hexane:ethyl acetate) with ~5% tetracyclododecene compounds.

6.29a (1.02:1.00 mixture of isomers)**:** ^{1}H NMR ($CDCl_3$, 300 MHz, ppm): δ 6.28 (m, 1H), 6.20 (s, 1H), 6.13 (m, 1H), 5.80 (s, 1H), 3.78 (s, 3H), 3.72 (s, 3H), 3.24 (s, 1H), 3.19 (s, 1H), 2.91 (s, 1H), 2.77 (t, *J* = 3.9 Hz, 1H), 2.66 (m, 1H), 2.56 (m, 1H), 2.35 (m, 1H), 2.30 (m, 1H), 2.15 (m, 1H), 2.11 (m, 1H), 2.07 (m, 1H), 1.98 (m, 1H), 1.7-1.6 (m, 2H), 1.6-1.45 (m, 3H). ^{19}F NMR ($CDCl_3$, 282 MHz, ppm): δ -76.23(q, 3F, major), -76.58 (q, 3F, minor), -78.70 (q, 3F, major), -78.91 (q, 3F, minor). GC-MS: 91.8% **6.29a**, *m/z* = 332, and 5.2% tetracyclodecenes, *m/z* = 398.

***t*-Butyl 3-(3,3,3-trifluoro-2-hydroxy-2-trifluoromethyl-propyl)-bicyclo[2.2.1]hept-5-ene-2-carboxylic acid ester (6.29b).** To a 10 mL thick-walled Schlenk tube was added ***E*-6.18b** (1.5 g, 4.87 mmol, 1 eq.), MEHQ (10 mg), and 5 mL benzene followed by freshly cracked cyclopentadiene (386 mg, 5.84 mmol, 1.2 eq.). The reaction mixture was degassed via 3 freeze-pump thaw cycles and the vessel sealed under argon. The reaction was heated at 80 °C for 16 hours, after which time 26 % conversion had been reached. The addition of 1.2 equivalents of

additional cyclopentadiene and heating at 115 °C for 12 hours afforded 53% conversion, at which time the reaction was purified by silica gel column chromatography (10:1 hexane:ethyl acetate) to afford 0.86 g (47%) of **6.29b** as a 1.04:1.00 mixture of isomers (R_f = 0.56, 85:15 hexane:ethyl acetate) and recovery of 0.47 g (31 %) of **6.18b** (R_f = 0.35, 85:15 hexane:ethyl acetate).

6.29b (1.04:1.00 mixture of isomers)**:** ^{1}H NMR ($CDCl_3$, 300 MHz, ppm): δ 6.73 (s, 1H), 6.47 (s, 1H), 6.27 (m, 2H), 6.14 (m, 2H), 3.18 (s, 1H), 3.14 (s, 1H), 2.87 (s, 1H), 2.72 (t, *J* = 9.9 Hz, 1 H), 2.47 (dm. *J* = 6.0 Hz, 1 H), 2.34 (s, 1H), 2.29 (s, 1H), 2.18 (s, 1H), 2.13 (s, 1H), 2.07(dm, *J* = 14.7 Hz, 1H), 1.99 (dd, *J* = 4.5 Hz, 1H), 1.93(dm, *J* = 8.7 Hz, 1H), 1.75-1.5 (m, 6H), 1.49 (s, 9H). 1.44 (s, 9H). ^{13}C NMR ($CDCl_3$, 75 MHz, ppm): δ 177.11, 176.80, 138.01, 137.58, 135.37, 134.88, 123.91 (q, *J* = 288 Hz), 123.31 (q, *J* = 288 Hz), 83.26, 83.12, 54.67, 52.74, 50.13, 48.14, 46.17, 46.03, 45.36, 39.29, 38.18, 36.87, 35.27, 28.13, 18.07. ^{19}F NMR ($CDCl_3$, 282 MHz, ppm): δ -75.81(q, *J* = 9.9 Hz, 3F, minor), -76.53 (q, *J* = 10.5 Hz, 3F, major), -78.94 (q, *J* = 9.9 Hz, 3F), -79.05 (q, *J* = 9.9 Hz, 3F). HRMS-[FAB+] (m/z): [M+H]+ calc'd for $C_{16}H_{21}F_6O_3$, 375.1395; found, 375.1391.

3-(3,3,3-Trifluoro-2-hydroxy-2-trifluoromethyl-propyl)-bicyclo[2.2.1]hept-5-ene-2-carboxylic acid (6.30). *t*-Butyl ester **6.29b** (108 mg, 0.288 mmol, 1 eq.) and *p*-toluenesulfonic acid monohydrate (8.5 mg, 0.045 mmol, 0.15 eq.) were added to a 10 mL 2 neck flask with 2 mL of benzene. The reaction was heated at 80 °C for 10 hours. Silica gel column chromatography (10:1 CH_2Cl_2: MeOH) afforded 85 mg (89%) of **6.30**. ^{1}H NMR ($CDCl_3$, 300 MHz, ppm): δ 6.8-6.3 (br s, 2 H, OH), 6.25 (m, 2H), 6.12 (m, 2H), 3.17 (m, 1H), 3.08 (m, 1H), 2.87 (m, 1H), 2.17 (t, *J* = 3.3 Hz, 1H), 2.65 (m, 1H), 2.54 (m, 1H), 2.45 (s, 1H), 2.29 (d, *J* = 14.1 Hz, 1H), 2.12 (d, *J* = 15.6 Hz, 1H), 2.09 (d, *J* = 15.9 Hz, 1H), 1.96 (m, 2H), 1.67 (d, *J* = 10.5 Hz, 1H), 1.62 (d, *J* = 10.5 Hz, 1H), 1.49 (d, *J* = 10.8 Hz, 4H). ^{13}C NMR ($CDCl_3$, 75 MHz, ppm): δ 184.18, 183.28, 138.14, 137.63, 135.15, 14.86, 123.73 (q, *J* = 288 Hz), 123.27 (q, *J* = 287 Hz), 54.09, 52.47, 50.05, 47.92, 47.82, 46.66, 46.37, 45.53, 38.91, 37.83, 36.57, 34.87., 135.37, 134.88, 123.91 123.31 (q, *J* = 288

Hz), 83.26, 83.12, 54.67, 52.74, 50.13, 48.14, 46.17, 46.03, 45.36, 39.29, 38.18, 36.87, 35.27, 28.13, 18.07. ^{19}F NMR ($CDCl_3$, 282 MHz, ppm): δ -76.61 (m, 3F), -76.77 (q, 3F), -78.65 (m, 3F), -78.88 (q, 3F). HRMS-[DIP-EI+] (m/z): [M•]+ calc'd for $C_{12}H_{12}F_6O_3$, 318.0691; found, 318.0695.

3-(3,3,3-Trifluoro-2-hydroxy-2-trifluoromethyl-propyl)-bicyclo[2.2.1]heptane-2-carboxylic acid methyl ester (6.33a). To a 100 mL round bottom flask was added **6.29a** (0.50 g, 1.50 mmol, 1 eq.) and Pd/C (10 wt % Pd, ~60 mg), and 15 mL ethyl acetate. The reaction mixture was degassed via 3 freeze-pump thaw cycles and the placed under a balloon of hydrogen. The reaction was stirred for 16 hours, at which time the catalyst was filtered off with a 0.45 μm^{-1} PTFE syringe filter. Removal of the solvent *in vacuo* afforded **6.33a** (95 %) as a colorless liquid (contains ~6 % tetracyclododecane compounds).

6.33a (1.07:1.00 mixture of isomers)**:** ^{1}H NMR ($CDCl_3$, 300 MHz, ppm): δ 6.17 (s, 1H), 5.42 (s, 1H), 3.76 (s, 6H), 2.69 (m, 1H), 2.64 (m, 1H), 2.53 (s, 1H), 2.5-1.8 (11H), 1.8-1.3 (15H). ^{13}C NMR ($CDCl_3$, 75 MHz, ppm): δ 178.55, 177.42, 66.06, 57.06, 55.23, 53.00, 52.68, 44.74, 42.64, 40.53, 40.29, 38.70, 38.56, 37.47, 37.31, 33.52, 30.11, 29.09, 24.26, 22.06, 15.46. ^{19}F NMR ($CDCl_3$, 282 MHz, ppm): δ -75.73(q, 3F, minor), -76.61 (q, 3F, major), -78.34 (q, 3F, minor), -78.43 (q, 3F, major). GC/MS: 91.6% **6.33a**, *m/z* = 334 (Ratio: 1.07:1), 6.0% Tetracyclododecanes, *m/z* = 400 (ratio 1.29:1).

3-(3,3,3-Trifluoro-2-hydroxy-2-trifluoromethyl-propyl)-bicyclo[2.2.1]heptane-2-carboxylic acid *t*-butyl ester (6.33b). To a 100 mL round bottom flask was added **6.29b** (0.83 g, 2.22 mmol, 1 eq.) and Pd/C (10 wt % Pd, ~150 mg), and 15 mL dry benzene. The reaction mixture was degassed via 3 freeze-pump thaw cycles and placed under a balloon of hydrogen. The reaction was stirred for 6 hours, at which time the catalyst was filtered off with a 0.45 μm^{-1} PTFE syringe filter. Removal of the solvent *in vacuo* afforded **6.33b** (95 %) as a colorless liquid.

6.33b (1.05:1.00 mixture of isomers)**:** ^{1}H NMR ($CDCl_3$, 300 MHz, ppm): δ 6.77 (s, 1H), 5.96 (s, 1H), 2.7-2.55 (m, 2H), 2.46 (m, 1H), 2.4-2.15 (m, 4H), 2.15-2.05 (m, 2H), 2.05-1.85 (m, 3H), 1.75-1.20 (12H), 1.48 (s, 9H). 1.47 (s, 9H). ^{13}C NMR ($CDCl_3$, 75 MHz, ppm): δ 177.63, 176.63, 123.79 (q, *J* = 288 Hz), 123.54 (q, *J* = 288 Hz), 83.06, 82.68, 58.14, 55.19, 45.07, 42.72, 40.61, 40.49, 38.69, 38.50, 38.36, 37.46, 37.40, 33.76, 30.29, 28.80, 28.20, 28.05, 23.98, 22.12. . ^{19}F NMR ($CDCl_3$, 282 MHz, ppm): δ -75.41(q, 3F, minor), -76.67 (q, 3F, major), -78.39 (q, 3F, major), -78.52 (q, 3F, minor). HRMS-[FAB+] (m/z): [M+H]+ calc'd for $C_{16}H_{23}F_6O_3$, 377.1551; found, 377.1566.

Acrylic acid 1,1-bis-trifluoromethyl-but-3-enyl ester (6.34). To a flame-dried 25 mL 2-neck flask was added sodium hydride (253 mg, 10.6 mmol, 1.1 eq.). 15 mL of dry degassed tetrahydrofuran was added via cannula. The solution was cooled to 0 °C. To the stirring suspension was added hexafluorocarbinol **6.14** (2.0 g, 9.60 mmol, 1.0 eq.) slowly via syringe. After bubbling ceased, the reaction was warmed for 20 minutes at 40 °C. The reaction was cooled to 0 °C and *N,N*-dimethylaminopyridine (0.12 g, 0.96 mmol, 0.1 eq.) was added. Acryloyl chloride was slowly injected via syringe. The reaction was allowed to stir for 6 hours. The solution was concentrated and purified directly by silica gel chromatography (20:1 pentane:ether) to afford 1.36 g (54%) of **6.34** as a colorless liquid. R_f = 0.49 (20:1 hexane:ethyl acetate). ^{1}H NMR ($CDCl_3$, 300 MHz, ppm): δ 6.50 (dd, *J* = 1.2, 17.1 Hz, 1H), 6.14 (dd, *J* = 10.5, 17.1 Hz, 1H), 5.99 (dd, *J* = 1.2, 10.5 Hz, 1H), 5.75-5.65 (m, 1H), 5.35-5.2 (m, 2H), 3.28(d, *J* = 7.2 Hz, 2H). ^{13}C NMR ($CDCl_3$, 75 MHz, ppm): δ 162.05, 133.89, 127.80, 127.29, 122.01, 31.83. ^{19}F NMR ($CDCl_3$, 282 MHz, ppm): δ -72.68 (s). HRMS-[GC-EI+] (m/z): [M•]+ calc'd for $C_9H_8F_6O_2$, 262.0464; found, 262.0429.

6,6-Bis-trifluoromethyl-5,6-dihydro-pyran-2-one (6.35). To a flame-dried 300 mL airless flask with reflux condenser was added catalyst **6.2** (39 mg, 0.046 mmol, 0.01 eq.). 100 mL of dry degassed dichloromethane was added via cannula followed by **6.34** (0.95 g, 3.62 mmol, 1 eq.).

The reaction was heated on an oil bath at 40 °C for 24 hours under nitrogen. The solution was concentrated and purified directly by silica gel chromatography (3:1 pentane:ether) to afford 0.40 g (47 %) of **6.35** as a colorless liquid. The product coeluted with ~5 % of 6,6-bis-trifluoromethyl-3,6-dihydro-pyran-2-one **(6.36)**. R_f = 0.23 (80:20 hexane:ethyl acetate). ^{1}H NMR ($CDCl_3$, 300 MHz, ppm): δ 6.84 (dd, *J* = 1.2, 10.2 Hz, 1H), 6.15 (dd, *J* = 2.1, 10.5 Hz, 1H), 2.95 (m, 1H). ^{13}C NMR ($CDCl_3$, 75 MHz, ppm): δ 156.93, 140.56, 121.87 (q, J = 287 Hz), 119.53, 22.57. ^{19}F NMR ($CDCl_3$, 282 MHz, ppm): δ -78.06 (s). HRMS-[CI+] (m/z): [M•]+ calc'd for $C_7H_4F_6O_2$, 234.0115; found, 234.0107.

6,6-Bis-trifluoromethyl-3,6-dihydro-pyran-2-one (6.36) ^{1}H NMR ($CDCl_3$, 300 MHz, ppm): δ 6.5-6.4 (dt, 1H), 6.07-6.0 (dt, 1H), 3.35-3.30 (dd, 1H). ^{19}F NMR ($CDCl_3$, 282 MHz, ppm): δ -77.34 (s).

5,5-Bis-trifluoromethyl-4-oxa-tricyclo[6.2.1.02,7]undec-9-en-3-one (6.37). Freshly cracked cyclopentadiene (0.67 mL, 8.4 mmol, 2 eq.) and **6.35** (0.97g, 4.2 mmol, 1 eq.) were added to a 10 mL thick walled Schlenk tube. The system was degassed via 3 freeze-pump-thaw cycles and sealed under argon. The tube was heated to 120 °C for 68 hours. The reaction products were purified by silica gel column chromatography (15:1 pentane:ether) to afford 0.40 g (32%) of ***endo*-6.37** and 0.13 g (9%) of ***exo*-6.37**. endo/exo = 3.6:1. Total yield: 41 %.

***endo*-6.37.** ^{1}H NMR ($CDCl_3$, 300 MHz, ppm): δ 6.36 (dd, *J* = 3.0, 5.7 Hz, 1H), 6.19 (dd, *J* = 3.0, 5.7 Hz, 1H), 3.42 (m, 1H), 3.11 (ddd, *J* = 1.2, 3.9, 10.2 Hz, 1H), 3.03 (s, 1H), 2.79 (m, 1H), 1.66 (dt, *J* = 1.8, 9.0 Hz, 1H), 1.66 (dt, *J* = 1.8, 10.5 Hz, 1H), 1.44 (dt, *J* = 1.5, 7.5 Hz, 1 H). ^{13}C NMR ($CDCl_3$, 75 MHz, ppm): δ 169.29, 138.42, 135.25, 122.23 (q, *J* = 288 Hz), 121.47 (q, *J* = 288 Hz), 81.72 (m), 48.28, 46.45, 45.99, 42.92, 34.53, 26.54. ^{19}F NMR ($CDCl_3$, 282 MHz, ppm): δ -72.81 (q, 3F), -77.96 (q, 3F). HRMS-[CI+] (m/z): [M•]+ calc'd for $C_{12}H_{10}F_6O_2$, 300.0585; found, 300.0581.

***exo*-6.37.** ^{1}H NMR ($CDCl_3$, 300 MHz, ppm): δ 6.3-6.2 (m, 2H), 3.47 (m, 1H), 2.77 (s, 1H), 2.67 (dd, *J* = 7.2, 15.0 Hz, 1H), 2.43 (d, *J* = 9 Hz, 1H), 2.3-2.0 (m, 1H), 1.72-1.67 (m, 1H), 1.51 (d, *J* = 9.6 Hz, 1H), 1.34 (d, *J* = 9.9 Hz, 1 H). ^{13}C NMR ($CDCl_3$, 75 MHz, ppm): δ 169.40, 136.90, 136.44, 122.29 (q, *J* = 288 Hz), 121.52 (q, *J* = 284 Hz), 81.03 (m), 47.24, 46.38, 44.14, 42.72, 33.32, 27.89. ^{19}F NMR ($CDCl_3$, 282 MHz, ppm): δ -72.67 (m, 3F), -77.97 (m, 3F).

Base-catalyzed hydrolysis of *endo*-6.37. ***Endo*-6.37** (0.20 g, 0.68 mmol, 1 eq.), potassium hydroxide (228 mg, 4.1 mmol, 6 eq.) and 5 mL methanol were added to a 2-necked flask with reflux condenser. The mixture was refluxed for 72 hours. The mixture was concentrated to dryness and taken up in water/ether. The mixture was acidified with 1M HCl solution. The product was extracted 3 times into ether. The organic layer was washed with brine until the washings were neutral. The solvent was removed *in vacuo* and the slightly yellowish solid washed with hexanes to produce 0.133 g (62%) of 3-*endo*-(3,3,3-Trifluoro-2-hydroxy-2-trifluoromethyl-propyl)-bicyclo[2.2.1]hept-5-ene-2-*exo*-carboxylic acid (***endo*,*exo*-6.30**) as a snow white solid. ^{1}H NMR ($CDCl_3$, 300 MHz, ppm): δ 6.33 (dd, J = 3.0, 5.7 Hz, 1H), 6.18 (dd, *J* = 3.0, 5.7 Hz, 1H), 4.8 (br s, 0.5H), 3.20 (s, 1H), 2.97 (s, 1H), 2.66 (m, 1H), 2.10 (dd, *J* = 3.6 Hz, 1H), 2.07 (d, *J* = 6.3 Hz, 1H), 1.72 (ddd, *J* = 1.5, 6.6, 15.3 Hz, 1H), 1.58 (m, 2H). ^{13}C NMR ($CDCl_3$, 75 MHz, ppm): δ 183.07, 137.54, 135.19, 51.70, 47.91, 46.75, 39.11, 34.73. ^{19}F NMR ($CDCl_3$, 282 MHz, ppm): δ -73.28 (q, *J* = 10.0 Hz), -78.43 (q, *J* = 9.9 Hz). HRMS-[CI+] (m/z): [M•]+ calc'd for $C_{12}H_{12}F_6O_3$, 318.0691; found, 318.1689.

2,2-Bis-trifluoromethyl-3,6-dihydro-2H-pyran (6.38). To a 100 mL oven-dried Fischer-Porter bottle was added 25 mg 4-*t*-butyl catechol. The pressure bottle was sealed and 1,3-butadiene was condensed in at -78 °C. The bottle was cooled with liquid nitrogen while the hexafluoroacetone tank was attached. 2 pump backfill cycles were used to remove any air that had entered the system. Hexafluoroacetone was condensed into the bottle at -78 °C, forming two distinct layers. The bottle was sealed and the temperature slowly warmed to room temperature. Gradually, the

system formed one phase and the pressure rose to 80 psi. The vessel was heated at 55 °C overnight. The excess gases were vented in the hood through a saturated potassium hydroxide solution. The product was purified by Kugelrohr distillation at room temperature. R_f = 0.53 (20:1 hexane:ethyl acetate). ^{1}H NMR ($CDCl_3$, 300 MHz, ppm): δ 6.0-5.9 (m, 2H), 4.38 (m 2H), 2.51 (m, 2H). ^{19}F NMR ($CDCl_3$, 282 MHz, ppm): δ -77.49 (s). HRMS-[CI+] (m/z): [M•]+ calc'd for $C_7H_6F_6O$, 220.0323; found, 220.0313.

Allylic Oxidation of 6.38. Compound **6.38** was oxidized with pyridinium chlorochromate according to the procedure of Bonini *et al.*[45] Aliquots were extracted for analysis by NMR. After 6 hours at 70 °C, NMR analysis revealed the reaction to contain: 68% **6.38**, 24% **6.35**, and 9% 24% 2,2-Bis-trifluoromethyl-2,3-dihydro-pyran-4-one **(6.39**). Adding more oxidant and increasing the temperature gradually increased the conversion to ~35% **6.35** (with about 3% of the isomeric **6.36**); however, heating above 100 °C resulted in the production of many degradation products. Structural assignments were confirmed by comparing spectra with independently synthesized **6.35** (see above) and column chromatography of the reaction mixture to afford samples for NMR analysis. The addition of 1 equivalent of pyridine per equivalent PCC seemed to accelerate the formation of by-products.

Similarly, oxidation with pyridinium dichromate/*t*-butyl hydroperoxide according to the procedure of Chandrasekaran *et al.*[47] was unable to increase the yields of the desired product.

2,2-Bis-trifluoromethyl-2,3-dihydro-pyran-4-one (6.39). Silica gel column chromatography (4:1 pentane: ether) on the reaction mixture from the PCC oxidation of **6.38** afforded a mixture of two side products: **6.39** and an overoxidized product in a 2:1 ratio, respectively. R_f = 0.36 (85:15 hexane/ethyl acetate).

(6.39). ^{1}H NMR ($CDCl_3$, 300 MHz, ppm): δ 7.31 (d, J = 6.3 Hz, 1H), 5.62 (d, J = 6.6 Hz, 1H), 3.07 (s, 2H). ^{19}F NMR ($CDCl_3$, 282 MHz, ppm): δ -77.41 (s). GC/MS: m/z = 234.

Overoxidized product: ^{1}H NMR ($CDCl_3$, 300 MHz, ppm): δ 7.49 (d, J = 5.4 Hz, 1H), 6.65 (d, J = 6.0 Hz, 1H). ^{19}F NMR ($CDCl_3$, 282 MHz, ppm): δ -74.53 (s). GC/MS: m/z = 248.

References and Notes

(1) (a). Trinque, B. C.; Chambers, C. R.; Osborn, B. P.; Callahan, R. P.; Lee, G. S.; Kusumoto, S.; Sanders, D. P.; Grubbs, R. H.; Conley, W. E.; C. Willson, C. G. *J. Fluorine Chem*. **2003**, *122*, 17-26. (b). Chiba, T.; Hung, R. J.; Yamada, S.; Trinque, B.; Yamachika, M.; Brodsky, C.; Patterson, K.; Vander Heyden, A.; Jamison, A.; Lin, S. H.; Somervell, M.; Byers, J.; Conley, W.; Willson, C. G. *J. Photopolymer Sci. Technol.* **2000**, *13*, 657-664. (c). Brodsky, C.; Byers, J.; Conley, W.; Hung, R.; Yamada, S.; Patterson, K.; Somervell, M.; Trinque, B.; Tran, H. V.; Cho, S.; Chiba, T.; Lin, S-H.; Jamieson, A.; Johnson, H.; Vander Heyden, T.; Willson, C. G. *J. Vac. Sci. Technol. B.* **2000**, *18*, 3396-3401. (d). Kunz, R. R.; Bloomstein, T. M.; Hardy, D. E.; Goodman, R. B.; Downs, D. K.; Curtin, J. E. *J. Vac. Sci. Technol. B* **1999**, *17*, 3267-3272. (e). Kunz, R. R.; Bloomstein, T. M.; Hardy, D. E.; Goodman, R. B.; Downs, D. K.; Curtin, J. E. *J. Photopolym. Sci. Technol.* **1999**, *12*, 561-570.

(2) (a). Sanders, D. P.; Connor, E. F.; Grubbs, R. H.; Hung, R. J.; Osborn, B. P.; Chiba, T.; MacDonald, S. A.; Willson, C. G.; Conley, W. *Macromolecules* **2003**, *36*, 1534-1542. (b). Tran, H. V.; Hung, R. J.; Chiba, T.; Yamada, S.; Mrozek, T.; Hsieh, Y-T.; Chambers, C. R.; Osborn, B. P.; Trinque, B. C.; Pinnow, M. J.; MacDonald, S. A.; Willson, C. G.; Sanders, D. P.; Connor, E. F.; Grubbs, R. H.; Conley, W. *Macromolecules* **2002**, *35*, 6539-6549. (c). Willson, C. G.; Trinque, B. C.; Osborn, B. P.; Chambers, C. R.; Hsieh, Y-T.; Chiba, T.; Zimmerman, P.; Miller, D.; Conley, W. *J. Photopolym. Sci. Technol.* **2002**, *15*, 583-590. (d). Tran, H. V.; Hung, R. J.; Chiba, T.; Yamada, S.; Mrozek, T.; Hsieh, Y-T.; Chambers, C. R.; Osborn, B. P.; Trinque, B. C.; Pinnow, M. J.; Sanders, D. P.; Connor, E. F.; Grubbs, R. H.; Conley, W.; MacDonald, S. A.; Willson, C. G. *J. Photopolym. Sci. Technol.* **2001**,

14, 669-674. (e). Chiba, T.; Hung, R. J.; Yamada, S.; Trinque, B.; Yamachika, M.; Brodsky, C.; Patterson, K.; Vander Heyden, A.; Jamison, A.; Lin, S-H.; Somervell, M.; Byers, J.; Conley, W; Willson, C. G. *J. Photopolym. Sci. Technol.* **2000**, *13*, 657-664.

(3) (a). Ito, H.; Wallraff, G. M.; Brock, P. J.; Fender, N.; Truong, H.; Breyta, G.; Miller, D. C.; Sherwood, M. H.; Allen, R. D. *Proc. SPIE* **2001**, *4345*, 273-284. (b). Trinque, B. C.; Chiba, T.; Hung, R. J.; Chambers, C. R.; Pinnow, M. J.; Osborn, B. P.; Tran, H. V.; Wunderlich, J.; Hsieh, Y-T.; Thomas, B. H.; Shafer, G.; DesMarteau, D. D.; Conley, W.; Willson, C. G. *J. Vac. Sci. & Technol. B* **2002**, *20*, 531-536. (c). Trinque, B. C.; Osborn, B. P.; Chambers, C. R.; Hsieh, Y-T.; Corry, S. B.; Chiba, T.; Hung, Raymond J-P.; Tran, H. V.; Zimmerman, P.; Miller, D.; Conley, W.; Willson, C. G. *Proc. SPIE* **2002**, *4690*, 58-68.

(4) (a). Feiring, A. E.; Crawford, M.; Feldman, J.; Farnham, W. B.; Feldman, J.; French, R. H.; Leffew, K. W.; Petrov, V. A.; Schadt, F. L., III; Whelanad, R.C.; Zumsteg, F. C. *J. Fluorine Chem.* **2003**, *122*, 11-16. (b). Toriumi, M.; Ishikawa, T.; Kodani, T.; Koh, M.; Moriya, T.; Araki, T.; Aoyama, H.; Yamashita, T.; Yamazaki, T.; Itani, T.; *J. Photopolym. Sci. Technol.* **2003**, *16*, 607-614. (c). Sharif, I.; DesMarteau, D.; Ford, L.; Shafer, G. J.; Thomas, B.; Conley, W.; Zimmerman, P.; Miller, D.; Lee, G. S.; Chambers, C. R.; Trinque, B. C.; Chiba, T.; Osborn, B. P.; Willson, C. G. *Proc. SPIE* **2003**, *5039*, 33-42.

(5) (a). Itani, T.; Ishikawa, S.; Irie, S.; Hagiwara, T. *J. Vac. Sci. Technol. B.* **2003**, *21*, 3181-3184. (b). Irie, S.; Ishikawa, S.; Hagiwara, T.; Yamazaki, T.; Furukawa, T.; Itani, T.; Kawaguchi, Y.; Kodama, S.; Yokokoji, O.; Kaneko, I.; Takebe, Y.; Okada, S. *Jap. J. Appl. Phys. Pt. 1*. **2003**, *42*(6B), 3743-3747.

(6) (a). Patterson, K.; Yamachika, M.; Hung, R. J.; Brodsky, C. J.; Yamada, S.; Somervell, M. H.; Osborn, B.; Hall, D.; Dukovic, G.; Byers, J.; Conley, W.; Willson, C. G. *Proc. SPIE* **2000**, *3999*, 365-374. (b). Brodsky, C.; Byers, J.; Conley, W.; Hung, R.; Yamada, S.; Patterson, K.; Somervell, M.; Trinque, B.; Tran, H. V.; Cho, S.; Chiba, T.; Lin, S-H.;

Jamieson, A.; Johnson, H.; Vander Heyden, T.; Willson, C. G. *J. Vac. Sci. Technol.* B **2000**, *18*, 3396-3401.

(7) (a). Ito, H. *IBM J. Res. Dev.* **2001**, *45*, 683-695. (b). Hoskins, T.; Chung, W. J.; Agrawal, A.; Ludovice, P. J.; Henderson, C. L.; Seger, L. D.; Rhodes, L. F.; Shick, R. A. *Macromolecules* **2004**, *37*, 4512-4518.

(8) Gandler, J. R.; Jencks, W. P. *J. Am. Chem. Soc.* **1982**, *104*, 1937-51.

(9) Madan, R.; Srivastava, A.; Anand, R. C.; Varma, I. K. *Prog. Polym. Sci.* **1998**, *23*, 621-663.

(10) Gaylord, N. G.; Deshpane, A. B.; Mandal, B. M.; Martan, M. *J. Macromol. Sci. Chem.* **1977**, *A11*, 1053-1070.

(11) (a). Barnes, D. A.; Benedikt, G. M.; Goodall, B. L.; Huang, S. S.; Kalamarides, H. A.; Lenhard, S.; McIntosh, L. H., III; Selvy, K. T.; Schick, R. A.; Rhodes, L. F. *Macromolecules* **2003**, *36*, 2623-2632. (b). Benedikt, G. M.; Elce, E.; Goodall, B. L.; Kalamarides, H. A.; McIntosh, L. H., III.; Rhodes, L. F.; Selvy, K. T.; Andes, C.; Oyler, K.; Sen, A. *Macromolecules* **2002**, *35*, 8978-8988.

(12) (a). Mathew, J. P.; Reinmuth, A.; Melia, J.; Swords, N.; Risse, W. *Macromolecules* **1996**, *29*, 2755-2763. (b). Lipian, J.; Mimna, R. A.; Fondran, J. C.; Yandulov, D.; Shick, R. A.; Goodall, B. L.; Rhodes, L. F.; Huffman, J. C. *Macromolecules* **2002**, *35*, 8969-8977. (c). Hennis, A. D.; Polley, J. D.; Long, G. S.; Sen, A.; Yandulov, D.; Lipian, J.; Benedikt, G. M.; Rhodes, L. F.; Huffman, J. *Organometallics* **2001**, *20*, 2802-2812.

(13) For recent reviews on development of olefin metathesis catalysts and their application to ring-opening metathesis polymerization, see: (a). Buchmeiser, M. R. *Chem. Rev.* **2000**, *100*, 1565-1604. (b) Frenzel, U.; Nuyken, O. *J. Polym. Sci. A Polym. Chem.* **2002**, *40*, 28956-2916. (c). Slugovc, C. *Macromol. Rapid Commun.* **2004**, *25*, 1283-1297. (d). Trnka, T. M.; Grubbs, R. H. *Acc. Chem. Res.* **2001**, *34*, 18-29.

(14) (a). Patterson, K. W. *Ph.D. Dissertation* University of Texas, Austin, **2000**. (b). Okoroanyanu, U.; Shimokawa, T.; Byers, J.; Willson, C. G. *Chem. Mater.* **1998**, *10*, 3319-

3327. (c). Okoroanyanu, U.; Byers, J.; Shimokawa, T.; Willson, C. G. *Chem. Mater.* **1998**, *10*, 3328-3333.

(15) Bielawski, C. W.; Benitez, D.; Morita, T.; Grubbs, R. H. *Macromolecules* **2001**, *34*, 8610-8618.

(16) Osborn, B. P. *Ph.D. Dissertation*, University of Texas, Austin, **2004**.

(17) Cho, J. H.; Kim, B. M. *Org. Lett.* **2003**, *5*, 531-533.

(18) Maynard, H. D.; Grubbs, R. H. *Tetrahedron Lett.* **1999**, *40*, 4137-4140.

(19) Sanders, D. P. *Ph.D. Dissertation*, California Institute of Technology, **2004**.

(20) (a). Dixon, D. A.; Matsuzawa, N. N.; Ishitani, A.; Uda, T. *Phys. Stat. Sol. B* **2001**, *226*, 69-77. (b). Matsuzawa, N. N.; Ishitani, A.; Dixon, D. A.; Uda, T. *Proc. SPIE* **2001**, *4345*, 396-404. (c). Matsuzawa, N. N.; Mori, S.; Okazaki, S.; Ishitani, A.; Dixon, D. A.; *Proc. SPIE* **2000**, *3999*, 375-384.

(21) (a). Yoshida, Y.; Goto, K.; Komiya, Z. *J. Appl. Polym. Sci.* **1997**, *66*, 367-375. (b). Mol, J. C.; *J. Molec. Catal. A. Chem.* **2004**, *213*, 39-45. (c). Yamazaki, M. *J. Molec. Catal. A. Chem.* **2004**, *213*, 81-87.

(22) Preishuber-Pfugl, P.; Eder, E.; Stelzer, F.; Reisinger, H.; Mulhaupt, R.; Forsyth, J.; Perena, J. M. *Macromol. Chem. Phys.* **2001**, *202*, 1130-1137.

(23) Amir-Ebrahimi,V.; Corry, D. A.; Hamilton, J. G.; Thompson, J. M.; Rooney, J. J. *Macromolecules* **2000**, *33*, 717-724.

(24) Morgan, J. P. *Ph.D. Dissertation*, California Institute of Technology, **2002**.

(25) For a recent review see: Schwendeman, J. E.; Church, A. C.; Wagener, K. B. *Adv. Synth. Catal.* **2002**, *344*, 597-613.

(26) For recent reviews on enyne metathesis, see: (a). Diver, S. T.; Giessert, A. J. *Chem. Rev.* **2004**, *104*, 1317-1382. (b). Mori, M. *J. Molec. Catal. A* **2004**, *213*, 73-79.

(27) Banti, D.; North, M. *Adv. Synth. Catal.* **2002**, *344*, 694-704.

(28) Ho, B.-C.; Yueh, W.; Willson, C. G. *Unpublished results.*

(29) Sworen, J. C.; Pawlow, J. H.; Case, W.; Lever, J.; Wagener, K. B. *J. Molec. Catal. A* **2003**, *194*, 69-78.

(30) (a). Chambers, C. R.; Kusumoto, S.; Lee, G. S.; Vasudev, A.; Walthal, L.; Osborn, B. P.; Zimmerman, P.; Conley, W.; Willson, C. G. *Proc. SPIE* **2003**, *5039*, 93-102. (b). Fresco, Z. M.; Bensel, N.; Suez, I.; Backer, S. A.; Frechet, J. M. J.; Conley, W. *J. Photopolym. Sci. Technol.* **2003**, *16*, 27-36. (c). Conley, W.; Miller, D.; Chambers, C.; Obsorn, B.; Hung, R. J.; Tran, H. V.; Trinque, B. C.; Pinnow, M.: Chiba, T.; McDonald, S.; Zimmerman, P.; Dammel, R.; Romano, A.; Willson, C. G. *Proc. SPIE* **2002**, *4690*, 69-75. (d). Conley, W.; Miller, D.; Chambers, C.; Trinque, B. C.; Obsorn, B.; Chiba, T.; McDonald, S.; Zimmerman, P.; Dammel, R.; Romano, A.; Willson, C. G. *J. Photopolym. Sci. Technol.* **2002**, *15*, 613-618.

(31) Chatterjee, A. K.; Choi, T.-L.; Sanders, D. P.; Grubbs, R. H. *J. Am. Chem. Soc.* **2003**, *125*, 11360-11370.

(32) (a). Chatterjee, A. K.; Morgan, J. P.; Scholl, M.; Grubbs, R. H. *J. Am. Chem. Soc.* **2000**, *122*, 3783-3784. (b). Choi, T.-L.; Chatterjee, A. K.; Grubbs, R. H. *Angew. Chem. Int. Ed.* **2001**, *40*, 1277-1279. (c). Chatterjee, A. K.; Choi, T.-L.; Grubbs, R. H. *Synlett.* **2001**, 1034-1037. (d). Chatterjee, A. K.; Grubbs, R. H. *Angew. Chem. Int. Ed.* **2002**, *41*, 3171-3174. (e). Connon, S. J.; Blechert, S. *Angew. Chem. Int. Ed.* **2003**, *42*, 1900-1923.

(33) Bott, G.; Field, L. D.; Sternhell, S. *J. Am. Chem. Soc.* **1980**, *102*, 5618-5626.

(34) Herold, P.; Mohr, P.; Tamm, C. *Helv. Chim. Acta* **1983**, *66*, 744-754.

(35) (a). Schmidt, B. *Eur. J. Org. Chem.* **2004**, *9*, 1865-1880. (b). Schmidt, B.; Pohler, M.; Costisella, B. *J. Org. Chem.* **2004**, *69*, 1421-1424. (c). Schmidt, B. *Angew. Chem. Int. Ed.* **2003**, *42,* 4996-4999.

(36) (a). McGrath, D. V.; Grubbs, R. H. *Organometallics* **1994**, *13*, 224-235. (b). Bourgeois, D.; Pancrazi, A.; Nolan, S. P.; Prunet, J. *J. Organomet. Chem.* **2002**, *662*, 247-252.

(37) (a). Dinger, M. B.; Mol, J. C. *Organometallics* **2003**, *22*, 1089-1095. (b). Dinger, M. B.; Mol, J. C. *Eur. J. Inorg. Chem.* **2003**, 2827-2833. (c). Banti, D.; Mol, J. C. *J. Organomet. Chem.* **2004**, *689*, 3113-3116. (d). Schmidt, B. *J. Org. Chem.* **2004**, *69*, 7672-7687.

(38) Hong, S. H.; Day, M. W.; Grubbs, R. H. *J. Am. Chem. Soc.* **2004**, *126*, 7414-7415.

(39) Pederson, R. L.; Fellows, I. M.; Ung, T. A.; Ishihara, H.; Hajela, S. *Adv. Synth. Catal.* **2002**, *344*, 728-735.

(40) Morgan, J. P.; Grubbs, R. H. *Org. Lett.* **2000**, *2*, 3153-3155.

(41) Pederson, R. C.; Lee, C.-W., Hong, S. H.; Sanders, D. P.; Grubbs, R. H. *Pat. Appl.* **2004**.

(42) Kobuke, Y.; Fueno, T.; Furukawa, J.; *J. Am. Chem. Soc.* **1970**, *92*, 6548-6553.

(43) (a). Pinnow, M.J.; Noyes, B.F., III; Tran, H.V.; Tattersall, P.I.; Cho, S.; Klopp, J.M.; Bensel, N.; Frechet, J.M.J.; Sanders, D.P.; Grubbs, R.H.; Willson, C.G. *PMSE Prepr*. **2002**, *87*, 403. (b). Kim, J. B.; Lee, J. J. *Polymer* **2002**, *43*, 1963-1967.

(44) (a). Ikeda, T.; Yue, S.; Hutchinson, C. R. *J. Org. Chem.* **1985**, *50*, 5193-5199. (b). Inukai, T.; Kojima, T. *J. Org. Chem.* **1966**, *31*, 2032-2033.

(45) (a). Bonadies, F.; Di Fabio, R.; Bonini, C. *J. Org. Chem.* **1984**, *49*, 1647-1649. (b). Bonadies, F.; Bonini, C. *Synth. Commun.* **1988**, *49*, 1573-1580.

(46) (a). Zeifman, Y. V.; Gambaryan, N. P.; Knunyants, I. L. *Izvestiya Akademii Nauk. SSSR Ser. Kimicheskaya* **1965**, *8*, 1472-1474. (b). Linn, W. J. *J. Org. Chem.* **1964**, *29*, 3111-3113.

(47) Chidambaram, N.; Satyanarayana, K.; Chandrasekaran, S. *Tetrahedron Lett.* **1989**, *30*, 2429-2432.

(48) Pangborn, A. B.; Giardello, M. A.; Grubbs, R. H.; Rosen, R. K. Trimmers, F. J. *Organometallics* **1996**, *15*, 1518-1520.

(49) Sanford, M. S.; Love, J. A.; Grubbs, R. H. *Organometallics* **2001**, *20*, 5314-5318.

(50) Masuyama, Y.; Saeki, K.; Horiguchi, S.; Kurusu, Y. *Synlett.* **2001**, *11*, 1802-1804.

(51) Herold, P.; Mohr, P.; Tamm, C. *Helv. Chim. Acta.* **1983**, *66*, 744-754.

CHAPTER 7

Formation of Trisubstituted Olefins via Ruthenium-Catalyzed Cross-Metathesis

Formation of Trisubstituted Olefins via Ruthenium-Catalyzed Cross-Metathesis

Abstract Symmetric trisubstituted alkenes can be prepared via intermolecular olefin cross-metathesis between α-olefins and isobutylene using a second-generation ruthenium benzylidene catalyst. Mechanistic studies of the reaction pathway in isobutylene cross-metathesis reveal that formation of the ruthenium isopropylidene is kinetically favored over the formation of the ruthenium methylidene. In order to kinetically favor the desired cross-metathesis product, 2-methyl-2-butene was employed as an isobutylene surrogate. Cross-metathesis of 2-methyl-2-butene with a variety of α-olefins constitutes a particularly mild and effective method to generate isoprenoid/prenyl groups, requiring only benchtop manipulations, standard glassware, low (room) temperatures, and low catalyst loadings. Understanding of the reactivity patterns of geminally-disubstituted and trisubstituted olefins in cross-metathesis has allowed the formation of trisubstituted olefins via the ring-opening cross-metathesis of low strain cyclic olefins and three-component cross-metathesis reactions.

Introduction

The development of new synthetic methods to create trisubstituted olefins remains an ongoing challenge in synthetic organic chemistry as trisubstituted olefins are present in a wide range of natural products and other molecules of biological and medicinal interest. While Wittig olefinations remain the most commonly used method to synthesized trisubstituted olefins,[1] olefin cross-metathesis (CM) offers a mild and convenient route to these structures that is orthogonal to Wittig chemistry. The commercial availability of well-defined single-component homogeneous olefin metathesis catalysts,[2] such as the molybdenum imido catalyst **7.1** (Figure 7.1) developed by Schrock *et al.*,[3] and ruthenium benzylidene catalyst **7.2** developed by Grubbs *et al.*,[4] has helped olefin metathesis gain prominence in synthetic organic chemistry as a facile methodology for

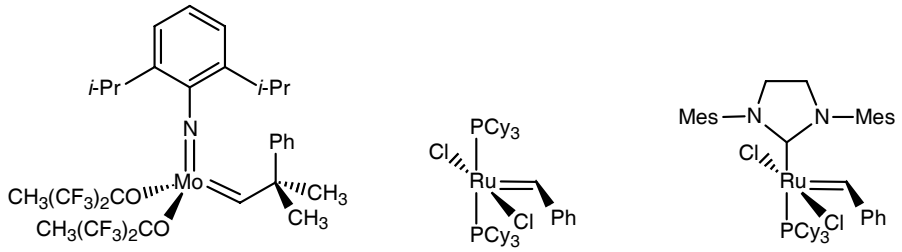

7.1 **7.2** **7.3**

Figure 7.1. Olefin metathesis catalysts

olefin formation.[5,6] In particular, the combination of high activity and high functional group tolerance of late transition metal ruthenium metathesis catalysts such as **7.2** and **7.3**[7] has made the olefin metathesis reaction practical for small molecule and natural product synthesis.

The molybdenum imido catalyst **7.1** displays mixed reactivities toward 1,1-disubstituted olefins. While Wagener *et al.* showed this catalyst was able to polymerize 2-methyl-1,5-hexadiene via acyclic diene metathesis (ADMET) polymerization to reasonable molecular weights,[8] Crowe *et al.* found during cross-metathesis of the same diene with styrene that the geminally disubstituted olefin was unreactive (Figure 7.2).[9]

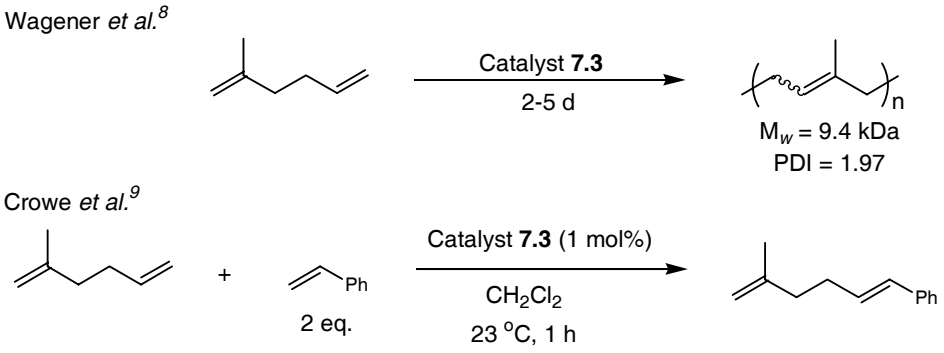

Figure 7.2. Reactivity of 1,1-disubstituted olefins in cross-metathesis with **7.3**

Ring-closing metathesis (RCM) reactions have been widely utilized in the construction of a variety of organic molecules.[6,10] The ring-closing metathesis activity of catalysts **7.1-3** with a

variety of substrates was examined by Grubbs *et al.*, as shown in Table **7.1**.[7a] While the molybdenum catalyst **7.1** is able to form even tetrasubstituted olefins via RCM, the less reactive bisphosphine-based ruthenium catalyst **7.2** affords only low yields of trisubstituted product and cannot form tetrasubstituted olefins. Fortunately, the development of *N*-heterocyclic carbene-based "second-generation" ruthenium metathesis catalysts such as **7.3** has resulted in catalysts with higher functional group tolerance than **7.2**, yet recovering much (if not all) of the activity loss associated with moving to a late transition metal.[2b,7] Catalyst **7.3** can produce trisubstituted olefins via RCM easily and can afford moderate yields of tetrasubstituted products as well. This

Table 7.1. Formation of substituted olefins via ring-closing metathesis[7a]

Substrate	Product	Time	^{1}H NMR Conversion 7.1	7.2	7.3
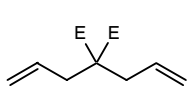	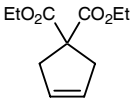	10 min	quant.	quant.	quant.
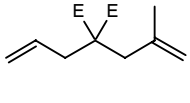	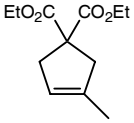	10 min	quant.	20 %	quant.
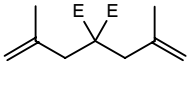	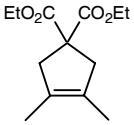	24 h	93 %	0 %	31 %

E = CO_2Et

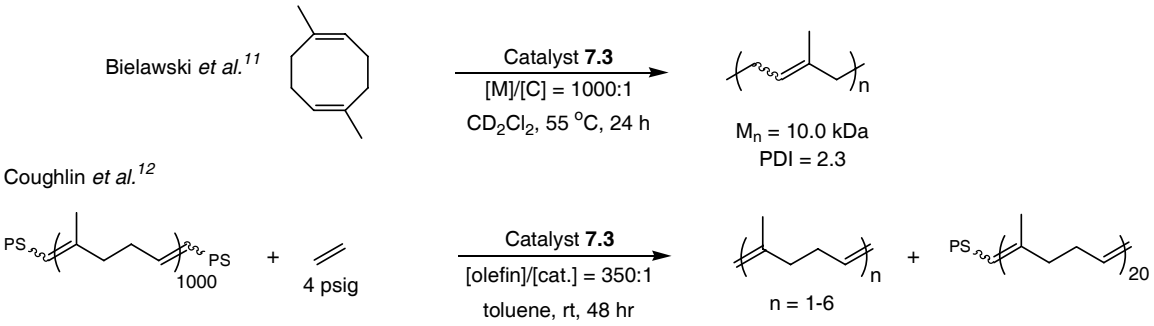

Figure 7.3. Polyisoprene structures in olefin metathesis catalyzed by **7.3**

increased tolerance to olefin substitution by **7.3** is also illustrated by its ability to polymerize 1,5-dimethyl-1,5-cyclooctadiene to form poly-1,4-isoprene[11] and to depolymerize poly(styrene-*b*-1,4-isoprene) in the presence of ethylene to polystyrene and polyisoprene oligomers (Figure 7.3).[12]

Formation of Trisubstituted Olefins via Cross-Metathesis The high functional group tolerance of **7.3**, coupled with its high reactivity with more substituted olefins, has renewed interest in the formation of trisubstituted olefins via intermolecular cross-metathesis.[1] Initial explorations showed that catalyst **7.3** is able to catalyze the formation of trisubstituted olefins from geminally disubstituted olefins with a wide variety of terminal olefins, including α,β-unsaturated carbonyl compounds, some of which are shown in Table 7.2.[1,13,14] Unfortunately, the low stereoselectivities of these reactions (an issue that has long complicated the use of cross-metathesis as a general synthetic technique) reduces the synthetic utility of the cross-metathesis approach.[5,15]

Table 7.2. Synthesis of trisubstituted olefins via cross-metathesis[1,13,14]

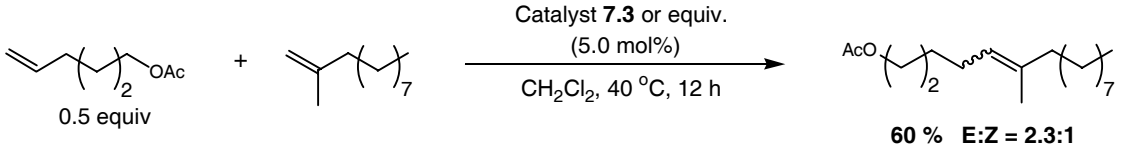

α-Olefin	1,1-Disubstituted Olefin	Product	Yield (%)	E/Z ratio
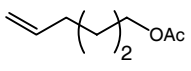	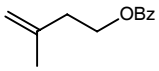	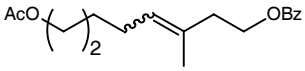	80	2.8:1
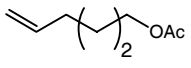	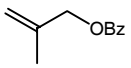	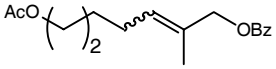	81	4.1:1
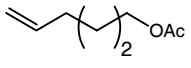	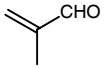	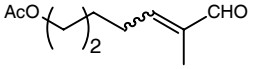	92	> 20:1
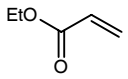	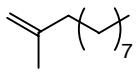	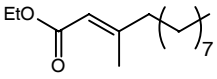	55	2:1

However, cross-metathesis reactions using disubstituted olefins with identical geminal substituents are not complicated by the issue of poor stereoselectivity. A number of 1,1-disubstituted olefins have been successfully employed in cross-metathesis using catalyst **7.3,** with isobutylene being the most important and convenient example.[16] Most importantly, these reactions offer a synthetically convenient alternative to Wittig-type olefinations of aldehydes in the formation of prenyl groups. A number of examples of cross-metathesis performed in neat isobutylene are shown in Table 7.3.[16] Although a small amount of tetramethylethylene (2,3-dimethyl-2-butene) was formed during the reaction, this background reaction did not lower overall cross-metathesis efficiency. The inability of isobutylene to undergo homodimerization via CM allows it to serve both as a reaction solvent and as an effective cross partner. This is evidenced by the very low amount of catalyst loading required relative to the amount of bulk olefin in the reaction (~ 0.0001 eq.).

Table 7.3. Cross-metathesis with isobutylene[16]

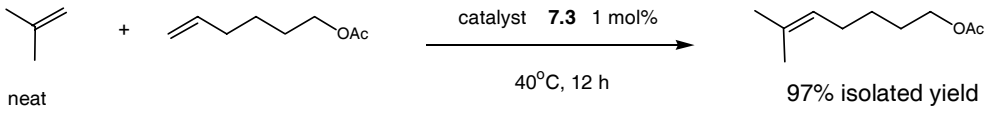

Entry	Metathesis Partner	Product	Isolated Yield
1	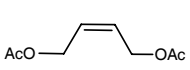	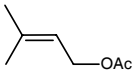	88
2	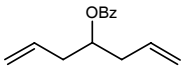	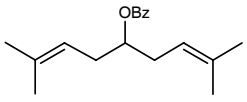	96
3	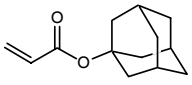	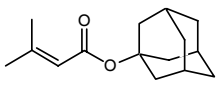	83
4	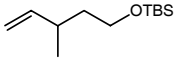	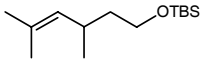	72
5	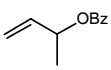	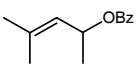	99

As a general synthetic technique, formation of trisubstituted olefins by ruthenium-catalyzed cross-metathesis is limited by the generally poor tolerance to geminal substituents larger than a methyl group.[1,13,14] In order to tune the ligand system of **7.3** to accommodate bulkier substituents or afford higher stereoselectivities, a more detailed understanding of the mechanistic pathway involved in this reaction is required. Isobutylene, with its low cost, ready availability, and symmetric structure, is the most promising geminally disubstituted olefin for use as a probe into the intricacies of this catalytic process.

Results and Discussion

Systematic evaluation of a wide variety of cross-metathesis reactions with a number of commercially available catalysts has enabled a general ranking of olefin reactivities to be established.[14] Since the actual catalytic process involves numerous ruthenium alkylidene intermediates reacting with starting materials to form products, undergoing degenerate metathesis, and performing secondary metathesis on product olefins, a complete understanding of the mechanistic pathways responsible for product formation requires a detailed analysis of a vary large number of substrate and catalyst specific rate constants. The empirical olefin categorization approach dramatically simplifies this analysis by generalizing reactivities of classes of olefins in terms of the accessibility of their respective ruthenium alkylidenes, their rates of homodimerization, and the susceptibility of their homodimers to undergo secondary metathesis events (Figure 7.4).[14]

Understanding of reactivities of general classes of olefin reactivities allows the prediction of product selective cross-metathesis reactions and facilitates the planning of cross-metathesis reactions as part of a larger synthetic effort. Selective reactions occur when olefins of different reactivities are employed in a cross-metathesis reaction. Since the less reactive olefin can only be consumed in reactions with the more reactive olefin (or its homodimer), as the reaction is driven to completion by the removal of ethylene the product mixture is driven towards the desired cross-product (Figure 7.5).[14]

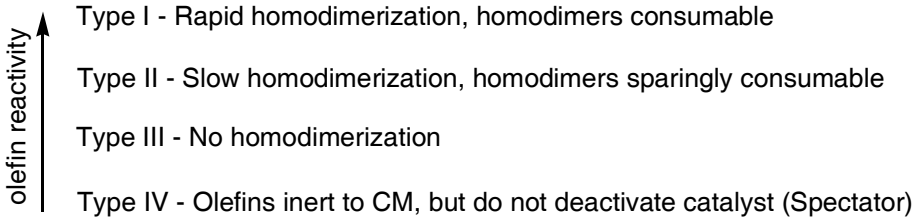

Reaction between two olefins of Type I = *Statistical CM*
Reaction between two olefins of same type (Type II or III) = *Non-selective CM*
Reaction between olefins of two different types = *Selective CM*

Figure 7.4. Olefin categorization and rules for product selectivity[14]

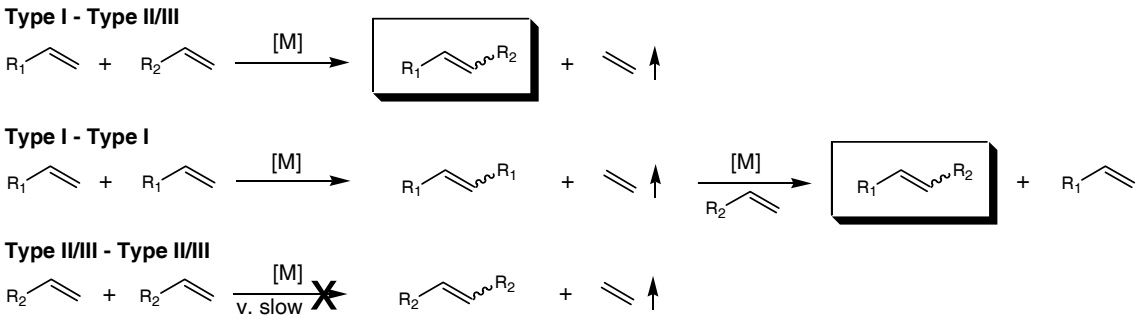

Figure 7.5. Primary reactions in cross-metathesis of Type I with Type II/III olefins[14]

While this approach is useful as a general guide towards the successful application of olefin metathesis in organic synthesis, it offers insufficient insight into the actual catalytic process upon which to base ligand and catalyst design decisions. In order to develop catalysts (i.e., ligand sets) with higher stereoselectivities, it would be useful to understand if the primary mechanistic pathway(s) involves coordination of the 1,1-disubstituted olefin to the monosubstituted ruthenium alkylidene, coordination of the α-olefin to the geminally disusbstituted ruthenium alkylidene, or both.

Kinetic Products of Catalyst Reactions with Substituted Olefins Consistent with earlier findings,[4b] the kinetic reaction product of ruthenium catalysts **7.3** with a simple terminal olefin such as propene (or *cis*-2-butene) is the formation of the ruthenium ethylidene **7.4** and styrene

(Figure 7.6). Because this pseudo-degenerate alkylidene "exchange" reaction is kinetically favored, CM reactions are driven to completion using Le Chatlier's principle (in this case, the removal of ethylene from the system). Only after extended reaction time was the ruthenium methylidene **7.5** characteristic of a productive metathesis event observed. The ability of olefins such as 3,3-dimethyl-1-butene to participate in CM reactions, yet not react to form the *t*-butyl-substituted ruthenium alkylidene, was rationalized by the ability of the metallacycle to form with the bulky *t*-butyl group located on the opposite corner of the metallacyclobutane ring.[4b] Because of the additional bulk of the geminal methyl groups of isobutylene, it was presumed that similar behavior would predominate and result in the formation of the ruthenium methylidene as the kinetic and thermodynamic product of the reaction between **7.3** and isobutylene. Surprisingly, NMR experiments showed that the ruthenium isopropylidene **7.6** was formed as the kinetic

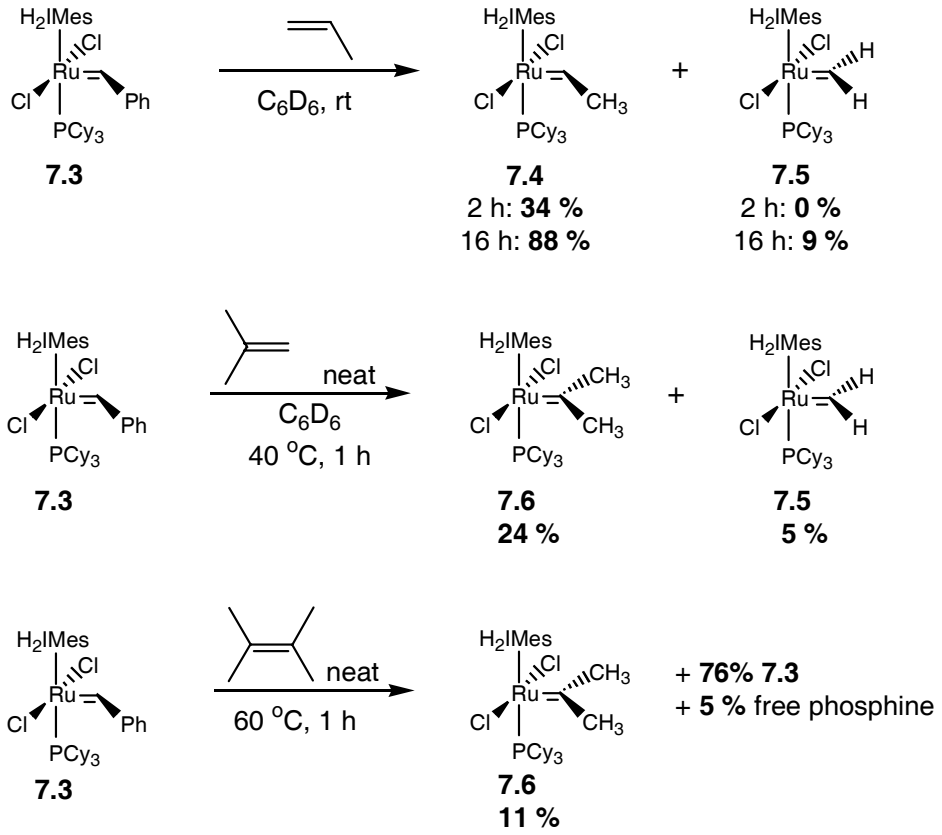

Figure 7.6. NMR initiation experiments with substituted olefins

product. Consistent with the low overall reactivity of isobutylene, this initiation reaction required heating at moderate temperatures for extended reaction times to achieve moderate conversions. Apparently, the additional sterics imparted by the geminal methyl groups is insufficient to disfavor the formation of the more electron rich ruthenium isopropylidene. During the extended reactions, **7.6** was observed to react with additional isobutylene to form 2,3-dimethyl-2-butene and methylidene **7.5.** Isopropylidene **7.6**, unlike the ruthenium benzylidenes **7.3**, is relatively unstable and could not be isolated by column chromatography from **7.5** and residual **7.3**. Use of more reactive catalysts such as the triphenylphosphine and bispyridine-based catalysts (**7.7** and **7.8**, respectively (Figure 7.7) led only to an acceleration of the overall process. The rates of initiation (L-type ligand dissociation) and further reaction are apparently similar between the benzylidene and isopropylidene.[17] Interestingly, NMR tube experiments show that the bisphosphine catalyst **7.2** also forms the isopropylidene as the kinetic product. If catalyst **7.2** can form the isopropylidene, it begs the question why this catalyst is unable to perform productive cross-metathesis with isobutylene.

Catalyst **7.3** was also able to initiate with the tetrasubstituted olefin 2,3-dimethyl-2-butene, albeit at higher temperatures and longer reaction times with low efficiency. This indicates the facile formation and reaction of tetrasubstituted olefins via intermolecular cross-metathesis is a future possibility. Catalyst **7.3** has sufficient reactivity to perform the reaction; however, the mesityl groups are perhaps too bulky to accommodate the additional sterics of the

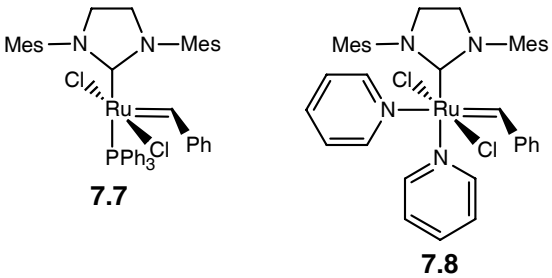

Figure 7.7. Metathesis catalysts with faster initiation rates

heavily substituted metallacycle. A number of approaches to scale back ligand bulk and enable the synthetically useful formation of tetrasubstituted olefins via RCM and CM are underway in our lab.[18]

Cross-Metathesis with 2-Methyl-2-Butene While the rate of reaction of **7.3** with simple terminal olefins is significantly higher than with isobutylene, the huge excess of isobutylene likely renders this process competitive. Unfortunately, the kinetic products of these reactions are not the desired cross-products. In order to design a reaction in which the *gem*-dimethyl groups would be transferred to the product olefin in the kinetic product, we sought to take advantage of the preference of the ruthenium catalysts to form electron rich alkylidenes while being tolerant of the bulk of a simple methyl group. 2-Methyl-2-butene seemed to be an ideal isobutylene surrogate for these types of cross-metathesis reactions. Reaction with the terminal olefin cross-partner should be much faster than with the trisubstituted olefin, ensuring a high relative concentration of the desired ruthenium alkylidene. The sterics and electronics of the subsequent metallacyclobutane formation should now lead to the desired cross-product being the kinetic product (as shown in Figure 7.8).

Productive reaction affords ruthenium isopropylidene and methyl-substituted product

Productive reaction affords ruthenium ethylidene and desired product

Figure 7.8. Regiochemistry of metallacyclobutane formation

Reaction of catalyst **7.3** with 2-methyl-2-butene affords exclusive production of the ruthenium ethylidene **7.4** as expected (Figure 7.9). In addition, this reaction proceeds more

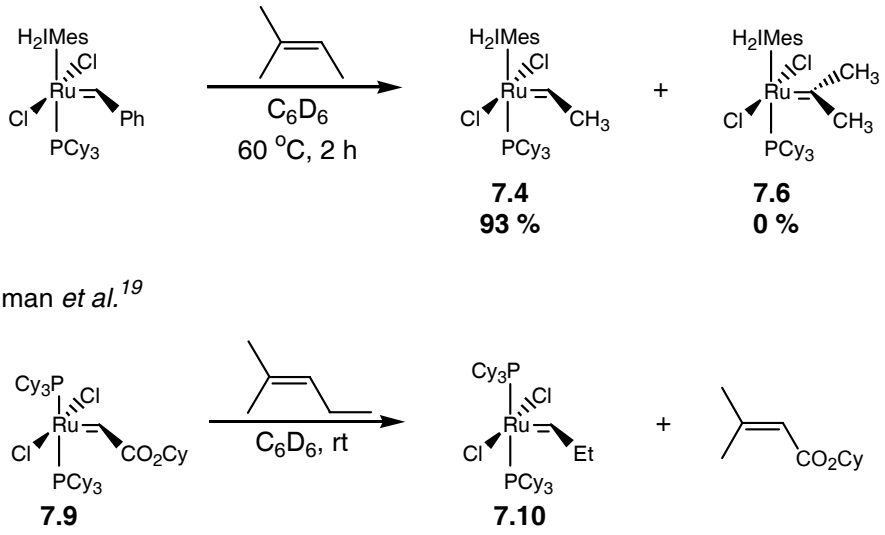

Figure 7.9. NMR initiation experiments with trisubstituted olefins

rapidly than reaction with the disubstituted isobutylene, indicating that benefits of the more electron rich olefin and less bulky resultant alkylidene outweigh the steric hindrance due to the additional methyl group during metallacyclobutane formation. The regioselectivity of the cross-metathesis reaction is identical to that observed by Ulman *et al.* with the bisphosphine-based enoic carbene **7.9**.[19] While the parent catalyst **7.2** was unreactive with trisubstituted olefins, catalyst **7.9** undergoes one turnover with 2-methyl-2-pentene to afford the ruthenium ethylidene **7.10** exclusively.

Unlike the high boiling tetrasubstituted 2,3-dimethyl-2-butene (bp 73 °C), 2-methyl-2-butene (bp 35-38 °C) serves as a synthetically useful isobutylene surrogate in cross-metathesis (Table 7.4).[16] The higher boiling point of 2-methyl-2-butene relative to isobutylene allows for reactions to be run with a standard reflux condenser rather than in more specialized pressure vessels and the higher reactivity of 2-methyl-2-butene allows reactions to be run efficiently at room temperature with lower catalyst loadings (~1 mol%). In addition to greatly enhancing the synthetic ease of the reaction relative to the use of isobutylene, this use of 2-methyl-2-butene represents the first productive CM of trisubstituted olefins at room temperature. Cross-metathesis

Table 7.4. Cross-metathesis with 2-methyl-2-butene[16]

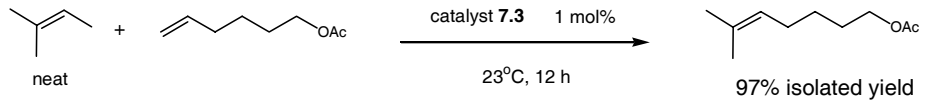

Entry	Metathesis Partner	Product	Isolated Yield
1	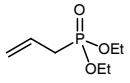	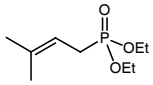	97
2	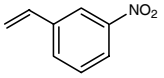	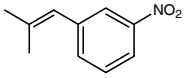	96
3	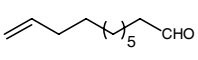	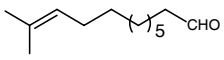	91
4	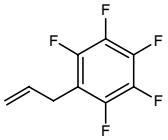	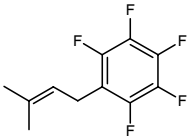	91
5	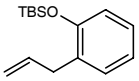	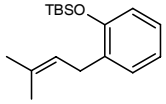	99

with diethyl allylphosphonate (Entry 1, Table 7.4) affords diethyl prenylphosphonate, a useful Wittig-type reagent. Unprotected aldehydes are readily tolerated as well, illustrating the direct orthogonality of this cross-metathesis approach to Wittig methods (Entry 4, Table 7.4). Perhaps the most important example is the CM reaction with a protected phenolic allylbenzene, affording nearly quantitative yields of the prenyl compound (Entry 5 Table 7.4). This cross-metathesis reaction is a convenient alternative to the standard synthetic route involving the Claisen rearrangement of a tertiary allylic phenoxy ether.

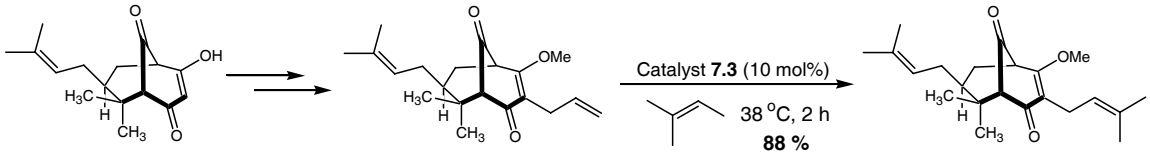

Figure 7.10. Synthesis of polyprenylated core of Garsubellin A[20]

This CM methodology has been employed by Stoltz *et al.* in the synthesis of the bicyclic core of the polyprenylated phloroglucin natural product Garsubellin A (as shown in Figure 7.10). In this synthesis, installation of an allyl group via a simple alkylation is followed by a Claisen rearrangement. Conversion of the allyl group to a prenyl group was achieved in high yield via cross-metathesis with 2-methyl-2-butene. This masking of prenyl groups as more robust allyl groups capable of being converted to prenyl groups via metathesis with 2-methyl-2-butene is being considered as the end-game strategy of other planned syntheses of polycyclic polyprenylated acylphloroglucinols.[21]

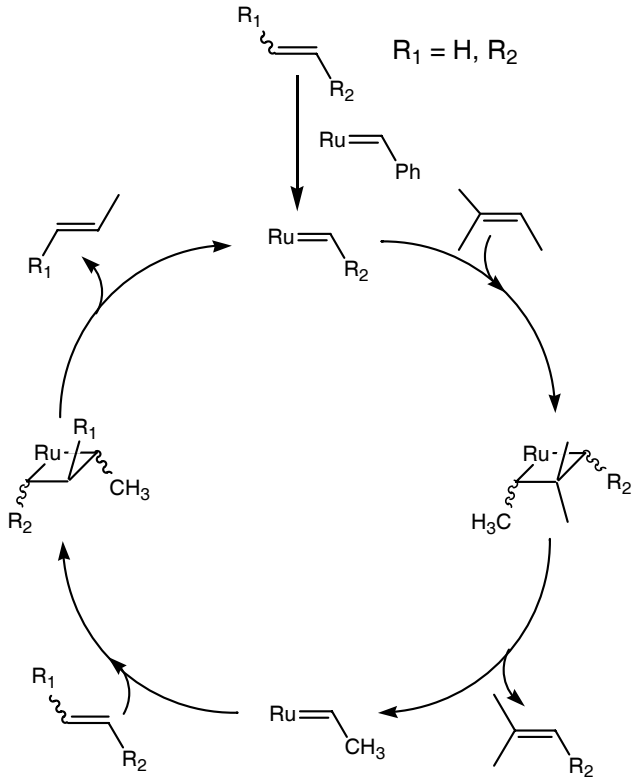

Figure 7.11. Proposed 2-methyl-2-butene cross-metathesis reaction pathway

These results indicate that the general reaction pathway for 2-methyl-2-butene cross-metathesis is that shown in Figure 7.11. Due to the higher reactivity of terminal olefins towards

CM, a significant portion of the terminal olefin may homodimerize via self-metathesis before the CM reaction with 2-methyl-2-butene (represented by $R_1 = R_2$). However, these homodimers are still generally more reactive than a trisubstituted olefin, ensuring facile access to the appropriately substituted ruthenium alkylidene. Cross-metathesis with 2-methyl-2-butene produces the ruthenium ethylidene and the geminally dimethyl-substituted product. Depending upon the nature of R_2, this trisubstituted olefin may be kinetically resistant to further metathesis. The ruthenium ethylidene reacts with another equivalent of olefin to regenerate the appropriate ruthenium alkylidene and release a methyl-substituted olefin. In the case where R_1 = H or CH_3, this volatile propene or 2-butene boils off at room temperature effectively removing the methyl endgroups from the reaction and driving the reaction towards the desired product. Higher molecular weight homologues of 2-methyl-2-butene such as 2-methyl-2-pentene and 2-methyl-2-hexene may be used as well; however, the higher boiling butene and pentene fragments are more difficult to drive out of the system at room temperature, resulting in a larger fraction of ethyl- and propyl-substituted products (Table 7.5).

Table 7.5. Cross-metathesis with 2-methyl-2-butene homologues

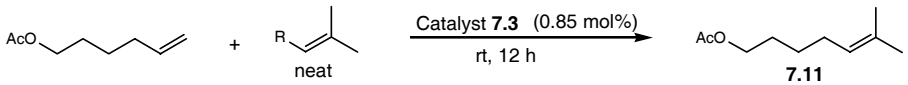

Trisubstituted Olefin	^{1}H NMR Product Distribution				
	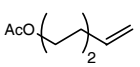 0%	3%	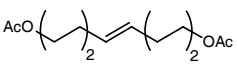 7.12	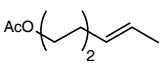 5%	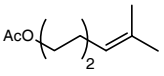 92%
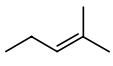	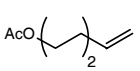 0%		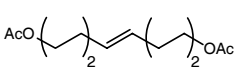 0%	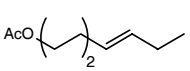 17%	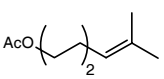 83%
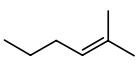	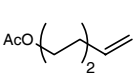 18%		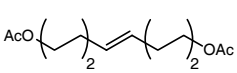 21%	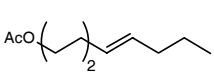	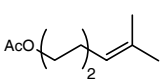 61%

Reaction with 2-methyl-2-butene performed by Arnab K. Chatterjee (Grubbs Group)

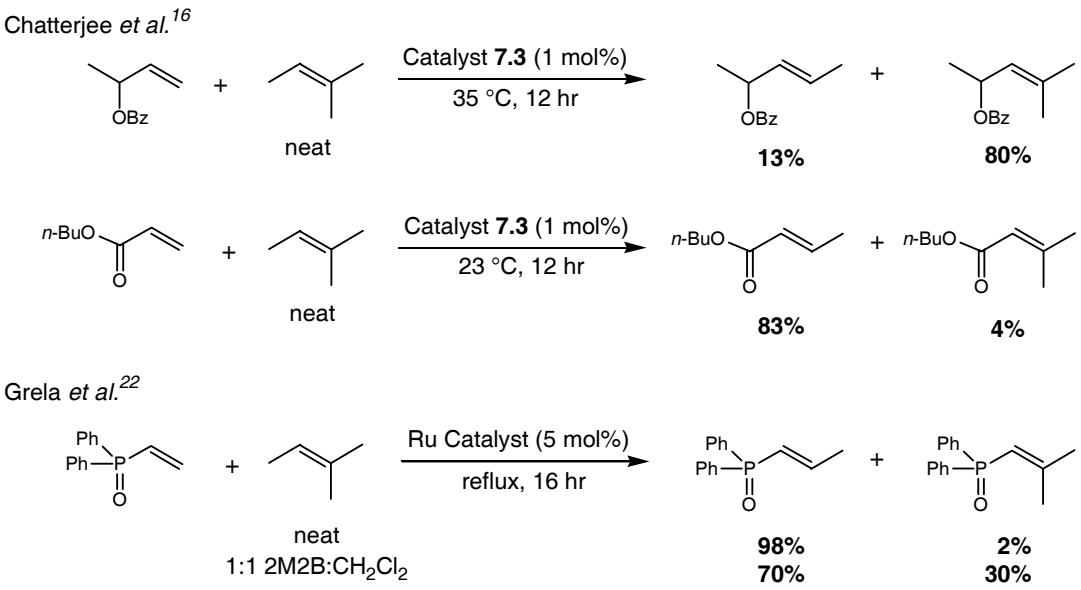

Figure 7.12. 2-Methyl-2-butene cross-metathesis with less active olefins[16]

While cross-metathesis with 2-methyl-2-butene is highly efficient for reactive olefins (Type I olefins), reaction with the less reactive allylic benzoate (Figure 7.12) results in a 6:1 mixture of dimethyl- and methyl-substituted products which cannot be driven to produce the desired cross-product in high conversion.[16] With even more unreactive olefins (Type II olefins, Figure 7.4), a mechanistic reversal is observed. This reversal is exemplified by the cross-metathesis of *n*-butyl acrylate with 2-methyl-2-butene which affords *E*-*n*-butyl crotonate in 83% conversion by ^{1}H-NMR.[16]

Unlike the examples shown in Table 7.4, when it is unfavorable for the terminal olefin to cross onto the ruthenium (such as in the case of acrylates), a second reaction pathway illustrated in Figure 7.13 is primarily responsible for the observed product distribution. In this system, the 2-methyl-2-butene is the more reactive olefin and reacts with the catalyst to produce a ruthenium ethylidene. This ethylidene species undergoes a productive metathesis reaction with the terminal olefin to produce a methyl-substituted olefin and ruthenium methylidene. The methylidene subsequently reacts with the large excess of 2-methyl-2-butene to produce isobutylene and

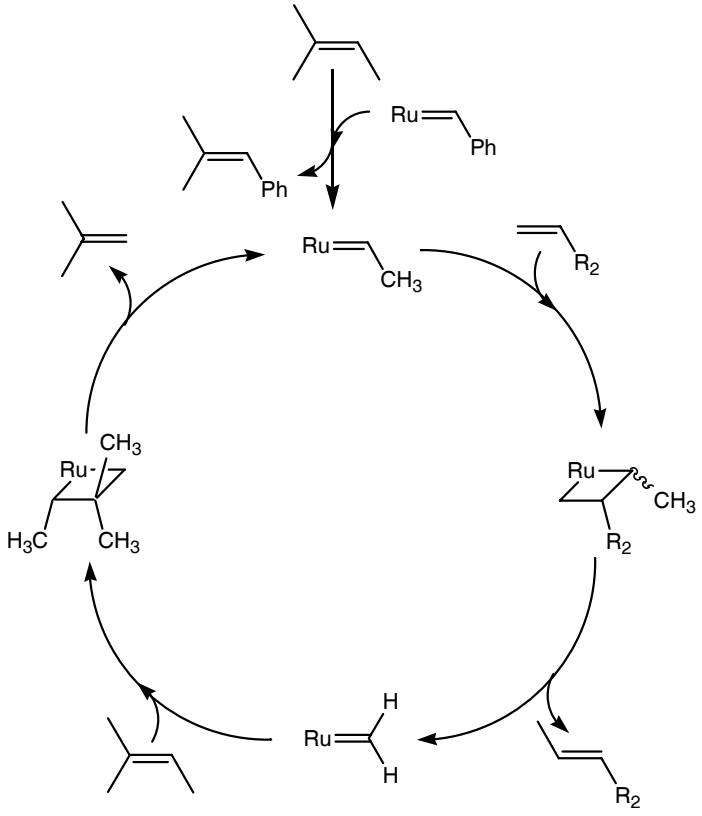

Figure 7.13. Proposed cross-metathesis pathway with less reactive olefins

regenerate the propagating ethylidene. In this pathway, the isobutylene boils off and effectively removes the geminal methyl endgroups from the reaction, resulting in the preferential generation of methyl-substituted olefins. With these less reactive olefinic substrates, the 2-methyl-2- butene may serve as practical substitute for propene or 2-butene in cross-metathesis. In terms of the categorization model discussed previously, 2-methyl-2-butene lies somewhere on the boundary between Types II and III. It serves as a moderately reactive Type III olefin when reacting with Type I and Type II olefins; however, its ability to form a new ruthenium ethylidene by reacting with the catalyst presumably will allow it to act like a Type II olefin during reaction with Type III olefins.

Grela *et al.* have subsequently employed this methodology in the synthesis of diphenyl-(*Z)*-prop-1-enyl phosphine oxide from diphenyl vinylphosphine oxide (Figure 7.12).[22] Using neat

2-methyl-2-butene, the methyl to dimethyl-substituted product ratio was 98:2; however, using less trisubstituted olefin (1:1 2-methyl-2-butene:CH_2Cl_2) resulted in a significantly higher ratio of disubstituted product (70:30).[22] Grela's results offer additional support for the mechanistic pathways for metathesis with 2-methyl-2-butene outlined here.

In order to convert simple terminal olefins into prenyl groups, cross-metathesis with 2-methyl-2-butene is the preferred methodology. However, given the inability to separate the methyl-substituted products via standard silica gel chromatography, cross-metathesis with isobutylene is the preferred route to the desired cross-product with substrates that form methyl-substituted products resistant to secondary metathesis and the only route to exclusively dimethyl-substituted products when less reactive olefins (such as Type II olefins) are used.

Formation of Trisubstituted Olefins via Ring-Opening Cross Metathesis Ring-opening cross-metathesis (ROCM) involves the ring-opening metathesis of a cyclic olefin in the presence of an acyclic olefin to generate a ring-opened structure with functionalized end-groups. Recent work has shown that 5-and 6-membered rings such as cyclopentene and cyclohexene with low ring-strain can be ring-opened in the presence of an electron deficient olefin such as an acylate in moderate yields.[5b, 23] While the equilibria in these reactions lie heavily on the side of the ring-closed starting material, ring-opening reactions which lead to the formation of an electron-deficient olefin such as the α, β-unsaturated ester allow the olefin to resist the secondary metathesis necessary for ring-closing.[24] The high reactivity of the electron-deficient ruthenium enoic carbenes results in the formation of monomeric and ring-opened structures with α, β-unsaturated ester endgroups.[23a] Instead of relying on olefin electronics to afford ring-opened product, use of sterically bulky endgroups should offer similar capabilities. As shown previously, the reluctance of the catalyst to couple *gem*-dimethyl-substituted olefins to form 2,3-dimethyl-2-butene is greater than its reluctance to couple α, β-unsaturated esters to form fumarates or

maleates.[14] Therefore, ROCM of cyclohexene in isobutylene should afford the monomeric 2,9-dimethyl-2,9-decadiene.

The ROCM of cyclooctene and cyclohexene with isobutylene and 2-methyl-2-butene are shown in Table 7.6. The higher ring-strain of cyclooctene results in quantitative conversion of ring-opened product. The lower reactivity of internal olefins slows secondary metathesis and results in a small amount of monomethyl-substituted product in the case of 2-methyl-2-butene. With cyclohexene, only the product with both olefins capped with *gem*-dimethyl groups is sufficiently resistant to subsequent RCM. Both isobutylene and 2-methyl-2-butene offer similar conversions under identical conditions (pressure vessel, 40 °C). These results are comparable to the results of ROCM using acrylates.[23a,b]

Table 7.6. Ring-opening cross-metathesis of cyclic olefins

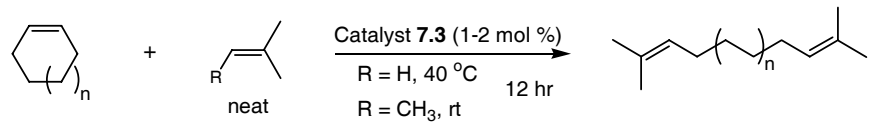

Trisubstituted Olefin	Cyclic Olefin	Products (% isolated yield)
		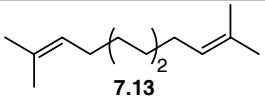 **7.13** **97%**
		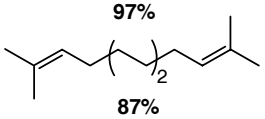 **87%** 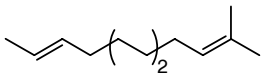 **13%**
		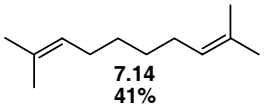 **7.14** **41%**
		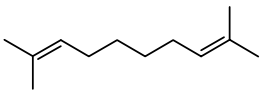 **19%** RT **29%** F-P bottle, 40 °C

ROCM of cyclohexene with isobutylene performed in conjuction with Arnab K. Chatterjee (Grubbs Group)

Three Component Olefin Metathesis Reactions: As mentioned previously, use of the categorization model allows for the design of highly selective cross-metathesis reactions. One of the first reactions to be conceived by this approach was a three component coupling reaction between a Type I α,ω-diene and Type II and Type III olefin.[14] The inability of the Type II and Type III olefins to efficiently couple via metathesis is the key to preventing these olefins from being consumed in non-productive metathesis reactions. The ability of isobutylene to serve as a reactive solvent and as a Type III olefin makes it an ideal choice for such a reaction. Three component coupling reactions between 1,5-hexadiene, isobutylene, and a variety of Type II olefins are shown in Table 7.7.[14] Coupling of a Type I and a Type II olefin to a Type I α,ω-diene in a stepwise reaction (Entry 4, Table 7.7) is considerably less efficient than using a Type III olefin in a simultaneous one-pot strategy (Entries 1-3, Table 7.7).

Table 7.7. Three component cross-metathesis reactions[14]

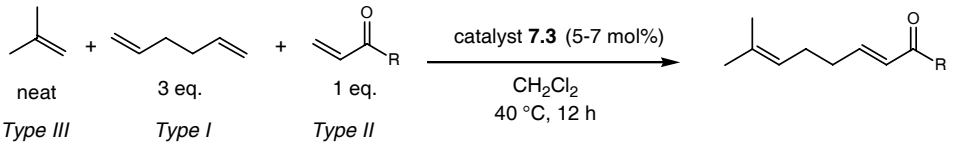

Entry	Method	CM partner Y	CM partner Z	Ratio (Diene:Y:Z)	Product	Isolated Yield (%)
1[a]	A			3:neat:1	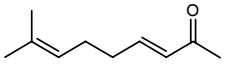 **7.15**	89
2	A		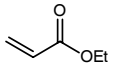	3:neat:1	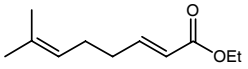 **7.16**	60
3	A		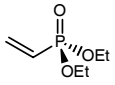	1:neat:1	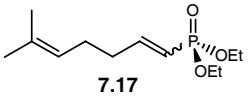 **7.17**	57[b]
4[a]	B		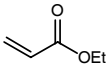	1:3:1	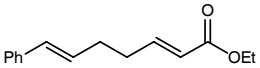 **7.18**	34

[a] Reaction performed by Arnab K. Chatterjee (Grubbs Group) [b] *E/Z* = 8:1 by ^{1}H NMR [c] Reaction at 23 °C
Method A = Added all components at one time
Method B = Added component Z, then added component Y after 4 hours

The origin of the remarkably high product selectivity in the reaction can be understood by looking at the various mechanistic pathways outlined in Figure 7.14. Since the isobutylene solvent is the least active towards metathesis, the majority of the α,ω-diene starting material is preferentially consumed in cross-metathesis reactions with the Type II acrylate or in self-metathesis reactions leading to oligoalkenamers. Stoichiometry is used to ensure roughly one Type II olefin is coupled to each α,ω-diene. The remaining terminal olefins undergo reaction with the Type III olefin. If an α,ω-diene is capped on both ends by *gem*-dimethyl endgroups, these trisubstituted olefins are simple 2-methyl-2-butene homologues which will react regioselectively with the Type II olefin to form the desired product. Presumably, any olefin formed via the reaction of the α,ω- diene with the Type II olefin is the least reactive olefin towards secondary metathesis and redistribution. Since premature coupling of all the isobutylene to form 2,3-dimethyl-2-butene is unlikely, the key limiting reactions (provided the catalyst is

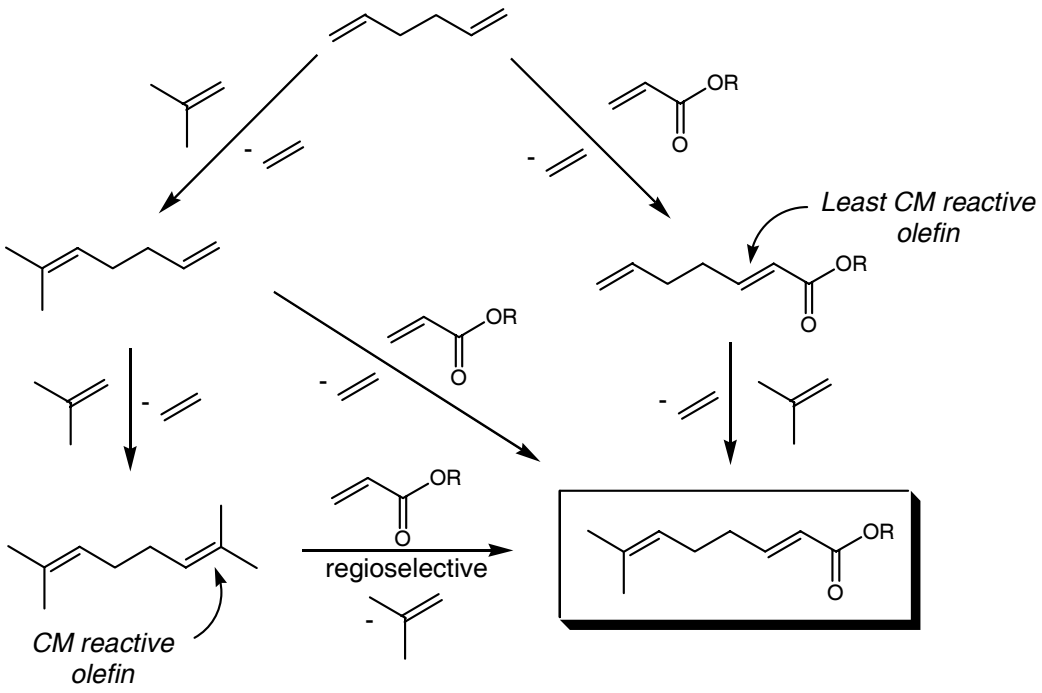

Figure 7.14. Mechanistic pathways for 3-component cross-metathesis reaction

sufficiently long-lived) are the homodimerization of the Type II olefin and cross-metathesis of the Type II olefin with isobutylene, both of which form a product olefin (such as a fumarate) which is kinetically inert to further metathesis.

Conclusions

In conclusion, a mechanistic understanding of the cross-metathesis reactions between isobutylene and terminal olefins employing the ruthenium benzylidenes catalyst **7.3** has been presented. This mechanistic understanding of the reactivity of olefins with various substitution patterns with the ruthenium catalyst has enabled the discovery of the ability of 2-methyl-2-butene to serve as a synthetically convenient surrogate for the gaseous olefins isobutylene or propene/2-butene in cross-metathesis reactions with Type I and Type II olefin cross-partners, respectively. Of particular interest is the convenient conversion of terminal olefins to prenyl groups. In order to achieve exclusively trisubstituted olefin cross-products, the more convenient 2-methyl-2-butene may be employed with reactive terminal olefins; however, the more rigorous route using isobutylene must be employed with less reactive substrates to prevent the formation of 1,2-disubstituted products. Ring-opening cross-metathesis of unstrained cyclic olefins may be achieved using geminally-disubstituted olefin cross-partners. In addition, the unique reactivity of isobutylene and prenyl-type olefins in cross-metathesis has allowed the development of highly product-selective three-component cross-metathesis reactions. In total, these methods allow for the efficient one-step formation of trisubstituted olefins under mild reaction conditions and low catalyst loadings, and further demonstrate the utility of olefin metathesis in organic synthesis.

Experimental

Materials: All air sensitive manipulations and polymerizations were carried out in an N_2-filled drybox or using standard Schlenk techniques. All solvents were rigorously degassed in 18 L reservoirs and passed through two sequential purification columns consisting of activated alumina.[25] All starting materials were procured from Aldrich and used as received unless

otherwise noted. Ruthenium olefin metathesis catalysts **7.2** and **7.3** were obtained from Materia, Inc. Catalysts **7.7** and **7.8** were synthesized according to the literature procedures.[26]

***Methods**:* Nuclear magnetic resonance (NMR) spectra were obtained using a Varian *Mercury 300* spectrometer (^{1}H: 300 MHz, ^{13}C: 75 MHz). Shifts for NMR spectra are reported in ppm relative to the chemical shift of the residual proteo solvent. ^{31}P NMR spectra are reference to an external H_3PO_4 standard ($\delta = 0$). High-resolution mass spectra (EI and FAB) were provided by either the Caltech Mass Spectrometry Facility or the UCLA Mass Spectrometry Facility (University of California, Los Angeles).

Typical Isobutylene Cross-Metathesis Procedure: To an oven dried, 100 mL Fischer-Porter bottle with Teflon stir bar, ruthenium metathesis catalyst (15.0 mg, 0.018 mmol, 1.0 mol%) was added. The bottle was capped with a rubber septum and flushed with dry nitrogen and cooled to -78 °C (or temperature sufficient to freeze substrate). Substrate (1.0 mmol) was injected into the bottle. Once the substrate was frozen, a pressure regulator was attached to the bottle. The bottle was evacuated and backfilled with dry nitrogen 3 times. Subsequently, isobutylene (5-10 mL, 50-100 equiv.) was condensed into the bottle. The bottle was backfilled to ~2 psi with nitrogen, sealed, and allowed to slowly warm to room temperature, at which time it was transferred to an oil bath at 40 °C. After stirring for 12-18 hours, the bottle was removed from the oil bath and allowed to cool to room temperature. The isobutylene was slowly vented off at room temperature until the pressure apparatus could be safely disassembled. The remaining mixture was taken up in organic solvent for subsequent purification via silica gel chromatography and/or spectroscopic characterization.

Typical 2-Methyl-2-Butene Cross-Metathesis Procedure: Substrate (1.5 mmol) and 2-methyl-2-butene (3.2 mL) were added simultaneously via syringe to a flask containing catalyst **7.3** (0.015 mmol, 1.0 mol%) equipped with a reflux condenser under a nitrogen atmosphere. The reaction was allowed to stir at room temperature while cold water was circulated through the reflux

condenser to prevent evaporation of 2-methyl-2-butene. After 12 hours, the reaction mixture was reduced in volume to 0.5 mL and purified directly on a silica gel column to provide the cross-metathesis product.

Typical NMR Initiation Reaction: In a N_2-filled drybox, catalyst **7.3** (15.0 mg, 17.6 μmol) was added to screw-cap NMR tube along with 1 mL of C_6D_6. A teflon septum screwcap was used to seal the NMR tube. The substrate olefin was added to the NMR tube using microsyringe injection for liquid olefins or by bubbling the gaseous olefin through the NMR tube solution for 2-5 minutes with the aid of a long needle attached to the tank regulator. The NMR tube was heated in a temperature-controlled oil bath and removed at designated intervals for spectroscopic analysis.

(H_2Imes)(PCy_3)Cl_2Ru(=CHMe) (7.4). The ruthenium ethylidene was independently synthesized via reaction of **7.3** with cis-2-butene or propene. ^{31}P NMR (C_6D_6): δ = 29.05 (s). ^{1}H NMR (C_6D_6): δ = 19.03 (q, *J* = 5.7 Hz, 1H, Ru=C*H*CH_3), 2.81 (s, 6H, ortho CH_3), 2.57 (s, 6H, ortho CH_3), 2.18 (s, 3H, para CH_3), 2.10 (s, 3H, para CH_3), 1.91 (d, *J* = 5.7 Hz, 3H, Ru=CHC*H*$_3$).

(H_2Imes)(PCy_3)Cl_2Ru(=CH_2) (7.5). For complete spectroscopic characterization of the ruthenium methylidene, see reference 7b.

(H_2Imes)(PCy_3)Cl_2Ru(=C(CH_3)$_2$) (7.6). The ruthenium isopropylidene is extremely air sensitive and decomposes rapidly upon exposure to air. Only moderate amounts of isopropylidene in a mixture of other catalyst species could be obtained. As such, isolation via standard techniques was not possible. The isopropylidene could only be characterized via NMR spectroscopy. The far upfield shift of the tricyclohexylphosphine resonance is consistent with the shift observed by Trnka et al. for a related cyclic disubstituted complex (H_2Imes)(PCy_3)Cl_2Ru(=C(CH_2)$_3$).[27] ^{31}P NMR (C_6D_6): δ = 19.94 (s). ^{1}H NMR (C_6D_6): δ = 2.85 (s, 6H, ortho CH_3), 2.57 (s, 6H, ortho CH_3), 2.26 (s, 6H, Ru=C(C*H*$_3$)$_2$), 2.21 (s, 3H, para CH_3), 2.14 (s, 3H, para CH_3).

Reaction of 5-Hexenyl-1-Acetate with:

(A). 2-Methyl-2-butene. 2-Methyl-2-butene (3.0 mL) and 5-hexenyl-1-acetate (230 μL, 1.47 mmol) were reacted according to the general procedure (see above) using catalyst **7.3** (11 mg, 0.013 mmol, 0.85 mol%) under a nitrogen atmosphere for 12 hours. The flask was allowed to stir at room temperature for 12 hours. ^{1}H NMR analysis of the initial product distribution (analysis of vinylic protons) indicated the presence of 92% 2-methyl-hept-2-enyl-7-acetate (**7.11**), ~ 5% 5-heptenyl-1-acetate (**7.12**), and 3% 1,10-diacetoxy-*trans*-5-decene(**7.13**).

(B). 2-Methyl-2-pentene. 2-Methyl-2-pentene (1.18 g, 1.73 mL) and 5-hexenyl-1-acetate (0.200 g, 220 μL, 1.41 mmol) were reacted according to the general procedure (see above) using catalyst **7.3** (10.2 mg, 0.012 mmol, 0.85 mol%) under a nitrogen atmosphere for 12 hours. The flask was allowed to stir at room temperature for 12 hours. ^{1}H NMR analysis of the initial product distribution (analysis of vinylic protons) indicated the presence of 83% 2-methyl-hept-2-enyl-7-acetate (**7.11**), 17% 5-octenyl-1-acetate (**7.12**).

(C). 2-Methyl-2-hexene. 2-Methyl-2-hexene (3.0 mL) and 5-hexenyl-1-acetate (0.200 g, 220 μL, 1.41 mmol) were reacted according to the general procedure (see above) using catalyst **7.3** (10.2 mg, 0.012 mmol, 0.85 mol%) under a nitrogen atmosphere for 12 hours. The flask was allowed to stir at room temperature for 12 hours. ^{1}H NMR analysis of the initial product distribution (analysis of vinylic protons) indicated the presence of 61% 2-methyl-hept-2-enyl-7-acetate (**7.11**), ~ 21% 5-octenyl-1-acetate/1,10-diacetoxy-*trans*-dec-5-ene(**7.12**), and 18% 5-hexenyl-1-acetate starting material.

2-Methyl-hept-2-enyl-7-acetate (7.11). ^{1}H NMR (300 MHz, $CDCl_3$, ppm): δ 5.10 (tm, J = 5.4 Hz, 1H), 4.06 (2H, t, J = 6.9 Hz), 2.05 (s, 3H), 2.01 (m, 2H), 1.69 (s, 3H), 1.60 (s, 3H), 1.70-1.55 (m, 2H), 1.41-1.31 (m, 2H). R_f = 0.32 (20:1 hexane:ethyl acetate). HRMS-[GC-EI+] (m/z): [M•]+ calc'd for $C_{10}H_{18}O_2$, 170.1307; found, 170.1315.

1,10-Diacetoxy-*trans*-dec-5-ene (7.12). ^{1}H NMR (300 MHz, $CDCl_3$, ppm): δ 5.37 (t, J = 3.6 Hz, 2H, m), 4.02 (4H, t, J = 6.6 Hz, 4H), 2.02 (s, 6H), 2.00 (m, 4H), 1.60(m, 4H), 1.38 (m, 4H). R_f = 0.31 (85:15 hexane:ethyl acetate). ^{13}C NMR ($CDCl_3$, 75 MHz, ppm): δ 171.41, 130.40, 64.63, 32.25, 28.21, 25,96, 21.17. HRMS-[GC-EI+] (m/z): [M•]+ calc'd for $C_{14}H_{24}O_4$, 256.1675; found, 256.1664.

Ring-Opening Cross-Metathesis of Cyclic Olefins:

2,11-Dimethyl-dodeca-2,10-diene (7.13). ^{1}H NMR (300 MHz, $CDCl_3$, ppm): δ 5.13 (t, J = 2.5 Hz, 2H), 1.97 (d, J = 6.9 Hz, 4H), 1.69 (s, 6H), 1.61 (s, 6H), 1.29 (m, 8H). R_f = 0.87 (20:1 hexane:ethyl acetate). ^{13}C NMR ($CDCl_3$, 75 MHz, ppm): δ 131.29, 125.13, 30.08, 29.44, 28.23, 25.91, 17.85. HRMS-[GC-EI+] (m/z): [M•]+ calc'd for $C_{14}H_{26}$, 194.2035; found, 194.2038.

2,9-Dimethyl-deca-2,8-diene (7.14). ^{1}H NMR (300 MHz, $CDCl_3$, ppm): δ 5.13 (t, J = 2.5 Hz, 2H), 1.97 (d, J = 6.9 Hz, 4H), 1.70 (s, 6H), 1.61 (s, 6H), 1.33 (m, 4H). R_f = 0.90 (20:1 hexane:ethyl acetate). HRMS-[GC-EI+] (m/z): [M•]+ calc'd for $C_{12}H_{22}$, 166.1722; found, 166.1707.

Three Component Cross-Metathesis Reactions:

For characterization of **7.15** and **7.18**, see reference 14.

9-Methyl-deca-2,8-dienoic acid ethyl ester (7.16). 1,5-Hexadiene (266 μL, 2.25 mmol) and ethyl acrylate (81 μL, 0.75 mmol) were reacted with catalyst **7.3** (31.8 mg, 0.037 mmol, 5.0 mol%) according to the general isobutylene cross-metathesis procedure. After 12 hours at 40 °C, the reaction mixture was then reduced in volume to 0.5 ml and purified directly on a silica gel column (4x15 cm), eluting with 20:1 pentanes:diethyl ether to afford a clear oil (82 mg, 0.45 mmol, 60% yield). ^{1}H NMR (300 MHz, $CDCl_3$, ppm): δ 6.92 (dt, J = 15.6, 6.3 Hz, 1H), 5.77 (dt, J = 15.6, 1.5 Hz, 1H), 5.12-5.02 (m, 1H), 4.13 (q, J = 7.2 Hz, 2H), 2.26-2.05 (m, 4H), 1.64 (s, 3H), 1.56 (s, 3H), 1.24 (t, J = 7.8 Hz, 3H). ^{13}C NMR (75 MHz, $CDCl_3$, ppm): δ 166.85, 149.08,

132.86, 123.04, 121.56, 60.25, 32.59, 26.73, 25.80, 17.85, 14.41. R_f = 0.39 (20:1 hexane:ethyl acetate). HRMS (GC-EI) calcd for $C_{11}H_{18}O_2$ [M•] 182.1307, found 182.1314.

(8-Methyl-nona-1,7-dienyl)-phosphonic acid diethyl ester (7.17). 1,5-Hexadiene (266 μL, 2.25 mmol) and diethyl vinyl phosphonate (115 μL, 0.75 mmol) were reacted with catalyst **7.3** (31.8 mg, 0.037 mmol, 5.0 mol%) according to the general isobutylene cross-metathesis procedure. After 12 hours at 40 °C, the reaction mixture was then reduced in volume to 0.5 ml and purified directly on a silica gel column (4x15 cm), eluting with 1:2 hexane:ethyl acetate to afford a clear oil (104 mg, 0.427. mmol, 57% yield) *E:Z* = 8:1. *E* isomer: ^{1}H NMR (300 MHz, $CDCl_3$, ppm): δ 6.85-6.60 (m, 1H), 5.59 (dd, *J* = 21.3, 17.1 Hz, 1H,), 5.10-4.95 (m,1H), 4.01 (q, *J* = 7.2 Hz, 4H,), 2.35-2.00 (m, 4H), 1.62 (s, 3H), 1.54 (s, 3H), 1.26 (t, *J* = 7.2 Hz, 3H). ^{13}C NMR (75 MHz, $CDCl_3$, ppm): δ 153.66, 132.89, 122.92, 117.07 (d, *J* = 186 Hz), 61.73, 53.58, 34.58, 34.30, 26.47, 25.79, 17.87, 16.53. ^{31}P NMR (121 MHz, $CDCl_3$, ppm): δ 19.85. R_f = 0.24 (1:2 hexane:ethyl acetate). HRMS (FAB) calcd for $C_{12}H_{24}O_3P$ $[M + H]^+$ 247.1463, found 247.1455.

References and Notes

(1) Chatterjee, A. K.; Grubbs, R. H. *Org. Lett.* **1999**, *1*, 1751-1753 and references therein.

(2) For recent reviews on development of olefin metathesis catalysts, see: (a). Schrock, R. R. In *Handbook of Olefin Metathesis*, vol 1., Grubbs, R. H., Ed. Wiley-VCH, **2004**, pp. 8-32. (b). Nguyen, S. T..; Trnka, T. M. In *Handbook of Olefin Metathesis*, vol 1., Grubbs, R. H., Ed. Wiley-VCH, **2004**, pp. 61-85. (c). Grubbs, R. H. *Tetrahedron* **2004**, *60*, 7117-7140. (d). Trnka, T. M.; Grubbs, R. H. *Acc. Chem. Res.* **2001**, *34*, 18-29.

(3) (a). Schrock, R. R.; Murdzek, J. S.; Bazan, G. C.; Robbins, J.; Dimare, M.; O'Regan, M. *J. Am. Chem. Soc.* **1990**, *112*, 3875-3886. (b). Bazan, G. C.; Khosravi, E.; Schrock, R. R.; Feast, W. J.; Gibson, V. C.; O'Regan, M. B.; Thomas, J. K.; Davis, W. M. *J. Am. Chem.*

Soc. **1990**, *112*, 8378-8387. (c). Bazan, G. C.; Oskam, J. H.; Cho, H. N.; Park, L. Y.; Schrock, R. R. *J. Am. Chem. Soc.* **1991**, *113*, 6899-6907.

(4) (a). Schwab, P.; France, M. B.; Ziller, J. W.; Grubbs, R. H. *Angew. Chem. Int. Ed. Eng.* **1995**, *34*, 2039-2041. (b). Schwab, P.; Grubbs, R. H.; Ziller, J. W. *J. Am. Chem. Soc.* **1996**, *118*, 100-110. (c). Belderrain, T. R.; Grubbs, R. H. *Organometallics* **1997**, *16*, 4001-4003.

(5) For recent reviews on olefin cross-metathesis, see: (a). Chatterjee, A. K. In *Handbook of Olefin Metathesis*, vol 2., Grubbs, R. H., Ed. Wiley-VCH, **2004**, pp. 246-295. (b). Connon, S. J.; Blechert, S. *Angew. Chem. Int. Ed.* **2003**, *42*, 1900-1923.

(6) For recent reviews on the application of olefin metathesis to the synthesis of small and complex molecules, see: (a). Love, J. A. In *Handbook of Olefin Metathesis*, vol 2., Grubbs, R. H., Ed. Wiley-VCH, **2004**, pp. 296-322. (b). Furstner, A. *Angew. Chem. Int. Ed.* **2000**, *39,* 3012-3043.

(7) (a). Scholl, M.; Ding, S.; Lee, C. W.; Grubbs, R. H. *Org. Lett.* **1999**, *1*, 953-956. (b). Sanford, M. S.; Love, J. A.; Grubbs, R. H. *J. Am. Chem. Soc.* **2001**, *123*, 6543-6554.

(8) Konzelman, J.; Wagener, K. B.; *Macromolecules* **1995**, *28*, 4686-4692.

(9) Crowe, W. E.; Zhang, Z. *J. Am. Chem. Soc.* **1993**, *115*, 10998-10999.

(10) For reviews on ring-closing metathesis, see: (a). Maier, M. E. *Angew. Chem. Int. Ed.* **2000**, *39*, 2073-2077. (b). Grubbs, R. H.; Miller, S. J.; Fu, G. C. *Acc. Chem. Rec.* **1995**, *28*, 446-452.

(11) Bielawski, C. W.; Grubbs, R. H. *Angew. Chem. Int. Ed.* **2000**, *39*, 2903-2906.

(12) Craig, S. W.; Manzer, J. A.; Coughlin, E. B. *Macromolecules* **2001**, *34*, 7929-7931.

(13) Chatterjee, A. K.; Morgan, J. P.; Scholl, M.; Grubbs, R. H. *J. Am. Chem. Soc.* **2000**, *122*, 3783-3784.

(14) Chatterjee, A. K.; Choi, T.-L.; Sanders, D. P.; Grubbs, R. H. *J. Am. Chem. Soc.* **2003**, *125*, 11360-11370.

(15) Leading references using **7.1** and **7.2** in CM: (a). Crowe, W. E.; Goldberg, D. R. *J. Am. Chem. Soc.* **1995**, *117*, 5162-5163. (b). Brummer, O.; Ruckert, A.; Blechert, S. *Chem. Eur. J.* **1997**, *3*, 441-446. (c). Blackwell, H. E.; O'Leary, D. J.; Chatterjee, A. K.; Washenfelder, R. A.; Bussmann, D. A.; Grubbs, R. H. *J. Am. Chem. Soc.* **2000**, *122*, 58-71.

(16) Chatterjee, A. K.; Sanders, D. P.; Grubbs, R. H. *Org. Lett.* **2002**, *4*, 1939-1942.

(17) This is identical to the results of Schwab *et al.* who were unable to isolate the isopropyl-substituted ruthenium alkylidene $(PCy_3)_2Cl_2Ru(=CH$*i*-Pr) from the reaction of **7.2** with 3-methyl-1-butene. A small constant concentration of the desired alkylidene was observed via NMR throughout the reaction. See reference 4b.

(18) Funk, T.; Chelnov, A.; Grubbs, R. H. *Unpublished results.*

(19) Ulman, M.; Belderrain, T. R.; Grubbs, R. H. *Tetrahedron Lett.* **2000**, *41*, 4689-4693.

(20) Spessard, S. J.; Stoltz, B. M. *Org. Lett.* **2002**, *4*, 1943-1946.

(21) Ciochina, R.; Grossman, R. B. *Org. Lett.* **2003**, *5*, 4619-4621.

(22) Demchuk, O. M.; Pietrusiewicz, K. M.; Michrowska, A.; Grela, K. *Org. Lett.* **2003**, *5*, 3217-3220.

(23) (a). Choi, T.-L.; Lee, C. W.; Chatterjee, A. K.; Grubbs, R. H. *J. Am. Chem. Soc.* **2001**, *123*, 10417-10418. (b). Randl, S.; Connon, S. J.; Blechert, S. *Chem. Commun.* **2001**, 1796-1797. (c). Morgan, J. P.; Morrill, C.; Grubbs, R. H. *Org. Lett.* **2002**, *4*, 67-70.

(24) Enoic carbene complexes such as **7.9** undergo stoichiometric reactions with cyclohexene to afford the new ruthenium alkylidene $(PCy_3)_2Cl_2Ru(=CH(CH_2)_4CH=CHCO_2Cy)$. See reference 19.

(25) Pangborn, A. B.; Giardello, M. A.; Grubbs, R. H.; Rosen, R. K. Trimmers, F. J. *Organometallics* **1996**, *15*, 1518-1520.

(26) Sanford, M. S.; Love, J. A.; Grubbs, R. H. *Organometallics* **2001**, *20*, 5314-5318.

(27) Trnka, T. M. *Ph.D. Dissertation* California Institute of Technology, **2003**.

APPENDIX A

X-ray Crystallographic Data for:

4,4-Difluoro-3-(trifluoromethyl)-tricyclo[4.2.1.$0^{2,5}$]non-7-ene-3-carboxylic acid (**2.10**)

X-ray Experimental for Compound 2.10:

The crystal was cut from a larger crystal and had approximate dimensions: 0.48 x 0.24 x 0.19 mm. The data were collected on a Nonius Kappa CCD diffractometer using a graphite monochromator with MoKα radiation (λ = 0.71073 Å). A total of 347 frames of data were collected using ω-scans with a scan range of 1° and a counting time of 39 seconds per frame. The data were collected at -120 °C using an Oxford Cryostream low temperature device. Details of crystal data, data collection, and structure refinement are listed in Table 1. Data reduction were performed using DENZO-SMN.[1] The structure was solved by direct methods using SIR92[2] and refined by full-matrix least-squares on F^2 with anisotropic displacement parameters for the non-H atoms using SHELXL-97.[3] The hydrogen atom positions were located in a ΔF and refined with isotropic displacement parameters. The function, $\Sigma w(|F_0|^2 - |F_c|^2)^2$, was minimized, where $w = 1/[(\sigma(F_0))^2 + (0.0455*P)^2 + (0.4828*P)]$ and $P = (|F_0|^2 + 2|F_c|^2)/3$. $R_w(F^2)$ refined to 0.102, with R(F) equal to 0.0455 and a goodness of fit, S = 0.998. Definitions used for calculating R(F), $R_w(F^2)$, and the goodness of fit, S, are given below.[4] The data were corrected for secondary extinction effects. The correction takes the form: $F_{corr} = kF_c/[1+ (6(4)x10^{-6})*F_c^2\lambda^3/(\sin 2\theta)]^{0.25}$ where k is the overall scale factor. Neutral atom scattering factors and values used to calculate the linear absorption coefficient are from the International Tables for X-ray Crystallography (1992).[5] All figures were generated using SHELXTL/PC.[6] Tables of positional and thermal parameters, bond lengths and angles, figures and lists of observed and calculated structure factors are located in Tables 1 through 6.

References

1) DENZO-SMN. (1997). Z. Otwinowski and W. Minor, Methods in Enzymology, **276**: Macromolecular Crystallography, part A, 307 – 326, C. W. Carter, Jr. and R. M. Sweets, Editors, Academic Press.

2) SIR92. (1993). A program for crystal structure solution. Altomare, A., Cascarano, G., Giacovazzo, C. & Guagliardi, A. J. Appl. Cryst. 26, 343-350.

3) Sheldrick, G. M. (1994). SHELXL97. Program for the Refinement of Crystal Structures. University of Gottingen, Germany.

4) $R_w(F^2) = \{\Sigma w(|F_o|^2 - |F_c|^2)^2/\Sigma w(|F_o|)^4\}^{1/2}$ where w is the weight given each reflection.
$R(F) = \Sigma(|F_o| - |F_c|)/\Sigma|F_o|\}$ for reflections with $F_o > 4(\sigma(F_o))$.
$S = [\Sigma w(|F_o|^2 - |F_c|^2)^2/(n - p)]^{1/2}$, where n is the number of reflections and p is the number of refined parameters.

5) International Tables for X-ray Crystallography (1992). Vol. C, Tables 4.2.6.8 and 6.1.1.4, A. J. C. Wilson, editor, Boston: Kluwer Academic Press.

6) Sheldrick, G. M. (1994). SHELXTL/PC (Version 5.03). Siemens Analytical X-ray Instruments, Inc., Madison, Wisconsin, USA.

Table 1. Crystal data and structure refinement for 1.

Empirical formula	C11 H9 F5 O2	
Formula weight	268.18	
Temperature	153(2) K	
Wavelength	0.71073 Å	
Crystal system	Monoclinic	
Space group	P21/n	
Unit cell dimensions	a = 6.7504(2) Å	α= 90°.
	b = 19.0686(5) Å	β= 110.485(2)°.
	c = 8.9486(2) Å	γ = 90°.
Volume	1079.03(5) $Å^3$	
Z	4	
Density (calculated)	1.651 Mg/m^3	
Absorption coefficient	0.169 mm^{-1}	
F(000)	544	
Crystal size	0.48 x 0.24 x 0.19 mm	
Theta range for data collection	3.29 to 27.49°.	
Index ranges	-8<=h<=8, -22<=k<=24, -11<=l<=11	
Reflections collected	4338	
Independent reflections	2414 [R(int) = 0.0188]	
Completeness to theta = 27.49°	97.6 %	
Absorption correction	None	
Refinement method	Full-matrix least-squares on F^2	
Data / restraints / parameters	2414 / 0 / 200	
Goodness-of-fit on F^2	0.998	
Final R indices [I>2sigma(I)]	R1 = 0.0392, wR2 = 0.0915	
R indices (all data)	R1 = 0.0585, wR2 = 0.1016	
Extinction coefficient	$6(4)x10x10^{-6}$	
Largest diff. peak and hole	0.382 and -0.251 $e.Å^{-3}$	

Structure 1. View of **2.10** showing the atom labeling scheme. Thermal ellipsoids are scaled to the 30% probability level. Hydrogen atoms are drawn to an arbitrary size.

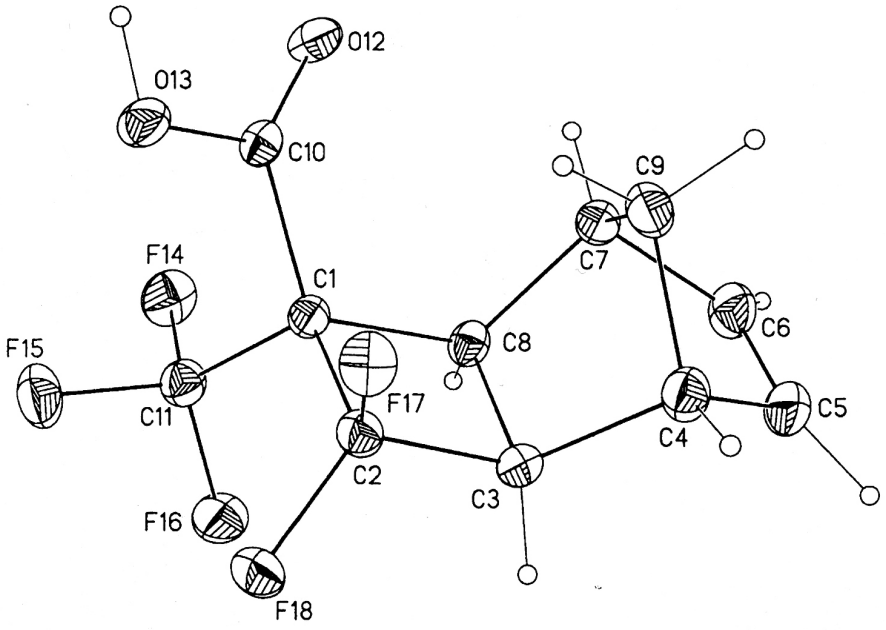

Structure 2. View of the H-bound dimers formed by **2.10**. The dimer lies around a crystallographic inversion center at 0, 1/2, ½. The geometry of the interaction is: O13-H13····O12 (related by –x, 1-y, 1-z), O····O 2.697(2)Å, H····O 1.85(3)Å, O-H····O 174(2)°. Thermal ellipsoids are scaled to the 30 % probability level. Hydrogen atoms are drawn to an arbitrary size.

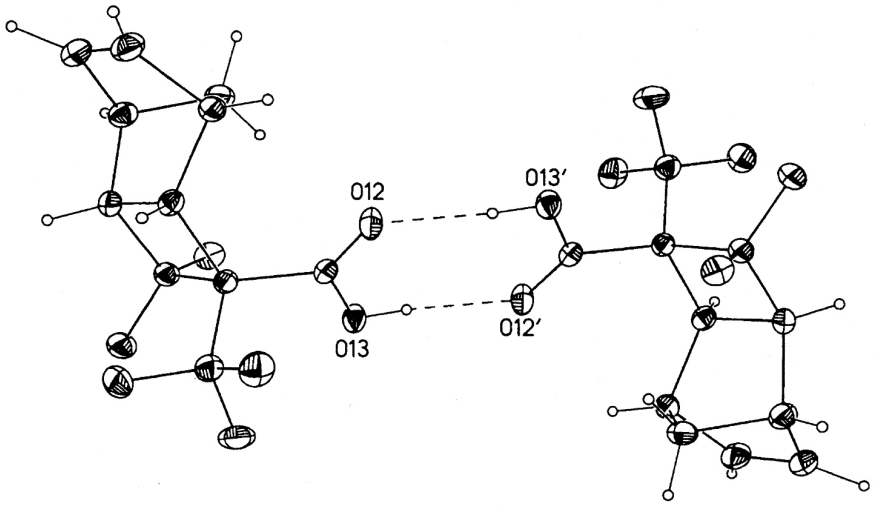

Table 2. Atomic coordinates (x 10^4) and equivalent isotropic displacement parameters ($Å^2$x 10^3) for 1. U(eq) is defined as one third of the trace of the orthogonalized U^{ij} tensor.

	x	y	z	U(eq)
C(1)	2305(2)	3607(1)	3784(2)	23(1)
C(2)	4730(2)	3586(1)	4102(2)	26(1)
C(3)	4345(3)	3470(1)	2335(2)	28(1)
C(4)	4800(3)	4081(1)	1362(2)	32(1)
C(5)	3661(3)	3859(1)	-365(2)	38(1)
C(6)	1613(3)	3916(1)	-667(2)	38(1)
C(7)	1299(3)	4179(1)	847(2)	30(1)
C(8)	1891(3)	3531(1)	1956(2)	26(1)
C(9)	3263(3)	4642(1)	1510(2)	33(1)
C(10)	1379(2)	4246(1)	4334(2)	24(1)
C(11)	1523(3)	2961(1)	4411(2)	31(1)
O(12)	-191(2)	4541(1)	3460(1)	33(1)
O(13)	2395(2)	4413(1)	5826(1)	32(1)
F(14)	-595(2)	2961(1)	3925(1)	42(1)
F(15)	2237(2)	2922(1)	6001(1)	44(1)
F(16)	2084(2)	2362(1)	3878(1)	41(1)
F(17)	5809(1)	4172(1)	4781(1)	33(1)
F(18)	5764(2)	3050(1)	5069(1)	37(1)

Table 3. Bond lengths [Å] and angles [°] for 1.

C(1)-C(11)	1.523(2)	C(6)-C(7)	1.527(3)
C(1)-C(10)	1.526(2)	C(6)-H(6)	1.01(2)
C(1)-C(2)	1.561(2)	C(7)-C(9)	1.529(3)
C(1)-C(8)	1.567(2)	C(7)-C(8)	1.548(2)
C(2)-F(17)	1.3563(19)	C(7)-H(7)	0.95(2)
C(2)-F(18)	1.3632(18)	C(8)-H(8)	0.981(19)
C(2)-C(3)	1.526(2)	C(9)-H(9A)	0.98(2)
C(3)-C(4)	1.549(2)	C(9)-H(9B)	1.00(2)
C(3)-C(8)	1.574(2)	C(10)-O(12)	1.2125(19)
C(3)-H(3)	0.96(2)	C(10)-O(13)	1.3094(19)
C(4)-C(5)	1.525(3)	C(11)-F(15)	1.335(2)
C(4)-C(9)	1.529(3)	C(11)-F(14)	1.341(2)
C(4)-H(4)	0.988(19)	C(11)-F(16)	1.341(2)
C(5)-C(6)	1.317(3)	O(13)-H(13)	0.85(3)
C(5)-H(5)	1.03(2)		

C(11)-C(1)-C(10)	107.03(13)	C(5)-C(4)-C(9)	99.51(14)
C(11)-C(1)-C(2)	112.84(13)	C(5)-C(4)-C(3)	103.46(15)
C(10)-C(1)-C(2)	118.94(13)	C(9)-C(4)-C(3)	101.77(13)
C(11)-C(1)-C(8)	110.56(13)	C(5)-C(4)-H(4)	118.8(11)
C(10)-C(1)-C(8)	117.86(13)	C(9)-C(4)-H(4)	118.6(12)
C(2)-C(1)-C(8)	88.86(11)	C(3)-C(4)-H(4)	112.2(11)
F(17)-C(2)-F(18)	104.97(12)	C(6)-C(5)-C(4)	107.82(16)
F(17)-C(2)-C(3)	117.02(13)	C(6)-C(5)-H(5)	127.3(13)
F(18)-C(2)-C(3)	114.35(14)	C(4)-C(5)-H(5)	124.3(13)
F(17)-C(2)-C(1)	115.12(13)	C(5)-C(6)-C(7)	107.84(16)
F(18)-C(2)-C(1)	113.99(13)	C(5)-C(6)-H(6)	127.9(12)
C(3)-C(2)-C(1)	91.57(11)	C(7)-C(6)-H(6)	124.0(12)
C(2)-C(3)-C(4)	118.56(15)	C(6)-C(7)-C(9)	99.42(15)
C(2)-C(3)-C(8)	89.86(12)	C(6)-C(7)-C(8)	102.78(14)
C(4)-C(3)-C(8)	102.91(13)	C(9)-C(7)-C(8)	102.60(13)
C(2)-C(3)-H(3)	112.1(12)	C(6)-C(7)-H(7)	118.1(11)
C(4)-C(3)-H(3)	113.6(12)	C(9)-C(7)-H(7)	116.6(12)
C(8)-C(3)-H(3)	117.6(11)	C(8)-C(7)-H(7)	114.9(11)

C(7)-C(8)-C(1)	120.45(14)	H(9A)-C(9)-H(9B)	108.6(16)
C(7)-C(8)-C(3)	102.34(13)	O(12)-C(10)-O(13)	124.93(15)
C(1)-C(8)-C(3)	89.55(11)	O(12)-C(10)-C(1)	121.73(14)
C(7)-C(8)-H(8)	113.0(11)	O(13)-C(10)-C(1)	113.28(14)
C(1)-C(8)-H(8)	111.1(11)	F(15)-C(11)-F(14)	106.96(13)
C(3)-C(8)-H(8)	118.4(11)	F(15)-C(11)-F(16)	106.85(14)
C(4)-C(9)-C(7)	94.83(14)	F(14)-C(11)-F(16)	106.65(14)
C(4)-C(9)-H(9A)	114.3(11)	F(15)-C(11)-C(1)	113.28(14)
C(7)-C(9)-H(9A)	115.1(11)	F(14)-C(11)-C(1)	110.38(14)
C(4)-C(9)-H(9B)	112.7(11)	F(16)-C(11)-C(1)	112.35(13)
C(7)-C(9)-H(9B)	110.8(11)	C(10)-O(13)-H(13)	106.8(16)

Table 4. Anisotropic displacement parameters ($Å^2 x\ 10^3$) for 1. The anisotropic displacement factor exponent takes the form: $-2\pi^2[\ h^2\ a^{*2}U^{11} + \ldots + 2\ h\ k\ a^*\ b^*\ U^{12}\ ]$

	U^{11}	U^{22}	U^{33}	U^{23}	U^{13}	U^{12}
C(1)	25(1)	23(1)	23(1)	-1(1)	10(1)	0(1)
C(2)	25(1)	28(1)	26(1)	3(1)	9(1)	2(1)
C(3)	30(1)	30(1)	28(1)	2(1)	13(1)	7(1)
C(4)	28(1)	41(1)	30(1)	5(1)	13(1)	2(1)
C(5)	45(1)	46(1)	28(1)	4(1)	18(1)	7(1)
C(6)	41(1)	48(1)	24(1)	2(1)	11(1)	3(1)
C(7)	28(1)	35(1)	26(1)	5(1)	10(1)	8(1)
C(8)	28(1)	26(1)	24(1)	-4(1)	11(1)	-3(1)
C(9)	40(1)	30(1)	29(1)	5(1)	13(1)	-1(1)
C(10)	24(1)	26(1)	24(1)	-2(1)	11(1)	-2(1)
C(11)	34(1)	29(1)	32(1)	0(1)	16(1)	-2(1)
O(12)	28(1)	39(1)	28(1)	-8(1)	6(1)	9(1)
O(13)	34(1)	36(1)	23(1)	-5(1)	7(1)	8(1)
F(14)	35(1)	43(1)	54(1)	-1(1)	23(1)	-10(1)
F(15)	60(1)	41(1)	33(1)	9(1)	21(1)	-4(1)
F(16)	54(1)	23(1)	53(1)	-1(1)	27(1)	-2(1)
F(17)	27(1)	39(1)	30(1)	-2(1)	7(1)	-7(1)
F(18)	33(1)	42(1)	36(1)	13(1)	12(1)	13(1)

Table 5. Hydrogen coordinates (x 10^4) and isotropic displacement parameters ($Å^2$x 10^3) for 1.

	x	y	z	U(eq)
H(3)	4880(30)	3027(11)	2140(20)	35(5)
H(4)	6320(30)	4195(10)	1710(20)	38(5)
H(5)	4390(40)	3634(12)	-1080(30)	55(6)
H(6)	420(30)	3772(11)	-1660(30)	43(6)
H(7)	-20(30)	4390(10)	750(20)	34(5)
H(8)	1000(30)	3121(10)	1510(20)	30(5)
H(9A)	3560(30)	4814(10)	2600(20)	37(5)
H(9B)	3170(30)	5056(11)	800(20)	40(5)
H(13)	1750(40)	4764(14)	6040(30)	63(7)

APPENDIX B

X-ray Crystallographic Data for:

5,5-Bis(trifluoromethyl)-4-oxa-tricyclo[4.3.$0^{1,6}$.$0^{3,7}$]nonane-8,9-diol (**4.6**)

Table 1. Crystal data and structure refinement for DPS01 (CCDC 203516).

Empirical formula	$C_{10}H_{10}F_6O_3$
Formula weight	292.18
Crystallization Solvent	Hexanes/ether
Crystal Habit	Block
Crystal size	0.35 x 0.30 x 0.21 mm^3
Crystal color	Colorless

Data Collection

Preliminary Photos	Rotation	
Type of diffractometer	Bruker SMART 1000	
Wavelength	0.71073 Å MoKα	
Data Collection Temperature	98(2) K	
θ range for 14175 reflections used in lattice determination	2.17 to 27.99°	
Unit cell dimensions	a = 7.6162(5) Å b = 11.4014(8) Å c = 13.4278(9) Å	α= 100.3010(10)° β= 98.5160(10)° γ = 100.6610(10)°
Volume	1107.44(13) $Å^3$	
Z	4	
Crystal system	Triclinic	
Space group	P-1	
Density (calculated)	1.752 Mg/m^3	
F(000)	592	
Data collection program	Bruker SMART v5.054	
θ range for data collection	1.86 to 28.07°	
Completeness to θ = 28.07°	92.1 %	
Index ranges	$-9 \leq h \leq 10$, $-14 \leq k \leq 14$, $-17 \leq l \leq 17$	
Data collection scan type	ω scans at 7 ϕ settings	
Data reduction program	Bruker SAINT v6.022	
Reflections collected	22015	
Independent reflections	4951 [R_{int}= 0.0398]	
Absorption coefficient	0.191 mm^{-1}	
Absorption correction	None	
Max. and min. transmission	0.9611 and 0.9363	

Table 1 (cont.)

Structure solution and Refinement

Structure solution program	SHELXS-97 (Sheldrick, 1990)
Primary solution method	Direct methods
Secondary solution method	Difference Fourier map
Hydrogen placement	Difference Fourier map
Structure refinement program	SHELXL-97 (Sheldrick, 1997)
Refinement method	Full matrix least-squares on F^2
Data / restraints / parameters	4951 / 0 / 423
Treatment of hydrogen atoms	Unrestrained
Goodness-of-fit on F^2	2.382
Final R indices [$I>2\sigma(I)$, 4252 reflections]	R1 = 0.0317, *w*R2 = 0.0656
R indices (all data)	R1 = 0.0378, *w*R2 = 0.0664
Type of weighting scheme used	Sigma
Weighting scheme used	$w=1/\sigma^2(Fo^2)$
Max shift/error	0.003
Average shift/error	0.000
Largest diff. peak and hole	0.416 and -0.320 e.Å^{-3}

Special Refinement Details

Refinement of F^2 against ALL reflections. The weighted R-factor (*w*R) and goodness of fit (S) are based on F^2, conventional R-factors (R) are based on F, with F set to zero for negative F^2. The threshold expression of $F^2 > 2\sigma(F^2)$ is used only for calculating R-factors(gt) etc. and is not relevant to the choice of reflections for refinement. R-factors based on F^2 are statistically about twice as large as those based on F, and R-factors based on ALL data will be even larger.

All esds (except the esd in the dihedral angle between two l.s. planes) are estimated using the full covariance matrix. The cell esds are taken into account individually in the estimation of esds in distances, angles and torsion angles; correlations between esds in cell parameters are only used when they are defined by crystal symmetry. An approximate (isotropic) treatment of cell esds is used for estimating esds involving l.s. planes.

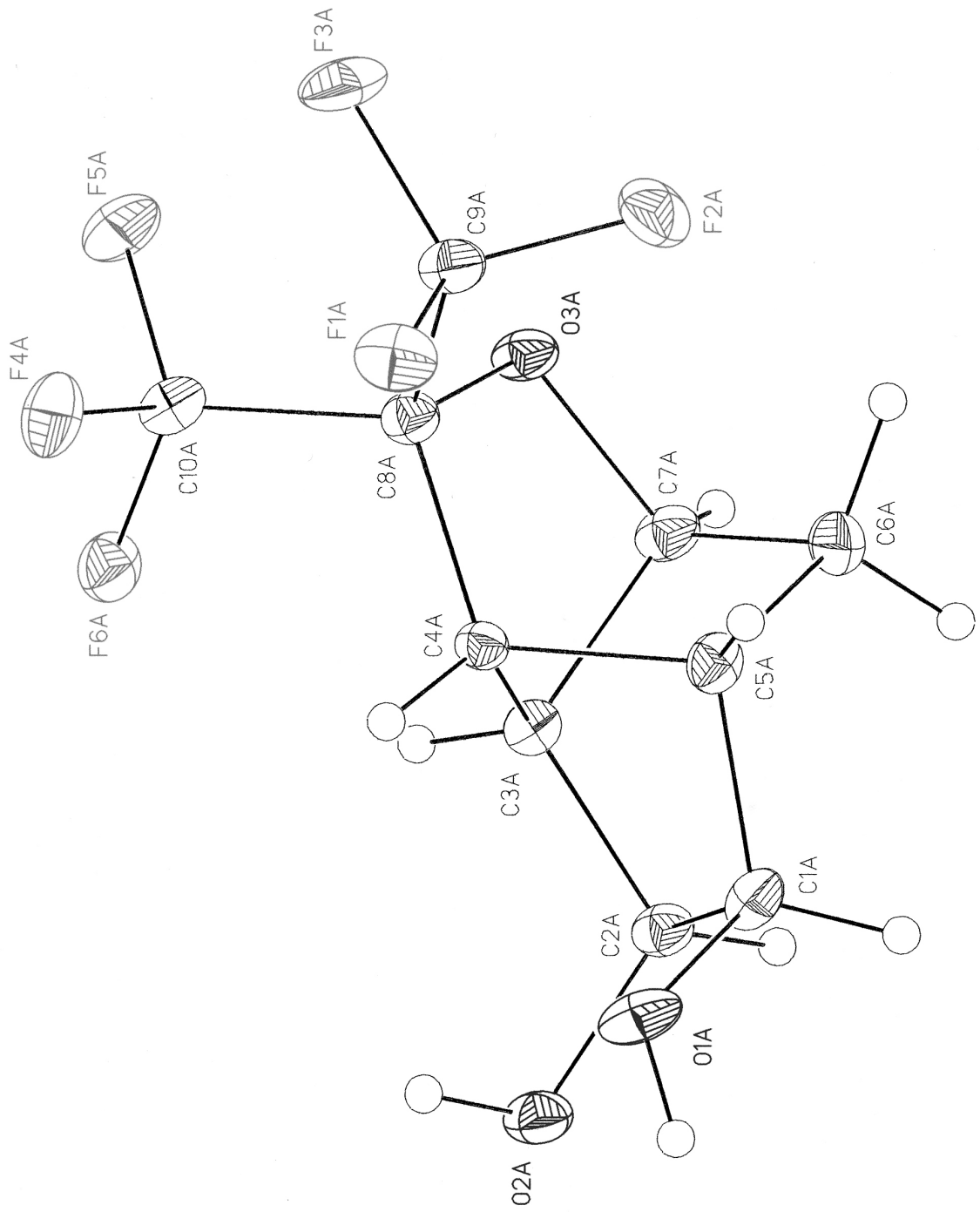
F3A
F5A
C9A
F2A
F1A
O3A
F4A
C10A
C8A
C7A
C6A
F6A
C4A
C5A
C3A
C1A
C2A
O1A
O2A

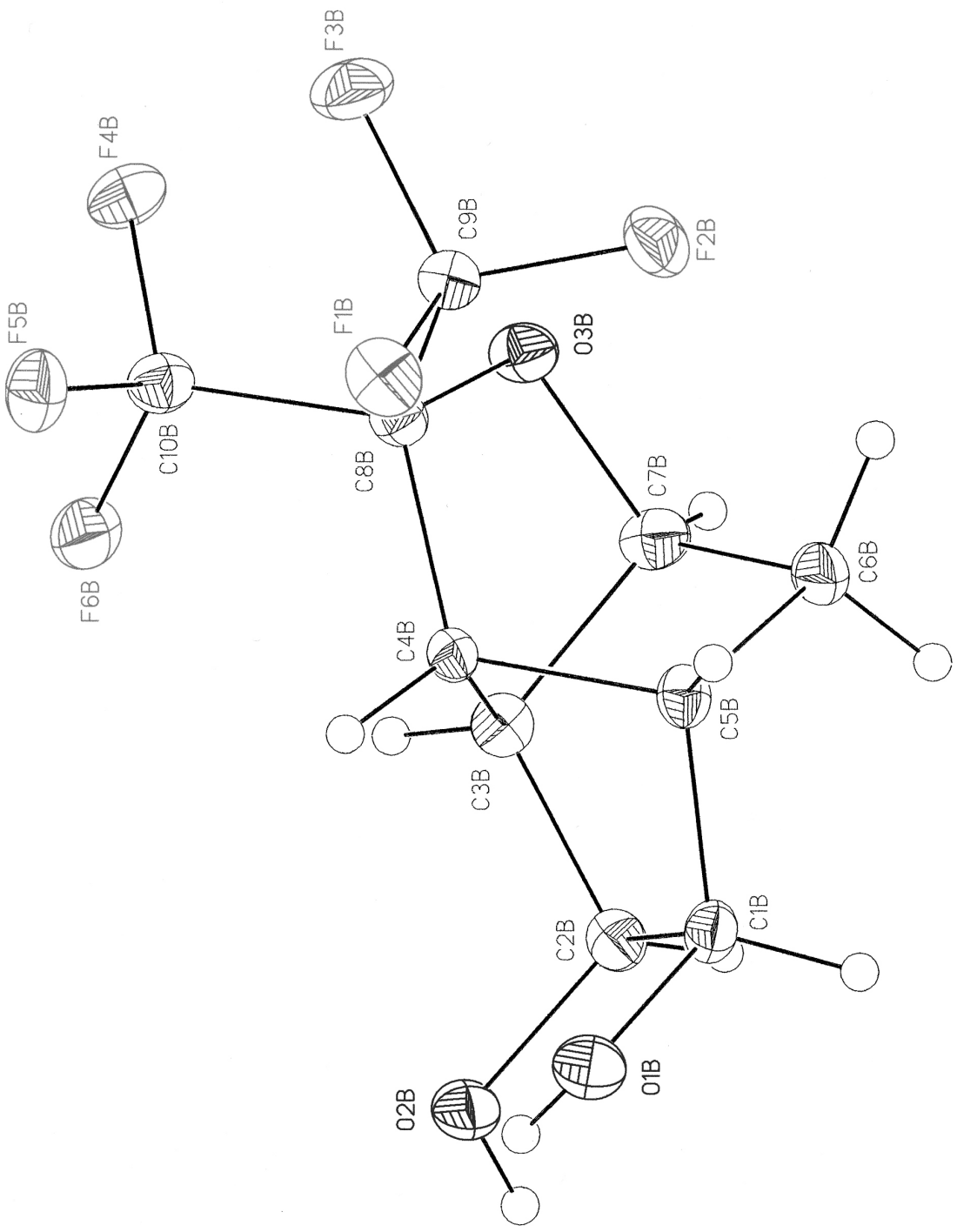
F3B
F4B
C9B
F2B
F5B
F1B
O3B
C10B
C8B
C7B
C6B
F6B
C4B
C5B
C3B
C2B
C1B
O1B
O2B

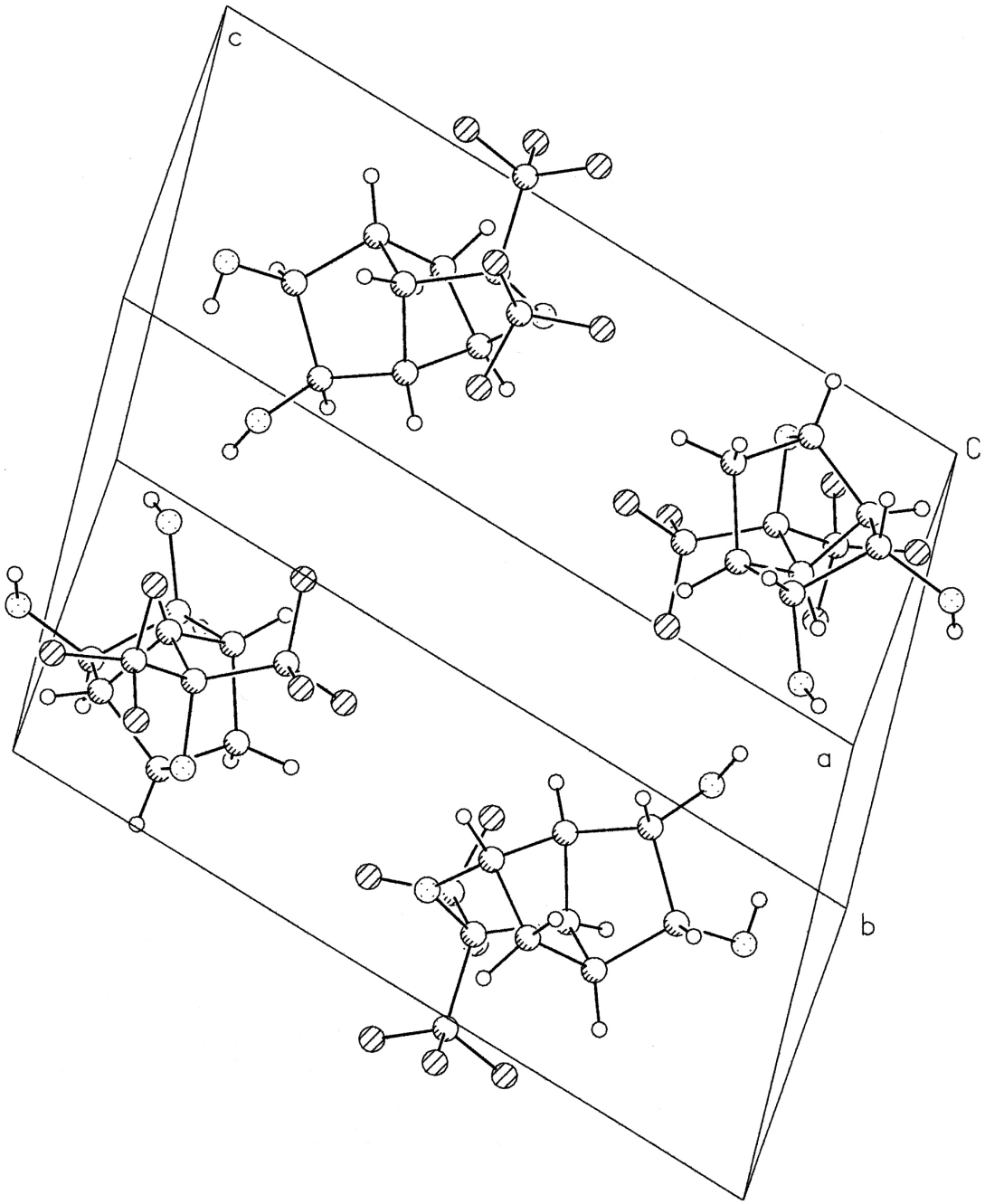
c
C
a
b

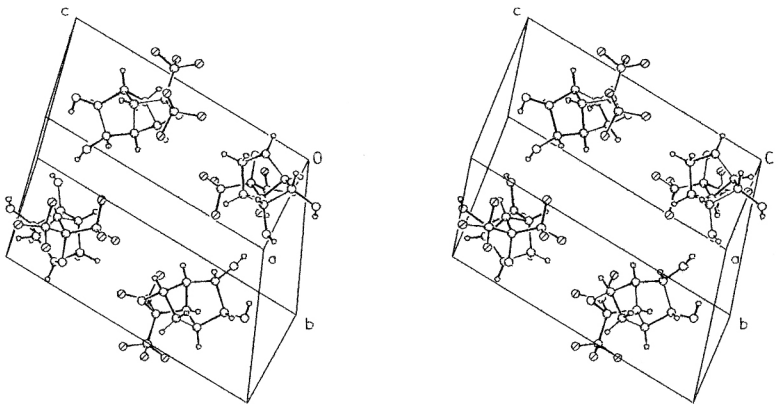
c
O
a
b
c
C
a
b

Table 2. Atomic coordinates (x 10^4) and equivalent isotropic displacement parameters ($Å^2$x 10^3) for DPS01 (CCDC 203516). U(eq) is defined as the trace of the orthogonalized U^{ij} tensor.

	x	y	z	U_{eq}
F(1A)	5587(1)	2914(1)	2740(1)	21(1)
F(2A)	3625(1)	2357(1)	3658(1)	22(1)
F(3A)	5154(1)	1093(1)	3042(1)	25(1)
F(4A)	5320(1)	1230(1)	997(1)	23(1)
F(5A)	3567(1)	-377(1)	1238(1)	25(1)
F(6A)	2639(1)	559(1)	82(1)	19(1)
O(1A)	1899(1)	4943(1)	1118(1)	19(1)
O(2A)	-633(1)	3299(1)	-335(1)	17(1)
O(3A)	1222(1)	847(1)	2020(1)	15(1)
C(1A)	615(2)	4189(1)	1531(1)	16(1)
C(2A)	-599(2)	3099(1)	686(1)	14(1)
C(3A)	259(2)	2014(1)	856(1)	13(1)
C(4A)	2238(2)	2607(1)	1421(1)	11(1)
C(5A)	1639(2)	3525(1)	2236(1)	14(1)
C(6A)	164(2)	2681(1)	2630(1)	18(1)
C(7A)	-209(2)	1522(1)	1792(1)	15(1)
C(8A)	2841(2)	1551(1)	1838(1)	13(1)
C(9A)	4305(2)	1977(1)	2831(1)	17(1)
C(10A)	3592(2)	729(1)	1036(1)	16(1)
F(1B)	12913(1)	8455(1)	3099(1)	21(1)
F(2B)	11792(1)	9781(1)	4008(1)	21(1)
F(3B)	13603(1)	8842(1)	4758(1)	25(1)
F(4B)	11998(1)	6859(1)	5331(1)	23(1)
F(5B)	12727(1)	6376(1)	3838(1)	22(1)
F(6B)	10107(1)	5572(1)	4104(1)	23(1)
O(1B)	7355(1)	6884(1)	836(1)	18(1)
O(2B)	5517(1)	5473(1)	1748(1)	19(1)
O(3B)	9542(1)	8092(1)	4688(1)	17(1)
C(1B)	6913(2)	7580(1)	1720(1)	15(1)
C(2B)	5972(2)	6692(1)	2343(1)	15(1)
C(3B)	7447(2)	6803(1)	3284(1)	15(1)
C(4B)	9266(2)	7239(1)	2936(1)	12(1)
C(5B)	8610(2)	8294(1)	2499(1)	14(1)
C(6B)	7876(2)	8956(1)	3417(1)	17(1)
C(7B)	7727(2)	7992(1)	4077(1)	17(1)
C(8B)	10601(2)	7673(1)	3969(1)	14(1)
C(9B)	12237(2)	8702(1)	3963(1)	16(1)
C(10B)	11364(2)	6615(1)	4320(1)	17(1)

Table 3. Bond lengths [Å] and angles [°] for DPS01 (CCDC 203516).

F(1A)-C(9A)	1.3436(14)	C(4B)-C(8B)	1.5347(17)
F(2A)-C(9A)	1.3304(15)	C(4B)-C(5B)	1.5574(16)
F(3A)-C(9A)	1.3423(14)	C(4B)-H(4B)	0.966(12)
F(4A)-C(10A)	1.3463(14)	C(5B)-C(6B)	1.5590(18)
F(5A)-C(10A)	1.3339(14)	C(5B)-H(5B)	0.940(13)
F(6A)-C(10A)	1.3386(14)	C(6B)-C(7B)	1.5292(19)
O(1A)-C(1A)	1.4223(15)	C(6B)-H(6B1)	0.959(12)
O(1A)-H(1A)	0.801(16)	C(6B)-H(6B2)	0.961(14)
O(2A)-C(2A)	1.4267(15)	C(7B)-H(7B)	0.966(13)
O(2A)-H(2A)	0.820(17)	C(8B)-C(9B)	1.5476(17)
O(3A)-C(8A)	1.4207(14)	C(8B)-C(10B)	1.5479(17)
O(3A)-C(7A)	1.4725(14)		
C(1A)-C(5A)	1.5275(17)	C(1A)-O(1A)-H(1A)	113.6(11)
C(1A)-C(2A)	1.5641(17)	C(2A)-O(2A)-H(2A)	107.7(12)
C(1A)-H(1A1)	0.958(12)	C(8A)-O(3A)-C(7A)	105.82(9)
C(2A)-C(3A)	1.5379(17)	O(1A)-C(1A)-C(5A)	108.60(10)
C(2A)-H(2A1)	0.987(12)	O(1A)-C(1A)-C(2A)	111.93(10)
C(3A)-C(7A)	1.5272(18)	C(5A)-C(1A)-C(2A)	101.77(10)
C(3A)-C(4A)	1.5508(16)	O(1A)-C(1A)-H(1A1)	110.5(8)
C(3A)-H(3A)	0.954(14)	C(5A)-C(1A)-H(1A1)	112.7(8)
C(4A)-C(8A)	1.5299(16)	C(2A)-C(1A)-H(1A1)	111.1(8)
C(4A)-C(5A)	1.5547(17)	O(2A)-C(2A)-C(3A)	112.11(10)
C(4A)-H(4A)	0.902(13)	O(2A)-C(2A)-C(1A)	113.23(10)
C(5A)-C(6A)	1.5575(18)	C(3A)-C(2A)-C(1A)	103.28(9)
C(5A)-H(5A)	0.949(13)	O(2A)-C(2A)-H(2A1)	105.0(7)
C(6A)-C(7A)	1.5254(19)	C(3A)-C(2A)-H(2A1)	112.6(7)
C(6A)-H(6A1)	0.992(14)	C(1A)-C(2A)-H(2A1)	110.8(7)
C(6A)-H(6A2)	0.950(14)	C(7A)-C(3A)-C(4A)	91.89(10)
C(7A)-H(7A)	0.948(13)	C(7A)-C(3A)-C(2A)	113.25(10)
C(8A)-C(10A)	1.5439(17)	C(4A)-C(3A)-C(2A)	104.61(9)
C(8A)-C(9A)	1.5452(17)	C(7A)-C(3A)-H(3A)	113.2(8)
F(1B)-C(9B)	1.3441(15)	C(4A)-C(3A)-H(3A)	117.1(8)
F(2B)-C(9B)	1.3291(14)	C(2A)-C(3A)-H(3A)	114.6(8)
F(3B)-C(9B)	1.3401(14)	C(8A)-C(4A)-C(5A)	113.61(10)
F(4B)-C(10B)	1.3321(14)	C(8A)-C(4A)-C(3A)	102.18(10)
F(5B)-C(10B)	1.3456(14)	C(5A)-C(4A)-C(3A)	93.49(9)
F(6B)-C(10B)	1.3368(15)	C(8A)-C(4A)-H(4A)	112.9(8)
O(1B)-C(1B)	1.4261(15)	C(5A)-C(4A)-H(4A)	116.4(8)
O(1B)-H(1B)	0.777(17)	C(3A)-C(4A)-H(4A)	116.0(8)
O(2B)-C(2B)	1.4262(15)	C(1A)-C(5A)-C(4A)	100.16(10)
O(2B)-H(2B)	0.815(15)	C(1A)-C(5A)-C(6A)	106.24(10)
O(3B)-C(8B)	1.4204(14)	C(4A)-C(5A)-C(6A)	102.61(10)
O(3B)-C(7B)	1.4723(15)	C(1A)-C(5A)-H(5A)	112.0(8)
C(1B)-C(2B)	1.5646(17)	C(4A)-C(5A)-H(5A)	117.5(8)
C(1B)-C(5B)	1.5271(17)	C(6A)-C(5A)-H(5A)	116.4(8)
C(1B)-H(1B1)	0.968(13)	C(7A)-C(6A)-C(5A)	100.57(10)
C(2B)-C(3B)	1.5318(17)	C(7A)-C(6A)-H(6A1)	113.4(8)
C(2B)-H(2B1)	0.948(13)	C(5A)-C(6A)-H(6A1)	112.7(8)
C(3B)-C(4B)	1.5508(17)	C(7A)-C(6A)-H(6A2)	110.6(8)
C(3B)-C(7B)	1.5261(18)	C(5A)-C(6A)-H(6A2)	111.9(8)
C(3B)-H(3B)	0.951(14)	H(6A1)-C(6A)-H(6A2)	107.7(11)

O(3A)-C(7A)-C(6A)	108.21(10)	C(2B)-C(3B)-H(3B)	110.0(8)
O(3A)-C(7A)-C(3A)	103.04(9)	C(8B)-C(4B)-C(5B)	113.80(10)
C(6A)-C(7A)-C(3A)	102.66(10)	C(8B)-C(4B)-C(3B)	101.88(10)
O(3A)-C(7A)-H(7A)	105.7(7)	C(5B)-C(4B)-C(3B)	93.75(9)
C(6A)-C(7A)-H(7A)	116.2(8)	C(8B)-C(4B)-H(4B)	113.9(7)
C(3A)-C(7A)-H(7A)	119.9(8)	C(5B)-C(4B)-H(4B)	113.8(7)
O(3A)-C(8A)-C(4A)	104.64(9)	C(3B)-C(4B)-H(4B)	117.8(7)
O(3A)-C(8A)-C(10A)	107.95(10)	C(6B)-C(5B)-C(4B)	102.24(10)
C(4A)-C(8A)-C(10A)	111.95(10)	C(6B)-C(5B)-C(1B)	104.95(10)
O(3A)-C(8A)-C(9A)	111.07(10)	C(4B)-C(5B)-C(1B)	100.74(10)
C(4A)-C(8A)-C(9A)	113.35(10)	C(6B)-C(5B)-H(5B)	115.3(8)
C(10A)-C(8A)-C(9A)	107.77(9)	C(4B)-C(5B)-H(5B)	116.7(8)
F(3A)-C(9A)-F(2A)	106.67(10)	C(1B)-C(5B)-H(5B)	114.9(8)
F(3A)-C(9A)-F(1A)	107.15(9)	C(5B)-C(6B)-C(7B)	100.75(10)
F(2A)-C(9A)-F(1A)	107.15(10)	C(5B)-C(6B)-H(6B1)	110.4(8)
F(3A)-C(9A)-C(8A)	112.70(10)	C(7B)-C(6B)-H(6B1)	109.2(8)
F(2A)-C(9A)-C(8A)	112.58(10)	C(5B)-C(6B)-H(6B2)	114.0(8)
F(1A)-C(9A)-C(8A)	110.27(10)	C(7B)-C(6B)-H(6B2)	111.1(8)
F(6A)-C(10A)-F(4A)	106.17(10)	H(6B1)-C(6B)-H(6B2)	111.0(11)
F(6A)-C(10A)-F(5A)	106.65(10)	O(3B)-C(7B)-C(3B)	103.01(10)
F(4A)-C(10A)-F(5A)	107.59(10)	O(3B)-C(7B)-C(6B)	108.23(10)
F(6A)-C(10A)-C(8A)	112.20(9)	C(3B)-C(7B)-C(6B)	102.74(10)
F(4A)-C(10A)-C(8A)	111.38(10)	O(3B)-C(7B)-H(7B)	105.9(7)
F(5A)-C(10A)-C(8A)	112.48(10)	C(3B)-C(7B)-H(7B)	118.4(8)
C(1B)-O(1B)-H(1B)	103.8(12)	C(6B)-C(7B)-H(7B)	117.4(7)
C(2B)-O(2B)-H(2B)	108.1(11)	O(3B)-C(8B)-C(4B)	104.71(9)
C(8B)-O(3B)-C(7B)	105.68(9)	O(3B)-C(8B)-C(9B)	110.45(10)
O(1B)-C(1B)-C(2B)	109.26(10)	C(4B)-C(8B)-C(9B)	113.74(10)
O(1B)-C(1B)-C(5B)	112.02(10)	O(3B)-C(8B)-C(10B)	108.05(10)
C(2B)-C(1B)-C(5B)	102.26(10)	C(4B)-C(8B)-C(10B)	112.01(10)
O(1B)-C(1B)-H(1B1)	109.4(8)	C(9B)-C(8B)-C(10B)	107.75(10)
C(2B)-C(1B)-H(1B1)	113.4(8)	F(1B)-C(9B)-F(3B)	106.96(10)
C(5B)-C(1B)-H(1B1)	110.4(8)	F(1B)-C(9B)-F(2B)	107.29(10)
O(2B)-C(2B)-C(3B)	109.98(10)	F(3B)-C(9B)-F(2B)	106.64(10)
O(2B)-C(2B)-C(1B)	109.92(10)	F(1B)-C(9B)-C(8B)	110.58(10)
C(3B)-C(2B)-C(1B)	103.43(10)	F(3B)-C(9B)-C(8B)	112.49(10)
O(2B)-C(2B)-H(2B1)	111.2(8)	F(2B)-C(9B)-C(8B)	112.55(10)
C(3B)-C(2B)-H(2B1)	110.1(8)	F(4B)-C(10B)-F(5B)	107.76(10)
C(1B)-C(2B)-H(2B1)	112.0(8)	F(4B)-C(10B)-F(6B)	106.82(10)
C(4B)-C(3B)-C(7B)	91.91(10)	F(5B)-C(10B)-F(6B)	106.22(10)
C(4B)-C(3B)-C(2B)	104.83(10)	F(4B)-C(10B)-C(8B)	112.23(10)
C(7B)-C(3B)-C(2B)	113.24(11)	F(5B)-C(10B)-C(8B)	111.20(10)
C(4B)-C(3B)-H(3B)	120.4(8)	F(6B)-C(10B)-C(8B)	112.27(10)
C(7B)-C(3B)-H(3B)	115.3(8)		

Table 4. Anisotropic displacement parameters ($Å^2 x 10^4$) for DPS01 (CCDC 203516). The anisotropic displacement factor exponent takes the form: $-2\pi^2 [h^2 a^{*2} U^{11} + ... + 2 h k a^* b^* U^{12}]$

	U^{11}	U^{22}	U^{33}	U^{23}	U^{13}	U^{12}
F(1A)	153(4)	222(4)	211(4)	58(3)	-27(3)	-13(3)
F(2A)	247(4)	299(5)	126(4)	46(3)	19(3)	65(3)
F(3A)	259(4)	250(4)	250(4)	102(4)	-42(3)	119(4)
F(4A)	138(4)	263(4)	282(5)	27(4)	70(3)	62(3)
F(5A)	346(5)	143(4)	316(5)	72(3)	72(4)	124(3)
F(6A)	219(4)	191(4)	156(4)	-10(3)	12(3)	70(3)
O(1A)	146(5)	132(5)	293(6)	99(4)	-9(4)	21(4)
O(2A)	146(5)	197(5)	184(5)	87(4)	12(4)	56(4)
O(3A)	120(4)	143(5)	201(5)	88(4)	31(4)	27(4)
C(1A)	147(6)	130(6)	208(7)	35(5)	41(5)	52(5)
C(2A)	105(6)	147(6)	170(7)	60(5)	16(5)	28(5)
C(3A)	117(6)	106(6)	141(7)	20(5)	12(5)	12(5)
C(4A)	114(6)	117(6)	117(6)	41(5)	24(5)	22(5)
C(5A)	148(6)	116(6)	139(7)	-3(5)	14(5)	28(5)
C(6A)	155(7)	226(7)	177(7)	67(6)	67(5)	71(6)
C(7A)	100(6)	163(7)	213(7)	80(5)	29(5)	34(5)
C(8A)	115(6)	123(6)	149(6)	47(5)	23(5)	20(5)
C(9A)	164(6)	168(7)	173(7)	65(5)	18(5)	50(5)
C(10A)	151(6)	144(7)	196(7)	47(5)	14(5)	49(5)
F(1B)	195(4)	220(4)	233(4)	48(3)	105(3)	29(3)
F(2B)	219(4)	128(4)	261(4)	21(3)	36(3)	20(3)
F(3B)	179(4)	250(4)	259(4)	44(4)	-56(3)	-12(3)
F(4B)	272(4)	286(4)	137(4)	60(3)	-19(3)	73(4)
F(5B)	231(4)	233(4)	251(4)	69(3)	79(3)	119(3)
F(6B)	243(4)	167(4)	258(4)	94(3)	-17(3)	9(3)
O(1B)	197(5)	203(5)	147(5)	29(4)	44(4)	28(4)
O(2B)	138(5)	161(5)	225(5)	7(4)	0(4)	1(4)
O(3B)	149(4)	213(5)	134(5)	8(4)	38(4)	43(4)
C(1B)	154(6)	156(7)	152(7)	41(5)	33(5)	67(5)
C(2B)	130(6)	147(7)	178(7)	23(5)	42(5)	27(5)
C(3B)	151(6)	150(7)	149(7)	54(5)	49(5)	19(5)
C(4B)	135(6)	116(6)	119(6)	16(5)	25(5)	41(5)
C(5B)	142(6)	119(6)	166(7)	52(5)	43(5)	29(5)
C(6B)	152(7)	162(7)	194(7)	0(6)	25(5)	59(5)
C(7B)	125(6)	229(7)	153(7)	14(6)	39(5)	38(5)
C(8B)	147(6)	144(6)	115(6)	15(5)	35(5)	36(5)
C(9B)	171(6)	158(7)	154(7)	20(5)	16(5)	36(5)
C(10B)	175(7)	180(7)	146(7)	38(5)	19(5)	28(5)

Table 5. Hydrogen coordinates (x 10^4) and isotropic displacement parameters ($Å^2$x 10^3) for DPS01 (CCDC 203516).

	x	y	z	U_{iso}
H(1A)	1490(20)	5438(15)	858(12)	35(5)
H(2A)	330(20)	3195(15)	-501(13)	40(5)
H(1A1)	-115(17)	4665(12)	1878(10)	12(3)
H(2A1)	-1880(17)	2972(11)	772(9)	11(3)
H(3A)	101(17)	1389(12)	254(11)	16(3)
H(4A)	2993(16)	2933(11)	1036(10)	9(3)
H(5A)	2565(17)	4074(12)	2748(10)	15(3)
H(6A1)	597(17)	2557(12)	3329(11)	16(3)
H(6A2)	-905(19)	2996(12)	2649(10)	20(4)
H(7A)	-1326(17)	963(12)	1733(10)	12(3)
H(1B)	6820(20)	6224(16)	803(13)	34(5)
H(2B)	4420(20)	5288(14)	1545(12)	29(5)
H(1B1)	6177(17)	8130(12)	1506(10)	17(3)
H(2B1)	4935(18)	6932(12)	2555(10)	14(3)
H(3B)	7247(18)	6079(13)	3549(10)	18(4)
H(4B)	9649(16)	6668(11)	2435(9)	6(3)
H(5B)	9458(17)	8799(12)	2231(10)	13(3)
H(6B1)	6685(17)	9081(11)	3184(10)	11(3)
H(6B2)	8676(18)	9709(13)	3795(11)	19(4)
H(7B)	6919(17)	8041(11)	4566(10)	11(3)

Table 6. Hydrogen bonds for DPS01 (CCDC 203516) [Å and °].

D-H...A	d(D-H)	d(H...A)	d(D...A)	<(DHA)
O(1A)-H(1A)...O(2A)#1	0.801(16)	1.888(17)	2.6873(13)	175.4(17)
O(2A)-H(2A)...O(1B)#2	0.820(17)	1.897(17)	2.7143(14)	174.5(17)
O(1B)-H(1B)...O(2B)	0.777(17)	1.943(17)	2.5346(14)	132.7(16)
O(2B)-H(2B)...O(1A)	0.815(15)	1.867(16)	2.6803(13)	177.0(16)

Symmetry transformations used to generate equivalent atoms:
#1 -x,-y+1,-z #2 -x+1,-y+1,-z